Hydrological Models - Development and Application

Institute for Water Research
Rhodes University

WRC Report No. 235/1/93

HYDROLOGICAL MODELS - DEVELOPMENT AND APPLICATION

Final report to the Water Research Commission
on the project :

"Hydrological modelling in the Eastern Cape"

by the

INSTITUTE FOR WATER RESEARCH
Rhodes University
Grahamstown, South Africa

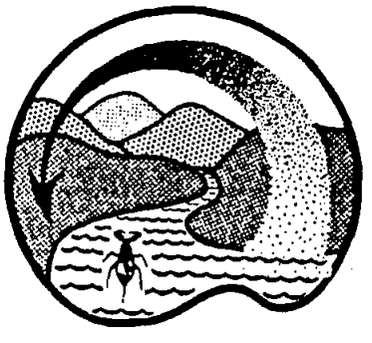

D A Hughes, K Sami and K A Murdoch

November 1993

IWR Report No. 2/93
WRC Report No. 235/1/93
ISBN 1 86845 026 0

Table of Contents Page

LIST OF FIGURES

LIST OF TABLES

FORWARD

The original proposal to the Water Research Commission to carry out this research project was compiled by Dr Denis Hughes and Dr John Herald of the former Hydrological Research HRU) Unit of the Department of Geography at Rhodes University. The HRU had been involved in research in the field of mathematical modelling of the processes of rainfall-runoff since its inception in 1974. Former senior research staff of the HRU have included Dr Peter Roberts, Dr Andre Görgens and Prof. Hulme Moolman. All of these scientists have contributed to the success that the HRU has enjoyed throughout its existence. However, the one person who contributed to the success of the HRU during the majority of the time that it was in existence was Prof. John Daniel, former Head of the Department of Geography. Prof Daniel was mainly responsible for establishing the HRU and gave his whole hearted support right up to the time of his retirement in 1989.

The earlier projects undertaken by the HRU concentrated on modelling semi-arid hydrology and were largely based in the Ecca research catchments, situated some 20km north-east of Grahamstown. Later work expanded into modelling the hydrology of the humid, southern Cape catchments between George and Knysna. A component of the work in the latter area involved attempts to improve the simulation of isolated flood events and this led to a major project to develop and evaluate flood models, some of the concepts of which have been incorporated into the work of the current project.

One diversification from the original research thrust of the HRU was into the field of hydrosalinity processes and their simulation. Specifically, this led to a long term study of the mineralisation processes involved in the irrigated areas of the Lower Sundays River Valley. One of the main aims was to obtain a better understanding of the sources of the highly mineralised return flow entering the Sundays River and to evaluate the ability of appropriate models to simulate the processes involved. Before the project discussed in this report began, Dr John Herald became the principle research officer in charge of the Sundays River project. While therefore making a major contribution to the proposal, he did not actually work on this project.

During the latter part of the 1980's, the Department of Water Affairs and Forestry began a major water supply scheme in the valley of the Ecca River (The Lower Fish River Irrigation Scheme). This development involved the construction of a dam and canal works within the former research catchments, meaning that they could no longer be considered representative of natural semi-arid conditions. It was therefore necessary to develop new research catchments and the area chosen was the Nyara River in the Bedford district, some 90km north of Grahamstown. The establishment of these catchments formed part of the project discussed in this report.

The Hydrological Research Unit ceased to exist in July 1991, not for any negative reasons, but because it combined with the former Institute for Freshwater Studies (IFWS) to become the Institute for Water Research (IWR). The IWR is now a broad based research institute that is designed to cover the fields of hydrology (surface and groundwater), freshwater ecology and water quality problems within a strongly multi-disciplinary framework. The IWR is concerned not only with scientific research, but also with the application of research

to the solution of real water resource problems, as well as the training of future water scientists. It is appropriate to thank those who were primarily involved in establishing the IWR; Prof. Wesley Kotzé (former Dean of Science at Rhodes and Chairman of the Institutes Board of Control), Prof. Randall Hepburn (Head of the Department of Zoology and Entomology), Prof Colin Lewis (Head of the Department of Geography) as well as the senior members of the two former research units (Dr Jay O'Keeffe - IFWS and Dr John Herald). Although no longer part of the Department of Geography, the staff of the IWR continue to maintain strong links with the department. This is mainly through their contribution to the honours courses given in Applied Hydrology, Groundwater Hydrology and Water Resources Management, as well as the supervision of undergraduate and honours projects and postgraduate research programmes.

As the amalgamation occurred during the course of this project, it was inevitable that some modifications to the aims and objectives occurred. However, these have only been of a minor nature and hopefully will be considered as contributing to a better final result, rather than detracting from the original aims.

The majority of the hydrological modelling research carried out within both the former HRU as well as the existing IWR would not have been possible without the tremendous support that the Water Research Commission has extended to Rhodes University over the years since 1974. As the current Director of the new Institute, I would like to express my thanks, as well as the thanks of the former and present Heads of the Department of Geography (Professors Daniel and Lewis) for this support.

Dr D A Hughes
(Associate Professor and Director of the IWR, Rhodes University)

ACKNOWLEDGEMENTS

The authors would like to thank their present and former colleagues in the Institute for Water Research and the Department of Geography. Dr John Herald made a major contribution to the design of this project and to the establishment of the instrumentation in the Bedford catchments. He also contributed to some of the conceptual ideas forming the basis of some of the models referred to in the report. Anne Beater worked on the project during its early stages and made important contributions to the collection and analysis of some of the Bedford catchment data. John Landman and Stanley Kara are thanked for their roles as field technicians and collecting the majority of the hydrometeorological and soil moisture data from the Bedford catchments, while several groups of Rhodes students contributed greatly to the collection of most of the physiographic data. Juanita Mclean is to be thanked for her role as secretary in the IWR for assisting with the administration of the project.

Professors John Daniel and Colin Lewis provided support to the research team during the time that the project was being run under the auspices of the Hydrological Research Unit. We are also indebted to the members of the Board of Control of the Institute for Water Research for their assistance and support, especially Prof. Wesley Kotzé, the chairman. Dr Jay O'Keeffe and Mrs Carin van Ginkel have provided food for thought about some of the developments that have formed part of this project by offering a perspective from other scientific disciplines. Mrs van Ginkel also worked closely with the senior author on the example simulations of several aspects of the Buffalo River and provided much of the necessary background information. Mrs Elizabeth Filmalter, a member of the IWR staff working in the southern Cape region provided some very useful information about the characteristics of these catchments. Dr Vladimir Smakhtin, a recent arrival in the IWR from Russia, has also made some contributions through constructive criticism, as well as beginning to add routines of his own to the modelling system (HYMAS) developed as part of the project.

We are indebted to Rhodes University for their general support of the IWR, as well as their specific support in the form of financial and personnel administration.

The landowners of the Bedford catchments are thanked for their assistance in permitting access to their land for the siting and servicing of instrumentation and for carrying out specific surveys or studies of the catchments characteristics.

The Computing Centre for Water Research is thanked for providing a great deal of data on rainfall, runoff and evaporation for several areas of South Africa, although most of this data originates with the Weather Bureau and the Department of Water Affairs and Forstry. The US Department of Agriculture provided the rainfall and runoff data for the USA catchments. The Institute for Soil, Climate and Water of the Agricultural Research Council provided important unpublished information about the soil characteristics of the Bedford area and the Geological Survey of South Africa provided unpublished information about the geology.

Several groups have provided constructive criticism of the modelling system. Special thanks are due to Dr Andre Görgens and some of the staff of the Cape Town office of Ninham Shand Inc., as well as Dr Gerard Chetboum and staff of the Lesotho Highlands Development

Authority for taking time to listen to presentations on HYMAS and suggesting improvements.

Last but far from least, the following persons comprised the Water Research Commission Steering Committee for this project and the authors are grateful to them for their valued contributions. Special thanks are due to Mr Hugo Maaren for guidance throughout the project in his role as the responsible WRC Research Manager and to Mr Malcolm Hensley for a great deal of assistance with characterising the soil properties of the Bedford catchments.

Mr H Maaren : Water Research Commission (Chairman)
Mr P W Weideman : Water Research Commission (Committee Secretary)
Mr J M Bosch : Forestek, CSIR
Mr H C Chapman : Water Research Commission
Dr M C Dent : Computing Centre for Water Research
Dr M Hensley : Agricultural Research Council
Dr J J Lambourne : University of the Witwatersrand
Prof. C Lewis : University of Rhodes
Prof. R E Schulze : University of Natal
Dr A Seed : Department of Water Affairs and Forestry

1. INTRODUCTION

The purpose of this introductory chapter is to outline the original aims and objectives of the project and to highlight where these have been modified during the five years that the project has been in operation. It also provides some background about how the project was organised, how the specific research tasks undertaken were influenced by developments in other projects related to this one and a brief introduction to the way in which the final report is structured.

1.1 AIMS AND OBJECTIVES OF THE PROJECT

The main aim of the project, as defined in the original proposal, was

> *"to contribute to an improvement in the applicability of hydrological models in South Africa with an emphasis on semi-arid environments."*

This was to be achieved through three primary objectives.

- To quantify the physical characteristics (relief, soil, landuse, etc.) of the Bedford catchments so that they can be established as long term research areas in a semi-arid environment.

- To improve the general applicability of hydrological models through the development of a flexible approach to their basic structure.

- To improve the soil moisture budgeting component of hydrological models by concentrating on monitoring and modelling vertical and lateral moisture fluxes at or near the base of the root zone.

The first objective arose out of the closure of the former Ecca research catchments due to the development of a major water supply scheme within their boundaries. It was considered at the time that it was important to replace the Ecca catchments as they were the only instrumented semi-arid research catchments in South Africa. To effectively replace them it was necessary to not only select a new area, but also to establish instrumentation and to carry out some baseline surveys of their characteristics. It would then be possible to not only use them to provide a basis for some of the process studies and model developments that form a part of this project, but also to establish them for future research efforts by Rhodes University scientists and others. This objective has remained unchanged throughout the project.

The second objective refers to improving the general applicability of hydrological models. It was realised early in the project that this objective could not be achieved by simply developing existing or new models. It was necessary to pursue this objective within a more general framework of the techniques used to set up the information that models require, run the models and examine the simulation results. The objective was therefore eventually interpreted to mean that the project would attempt to improve the approaches to applying a

range of hydrological models, as well as developing a more flexible approach to the basic structure of some models. One example is allowing a choice of methods for simulating some sub-components of catchment hydrology on the basis of the amount of information available or the specific-response characteristics of the catchment being modelled.

The final objective has also undergone some modification during the course of the project. The essence of the objective was to use field based process studies of soil moisture and groundwater recharge, carried out within the Bedford catchments to gain a better understanding of soil moisture fluxes within semi-arid soils. The results from these field studies would then be used to develop new and improved approaches to the soil moisture budgeting component of catchment hydrological models. While the essence of the objective has remained unchanged, the project team has not restricted itself to the 'base of the root zone', but has investigated various aspects of the hydrology of semi-arid soils, including infiltration characteristics, channel transmission losses into alluvial material, re-infiltration of slope runoff, as well as the mechanisms involved in groundwater recharge into fractured rock aquifers and the estimation of recharge rates.

1.2 PROCEDURES ADOPTED AND PROJECT ORGANISATION

It is clear from the above section, that despite being formulated over seven years previously, the aims and objectives of the project have been retained, largely unmodified. The only changes that have occurred have been in response to the changing requirements of the hydrological science community, as perceived by those involved in this project.

Although highly interrelated, the three objectives could also be reasonably well defined in the context of project organisation and management. An initial priority was to establish the instrumentation and baseline characteristics of the Bedford catchments. Only then was it possible for the project team determine where within the whole area it would be most beneficial to concentrate their more detailed studies. There was also a need to allow some time to pass for a database of hydrometeorological and soil moisture information to develop.

It was also recognised that the development of a user-friendly model application system would suffer from a number of false starts and returns to the proverbial drawing board and that feedback from other potential users would be important. However, it was also recognised that this development had to proceed fairly rapidly if the system was to be used effectively by the project team itself to improve the efficiency of their own model development and testing. It was further recognised that there would be research developments in this general area by other groups not directly associated with the project. Where these could be clearly identified, it was considered better not to duplicate these efforts and only carry out the minimum research necessary to assist with the primary purpose of the project. It was felt that further improvements could be made to the system at a later date (even after the end of the project) when relevant work carried out by other groups had reached fruition. One example of this was in the integration of GIS software and products with hydrological models.

The interpretation of the field studies and the final development and testing of new modelling approaches, necessarily lagged behind some of the other work. Fortunately, some of the modelling approaches were sufficiently well developed during the project to be useful in

investigating real applied problems. Such applications of the models has also contributed to their further modification and development.

The final stages of the project have mainly involved further testing, application and modification of both the modelling system and some of the models contained within it. The intention has been to produce an applied hydrological modelling 'product', that can be useful to others at the end of the project. This is not meant to imply that the 'product' should be considered to be in its final form. The authors accept that there is a great deal of room for improvement and believe that such a system requires continual up-dating and revision based on their own perceptions as well as constructive comment and criticism from other users.

1.3 ASSOCIATIONS WITH OTHER INSTITUTE RESEARCH PROJECTS

During the course of the project, there have been several developments in other projects undertaken at Rhodes which have influenced some parts of the work carried out for this project.

The first was a water quality situation analysis of the Buffalo River Catchment undertaken by Watertek of the CSIR and the Institute for Water Research (Van Ginkel, et al., 1993). Part of this project involved a modelling exercise to determine the long term streamflow characteristics of the whole Buffalo River catchment. The version of Pitman's monthly model included in the modelling system developed during this project was used to carry out these simulations. Due to the presence of several impoundments within the system, it was also necessary to make use of a reservoir simulation model. A further component of the Buffalo River project was to attempt to estimate the effect of low cost, high density urban development on the phosphorus input to the Buffalo River. In the absence of suitable and available alternative approaches, this modelling project contributed by designing a daily time step phosphate export model and including it as part of the model application system. The details of the Buffalo River monthly modelling exercise, the phosphate export model and some of the results of applying it, are discussed in later sections of this report.

The Institute is currently carrying out a project for the Department of Environment Affairs which is designed to investigate some aspects of the hydrology of the Wilderness Lakes catchments, particularly with reference to changes in land use. It was anticipated that some of the models being developed by the hydrological modelling project could be useful in this regard, but that they would need to cater for a situation where the parameter values could change over time. This prompted the inclusion of a 'dynamic parameter' approach (or parameter 'time-slicing') in all the models being used in the modelling system. The staff of Ninham Shand working on the Western Cape Systems Analysis also identified the need for this type of approach during a demonstration of an earlier version of the Rhodes modelling system. The details of the approach adopted by Rhodes is referred to in more than one section of this final report.

At the beginning of 1993, the Institute began a Water Research Commission project designed to address various issues of low flow hydrology. One of the identified requirements for low flow analysis was a better understanding of the requirements for different indices of low flows. The modelling system referred to in this report, presented an ideal vehicle to attach procedures to estimate a variety of low flow statistics or indices. The indices could then be

calculated using observed data or simulated data from any of the included models. This work is in the early stages, but some of the progress is reported in sections of this final report.

The contribution that the real application of models can make to the further development of their structure has already been referred to. The research team have carried out a number of short term consultancy projects, most of which have been of benefit in identifying areas where the models, or the system within which they operate, could be improved.

1.4 STRUCTURE OF THE FINAL REPORTS

The final report is divided up into three volumes plus an executive summary. The first (Hughes and Sami, 1992) deals with the physical and hydrological characteristics of the Bedford catchments and is designed to stand alone as an introduction to anyone wishing to carry out further studies in the area or make use of some of the data that has been collected. The report describes the hydrometeorological gauging network that has been established and operated during the last five to six years and interprets both the information gained from this source, as well as others, to provide a brief introduction to the climate of the area. The physical characteristics are described in sections on the geology, topography and drainage, soils and alluvial deposits, as well as the land use and vegetation. Most of the spatial information has been digitised using ArcInfo GIS and the coverages are readily available. The soil moisture, runoff and groundwater dynamics of the area are also covered in the report, although it should be appreciated that the length of records is too short to make any firm conclusions.

The second volume (Hughes and Murdoch, 1993) represents the current version of the user manual for the modelling system (HYMAS - HYdrological Model Application System). This manual provides a detailed overview of what HYMAS is and what it is designed to do and explains the use of all the various computer programs that form part of the system. It includes a guide to installing the system, various sections on how to set up a modelling application and the ways and means by which users can modify or customise certain components of the system to more readily suit their purposes. The models currently contained within HYMAS are also described in some detail, together with the procedures designed to assist with the estimation of their parameter values.

The third volume (this volume) represents the overall final report and contains some summary information from the other two, as well as the details of the hydrological process studies, the background to the development of some of the models and the modelling application system, examples of the application of the models and the overall conclusions and recommendations of the project. There is inevitably some overlap between this volume and the other two. This is necessary so that all three volumes can stand more or less alone and so that readers mainly interested in the contents of any one volume do not need to continually refer to one of the others.

The executive summary attempts to present the developments that have arisen out of the project and the project conclusions in a much abbreviated format.

2. SEMI-ARID HYDROLOGICAL PROCESS STUDIES

This section of the report deals with those studies carried out during the project that have concentrated on specific hydrological processes. Many of these studies have been carried out in the Bedford catchments, which were established for this very purpose, while additional supporting material has been drawn from the literature. All of the studies have been directed at obtaining a better quantitative understanding of the operation of some specific processes, with the ultimate objective of improving the way in which the processes are represented within hydrological models. Although a repetition of some of the contents of one of the other volumes of the final report (Hughes and Sami, 1993), a brief description of the Bedford catchments is provided as background.

2.1 THE BEDFORD CATCHMENTS

The catchments are situated in the eastern Cape Province some 150 km inland from the coast and about 90 km north west of Grahamstown. They represent the transition area between the gently sloping, semi-arid grassland regions lying at the foot of the Winterberg escarpment and the more hilly and dissected, valley bushveld and karoo type vegetation areas to the south. The mean annual rainfall is some 460 mm, with a seasonal distribution that favours spring and autumn, while the annual potential evaporation is of the order of 1400 mm.

Soils are generally thin (less than 400mm over large parts of the area), although deeper soils are to be found in the valley bottom areas, where they are associated with alluvial and colluvial sediment accumulations. Soil textures are mainly clay-loams and sandy-clay-loams. Vegetation cover consists of a mixture of grass, bush and trees. The denser areas of bush and trees are found within the main valley bottoms, while the slopes and hilltops consist of either grassland or low karoo shrubs with variable densities of thornbush. The latter seems to be mainly dependent on the history of grazing land use practices and management and is partly related to overgrazing in the past or present.

The main hydrometeorological instrumentation system was established during 1987 and 1988 and is illustrated in figure 2.1. Six flow measuring weirs have been established, each with continuous water level recorders (the main weir has two recorders as drowned conditions at high flow are considered likely). The total catchment area draining to the main weir at NYQ01 is 656.6 km^2, while the gauged sub-catchments vary from 111.8 km^2 (NYQ03) to 0.18 km^2 (NYQ07). Most of the structures are flat-vee Crump weirs, while the gauge at NYQ07 is an H-flume at the outlet of a small first order tributary. There are 28 continuously recording raingauges, 2 automatic weather stations (temperature, wind speed and direction, relative humidity and solar radiation) and soil mositure has been monitored at three groups of sites at roughly 2-weekly intervals using neutron access tubes. Two of the latter sites are located in valley bottom areas, where the access tubes extend into the alluvium, while the other is located in the small first order tributary above NYQ07.

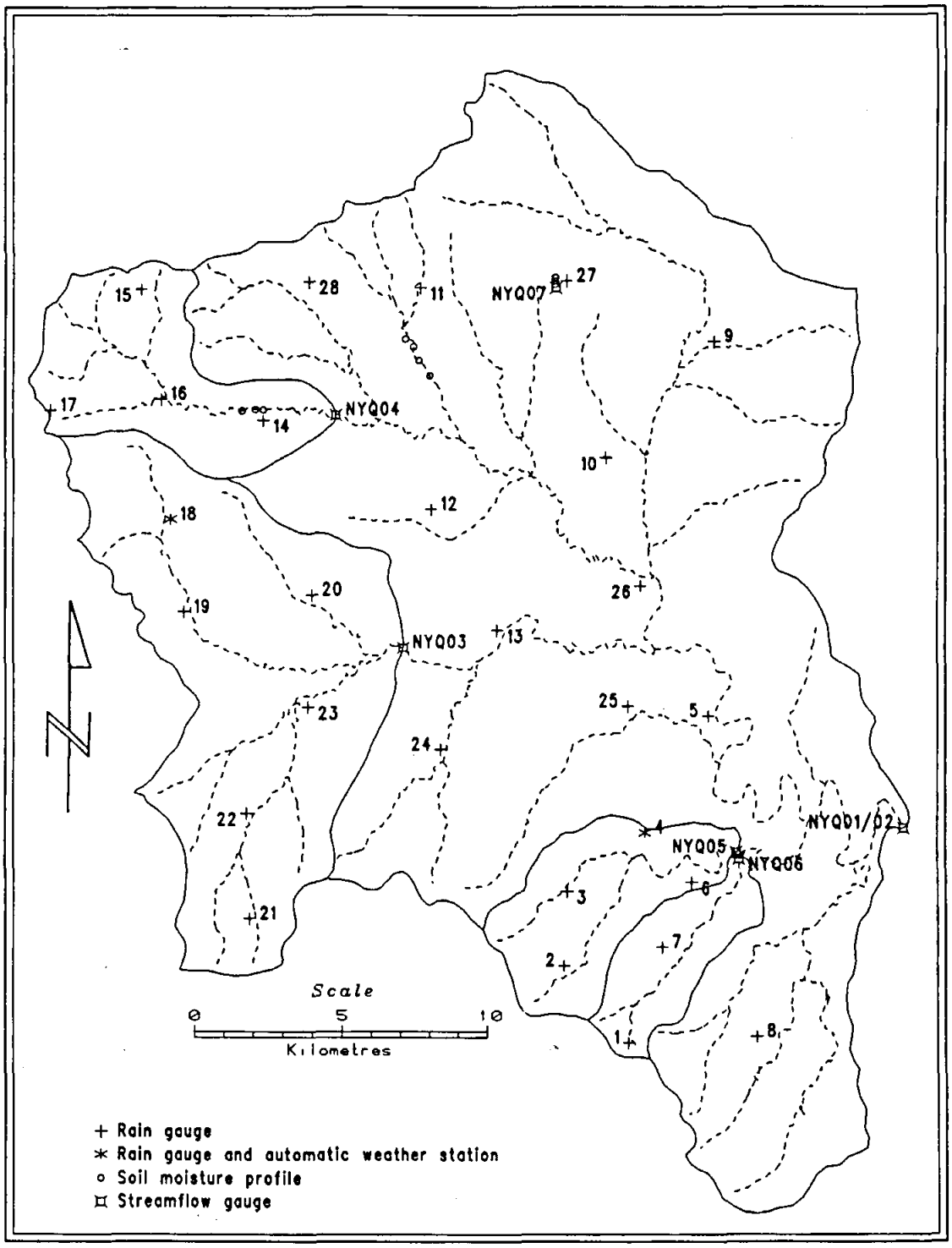

Figure 2.1 Instrumentation in the Bedford catchments.

The report on the physical characteristics of the catchments (Hughes and Sami, 1993), provides some detailed information about the climate, geology, topography, drainage, soils and land use. It also provides some insight into the perceived operation of hydrological processes, from the nature of the rainfall regime to estimates of the long term rates of groundwater recharge.

2.2 RAINFALL CHARACTERISTICS

As with many other semi-arid areas of southern Africa, annual rainfall totals are highly variable. At least part of this variability arises from the relative frequency of occurrence of the two types of rainfall that can prevail over the region. The first type are short duration and high intensity convective storms that occur mainly in the summer months. These are typified by small areal extents, giving rise to large spatial variations in short period intensities and total storm depths. They also rarely give rise to widespread runoff within the catchment, although fairly spectacular amounts of localised slope runoff have been observed.

The second major type are longer duration and variable intensity storms that are associated with the passage of cold fronts along the southern African coast or advection of moist air from the Indian Ocean. There does not seem to be any preferential season for these type of events and they appear to have similar probabilities of occurrence throughout the year. Total storm depths are very variable (from a few mm to well over 100 mm). Spatial variability during these events is generally much lower than during the convective events. The major cause of widespread streamflow in the catchments are the long duration events resulting from a low pressure cell over the interior of the sub-continent and high pressure cells over the oceans to the south.

The total rainfall during convective storms appears to vary from very small amounts up to about 30mm. Total durations vary from less than 1 hour up to more than 6 hours, although the main part of the latter also usually last for less than about 2 hours. Maximum 5 minute intensities are in excess of 120 mm h^{-1}, dropping to about 70 mm h^{-1} over 15 minutes and about 25 mm h^{-1} over 1 hour durations. Given the density of the gauging network that exists in the Bedford area, it has been estimated that the mean cell size of these storms is about 8 km^2 (based on the number of grids with rainfall greater than 0.8 times the maximum rainfall). It is quite possible that the density of the gauging network is insufficient in some parts of the catchment (fig. 2.1) to adequately define the size of some of the small area storms.

In comparison, the large area storms have durations of generally greater than 6 hours and sometimes in excess of 2 days. Intensities are variable but not greater than about 15 mm h^{-1} over 1 hour durations, occasionally increasing to about 50 mm h^{-1} over 15 minute durations, but generally not increasing very much over shorter durations. The largest event recorded (November 1989) consisted of between 90 and 140 mm over a duration of about 36 hours. The mean cell size of three events of this type (based on the same definition given above) has been estimated as about 70 km^2. However, this figure does not reflect the fact that the grids having rain falling below 0.8 times the maximum are not much lower. In the case of the convectional events, many of the grids not defined as part of a storm cell have rainfall well below the figure of 0.8 times the maximum.

The differences in the spatial and temporal variability of the rainfall events experienced in the Bedford catchments serve to highlight the spatial and temporal resolutions that might be required within a hydrological model used to simulate the hydrology of the area. From the point of view of simulating flow from relatively large sub-catchments within the area, or from the total area, the resolutions may not be all that important. It is only the large area storms, with depths greater than the normal convective storm, that cause widespread channel flow. These storms have much more uniform (spatially and temporally) intensities and the need for fine time interval modelling may be unnecessary. Hughes (1993) illustrates that using model time steps of below 2 hours does not significantly improve the simulation results of these large storms. However, a time step of 1 day, without some form of intra step iteration and assumptions about the shorter period time distribution of rainfall, proved to be inadequate.

If there is a need for additional detailed output from a model, with respect to the nature of the hydrological processes occurring during different types of storms, it is clear that a relatively small time step of modelling (less than or equal to 15 mins), as well as an appropriate spatial resolution, will be required. However, the information available for this catchment is relatively unique and it is rare to have as many raingauges or rainfall information with a time resolution of better than one day. The question therefore arises as to whether it is worthwhile designing a model around the level of information that is required to satisfactorily define the rainfall input, or is it better to design for the level of information that is commonly available. Ultimately, either approach will potentially suffer from the same problem of incorrectly describing the real rainfall intensity input to the model if only daily rainfall information is available and the intensities are as variable as they are in the Bedford catchments.

2.3 INFILTRATION CHARACTERISTICS

Infiltration studies conducted during the course of this project focused on two objectives. First, a literature review was conducted in order to quantify the range of infiltration rates encountered over various soil textural classes and to identify other physical indices affecting infiltration. These data were used to develop and calibrate infiltration parameter estimation techniques incorporated into the VTI model. Second, the infiltration characteristics of the various Soil Forms in the Bedford catchments under different vegetation types and veld conditions were quantified. These data were used to further calibrate the parameter estimation functions and test their validity under various conditions encountered in semi-arid areas.

2.3.1 Derivation of infiltration envelope curves

The range of characteristic cumulative infiltration curves for each of the various soil textural classes were derived from the theoretical maxima and minima of the Green-Ampt infiltration parameters (effective porosity, ϕ and capillary pressure head, ψ - table 2.1) found in the literature (e.g. Rawls and Brakensiek, 1983). Subsequently, the time required to infiltrate known depths of water was determined from using the integrated form of the Green-Ampt equation:

$$Kt = I - (\phi * \psi) * \ln(1 + \frac{I}{\psi}) \quad \text{Eq. 2.1}$$

where I is cumulative infiltration in cm h^{-1}
t is time in hours.

Infiltration rates at specific moments (i) were calculated by:

$$i = K(1 + \phi \frac{\psi}{I}) \quad \text{Eq. 2.2}$$

The range of infiltration rates obtained for each soil texture class were then used to construct envelope curves for various soil textures (figures 2.2 to 2.5). These curves were subsequently defined by the two empirical constants, k and c, of the Kostiakov infiltration function (Kostiakov, 1932):

$$i = kct^{k-1} \quad \text{Eq. 2.3}$$

This transformation was deemed necessary in order that infiltration parameters incorporated into the model be compatible with the South African Department of Agriculture's sprinkling infiltrometer (Reinders and Louw, 1984), which determines similar k and c infiltration parameters. The range of k and c required to bracket the infiltration envelope curves is shown in table 2.2.

The authors have identified several physical factors which may cause infiltration rates to vary within these ranges. These are the degree of macropore development and surface compaction, soil structure, sand grade, surface organics and roughness. The log normal distribution of infiltration rates encountered at the field scale, even across a relatively homogenous soil zone, can also be attributed to these factors (e.g. Sharma et al., 1983).

According to indices of these factors, parameter estimation functions have been developed to estimate the mean and upper standard deviation of k and c values for specified soil textures in order to derive a log normal distribution of infiltration rates for a given catchment. These functions are described in detail in the HYMAS user manual. Examples of k and c estimates derived from these functions are given in table 2.3. This table presents estimated mean k and c values and their standard deviations in catchments with loam, sandy clay loam and silt loam soils combined with different additional physical characteristics. While it was relatively straightforward to identify the range of parameter values for each soil texture class, it was found to be very difficult to adequately quantify the effects of the additional physical characteristics (structure, crusting, etc.) from the literature.

Table 2.1 Range of Green-Ampt infiltration parameters by soil textural class.

Soil Texture	Bulk density	Effective porosity (ϕ)	Capillary pressure head (ψ cm)	Sat. hyd. conductivity (K cm h^{-1})
Sand	1.50-1.60	0.35-0.40	5-6	11-20
Loamy sand	1.40-1.70	0.33-0.43	6-9	6-12
Sandy loam	1.25-1.27	0.32-0.50	8-15	1.5-12
Loam	1.35-1.55	0.35-0.45	16-30	0.3-2
Silt loam	1.00-1.50	0.43-0.52	15-50	0.1-3
Sa clay loam	1.55-1.70	0.29-0.35	8-25	0.2-11
Clay loam	1.30-1.55	0.33-0.41	24-55	0.08-0.3
Si Cl loam	1.30-1.50	0.38-0.42	40-90	0.04-0.2
Sandy clay	1.60-1.65	0.30-0.35	10-55	0.05-1
Silty clay	1.35-1.50	0.37-0.39	70-150	0.005-0.05
Clay	1.20-1.55	0.34-0.46	40-150	0.001-0.05

Table 2.2 Range of infiltration k and c by textural class.

Texture	k	c
Sand	0.75-0.80	3.4-7.6
Loamy sand	0.67-0.74	3.6-5.3
Sandy loam	0.60-0.67	2.1-8.5
Loam	0.54-0.58	1.3-6.3
Silt loam	0.50-0.56	1.2-9.7
Sa clay loam	0.58-0.65	0.7-9.3
Clay loam	0.52-0.52	1.0-3.2
Si Cl loam	0.51-0.51	1.0-3.5
Sandy clay	0.53-0.54	0.5-5.3
Silty clay	0.50-0.51	0.5-2.2
Clay	0.50-0.50	0.2-2.4

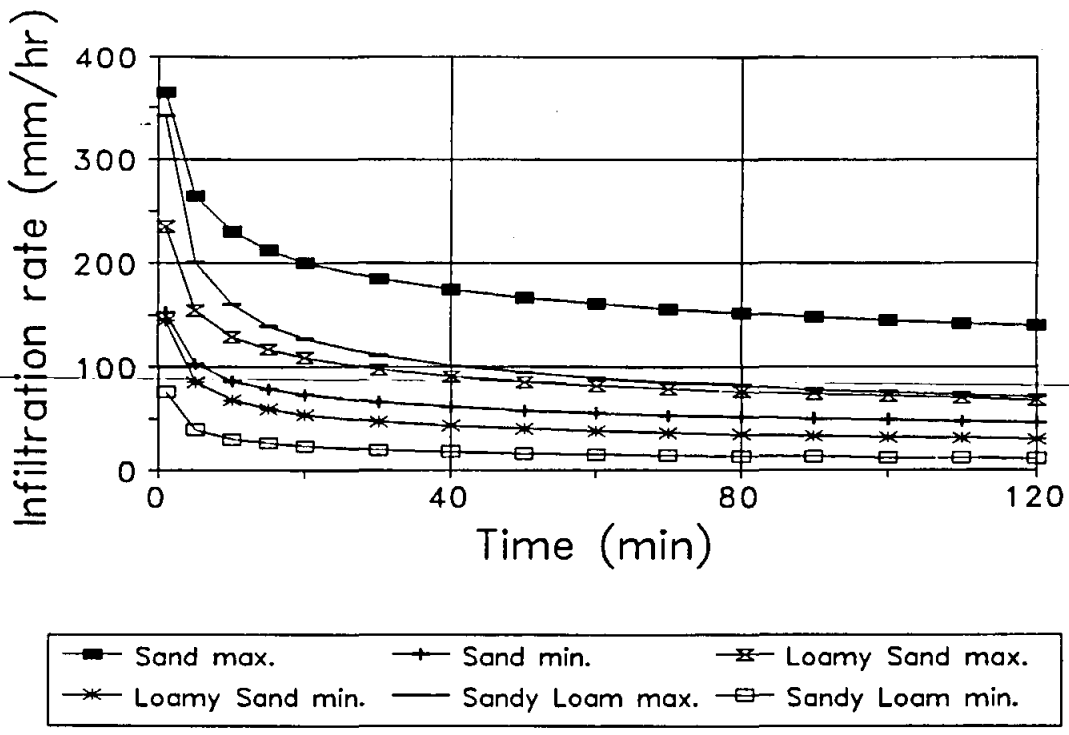

Figure 2.2 Maximum and minimum infiltration curves in coarse textured soils.

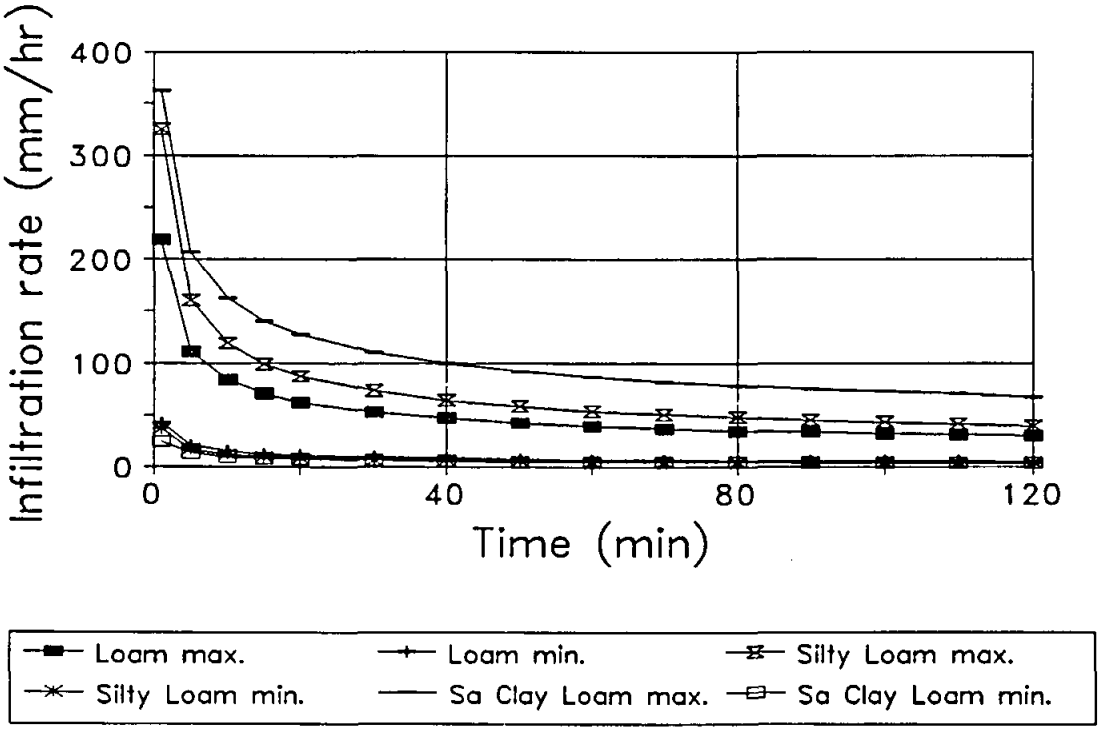

Figure 2.3 Maximum and minimum infiltration curves in intermediate soils.

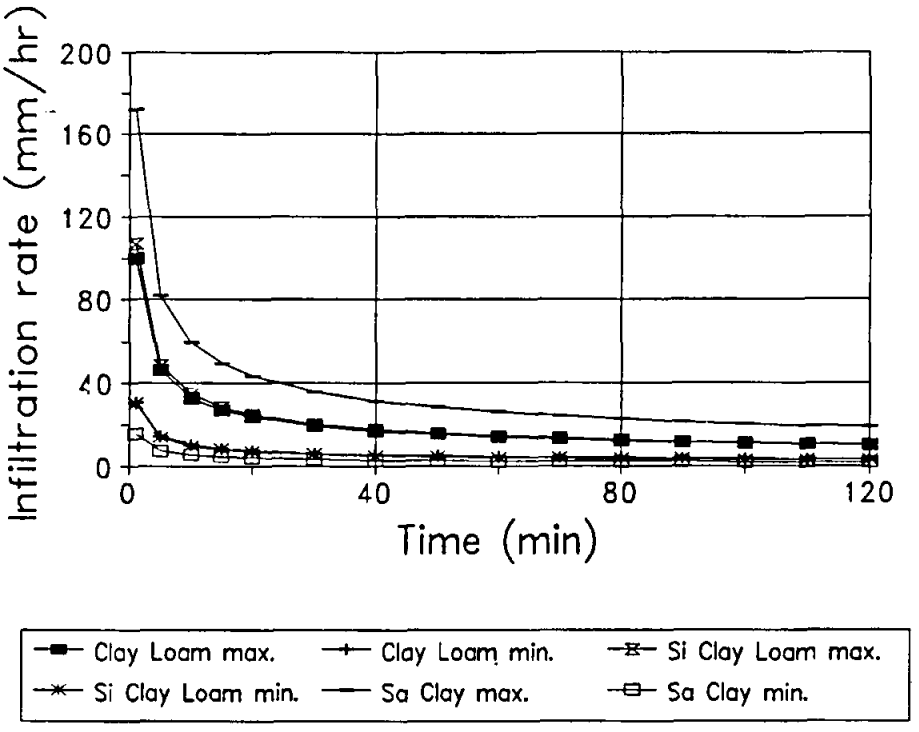

Figure 2.4 Maximum and minimum infiltration curves in intermediate soils.

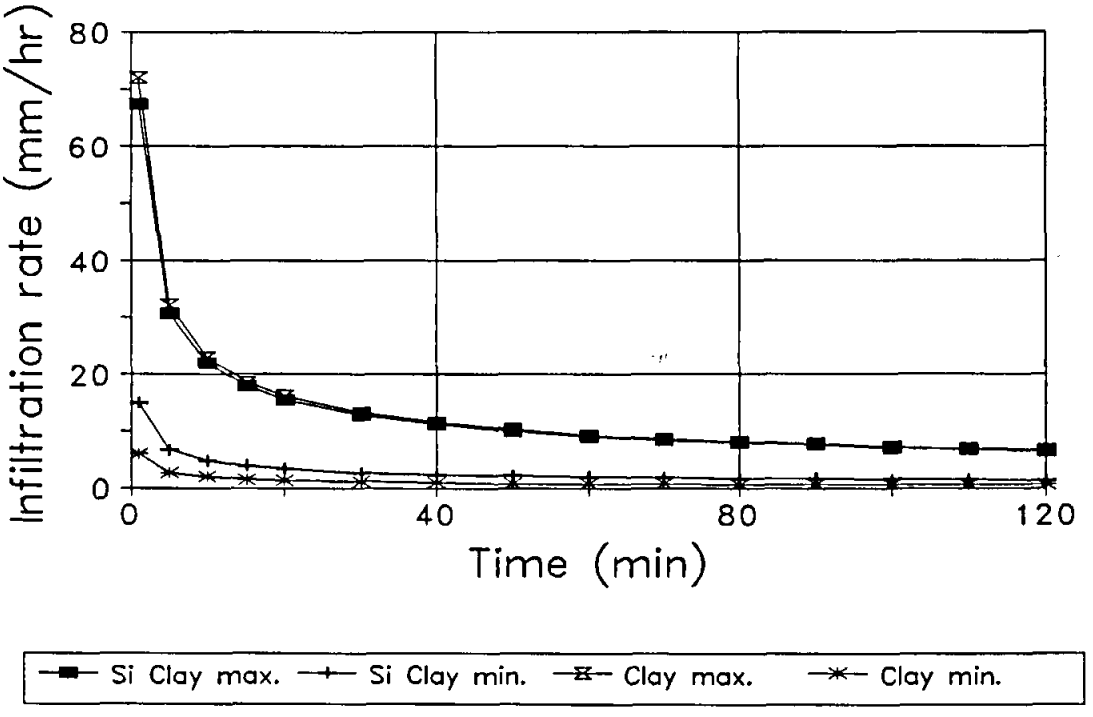

Figure 2.5 Maximum and minimum infiltration curves in fine textured soils.

Table 2.3 Infiltration parameters for a catchment covered by: A) loam, sandy clay loam and silt loam soils; B) with a high degree of macropore development; C) strong structural development; D) coarse sand in the sand component; E) severe surface compaction; F) high surface organic content; G) rough surface conditions; H) strong macropore and structural development, coarse sand, and a rough surface with a high organic content.

	A	B	C	D	E	F	G	H
k	0.54	0.562	0.562	0.562	0.432	0.648	0.562	0.734
k upper St.Dev.	0.015	0.015	0.015	0.007	0.023	0.015	0.015	0.007
c	2.5	2.575	2.575	2.75	2.25	2.75	2.575	3.225
c upper St.Dev.	2.0	2.1	2.1	2.2	1.8	1.8	2.1	2.3
Mean final inf. rate (mm/h)	8.95	10.67	10.67	11.39	3.84	19.82	10.67	39.75

2.3.2 Infiltration characteristics in the Bedford catchments

Soil and infiltration properties in the Bedford catchments are described in Hughes and Sami (1993). The Infiltration characteristics of these soils under various vegetation and surface conditions were derived from a field survey conducted by project staff. These soils generally have a very low organic content, a very fine sand component, are severely compacted with bulk densities of about 1.8, have weak structural and macropore development and exhibit surface crusting. The results were obtained using a Department of Agriculture sprinkling infiltrometer. The broad vegetation and soil groups, the resultant ranges and means of k and c values and final infiltration rates are listed in Table 2.4. Final infiltration rates have been defined arbitrarily as the rate after 120 minutes.

Table 2.4 Infiltration characteristics for various vegetation and soil conditions.

Dominant Vegetation Type	Soil Form and Condition	Text	N	k range and mean	c range and mean	Final Inf. rate (mm/h) range and mean
Karroid	Glenrosa, Mispah	SaClLm	7	0.11-0.36 0.25	1.46-3.8 2.13	0.16-2.07 1.09
Grass	Swartland, Glenrosa	SaClLm	17	0.15-0.55 0.33	1.16-5.48 2.43	0.35-12.53 3.34
Grass/riverine	Valsrivier, Augrabies	Sa Lm	6	0.32-0.56 0.40	1.61-3.00 2.19	1.55-8.58 3.46

The results show that the infiltration parameters are likely to be log normally distributed since means tend to lie closer to the lower range value. However, the sample sizes are too

small to present any statistically significant conclusions concerning spatial variability. In general, the lowest values were recorded where overgrazing has resulted in Karroid species domination and where surface crusting can develop. The highest infiltration rates are found on colluvial footslopes where denser vegetation and deeper soils are found. Similarly, hillslopes covered by thornbush and grass, usually well vegetated with relatively deep soils, also have high infiltration rates.

In general k values are much lower than has been recorded in the literature (table 2.2), however, few studies have been conducted in semi-arid regions where the effect of surface crusting may significantly affect infiltration. The consistently low k values observed in the field reflect the rapid reduction in infiltration rates which result from surface crusting. Crusting also causes final infiltration rates to occasionally lie below the theoretical minimum of 3.26 mm h^{-1} (figure 2.3).

Infiltration parameter estimation procedures developed during this project incorporate the effects of crusting on compacted soils. The predicted mean infiltration rate for existing soil conditions (3.84 mm h^{-1}) is similar to means observed in the field under grass conditions (3.34 mm h^{-1}). Similarly, the observed range of infiltration rates lie close to estimates of ± 1 standard deviations from the predicted mean final infiltration rate (figure 2.6).

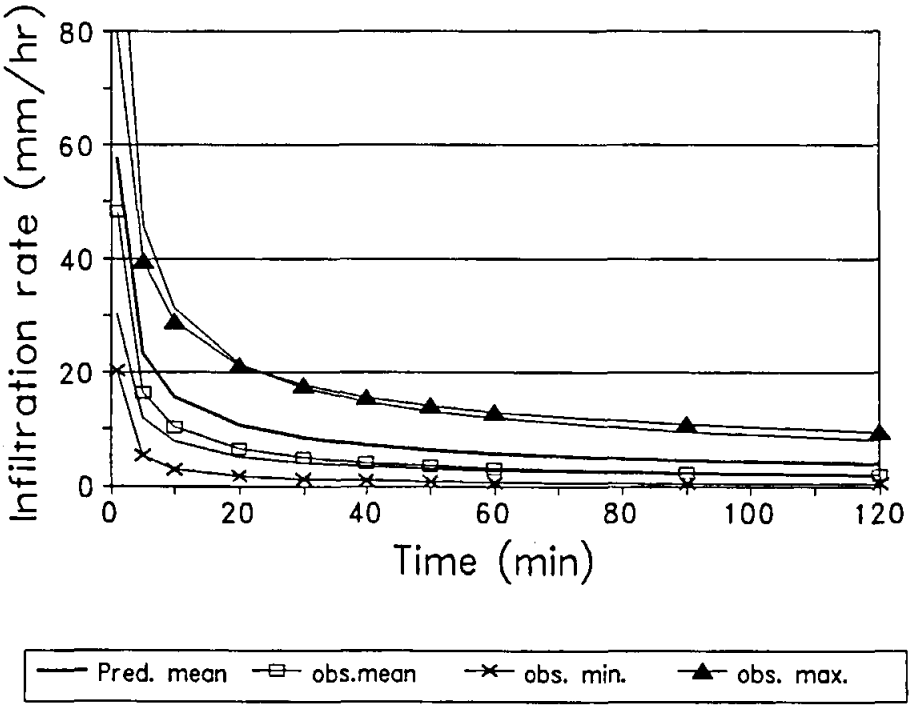

Figure 2.6 Range of observed infiltration rates and simulated mean ± 1 standard deviation (lines with no symbols) under grass conditions.

The large range of k values implies that there is a large variation in the rate at which infiltration capacity declines during a storm event. Consequently, there is a greater relative difference in initial infiltration rates than final infiltration rates. Hughes and Sami (1993) show that initial infiltration rates vary from about 10 mm h^{-1} to 150 mm h^{-1}, while final

infiltration rates range from less than 1 to 15 mm h^{-1} across the catchments. Where Karoo vegetation exists, initial infiltration rates are generally less than 30 mm h^{-1} (figure 2.7). As these regions also have low k values (table 2.4), infiltration rates decline rapidly to less than 10 mm h^{-1} in under 10 minutes. This reflects the high sorptivity of clay particles in the surface crust, which causes a rapid surface sealing once the surface layer is wetted. In well vegetated grassland and thornveld areas where crusting has not developed, such as those found on colluvial footslopes, initial infiltration rates exceed 80 mm h^{-1} and decline at a slower rate than other soils. Hillslopes which have been overgrazed, or where the soil cover is shallow, have infiltration capacities approximately six to seven times lower than well vegetated areas (figure 2.7). They also experience a more marked decline in infiltration rates over time due to crusting.

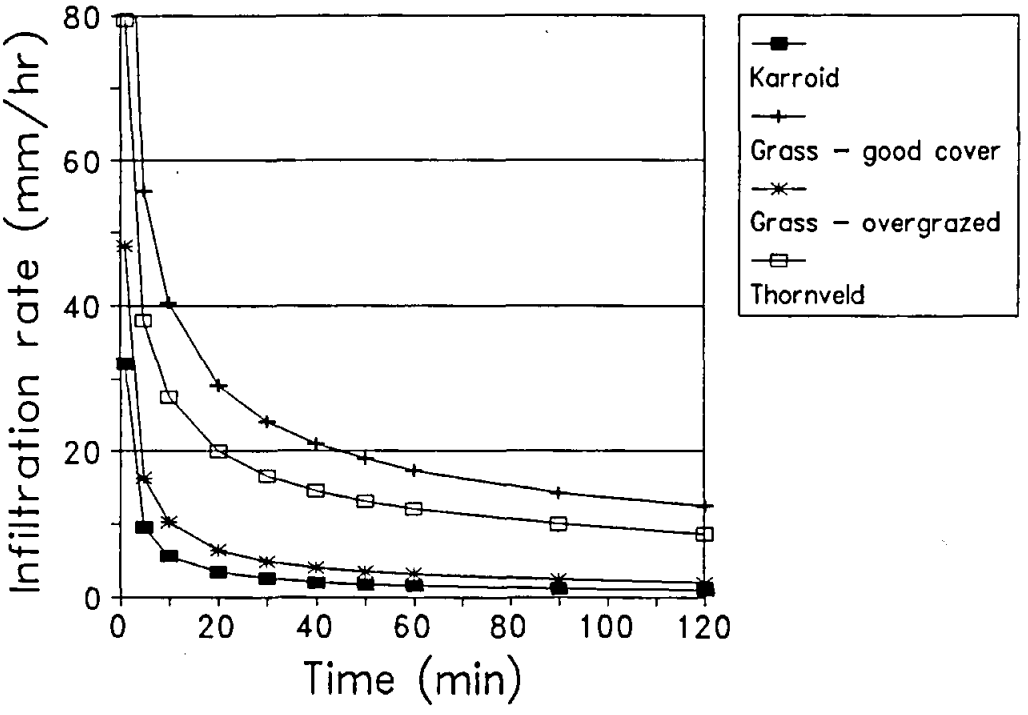

Figure 2.7 Representative infiltration curves in the Bedford catchments.

2.3.3 Infiltration and runoff generation processes

As a result of the large variations in initial infiltration rates, short duration storm events generate overland flow from partial areas of the catchment where the infiltration rate is exceeded by rainfall intensity. These would most likely be on hillslopes, where soils are shallower, or where overgrazing and surface crusting has occurred. The higher infiltration rates encountered on the footslopes and alluvial valley bottoms would result in the re-infiltration of overland flow derived from the upper slopes. With increasing storm duration infiltration rates, and their variability, decline rapidly. Consequently a larger the proportion of the catchment would generate intensity excess runoff. These processes have been frequently observed in the field during rainstorms of differing magnitudes and durations.

2.4 CHANNEL TRANSMISSION LOSSES

Transmission losses refer to the reduction in flow volume between upstream and downstream points in a channel system and are caused by infiltration into the material of the river bed or flooded surface during overbank flows, as well as losses through evaporation from water surfaces. The latter is not relevant to the Bedford catchments, but has been identified as a major consumer of water in large rivers such as the Orange (McKenzie, et al., 1993).

Various authors have quantified losses for several parts of the world, with some concentrating on the effects of transmission losses on channel flow and the derivation of techniques for estimating the effects on the downstream hydrograph (Cornish, 1961; Lane et al.,1971; Renard, 1971; Jordan, 1977; Peables, Smith and Yakowitz, 1981; Walters, 1990). Others have investigated the effects of losses on the recharge of alluvial aquifers (Crerar, Fry, Slater, van Langenhove and Wheeler, 1988). Most of the literature has concentrated on losses during flood events. Walters (1990) summarises much of the quantitative information available on transmission losses. According to the data given by Walters (1990), the proportion of flow lost from the upstream hydrograph varies from negligible over a 32km reach of the Trinity River in Texas to over 90% over a 12km reach of Walnut Gulch in Arizona. Equivalent data from wadi environments in Saudi Arabia range between 10% and 78% over two similar length (18km) reaches in the same drainage basin. Crerar et al. (1988) report losses of up to 12% over a 1.8km reach of the Swakop River in Namibia for the first flood of the season. However, subsequent floods demonstrate lower losses due to the formation of an impermeable silt layer.

The figures given above demonstrate that neglecting transmission losses in any modelling system designed to simulate runoff characteristics from semi-arid or arid catchments could result in serious errors. However, the amount of information on the processes involved is relatively modest and few models seem to account for transmission losses. There is, therefore, a need for further documentation and understanding of the nature of transmission losses in different environments, as well as the incorporation of this understanding in water resource estimation techniques. Apart from the paper by Crerar et al. (1988) no other southern African studies have been reported in detail. Consequently, any quantitative information that contributes to a better understanding will be of use. The details of the study reported in this section have been published in Hughes and Sami (1992).

The alluvial valley bottom referred to is located about 3km upstream from one of the Bedford gauging weirs (catchment area of 39.6km^2). Above the alluvial area the channel is incised, developed on bedrock and with bed material consisting mainly of large boulders. There is then a very rapid transition to a deep rectangular channel having alluvial banks up to 3.5m in height and approximately 6m wide with gravel bed material (figure 2.8, section A-A). The catchment area above this first section of alluvium is 26.3km^2. After some 2km the channel gradually decreases in size until disappearing as a truly continuous feature. It is replaced by a number of discontinuous trench like features which are highly variable in both width, depth and position on the valley floor (figure 2.8, sections B-B, C-C and D-D). The movement of gravel, both within these channel features and across the alluvial floor, is very much in evidence for several hundred metres after the disappearance of the single continuous channel but eventually only fine material is found on the surface. The valley floor is about 200m in width and the main relief features are discontinuous channel trenches and linear

depressions. About 1.5km from the gauging weir the width of the alluvial area decreases and a continuous channel with rock outcrops in the bed (figure 2.8, section E-E) is again in evidence. The catchment area draining into this section of channel is some 4.6 km².

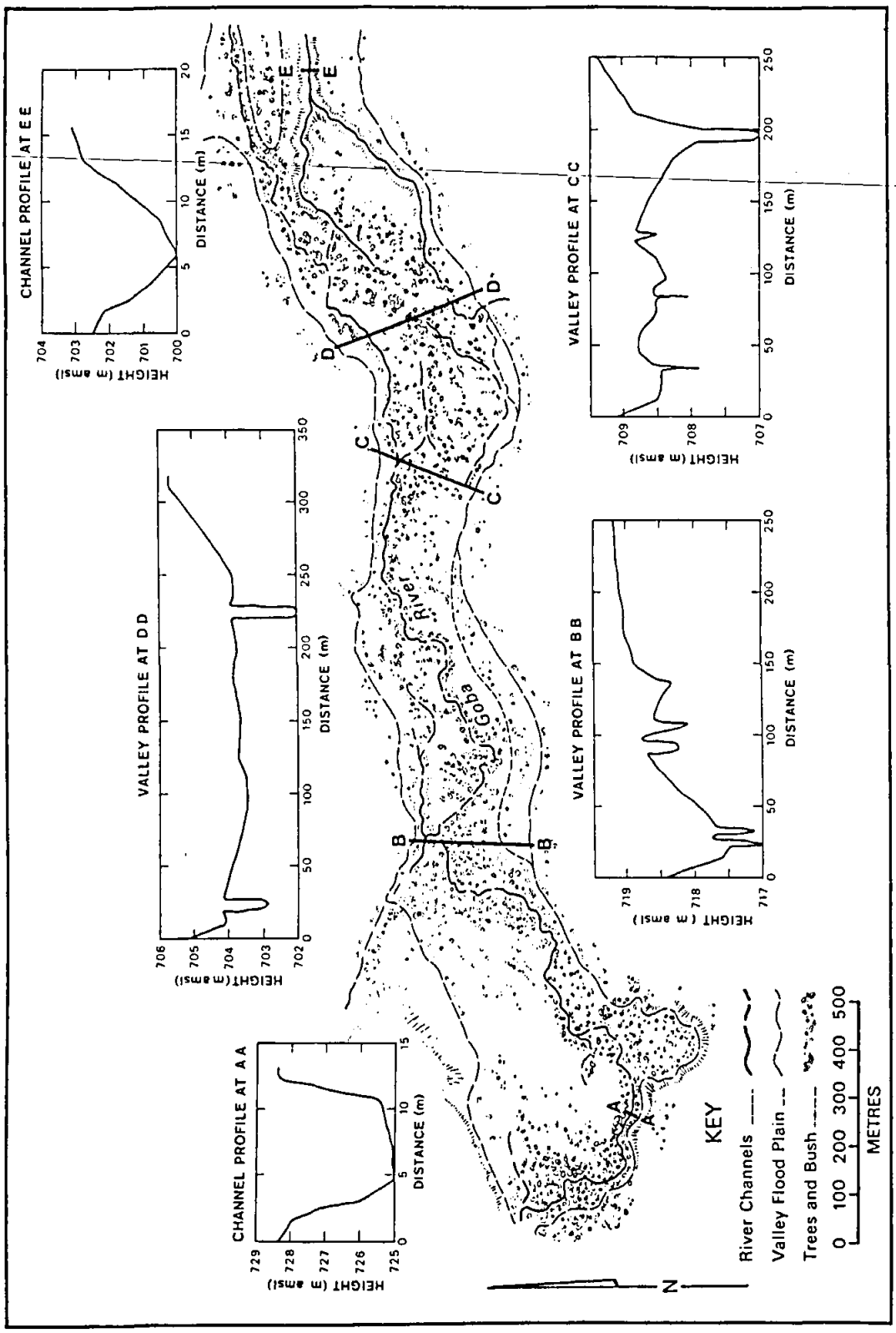

Figure 2.8 Plan map of the alluvial area and some channel and valley cross sections.

Vegetation consists of a mixture of grass, bush and trees. The denser areas of bush and trees follow the main linear channel features and thin out to open grass areas in the more elevated parts of the valley floor. This is clearly a response to the greater (or more frequent) availability of soil moisture close to the channel features. The density and height of the grass ground cover is partly seasonally determined, but also affected by the availability of moisture following the infrequent flow events.

Table 2.5 Textural characteristics of the alluvial material.

Sample Depths (m)	0.15, 0.3, 0.5	0.75, 1.0	1.5, 2.0	>2.0
Mean Bulk Density (gm cm^{-3})	1.51	1.76	1.81	1.75
St. Dev Bulk Density (gm cm^{-3})	0.20	0.29	0.23	0.23
Mean Porosity (% Vol)	42.8	35.6	31.7	33.8
Mean % Clay	30.7	27.3	29.6	23.7
St. Dev % Clay	6.4	10.6	5.9	9.6
Mean % Silt	12.7	12.0	13.1	10.8
St. Dev % Silt	2.4	3.6	2.3	3.9
Mean % Coarse	4.0	7.6	2.8	7.1
St. Dev. % Coarse	6.7	13.8	6.8	18.3

The available information on the characteristics of the alluvial material was obtained during the installation of a total of 12 neutron probe access tubes at the three cross-valley sections (B-B to D-D in figure 2.8). Unfortunately, the auger equipment used to sink the holes only reached a maximum depth of 6m and for 5 of the 12 holes the base of the alluvial material was not reached. The total area between B-B and D-D is approximately 320 000m^2. Table 2.5 summarises the observed dry bulk densities and the estimated porosity of the material for several depth horizons. The textural properties of the material have been estimated using a combination of hand texturing methods with verification of a sub-set of the samples using hydrometer analysis. Table 2.5 indicates that there is no noticeable trend in texture with depth and that most of the material can be considered to lie within the sandy clay loam class with relatively low coarse (> 2mm) fractions. The samples taken from gravelly layers, of which few were encountered, and the basal samples in weathered sandstone did have much higher coarse fractions (up to 75% in extreme cases).

2.4.1 Moisture changes following a runoff event

The description of the area given above indicates that the alluvial valley bottom area can be divided up into two main parts. The first is the upper alluvium, which is associated with a well defined gravel bed channel. The second is the lower area where no such well defined channel exists and where all the observations of soil moisture have been taken. The neutron probe access tubes were established over the period of 6 October to 8 November 1989. Fortunately, all the tubes were therefore in place before the major rainfall and runoff event that occurred over the period of 14 to 17 November 1989. Table 2.6 indicates that 131.9mm

of rainfall generated some 900 000 m^3 of runoff over a period of 72 hours and that the peak flow was 16.6m^3 s^{-1} at the downstream gauging station. This event has been estimated to have an annual return period of approximately 20 years. The pattern of moisture changes in the alluvium that resulted from this event have been extrapolated from the readings taken from the 12 access tubes and are discussed below. Some tentative estimations of the transmission losses that occurred during this event are also included in table 2.6 and an explanation of how these were obtained appears in a later section.

A storm on 2 and 3 October with similar characteristics in terms of intensity distribution and duration preceded the November event. However, the total rainfall depth was less than 90mm (table 2.6), the flow volume less than 30 000m^3, and the peak a mere 0.25m^3 s^{-1}. This event has a return period of about 5 years. As the access tubes had not been installed prior to this event, and in some cases not until 36 days later, it is difficult to make any firm conclusions about the nature of the moisture changes in the alluvium. Nevertheless, this report does include some speculative observations.

The November event.

Moisture increments to the alluvium were highly variable over the 12 access tubes and ranged from less than 20mm to greater than 800mm, with a mean of about 330mm. It is therefore apparent that a great deal more water was added than can be accounted for by rainfall on the alluvium (121.7mm). The additional input is assumed to originate from transmission losses. By weighting the moisture increment at each site by the fraction of the total area which that site can be considered to represent, it is estimated that the total increment to storage represents some 411.7mm. 290mm of this can be attributed to transmission losses. The weighting fraction was based on prevailing surface conditions (proximity to depressions or channels, etc.) and profile depth.

The nature of the moisture response at the access tube sites can be divided into three main categories. The first includes all those sites where an immediate response was observed throughout their depth. The term 'immediate'is taken to mean that the maximum moisture content was observed on the first visit after the flood water had largely receded (1 day after the peak). This category includes the two deep (>5.0m) sites on the upstream profile (B-B in figure 2.8) close to the termination of the gravel channel. The latter were the only sites where saturated conditions were observed and this occurred at a depth of 3.0m and below.

The second category includes those sites where an immediate response was observed in the layers down to between 2.0 and 3.0m. Within this category fall most of the relatively shallow (0.95 to 2.5m) sites close to the edge of the alluvium. Also included are several sites (> 2.5m deep) where a delayed response occurred in the deeper layers. Typical delays are between 7-14 days for the 3.0m layers of the two mid-valley sites of profile C-C and 21-28 days for the layers at 4.0m and below for the same sites. On the basis of the available data, it is difficult to ascertain whether this delay is a reflection of a vertically downward moving unsaturated wetting front, or a combination of this and some unsaturated lateral redistribution.

Table 2.6 Characteristics of the two events.

	October 3 1989	November 15 1989
Mean catchment rain (mm)	84.5	131.9
Rain on alluvium (mm)	86.3	121.7
Duration of streamflow (hr)	54	72
Peak streamflow ($m^3 s^{-1}$)	0.25	16.6
Streamflow volume (m^3)	29 504	907 200
Moisture increment to lower alluvial area (m^3)	*	131 750
Input to lower alluvium from rainfall (m^3)	*	38 950
Transmission losses to lower alluvium (m^3)	*	92 800
Transmission losses to upper alluvium (m^3)	** 88 900	88 900
Total estimated runoff volume (m^3)	*	1 088 900
Estimated runoff proportion (% rain)	3.7	20.8
Estimated total transmission losses (% runoff)	75	22

Notes : * Not enough data to allow a satisfactory estimate except that the input was similar to rainfall and transmission losses were small.

** Based on the assumptions discussed in the text.

The third category incorporates two sites, both of which are in slightly elevated areas of the valley floor which was not submerged by the flood waters. Both sites demonstrate very little immediate response at any depth (total profile increments of 10.2 and 16.4mm) suggesting a very effective surface crusting mechanism. The site located on section A-A (figure 2.8) down valley of the gravel bed channel crossing the valley floor transversely, shows a delayed (by approximately 21 days) response in the deeper layers. The deepest part of the profile, at 5.8m, responds somewhat sooner than the 5.0m layer. Sub-surface lateral flow at the base of the alluvium away from the higher input zone close to the gravel channel, therefore appears to be the dominant mechanism.

The October event.

Although this event occurred before the November event, there is less information available about the moisture response and is therefore discussed last. As none of the sites had been established prior to October 1989, any statements made about the response must be considered to be speculative. However, some information can be obtained given the assumption that the initial conditions prior to the October event were similar to the conditions almost 12 months after the November event. This assumption is based on the fact that all the profiles demonstrate a gradual drying over that period and the drying curves have almost flattened out for the majority of depths at all sites. There were also no major rainfall events in the 12 months prior to October 1989. The assumption is therefore equivalent to suggesting that the alluvial material was at, or close to, residual moisture content.

The first observation is that after the October event the profiles below 0.75m were still at residual moisture content and therefore assumed to have been unaffected. Several were

apparently unaffected even at the 0.5m depth. Only one of the sites is estimated to have had a moisture increment (approximately 150mm) much greater than the depth of rainfall and this is situated close to a channel segment on the north side of valley section C-C. The sites close to other channel segments, or similar depressions, do not exhibit the same pattern. One of the sites (on section D-D) that responded very little to the November event did respond in this event although by an amount (some 40-50mm) apparently less than the rainfall. It is therefore possible that the crusting effect may have been caused by the first event.

2.4.2 Approximations of transmission losses

Field observations after the October event indicate that channel flow was in evidence above the alluvial area. The evidence suggests that the moisture content of the lower alluvial area was unaffected by an input of transmission losses, which in turn suggests that any upstream runoff was lost to the upper alluvial area where the continuous gravel bed channel exists. This observation provides an opportunity to estimate a value for the amount of water that can be absorbed by the upper area. As no runoff seems to have passed this section during the October event, the potential for losses could of course be higher.

To estimate this value it is assumed that the flow at the gauging weir represents runoff from below the alluvial areas and from the tributary that enters from the south close to the downstream end of the alluvium (close to valley section D-D in figure 2.8). This catchment area is 9.3km^2 (34% of the total), which suggests a runoff depth of 3.2mm or a runoff proportion of 3.7% of rainfall. The vegetation and soils of the upper part of the catchment above the alluvium are similar to the lower parts of the catchment but the slopes are significantly higher. The runoff proportion is therefore unlikely to be less than some 4%, which yields a minimum runoff volume of 88 900m^3 (table 2.6) generated above the alluvium. The lower part of table 2.6 transfers this conservative estimate of the transmission losses during the October event to the November event. Combining it with the estimated losses from the neutron probe observations in the lower alluvium, a conservative estimate of the total losses in November is produced (181 700 m^3 or 22% of the estimated runoff into the alluvial valley bottom).

2.4.3 Conclusions

The estimated losses during the November event in the lower alluvial area are probably as good as can be obtained without a major expansion of the network of access tube sites. While based on an extrapolation from a limited number of observations, they should be at least the correct order of magnitude. The losses to the upper alluvial area for the November event are likely to be at least as high as the estimated value of 20%.

The results indicate that during flow events, even up to a return period of 5 years, all runoff from 66% of the catchment is likely to be absorbed, giving transmission losses as high as 75%. Larger events, such as the November storm, which are able to transmit runoff across both alluvial areas, are likely to have lower percentage losses, but the volume of loss is still substantial. It is apparent that ignoring transmission losses in deterministic catchment models will result in a serious over estimation of the surface runoff from catchments with similar characteristics. This issue is discussed further in the section on the development of the Variable Time Interval model.

2.5 SURFACE-SUBSURFACE INTERACTIONS

The aquifer in the Bedford catchments consists of Beaufort Series sandstones and mudstones and contains sediments deposited in a fluvial channel and floodplain environment during the late Carboniferous to the early Triassic. They are derived from previously weathered andesitic and felsic volcanic rocks from the Cape Sequence to the south. The sediments thus incorporate minerals which are resistant to weathering, such as quartz, albite and K-feldspars. These sediments were intruded by dolerite sills and dykes during the Jurassic resulting in severe jointing.

The study area is underlain by the Middleton Formation of this series, a formation exhibiting near horizontal bedding planes (less than 5° dip) dipping gently to the North-East. These beds consist of alternating cycles of fine-grained lithofeldspathic sandstone of variable lateral extent fining upward into mudstone. Sandstone lithosomes are from 1-2 m in thickness and represent 30-40% of the Formation. The composition of these rocks is as follows (Tordiffe 1978): sandstones consist of quartz (19%), feldspars (29%), rock fragments (35%), cement (2%), and a mostly illite matrix (14%); mudstones consist of quartz (15-25%), and a matrix of illite and chlorite. Below the Middleton lie the Koonap and Ecca Formations respectively. The Koonap represents a delta plain deposit of alternating cycles of sandstones and mudstones; a transitional environment from the shallow marine shales of the Ecca formation (Tordiffe 1978).

As these rocks are dense and have undergone severe compaction, groundwater is restricted to joints and the fracture zones adjacent to the dolerite intrusions. Because of semi-confining conditions, water levels represent a piezometric surface rather than a water table. Due to the slight dip of the bedding plane, groundwater flow follows the topography and flows to the south-east. Rest water levels vary between 5 m and 35 m below the surface.

Transmissivities measured in fractured Karoo rocks generally range from 5 to 150 $m^2 day^{-1}$ (Reynders et al. 1985, Kirchner et al. 1991, Hughes and Sami 1993) but can be highly variable due to the presence of fracture zones. Well yields in the catchment range from negligible to 80000 $l h^{-1}$. Storage coefficients range from 0.02 to 0. Groundwater conditions were found to be fairly stagnant as recorded water levels only dropped by approximately 1.5 m in 15 months without a recharge event.

2.5.1 Recharge processes in semi-arid regions

This investigation was initiated as part of a programme to estimate recharge and study the groundwater dynamics of the fractured rock aquifer system of the Bedford catchments. Since long term recharge ultimately controls an aquifer's sustainable yield, mean annual recharge is of great importance. Unfortunately, it is one of the most difficult of all hydrological components to estimate, especially in arid regions, where recharge can be extremely variable in space and time and represents a minor proportion of the overall water balance equation.

Conceptually, groundwater recharge can be divided into four components (Lloyd, 1986):

- Direct or diffuse recharge by infiltration through the soil matrix or preferential pathways;

- Indirect recharge from runoff over jointed outcrops;
- Indirect recharge through runoff ponding;
- Indirect recharge through transmission losses in stream channels.

In arid environments, large storm thresholds are required to overcome high soil moisture deficits and initiate direct recharge. As a result, direct recharge becomes increasingly less significant as aridity increases and it is likely to be a rare event. In regions covered by extensive sand dunes, however, direct recharge is well documented. Indirect recharge occurs following a horizontal redistribution of water at the surface and its concentration in ponds, channels or on outcrops of jointed or fractured rock. It is therefore highly localised in nature and occurs if significant overland runoff is generated, regardless of the existence of a soil moisture deficit. The correct flow mechanisms and source areas must therefore be identified prior to the selection of an appropriate recharge estimation model. Rushton (1987) lists many of the factors which influence recharge pathways.

2.5.2 Recharge estimation in semi-arid regions

Numerous techniques have been developed to quantify recharge, but all are based on constraints or assumptions which limit their range of application in semi-arid areas (Sami, 1991). In general, these techniques can be divided into physical and chemical methods. Physical methods attempt to estimate recharge from: water balances calculated from hydrometeorologic measurements, direct estimates of soil water fluxes based on soil physics, or changes in the aquifer's saturated volume based on water table fluctuations.

Water balances are of limited applicability in semi-arid regions since the recharge component is small in relation to errors in the measurement of evapotranspiration, runoff and precipitation. The accumulation of the error term in the recharge estimate of a water balance has been found to exceed several hundred percent (Gee & Hillel, 1988). Methods relying on the direct measurement of soil water fluxes are problematic because fluxes are low and difficult to detect (Lerner et al. 1990). Furthermore, since such methods assume that flow takes place through a matrix, they ignore localised or indirect recharge from surface ponding, transmission losses or from runoff over jointed rock outcrops. In arid areas, localised recharge is likely to predominate since large storm thresholds are required to overcome the large soil moisture deficits and initiate direct recharge through the soil matrix (Lloyd, 1986). Water table fluctuation measurements require accurate estimates of aquifer parameters to equate changes in saturated volume to recharge, however, these parameters are rarely constant (Sophocleous 1991, Rushton 1987, Johansson, 1987), especially in a fractured rock aquifer.

All these physical methods are prone to error in semi-arid areas because they measure recharge at specific moments and locations and thus rely on spatial and temporal extrapolations to derive values of mean annual recharge. The episodic and highly variable nature of recharge, suggests that long time series of observations are required to obtain realistic estimates of mean annual recharge. In addition, since the distribution of recharge in space is highly variable (Johnston, 1987) and may be restricted to specific areas of a catchment (Knutsson, 1988), especially when localised recharge is considered, it is difficult

to regionalise estimates from site specific measurements (Lerner et al. 1990, Sophocleous, 1992).

For these reasons, chemical recharge estimation methods based on the distribution of a tracer (^{2}H, ^{3}H, ^{14}C, ^{18}O and Cl being the most common), in the saturated or unsaturated zone have several advantages over physical methods in arid regions (Allison, 1987). First, in contrast to spatially variable precipitation, a tracer's concentration represents a spatially uniform input to the soil surface, or in the case of tritium its fallout history is known (Lerner et al. 1990). Second, whereas physical methods only provide data over the duration of the monitoring period, an aquifer or soil can store sufficient water to represent many years of recharge, from which an historical record can be derived (Allison et al. 1985). Third, the accuracy of the recharge estimate does not necessarily decrease as the moisture flux to groundwater decreases (Scanlon, 1991).

Most tracer studies in semi-arid areas have been based on tritium or chloride profiles in the unsaturated zone. Studies using environmental tritium profiles (e.g. Foster and Smith-Carrington 1980, Mazor et al., 1982, Dincer et al., 1974) are based on the depth of migration of the 1964 peak resulting from nuclear fallout (Munnich et al. 1967). However, such studies have been restricted to regions where the soils are deep enough, or recharge small enough, for post 1964 recharge to be contained in the unsaturated zone where flow is vertical (e.g. Solomon and Sudicky, 1991). Where bomb tritium peaks have passed out of the soil, injected tritium profiles have been used (e.g. Chandrasekharan et al. 1988, Sukhija et al., 1988).

Chloride has an advantage over tritium as a tracer since it is not volatile, none is lost by evaporation and it is easier to perform a mass balance. Studies based on unsaturated chloride profiles have assumed that inputs to the soil surface have occurred at a steady state and that chloride is conservative, being concentrated in the soil by evapotranspiration. Some of these studies have assumed that the flux of chloride below the root zone equals the input to the surface (e.g Johnston 1987, Sharma and Hughes 1985, Edmunds et al. 1992), while others have used transient state profiles (Walker et al. 1991, Thorburn et al. 1991). These studies have all calculated the input flux to the soil from the rate of atmospheric accession, hence they assume that all precipitation enters the soil. As the effect of any lateral redistribution on input fluxes is ignored, this method cannot be used where significant overland flow occurs.

As studies based on unsaturated zone profiles determine recharge rates from concentrations in soil water below the depth of the zero-flux plane, they are also restricted to areas where deep unconsolidated sediments extend below the root zone. Furthermore, since these methods can only provide point estimates of recharge through the soil matrix, they of limited value in regions where significant indirect recharge occurs. In South Africa, deep unconsolidated deposits are rarely encountered, except for those of limited lateral extent. In addition, very little flow percolates through the matrix to any significant depth in Karoo soils, even with exceptionally high rainfall (Inst. for Water Research, unpubl. data, Van Tonder and Kirchner 1990), implying that aquifers are recharged by indirect flowpaths. This situation suggests alternative methods are required in such environments.

The use of tracers in the saturated zone to quantitatively evaluate recharge has recieved

limited attention (Erriksson and Khunakasem 1969, Adar et al., 1988). Since long term average inputs are areally integrated in the saturated zone, such an approach would alleviate complexities resulting from diverse recharge pathways and spatial variability. As variations in geochemistry are more distinct in semi-arid areas than humid areas (Fontes and Edwards, 1989), especially in fractured rock aquifers where lateral mixing is restricted, geochemical variations resulting from variations in recharge may be used to estimate the distribution of recharge. This section presents such an attempt to trace the origin of chloride in an aquifer and estimate lateral and vertical groundwater flow rates from its distribution on a sub-area scale.

2.5.3 Recharge mechanisms and geochemical processes in the Bedford catchments.

More than 50% of South Africa is underlain by the sedimentary sandstones, mudstones and shales of the Karoo Sequence. In the eastern Cape Province, the greater part of the surface area is underlain by the fractured rocks of the Beaufort Series of this Sequence. This geological region is characterized by a semi-arid environment where annual rainfall is highly variable with a seasonal distribution that favours autumn and spring. As evaporation exceeds precipitation throughout most of the year, leaching is limited and soluble salts tend to accumulate near the soil surface. Runoff and percolation periodically flush these salts into streams and groundwater following large rain events. It has been suggested that connate marine water from the Ecca Series shales below may also contribute to groundwater salinity in the lower Formations of the Beaufort system by a process of upward filtration (Tordiffe 1978, 1981). However, no study has previously been undertaken to verify this hypothesis.

Relationships between the isotopic composition of groundwater and recharge processes.

The stable isotopes ^{18}O and ^{2}H are naturally occurring and form a constituent part of water molecules. Their concentration in water is usually expressed in parts per million (o/oo) difference relative to the Standard Mean Ocean Water (SMOW) (Craig, 1961). Since they are chemically conservative in the liquid phase when temperatures are below 60-80 °C (Issar and Gat, 1981), their concentrations are not affected by the geological setting. Once below the water table, the water's isotopic signature persists until it mixes with isotopically different waters. This signature reflects the water's history and origin prior to percolation, hence it can be used to interpret the mechanisms by which recharge occurs.

Although the isotopic content of precipitation is extremely variable, Craig (1961) found that precipitation that has not undergone significant evaporation shows a specific relationship between ^{18}O and ^{2}H so that $^{2}H = 8*^{18}O + d$. The variable d is termed the deuterium excess and has a value of 10 on a global basis. However, this value can vary locally, primarily as a function of humidity over the vapour source region (Merlivat and Jouzel, 1979). In general, it has been found that ^{18}O and ^{2}H concentrations in precipitation are temperature dependent and that their mean annual concentrations are directly related to the mean annual temperature (Dansgaard, 1964). Rain falling at cooler and higher elevations is therefore more isotopically depleted than that at warmer or lower elevations. This temperature dependence has been used to identify paleo-groundwaters recharged during a cooler period (e.g. Gat and Issar, 1974), groundwaters recharged from distant mountain drainage (e.g. Vogel et al., 1972) and the seasonality of recharge in temperate regions (e.g. Brinkmann et al., 1963).

Vogel (1963) found that the groundwater in semi-arid areas contained less heavy isotopes than the weighted mean annual precipitation but that it corresponded to the isotopic composition of exceptionally heavy downpours. This isotopic depletion in large rain events is due to the preferential fallout of heavy isotopes, which results in small rain events being more isotopically enriched than larger rain events (Levin et al. 1980). This effect is heightened by the enrichment of heavy isotopes which occurs by evaporative water loss from water droplets during smaller rain events (Levin et al., 1980). This evaporation process, however, alters the ^{18}O-^{2}H relationship of the rainfall.

When water evaporates from a surface water body or saturated soils, an enrichment of both ^{18}O and ^{2}H occurs in the residual liquid, although kinetic isotope fractionation results in a greater relative enrichment of ^{18}O than ^{2}H (Barnes and Allison, 1988). The relationship between ^{2}H and ^{18}O in the residual liquid consequently changes, exhibiting a slope of between 4 and 6 regardless of the original isotopic content (Payne, 1988). When evaporation occurs from an unsaturated profile the degree of kinetic fractionation increases; slopes of between 2-5 in the ^{18}O-^{2}H relationship have been recorded near the soil surface by Allison et al. (1984), with the lowest slopes generally produced by the driest soils. Because of this shift in the isotopic relationship, it is possible to identify whether recharging water has undergone significant evaporation in a riverbed, pan or soil profile prior to infiltration (e.g. Issar et al., 1984).

Relationships between the chemical composition of groundwater and solute sources.

Saline conditions in a sedimentary aquifer can originate from one or more of the following mechanisms:

- The intrusion of marine water from the sea.
- The mixing of meteoric water with connate water trapped during the deposition of sediments in a marine environment.
- The concentration of dissolved salts by evaporation or transpiration near the soil surface during slow diffuse recharge.
- The leaching of evaporitic salt deposits by water percolating rapidly through preferential pathways.
- The chemical weathering of the aquifer.

Each of these mechanisms will have a distinct effect on some of the geochemical and isotopic relationships of the groundwater. If the mixing of meteoric water with recent or connate marine water is the primary cause of salinity, then variations in the salinity of the aquifer are expected as a result of variations in the degree of mixing. The ^{18}O versus either deuterium or chloride values of groundwater should then be positively correlated and plot on a mixing line between seawater and the least saline groundwater (Payne, 1988).

If salinity is primarily due to the concentration of dissolved salts by evaporation, then the ^{18}O-^{2}H relationship will have a low slope reflecting kinetic fractionation. In addition, a plot of

chloride per mass of solution against either isotope will be positively correlated, since increased evaporation would result in isotopic enrichment as well as an increased chloride concentration (Payne, 1988). If transpiration is the predominant concentration mechanism, then the ^{18}O-^{2}H signature will have a slope similar to the regional rainfall, since transpiration results in no significant fractionation (Allison et al., 1984). The chloride versus isotope relationship would then define a line with a steep slope, since there would be little variation in isotopic content with increasing salinity. If waters with different chemical and isotopic signatures exist concurrently, lateral mixing of waters may obscure these chloride-isotope relationships. In this case poor correlations would be observed.

If salinity is due to the leaching of evaporitic salts by rapid percolation through preferential pathways, then the groundwater should retain an ^{18}O-^{2}H relationship similar to that of the regional rainfall. Since the leaching process does not affect the isotopic composition of water (Payne, 1988), there would be no correlation between either isotope and chloride.

Finally, if chemical weathering is the primary source of dissolved salts, then the anion and cation concentrations of specific salts should be strongly correlated, with increasing concentrations along the regional flowpath (Rosenthal, 1987). Furthermore, if marine connate salts and halite deposits can be geologically excluded so that chloride is solely of meteoric origin, the abundance of chloride compared to other ions can be used as an index of the relative contribution of meteoric salts to those resulting from mineral weathering.

Data collection and analysis.

Groundwater samples were collected from actively pumping windmills over a period of 18 months. Twenty-seven boreholes in the western half of the catchment were sampled intensively on a monthly basis. Using a borehole sampler and a submersible pump, it was determined that no vertical stratification exists. Other boreholes, including those in the eastern half, were only sampled once in order to detect regional patterns or chemical evolution along flowpaths. No regional pattern could be identified and large variations in salinity were encountered over distances of only several hundred meters. During the study period there was only one recharge event, however, this had little effect on groundwater chemistry. Unfortunately, only one flood water sample was collected for isotopic analysis following this event, and it was only obtained after several days had elapsed. The sample was therefore subject to evaporation prior to collection.

All groundwater samples were analyzed for chemical composition, using atomic absorbtion for cations and titrations for Cl and total alkalinity. The SO_4 concentration was estimated from a cation-anion milli-equivalent balance. Selected samples were analyzed for ^{18}O and ^{2}H by the Council for Scientific and Industrial Research (CSIR) in Pretoria. Results from the chemical analyses are reported in millimoles/litre and isotopic composition is given relative to SMOW. The regional South African meteoric relationship between ^{18}O and ^{2}H was established from the regression of rainfall data collected at De Aar and Dewetsdorp by the Institute for Groundwater Research of the University of the Orange Free State (Kirchner et al., 1991).

Isotopic data

The results of the isotopic and chemical analyses are shown in tables 2.7 and 2.8. The pH of groundwater ranged between 7 and 8.3, therefore, essentially all the dissolved carbonate and all of the alkalinity is in the form of HCO_3 (Drever 1982). The ^{18}O-^{2}H relationships are shown in figure 2.8. The regional relationship of ^{18}O-^{2}H in rainwater was calculated as $^{2}H = 7.45*^{18}O + 12.14$. This relationship differs slightly from the World Mean Meteoric Line of $^{2}H = 8 * ^{18}O + 10$. The groundwater ^{18}O-^{2}H is relationship is defined by a line where $^{2}H = 5.43*^{18}O - 4.79$, with a standard error of the y intercept equal to 1.57.

The ^{18}O-^{2}H relationship of groundwater does not fall on a mixing line with seawater, since the y intercept of the relationship does not intersect the composition of seawater within two standard errors. Furthermore, the correlation coefficient between ^{18}O and chloride is not significant (table 2.9). Increases in chloride concentration are, therefore, not correlated with a corresponding isotopic enrichment resulting from mixing with marine water. The presence of chloride is thus attributed to meteoric accumulation.

As the isotopic relationship of groundwater is displaced from that of meteoric water and plots along a line with a slope of 5.43, variable evaporative enrichment has occurred. This suggests that water is retained on or near the soil surface prior to deep percolation. In spite of this evaporative enrichment, no relationship can be observed between isotopic enrichment and increasing salinity in the chloride versus ^{18}O plot (figure 2.9). It is unlikely that this correlation could have been lost due to mixing with waters with a different isotopic relationship, since the fractured nature of the aquifer and the stagnant flow conditions preclude significant mixing. The constraints on mixing between waters in discrete fracture zones are reflected in the highly variable geochemical and isotopic conditions which exist in the groundwater. The poor correlation between ^{18}O and chloride (table 2.9) therefore suggests that the concentration of salts by evaporation is not the only significant salinization mechanism.

The approximate mean isotopic concentration of the rainwater from which the groundwater was derived can be reconstructed by projecting the groundwater relationship back to the meteoric line (figure 2.9). Such a projection suggests that the mean ^{18}O of rain events resulting in recharge is about -8 SMOW. The flood water sample generated by the only event resulting in any recharge, although somewhat enriched by evaporation, substantiates this prediction. An ^{18}O concentration of -8 SMOW corresponds to some of the most isotopically depleted rain events (figure 2.9). As these rain events tend to be those which have originated from oceanic evaporation (Turner et al. 1987, Vogel and Van Urk 1975), the largest events in the region, this suggests that recharge is limited to inputs from rain events which exceed a minimum threshold. Consequently, water inputs from events below this threshold are completely lost by evapotranspiration. The meteoric salt load from such events must therefore be precipitated out of solution at or near the soil surface.

A mechanism whereby these accumulated surficial salts are episodically redissolved and leached into the groundwater by large isotopically depleted rain events is suggested as a probable salinization mechanism. As the concentration of salts mobilised by leaching is not related to the water's isotopic composition, such a process can account for the poor correlation between observed isotope and chloride concentrations (table 2.9).

Table 2.7 Results of chemical analyses expressed in millimoles l^{-1}.

SITE	N	Cl	HCO3	SO4	Ca	Mg	Na	K
BAG04	4	3.64	3.40	0.72	0.88	0.97	4.62	0.17
HHG01	1	5.00	9.30	-0.01	1.52	1.97	7.22	0.05
BAG12	5	5.01	5.89	0.95	1.63	1.76	5.24	0.79
PHG01	1	5.49	5.60	0.19	0.82	1.32	7.05	0.15
PHG02	1	5.59	4.70	1.48	1.67	2.06	5.70	0.10
BBG27	6	5.71	5.68	0.88	1.26	1.53	7.03	0.53
DDG01	1	5.74	6.40	0.93	1.67	2.02	5.79	0.85
BBG24	6	5.77	9.55	0.68	2.09	1.93	8.58	0.07
BBG09	5	5.79	6.35	0.58	1.73	1.63	6.31	0.28
BCG09	1	5.90	5.00	0.73	1.82	1.65	5.35	0.08
BRG01	4	6.23	8.53	0.81	1.86	1.90	8.28	0.58
BAG14	5	6.56	6.60	0.60	1.58	1.46	8.10	0.19
BCG05	1	6.69	8.00	0.22	2.12	1.89	7.09	0.01
BBG02	12	6.93	7.53	1.18	1.83	1.58	9.93	0.09
GWG04	1	6.97	6.60	1.19	1.85	2.43	6.96	0.45
BBG22	3	7.32	7.10	0.71	1.69	1.44	9.47	0.10
BBG07	7	7.33	7.24	1.38	1.86	1.96	9.36	0.32
BBG03	17	7.36	7.00	0.36	1.52	1.34	9.25	0.11
BAG06	3	7.67	7.23	0.71	1.63	1.76	9.40	0.16
BBG14	1	7.81	3.50	1.05	1.32	1.73	7.00	0.31
BBG13	1	7.87	3.76	0.62	0.95	1.69	7.22	0.38
BRG06	1	7.98	7.70	1.17	2.42	2.51	8.05	0.11
BAG08	5	8.33	7.32	0.56	1.73	2.11	8.88	0.20
BCG07	8	8.40	8.14	-0.27	2.30	2.03	7.23	0.10
BCG08	1	9.39	8.00	-0.32	2.47	2.22	7.35	0.01
BRG02	2	9.49	8.50	-0.05	2.26	2.27	8.72	0.13
EFG07	1	9.51	7.20	-0.09	1.52	2.76	7.83	0.14
BAG05	5	9.61	7.18	0.65	1.62	1.69	11.27	0.21
MKG03	1	9.70	5.90	0.46	1.87	1.56	9.53	0.13
BCG01	13	9.78	7.60	0.41	2.46	2.11	8.95	0.12
BAG07	6	9.93	7.07	0.92	1.93	1.79	11.17	0.21
BBG10	1	10.49	6.00	0.99	2.02	2.10	9.92	0.31
BBG08	4	10.49	7.93	0.89	2.40	2.56	10.17	0.12
OFG15	1	10.59	7.80	-0.01	1.45	2.59	9.92	0.37

SITE	N	Cl	HCO3	SO4	Ca	Mg	Na	K
VFG01	1	10.69	7.90	0.33	2.22	2.67	9.14	0.33
BBG12	1	10.75	6.50	0.73	2.02	2.14	10.09	0.31
BAG03	7	11.15	9.96	0.66	2.43	2.75	11.68	0.38
BCG03	22	11.64	7.68	0.35	2.79	2.70	8.95	0.09
BBG05	23	11.71	7.04	0.72	2.29	2.39	10.51	0.31
BRG05	4	11.75	8.30	1.12	2.63	2.87	11.05	0.25
BAG13	5	11.80	7.72	0.85	2.43	2.51	10.92	0.43
BAG09	3	11.83	5.80	0.94	2.19	1.71	11.60	0.11
OFG13	1	11.87	6.50	1.03	2.05	2.43	11.01	0.49
BBG23	8	11.89	8.24	1.23	3.09	3.03	10.25	0.10
BAG02	1	11.99	10.00	0.83	3.42	2.76	11.18	0.12
BBG04	21	12.06	8.46	0.66	2.70	2.85	10.62	0.13
BCG02	11	12.07	7.22	0.21	2.17	1.71	11.83	0.12
MKG04	1	12.07	7.60	0.84	2.82	2.39	10.79	0.16
BBG11	1	12.30	6.50	0.55	2.15	2.26	10.74	0.33
BFG02	2	12.86	8.00	1.25	2.62	3.04	11.70	0.34
BBG26	5	13.06	8.54	1.29	2.97	3.03	12.06	0.12
HHG05	1	13.94	6.90	1.29	2.77	3.46	10.79	0.19
BCG06	1	14.36	7.00	0.98	2.64	3.00	12.01	0.01
BBG17	2	14.73	6.15	1.23	2.22	2.51	13.42	0.45
BAG10	6	15.16	7.90	1.01	3.39	3.06	12.01	0.17
BRG07	3	15.41	6.97	0.54	2.94	2.96	11.28	0.38
BBG01	20	16.06	6.29	0.93	2.72	2.64	13.15	0.33
BBG19	1	16.45	5.00	0.32	2.17	2.51	12.40	0.33
BBG06	6	17.43	7.26	1.71	3.53	3.91	12.96	0.28
MKG05	1	17.49	6.50	1.12	3.57	3.17	12.57	0.19
MKG01	1	17.98	8.00	0.53	3.62	3.58	12.48	0.17
BBG16	3	18.12	5.83	0.78	2.05	2.59	15.83	0.39
BBG21	19	18.20	9.00	3.86	4.97	5.17	12.93	1.71
BRG03	1	18.48	7.90	0.41	4.02	3.66	11.66	0.19
BFG01	2	18.77	8.90	0.60	2.20	3.54	17.05	0.35
BAG01	19	18.96	9.76	1.20	2.89	3.67	17.82	0.19
BBG18	1	19.18	7.00	1.41	2.45	3.04	17.66	0.36
BBG25	7	19.54	5.75	0.84	2.83	2.87	15.36	0.22
BBG20	21	20.23	6.37	0.76	4.20	3.85	11.71	0.31
BBG15	1	21.83	7.50	0.95	2.87	3.00	19.18	0.31

Table 2.8 Results of isotopic analyses expressed relative to SMOW.

SITE	^{18}O	^{2}H
BAG01	-3.6	-24
BAG06	-3.9	-26
BAG08	-4.0	-28
BAG09	-4.6	-29
BAG12	-3.7	-26
BAG13	-2.7	-22
BAG14	-4.0	-28
BBG01	-4.1	-26
BBG03	-3.9	-25
BBG04	-4.1	-25
BBG05	-3.3	-21
BBG16	-4.7	-32
BBG20	-2.8	-18
BBG21	-3.9	-25
BBG23	-4.3	-29
BBG27	-4.0	-27
BCG02	-4.5	-27
BCG03	-4.1	-29
Runoff	-8.8	-57

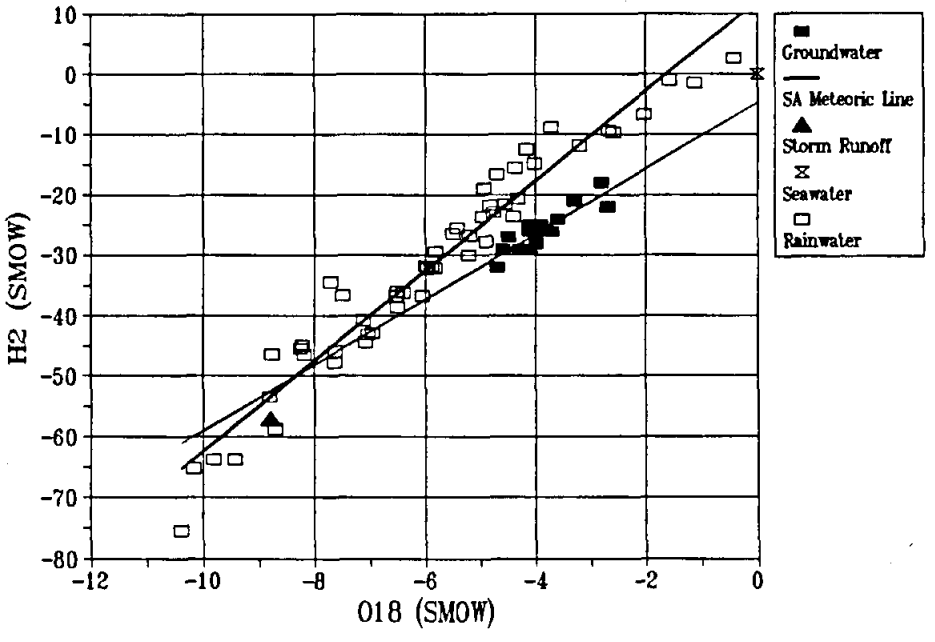

Figure 2.9 ^{18}O and ^{2}H relationships in groundwater, precipitation and storm runoff (the lighter line represents a regression through the groundwater data points).

Table 2.9 Correlation coefficients between chemical relationships in groundwater. Results shown in bold and underlined are significant at the 0.01 level, while those in bold only are significant at the 0.5 level.

	^{2}H	Cl	T.A.	Ca	Mg	Na	K
^{18}O	**0.89**	0.12	0.17	0.26	0.27	-0.08	0.16
^{2}H		0.26	0.20	0.39	0.34	0.04	0.14
Cl			0.35	**0.78**	**0.80**	**0.87**	0.21
T.A.				**0.51**	**0.61**	0.41	0.14
Ca					**0.94**	0.47	**0.50**
Mg						**0.56**	**0.56**
Na							0.02

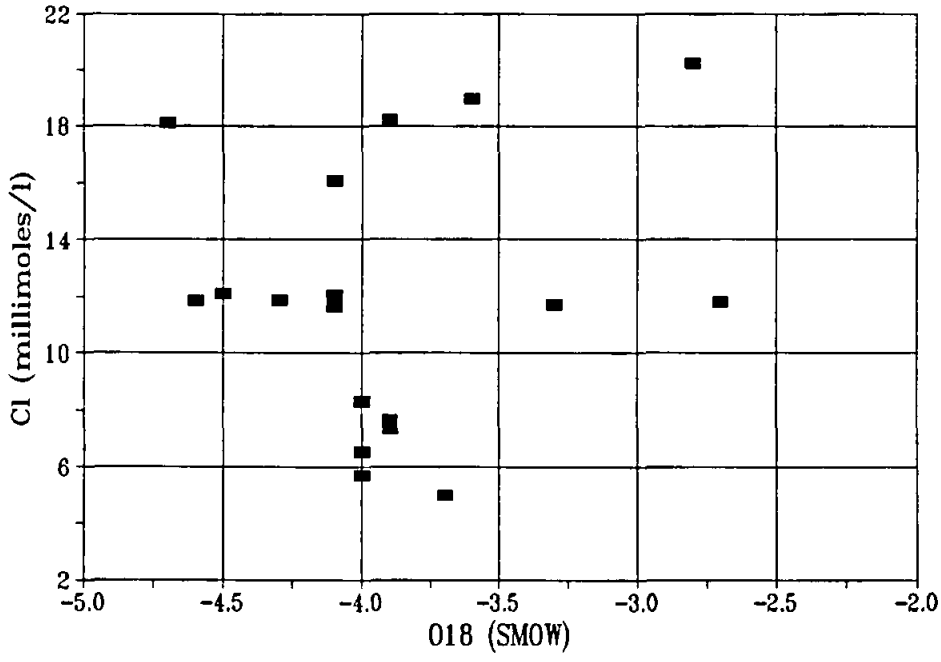

Figure 2.10 ^{18}O and chloride relationships in groundwater.

The leaching of salts by widespread diffuse recharge is unlikely to be due to low infiltration rates and frequent generation of overland flow. Indirect recharge from transmission losses or surface depressions, where concurrent evaporative losses lead to the isotopic enrichment of the leachate and the further concentration of mobilised salts, is the postulated recharge mechanism. Variations in salinity can be attributed a number of inter-related factors: spatial variations in surficial salt deposits resulting from their redistribution by overland flow; in recharge rates or the volume of water diluting mobilised salts; in the degree of evaporative or transpirative concentration to which percolating water has been subjected.

Geochemistry.

The groundwater was found to be predominantly of the Na-Cl type. This is attributed to the preferential leaching of highly soluble NaCl, which is completely dissolved during resolution. Less soluble salts, such as calcite and gypsum, may only be partially dissolved, depending on the volume of infiltrating water and its contact time with surficial salts. Subsequent evaporative concentration may also cause less soluble salts to precipitate out of solution. As a result, percolating water is enriched with highly soluble NaCl but has lost those salts that precipitate as less soluble compounds (Drever and Smith 1978). Groundwater molar ratios were studied to elucidate whether any subsequent evolution of water chemistry occurs.

mNa/mCl: This ratio ranges from 1.49 to 0.58 (figure 2.10), generally decreasing with increasing salinity. This trend shows that groundwater is not evolving towards an equilibrium reflecting inputs of oceanic water or halite dissolution, which would produce equilibrium ratios of 0.86 and 1.0 respectively. Ratios in excess of 1.0 at low salinities imply that meteoric NaCl is not the only source of Na. Albite weathering may be occurring in the sandstone, releasing Na, HCO_3 and montmorillonite according to the weathering reaction:

$$2.33NaAlSi_3O_8 + 8.64H_2O + 2CO_2 = Na_{0.33}Al_{2.33}Si_{3.67}O_{10}(OH)_2 + 2Na + 2HCO_3 + 3.32H_4SiO_4 \quad \text{Eq. 2.5.1}$$

Alternatively, increased Na concentrations at low salinities can be attributed to cation exchange processes in the aquifer matrix. Clay particles in the matrix may be adsorbing dissolved Ca and Mg in exchange for bound Na. Ca and Mg in solution would therefore have to be depleted relative to HCO_3. All possible lithologic sources of Ca and Mg result in Ca + Mg/HCO_3 ratios of 0.5 (discussed below), however, figure 2.11 shows that at low salinities, Ca + Mg/HCO_3 ratios are less than 0.5. The low Ca + Mg/HCO_3 ratios could be the result of either Ca and Mg depletion by cation exchange or HCO_3 enrichment.

With increasing salinity the Na/Cl ratio declines, which suggests that cation exchange processes adsorb Na in exchange for bound Ca and Mg, thereby depleting Na while enriching the Ca and Mg concentrations in solution with respect to HCO_3 (figure 2.11).

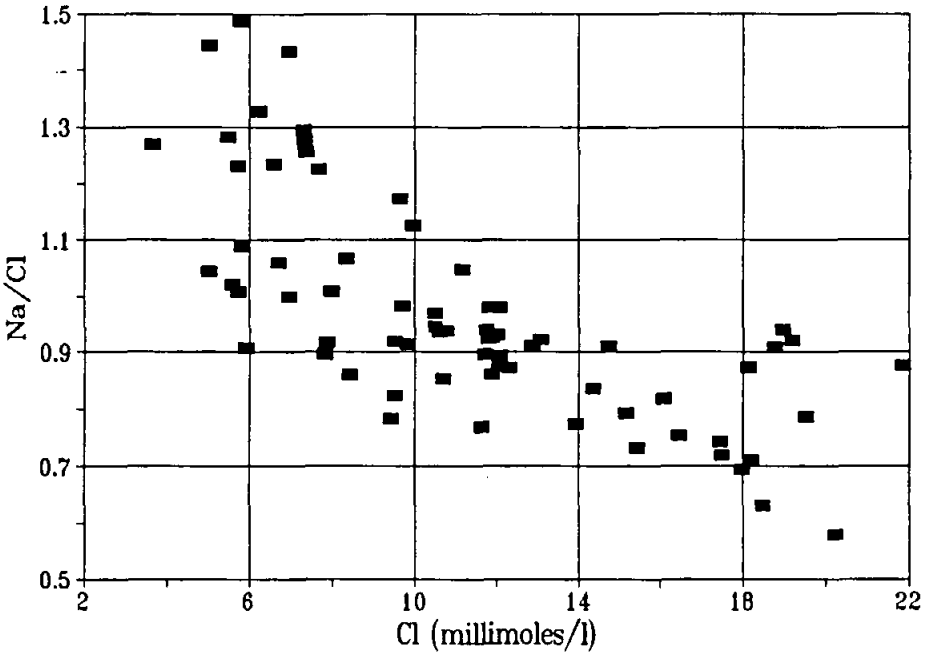

Figure 2.11 The relationship between the Na/Cl ratio and increasing salinity.

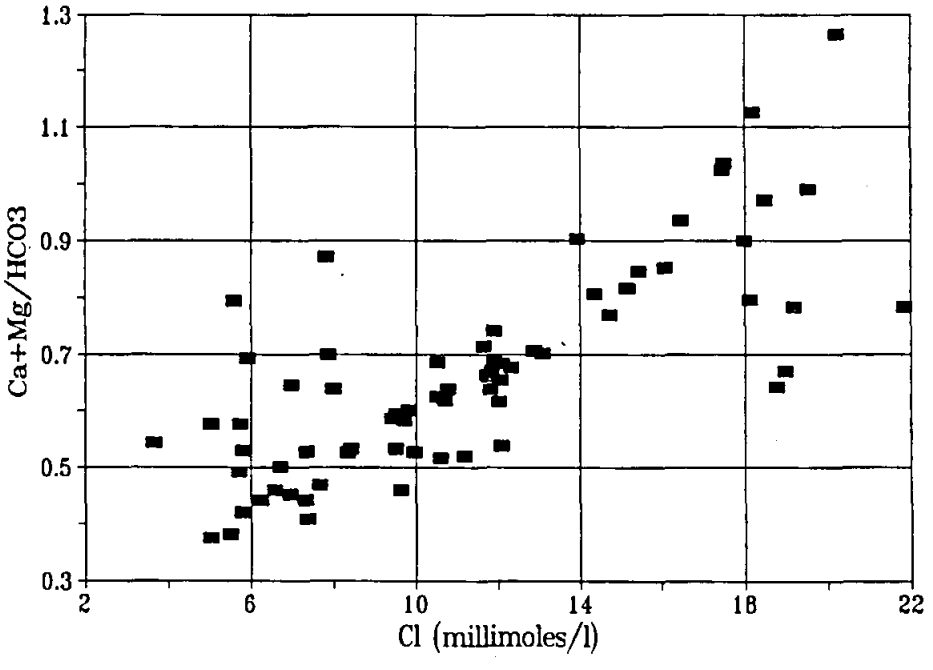

Figure 2.12 The relationship between the Ca+Mg/HCO_3 ratio and increasing salinity.

mMg/mCa: Figure 2.12 shows that this ratio varies between 1.81 and 0.78 over a wide range of salinities. As this ratio remains relatively uniform with increasing salinity, and as both ions are significantly correlated (table 2.9), Ca is not being depleted by $CaCO_3$ precipitation. As both ions are also significantly correlated to Cl, both Ca and Mg concentrations are increasing with salinity. This is attributed to the increased cation exchange of Na for bound Ca and Mg as salinity increases.

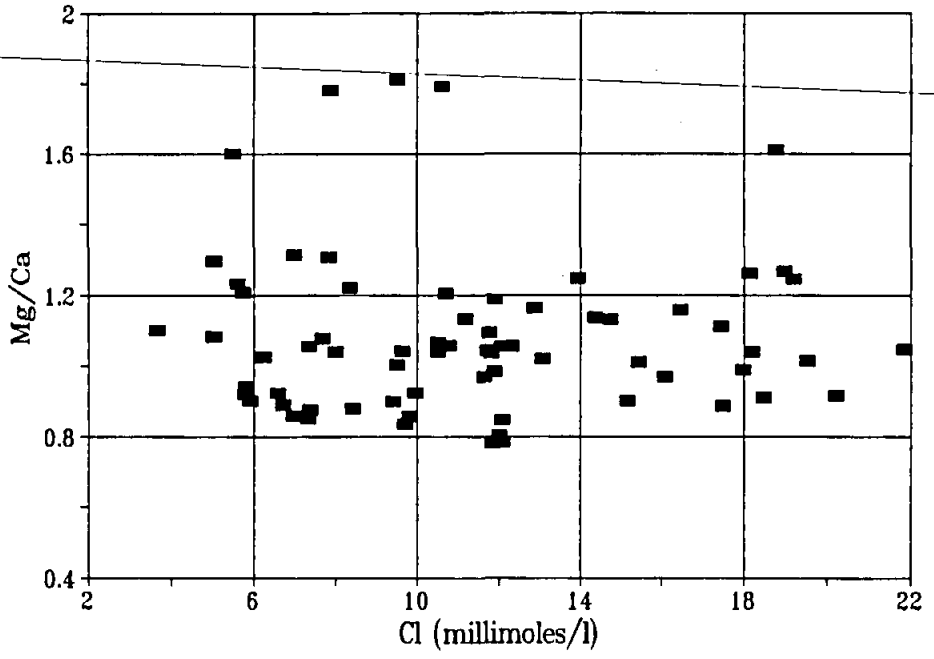

Figure 2.13 The relationship between the Mg/Ca ratio and increasing salinity.

mMg+mCa/mHCO$_3$: The sources of Ca and Mg in groundwater can be deduced from this ratio. As the ratio increases with salinity (figure 2.11), Mg and Ca are being added to solution at a greater rate than HCO_3. If Mg and Ca originate from the dissolution of carbonates in the aquifer cement or from the weathering of accessory pyroxene or amphibole minerals, this ratio would be about 0.5, since the governing weathering equations would be: for calcite:

$$CaCO_3 + H_2O + CO_2 = Ca + 2HCO_3 \quad \text{Eq. 2.5.2}$$

for pyroxene:

$$CaMg(Si_2O_6) + 4CO_2 + 6H_2O = Ca + Mg + 4HCO^3 + 2Si(OH)_4 \quad \text{Eq. 2.5.3}$$

for amphiboles:

$$Ca_2Mg_5Si_8O_{22}(OH)_2 + 14CO_2 + 22H_2O = 2Ca + 5Mg + 14HCO_3 + 8Si(OH)_4 \quad \text{Eq. 2.5.4}$$

High ratios cannot be attributed to HCO_3 depletion as, under the existing alkaline conditions, HCO_3 does not form carbonic acid (H_2CO_3) (Spears 1986). High ratios therefore indicate alternate sources of Ca and Mg, such as cation exchange or some meteoric contribution, such as gypsum.

Ca+Mg-SO_4/Na-Cl: This relationship provides information pertaining to the geologic sources of Ca and Mg in the aquifer. To account for meteoric Ca from the dissolution of evaporitic gypsum ($CaSO_4$), an amount of Ca equal to the concentration of SO_4 is subtracted from Ca and Mg totals. Assuming that all Na inputs are from NaCl, subtracting Cl from Na accounts for meteoric Na and provides a minimum value of Na depletion due to cation exchange. As clay particles adsorb 2Na to release one Ca or Mg ion, a 2:1 line shows how much Ca and Mg is contributed from cation exchange processes (figure 2.13). As observed Ca and Mg concentrations plot above the 2:1 line, cation exchange processes alone cannot account for the observed values. Therefore, weathering is also a prominent source of Ca and Mg ions.

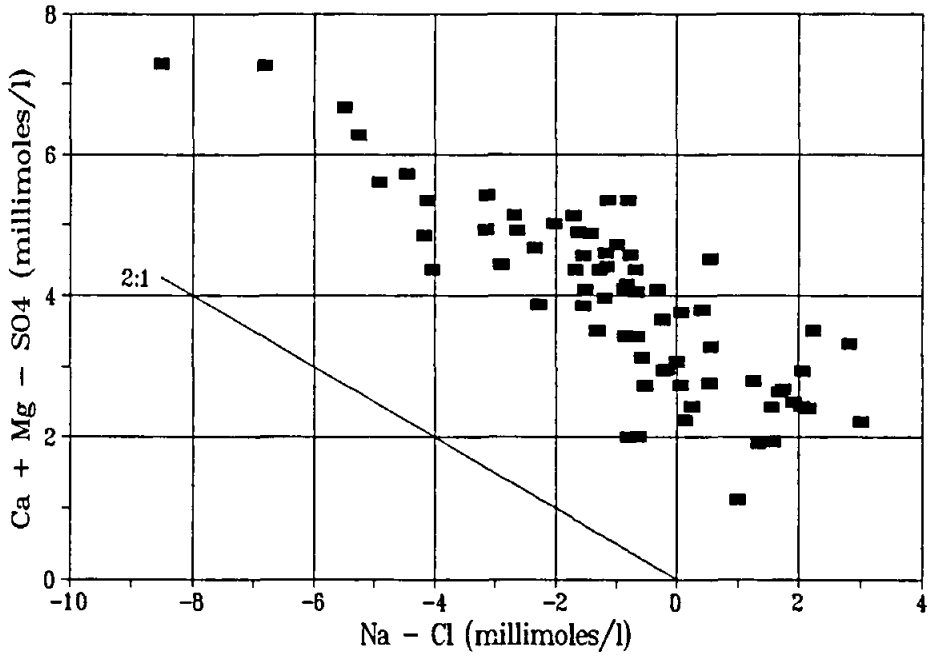

Figure 2.14 The relationship between geologic Ca+Mg and Na depletion.

m(Ca+Mg-SO_4+0.5*(Na-Cl))/mHCO_3: This ratio examines the relationship between the calculated lithologic Ca and Mg component and HCO_3 by adding or subtracting Ca and Mg originating from cation exchange (0.5*(Na-Cl)) from Ca and Mg of lithologic origin (Ca+Mg-SO_4). Figure 2.14 shows that the lithologic Ca+Mg/HCO_3 ratio is less than 0.5. Since weathering reactions of Ca and Mg produce HCO_3 in a ratio of 1:2, there is an accessory source of HCO_3. This indicates that some albite weathering may be occurring (eq. 2.5.1).

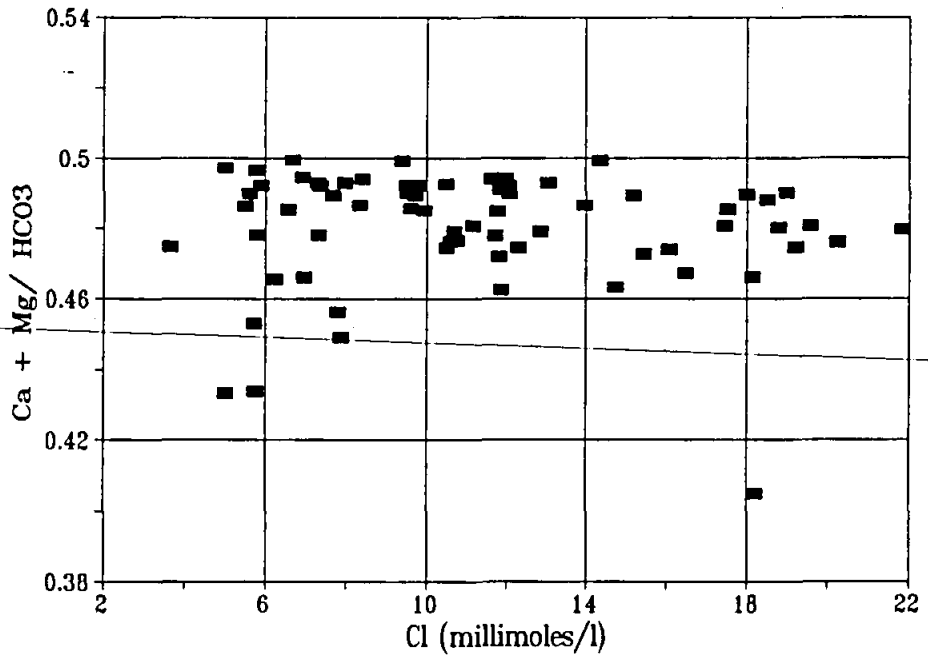

Figure 2.15 The relationship between Ca+Mg/HCO_3 and salinity.

It is possible to quantify dissolution rates in the aquifer from ionic concentrations which cannot be attributed to meteoric or cation exchange sources. Figure 2.15 shows Ca and Mg concentrations contributed by the dissolution of minerals according to equations 2, 3 and 4. These results show that weathering reactions contribute between 2.5 and 4.5 millimoles l^{-1} of Ca and Mg. At low salinities this represents greater than 60% of the total Ca and Mg, however, the relative contribution of mineral weathering drops as cation exchange increases with increasing salinity (figure 2.16). Albite weathering (eq. 2.5.1), calculated as being equivalent to the HCO_3 concentration surplus to Ca and Mg, contributes less than 0.4 millimoles l^{-1} of Na (figure 2.17), less than 5% of the total Na (figure 2.18). The main source of Na is from meteoric NaCl. At concentrations below 10 millimoles l^{-1} of Cl, however, cation exchange is also a significant source of Na ions.

The predominance of meteoric NaCl in the geochemistry is demonstrated by figure 2.19. In comparison, meteoric Ca and Mg salts are a relatively minor constituent due to their lower solubility. Chemical weathering contributes relatively little (approximately 4 millimoles l^{-1}) to the subsequent evolution of groundwater. In addition, since lithologic contributions are relatively constant with increasing salinity, all the samples may have a similar geologic residence time. Salinity increases, therefore, do not reflect increased residence times along a flow path. Instead, they probably reflect variable degrees of leaching of surficial salts.

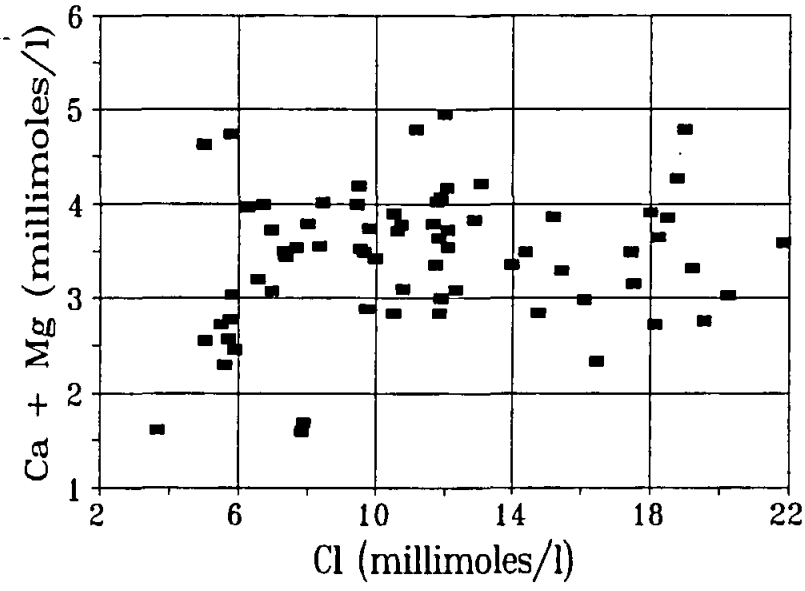

Figure 2.16 Ca+Mg concentrations derived from mineral weathering.

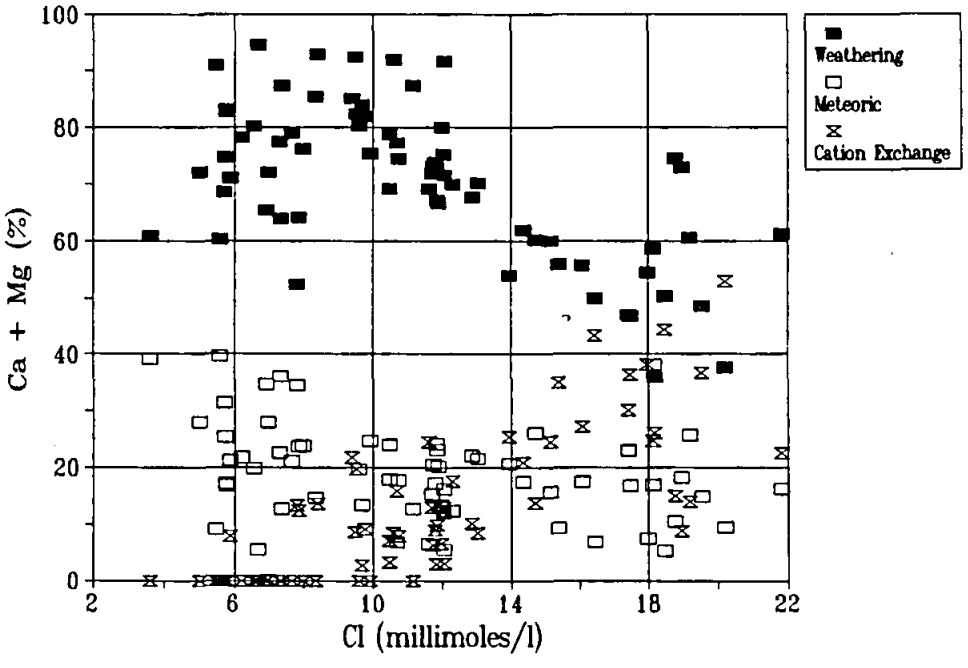

Figure 2.17 Sources of Ca+Mg as a percentage of total concentrations.

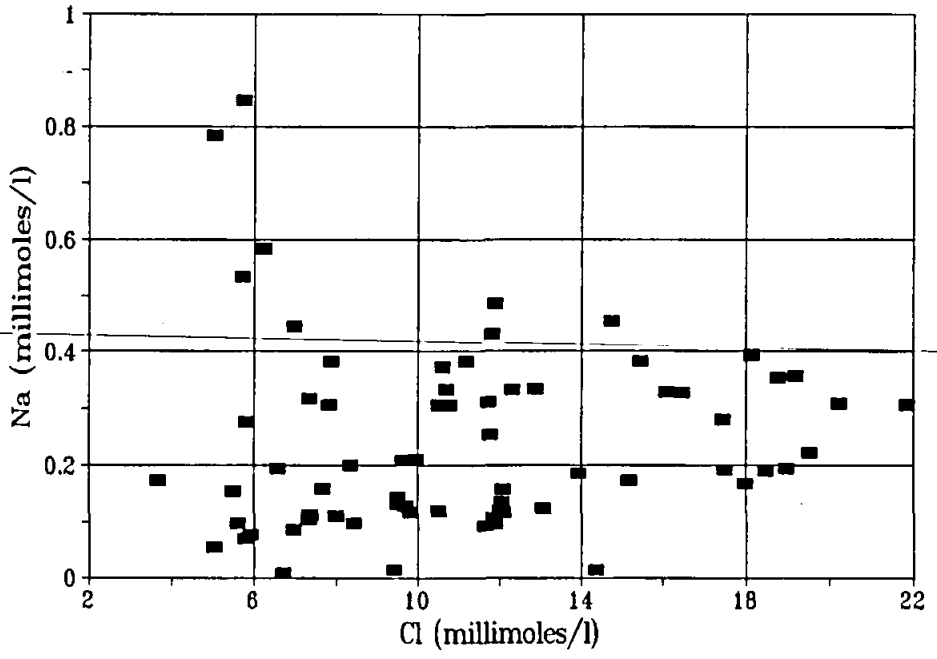

Figure 2.18 Na concentrations derived from mineral weathering.

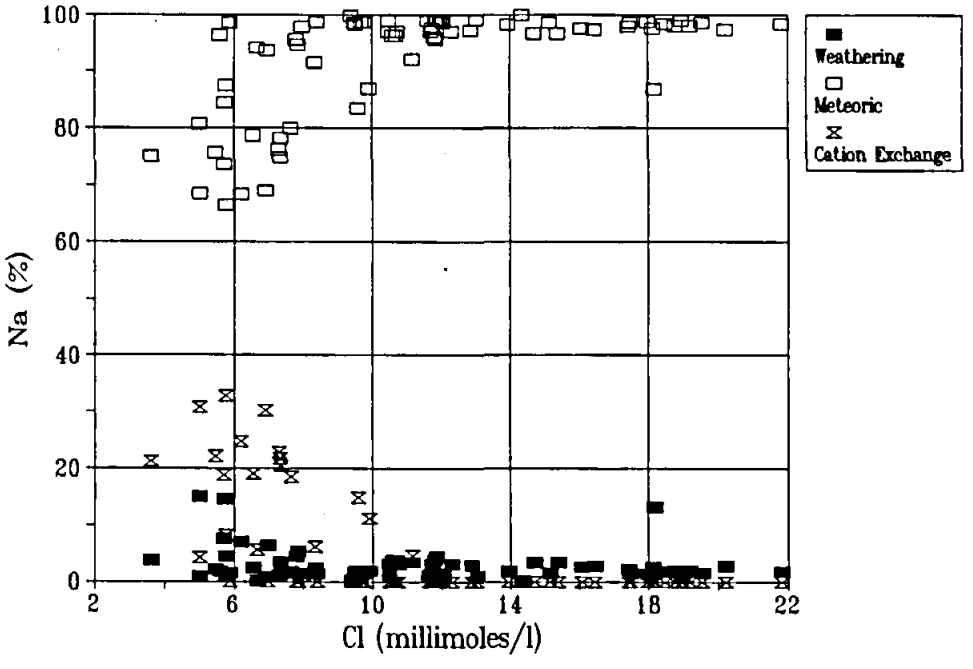

Figure 2.19 Sources of Na as a percentage of total concentration.

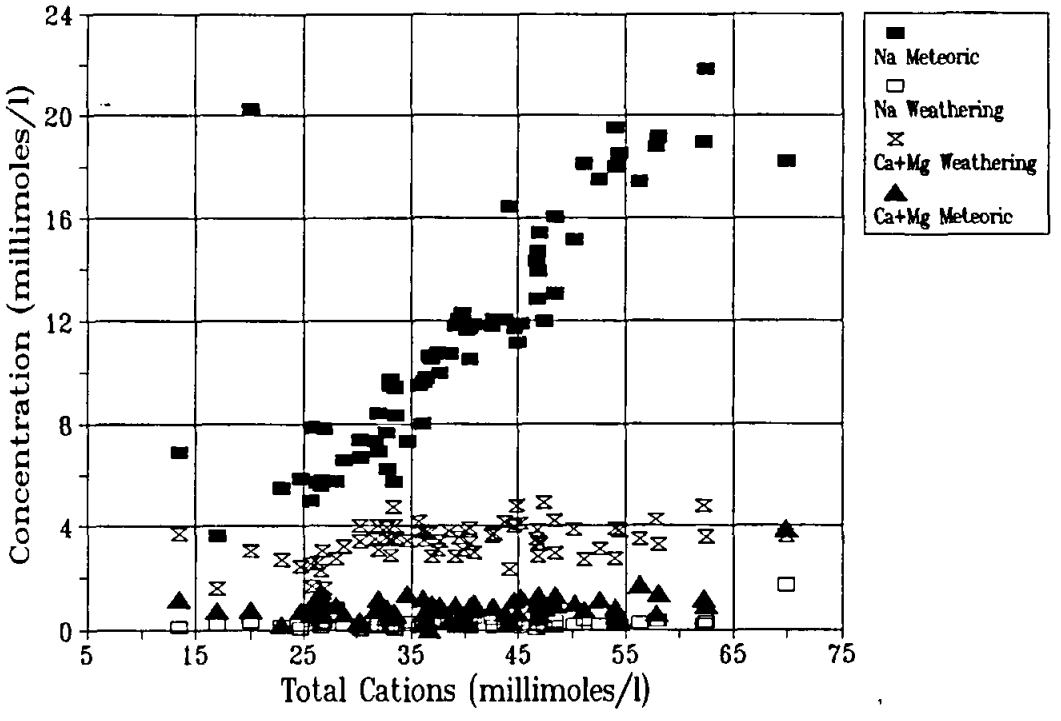

Figure 2.20 Source of dissolved cations with increasing salinity.

Conclusions

Environmental isotope techniques and geochemical data were utilized to gain an understanding of recharge mechanisms and the geochemical evolution of groundwater in an aquifer of variable salinity. The main points concluded are:

- Mixing with connate marine water does not contribute to saline conditions as the groundwater isotopic and chemical relationships do not fall on a mixing line with seawater.

- The isotopic enrichment of water by evaporation implies that an evaporative enrichment of solutes occurs at or near the soil surface prior to percolation. Rapid infiltration through preferential pathways is therefore not prevalent.

- Meteoric salts precipitate and accumulate at the surface following rain events which are completely absorbed by evapotranspiration losses. Infrequent large events subsequently dissolve these salts and leach them into the groundwater. NaCl is preferentially leached due to its high solubility, resulting in Na-Cl type groundwater.

- Variations in groundwater salinity are attributed to spatial variability in the accumulation of evaporitic salt deposits resulting from their redistribution by overland flow, in recharge volumes and in the degree of evaporative concentration.

- Several mechanisms contribute to the subsequent chemical evolution of groundwater.

Cation exchange from the illite and chlorite matrix of the mudstones adsorb Ca and Mg in exchange for Na at low salinity levels. Once the salinity exceeds 10 millimoles/l of Cl, however, the process reverses and bound Ca and Mg are increasingly exchanged for Na. Chemical weathering of the aquifer contributes little to the total dissolved solids due to the resistant nature of the material, however, it provides a significant fraction of the total Ca and Mg component.

2.5.4 Quantification of recharge in selected Bedford sub-catchments

The chloride balance method

The previous section has shown that chlorides in groundwater originate from wet or dry atmospheric deposition. As Hutton (1976) has shown that oceanic chloride from precipitation is dominant up to 300 km from the coast, and as a net accession from aeolian redistribution is unlikely in a catchment that is spatially uniform, estimates of the chloride flux can be obtained from bulk precipitation samples so that:

$$J_p = C_p P \quad \text{Eq. 2.5.5}$$

where J_p is the steady state vertical flux density (mg m^{-2} y^{-1}), Cp is the weighted mean chloride concentration in rainfall (mg l^{-1}) and P is mean annual precipitation (mm).

Under steady state conditions in catchments where surface runoff is negligible the flux of chloride to the surface is equal to the flux of chloride to the water table. The removal of chloride from surface inputs is unlikely since chloride does not form solutes unless concentrations are extremely high, the ion is not adsorbed on mineral surfaces and plays few biochemical roles (Dettinger, 1989). Fluxes to groundwater may be lost over the short term by the precipitation of chloride salts following rain events that are completely evapotranspirated and do not result in any recharge. Being the most soluable, chloride salts are the last to be precipitated and the first to be leached in subsequent rain events. As a result, virtually all chloride salts are dissolved in whatever volume of water reaches the groundwater and its concentration in recharging water reflects the fraction of rain water reaching the water table.

Under steady state conditions where hydrodynamic dispersion can be ignored (Allison et al. 1985) and flow is essentially vertical, this relationship can be expressed as:

$$R = J_p/C_r \quad \text{Eq. 2.5.6}$$

where R is the mean annual recharge (mm) and C_r the mean chloride concentration of percolating water (mg l^{-1}). This relationship is not strictly valid in groundwater as it does not account for variations in the horizontal transport of chloride below the water table. Local recharge cannot be calculated solely from local groundwater unless R and C_s are uniform.

According to Eriksson and Khunakasem (1969), one dimensional horizontal chloride flux from an aquifer that is well mixed vertically (J_c mg m-1 y^{-1}), would be related to the accumulated vertical flux from a horizontal distance x (m) beginning at the catchment boundary and extending along the flow path so that:

$$J_c = \int_0^x J_p \, dx \quad \text{Eq. 2.5.7}$$

since the lateral flux of chloride can also be expressed as:

$$J_c = 1000 \, Q_g \, C_g \quad \text{Eq. 2.5.8}$$

where Q_g is rate of steady state groundwater flux (m3 m^{-1} y^{-1}) and C_g is the chloride concentration of groundwater at distance x

$$Q_g = J_c / 1000 \, C_g \quad \text{Eq. 2.5.9}$$

Since, under state conditions groundwater flow is related to recharge:

$$R = dQ_g / dx \quad \text{Eq. 2.5.10}$$

or

$$R = (C_g J_p - dC_g / dx \int_0^x J_p \, dx)/C_g^2 \quad \text{Eq. 2.5.11}$$

Consequently, from the estimates of chloride fluxes to the surface from rainfall and a knowledge of the spatial distribution of chloride concentrations, groundwater recharge can be horizontally integrated along presumed unidirectional flow lines.

The major disadvantage with this method of computation is that equation 2.5.7 assumes uniform conditions in the aquifer so that chloride is only accumulated along a unidimensional flowpath. If flow convergences exist, or if some lateral redistribution of salts occurs prior to infiltration, the relationships discussed above would not be valid. In a semi-arid situation, infiltration excess runoff from the hillslopes, followed by re-infiltration or transmission losses in the valley bottom are common recharge mechanisms (e.g. Hughes and Sami 1992, Lloyd 1986). Furthermore, in a fractured rock aquifer percolating water is concentrated into discrete fracture zones. Chloride fluxes through these fracture zones are therefore related to the chloride load of the upflow sub-area from which the fracture zone collects water. The lateral redistribution of salts by surface runoff suggests that contributing sub-areas can be defined by the surface topography. Under steady state conditions chloride export is then related to the vertical chloride flux and the sum of the contributing catchment areas by:

$$J_e = J_p \Sigma A_j \quad \text{Eq. 2.5.12}$$

where J_e is the rate of chloride export (mg y^{-1}) and A is the catchment area (m^2). If it can then be assumed that discharge from a sub-area is of a uniform chloride content, annual sub-area groundwater discharge (m^3 y^{-1}) can be calculated by:

$$Q_d = J_e / 1000 \, C_g \quad \text{Eq. 2.5.13}$$

and sub-area recharge is:

$$R = 1000 \, (Q_{doj} - Q_{dij}) / A_j \quad \text{Eq. 2.5.14}$$

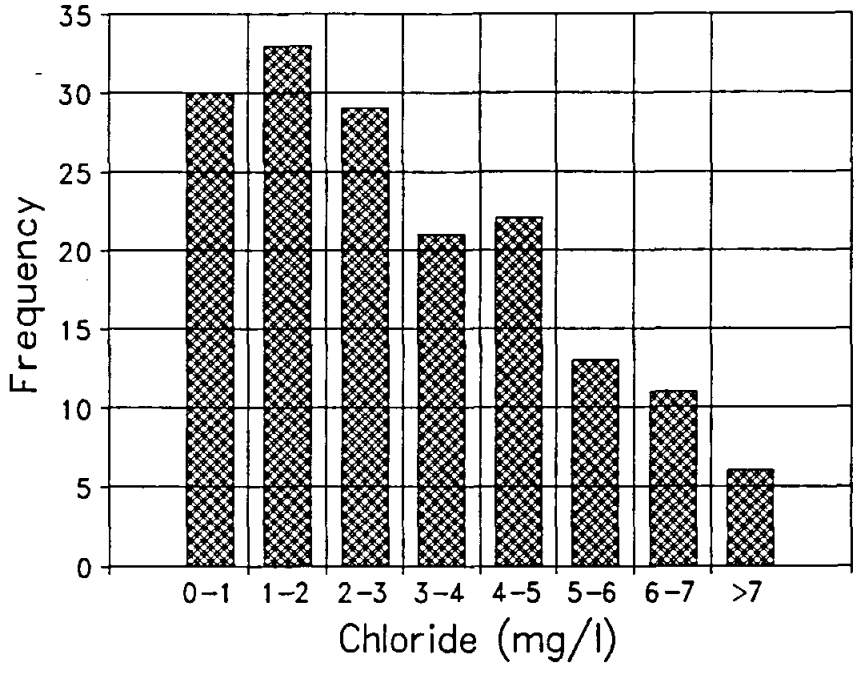

Figure 2.22 Chloride concentrations of rainfall in the Bedford catchments.

Table 2.10 Recharge estimates derived from a chloride mass balance in 12 Bedford sub-catchments.

Sub-area	Contrib. sub-areas	Area	G.water Cl (C_g)	Sub-area Cl load	Total Cl load (J_s)	G'water flow (Q_d)	Change in flow (Q_{do} - Q_{di})	Sub-area recharge
		(km^2)	(mg l^{-1})	(T y^{-1})	(T y^{-1})	(Ml y^{-1})	(Ml y^{-1})	(mm y^{-1})
1	1	17.74	395	35.2	35.2	89.1	89.1	5.03
2	2	1.07	546	2.1	2.1	3.9	3.9	3.64
3	2 & 3	4.45	336	8.8	10.7	31.9	28.4	6.40
4	2 - 4	3.52	416	7.0	17.7	42.6	10.6	3.03
5	5	0.73	509	1.4	1.4	2.8	2.8	3.90
6	5 & 6	17.69	272	35.1	36.5	134.4	131.5	7.44
7	7	4.91	261	9.7	17.0	65.3	38.4	7.84
8	5 - 7	6.94	412	13.8	57.6	139.9	0.0	0.0
9	5 - 9	11.65	346	23.18	80.8	233.4	93.59	8.03
10 & 11	5 - 11	30.89	425	61.3	159.8	376.0	100.0	3.24
12	1 - 12	12.18	537	24.2	152.0	283.1	0.0	0.0

where o and i are groundwater outflows and inflows to sub-area j.

Chloride concentrations in rainfall.

The mean annual rainfall since 1956 is 483 mm (figure 2.21). During a 729 day study period (1990-1992) between 622 and 996 mm of rain were recorded at the various rain gauges, with the average being 780 mm. Monthly rainfall varied between 0 and 135 mm. The chloride concentrations in rain water varied from barely detectable amounts to 10.3 mg l^{-1}, with a weighted average of about 4.11 mg l^{-1}. In general, much less variability was recorded in the chloride concentration of large rain events than in the smaller convective rain events. If the recorded weighted average concentration is representative of the long term rate of chloride deposition, then J_p is 1985.1 mg m^{-2} y^{-1}.

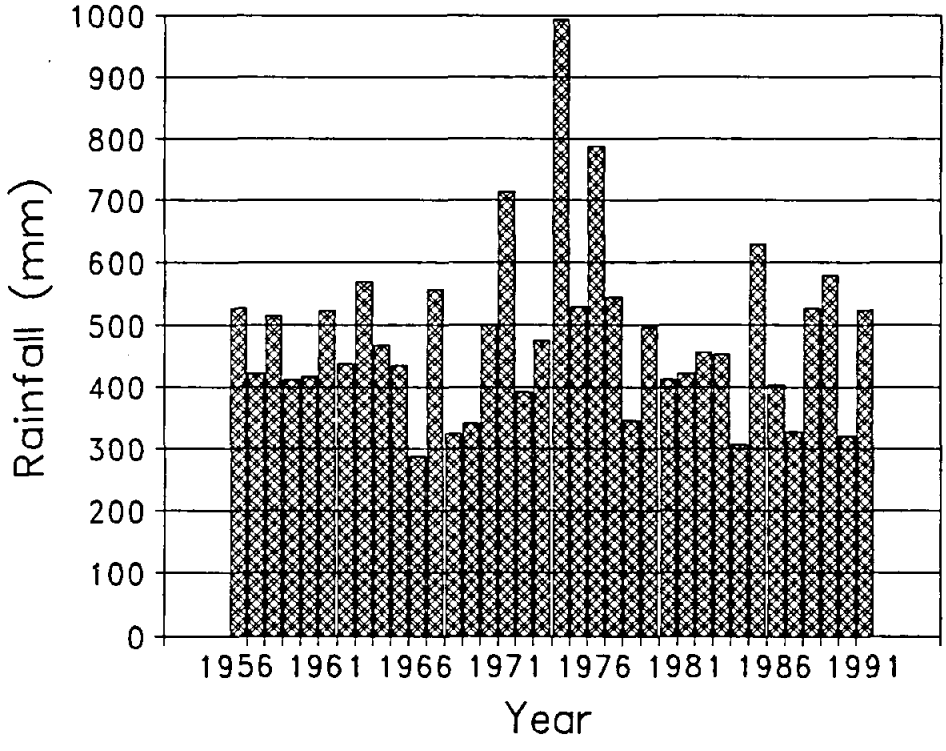

Figure 2.21 Annual rainfall at the Albertvale station.

Recharge estimates

Using the ARC/INFO GIS package, 12 sub-areas were defined according to borehole locations and topography. These cover the northwest quadrant of the Bedford catchments and constitute the 112 km^2 catchment area above borehole BAG10 (Hughes and Sami, 1993). Each sub-catchment represents the area contributing chloride to a monitored borehole (A_j) which defines the catchment outlet. Sub-catchment areas were progressively integrated from the catchment boundary along the regional hydraulic gradient in order to calculate the lateral chloride flux (J_j) through nested sub-catchments. The relevant physical parameters of these sub-areas are presented in 5.5. Results obtained by applying eqs. 2.5.12 to 2.5.14 are shown in table 2.10. The area weighted mean recharge rate is 4.45 mm y^{-1}.

3. AN INTEGRATED APPROACH TO DEVELOPING A HYDROLOGICAL MODEL APPLICATION SYSTEM

3.1 PHILOSOPHY OF THE APPROACH

In designing a computer based system which can be used to satisfy a number of different requirements in the broad field of hydrological simulation modelling, several initial criteria were developed.

- The first was that the system would be written for application on PC's with DOS based (or compatible) operating systems. While software written for UNIX based systems may be more transportable across different hardware platforms, there are a large number of potential users who are likely to remain with DOS based PC systems for a long time to come. This is particularly true as the expansion of local area network systems takes place and as these systems allow several different hardware platforms and operating systems to interconnect. The rapid advances in the power of DOS based PC's in recent years has meant that the old reliance on mainframes and minicomputers for the large processing power ('number crunching') required to efficiently run hydrological models has fallen away completely.

- An early decision was made to write the system using a low level computer language and 'C' was chosen for its functionalility and ease with which code can be written to interact with the hardware and the operating system. In many ways the choice of 'C' was also a personal preference and several other languages could have been used more or less as successfully (e.g. FORTRAN or PASCAL).

- The ideal system was perceived to be one in which a number of different problems in applied hydrological or water resource modelling could be addressed within a single integrated approach. This therefore meant that procedures which are common to a number of different modelling approaches had to be identified and linked together. This point is discussed in more detail in the next section.

- While great strides have been made recently, and are still being made, in coupling the application of hydrological models to other software developments (Geographical Information Systems and Digital Terrain Modelling, for example), it was also recognised that not all potential users would have, or require, access to such software. Consequently, although some work has been carried out in this area, the design philosophy was to ensure that none of the modelling procedures would be dependent upon the availability of such packages or their output. Similarly, it was recognised that other groups, more qualified to carry out such research, would be working on such problems during the course of this project. The project team believed that attempts to duplicate this work would not be productive. It was, however, considered necessary to bear in mind the direction of likely future developments and at least make some allowance for interfacing the system developed here with them.

- While the system was to be developed primarily as a model application tool, it was

recognised that it would also be useful to model developers in providing an established environment in which to create new models or adapt and add to existing ones.

- It was also recognised that some of the functions of the system (data handling and modelling) would require changing as new information and technology became available. It was therefore necessary to incorporate as much flexibility into the system as possible, where individual functions or components could be changed without affecting the rest of the system operation.

- As part of the concept of flexibility, it was understood that there would be some components, established on the basis of the developers ideas, that might not be acceptable to some users. It was therefore considered necessary to allow individual users the ability to customise certain approaches, without the need to access the source code and re-write the actual computer programs.

The authors accept that the version of the modelling system that is one of the products of this five year project does not completely satisfy all the demands identified above. However, all these criteria have been addressed at some stage in the development and even though there are clearly identifiable inadequacies, the basic framework has been established so that future improvements can proceed rapidly.

3.2 BASIC COMPONENTS OF AN APPLIED MODELLING SYSTEM

Given that a decision has been made about the objective of a modelling exercise and that a suitable model has been selected, it is possible to identify four major components or tasks that have to be carried during any application of a hydrological model.

The first is the quantification of the parameters that are used in the model algorithms and determine the way in which the input time series data will be transformed to the output data. This task may involve field work, map or aerial photograph studies, processing of digital elevation data, interpretation of GIS coverages, the use of existing regionalised relationships or informed guesswork. The amount and complexity of the work involved is highly dependent on the type of model as well as the existing availability and format of relevant information.

The second task is the preparation of the time-series data that form part of the input to the model, or will be used to compare the simulation results with the real world conditions. Time-series data includes rainfall, evaporation, temperature, soil moisture, streamflow, reservoir levels, etc. The interval between individual values in stored time-series data may be fixed at anything from 1 min to 1 year, or it may be variable depending on the rate of change of the process that has been measured (frequently referred to as 'break point' data). There are probably almost as many different formats used to store time-series data as there are agencies collecting such data. In some parts of the world, users are fortunate enough to have centralised agencies that either collect or collate the data into common formats. Nevertheless, users of hydrological time-series data are often faced with a variety of ASCII or binary formatted data which must be reduced to a format which is compatible with the

model input data requirements. Additional problems occur when the original data files contain codes to indicate missing data or the reliability of the individual data values.

The third task is the actual running of the model itself, which is normally trivial, but may involve some decisions to be taken by the user with respect to how the model should be run.

The final task is to assess the results and decide whether or not the first and third tasks should be repeated to try and improve the results. There are a number of ways of assessing the results and preferences vary between individual model users. The amount of information generated by a model is usually quite daunting and some form of summary is frequently required. Conventionally, this takes the form of a set of summary statistics of the simulated time-series and comparisons with the observed data if available. There are, of course, a wide variety of statistics that can be computed. An alternative is to utilise graphical plots of the results to permit a visual assessment of the results.

3.3 HYMAS - HYDROLOGICAL MODELLING APPLICATION SYSTEM

HYMAS consists of a set of computer programs written in 'C' code to perform the majority of the tasks referred to above. All of these programs or 'processes' are called from a master program which contains a menu system to permit the user to select which process is required to be run. The master program is therefore essentially a menu 'shell' which also passes parameters to the individual system processes to ensure that they will access the correct data files. A full explanation of what HYMAS is, what it can do and how to operate the system is contained within the user manual which forms one volume of the final report for this project (Hughes and Murdoch, 1993). This section of the report provides a brief overview of the system.

HYMAS uses the concept of 'project' files (having a fixed FLH extension), which are more or less unique to each application of the system. These files contain a project name and references to the locations and names of the files which need to be accessed to run any of the HYMAS processes for the application. In setting up an application, or modifying an existing one, the source directory and names of those files which are to be used or created are entered via a spreadsheet type of screen. The project files are standardised, in that they contain records referring to all the possible files that the system can use, regardless of whether a specific application requires them or not. The project files also contain flags to indicate the status of the files referred to. The status flag can indicate that the filename is invalid, that it is valid but the file does not exist or that one or more files do exist. The latter implies that a wild card (e.g. RAIN*.DAT) specification can also be used to define filenames. This is used, for example, in specifying input data files to distributed models, where each element of the distribution system has a separate data file(s) associated with it.

The master program accesses a process control file which contains information about the files that should be passed to each process (or separate program) and checks to ensure that the relevant filenames are valid and that the files exist if necessary. The master program then passes the name of the project file to the selected process and after completion, control is returned to the master program to allow the user to select a further process.

3.3.1 Parameter estimation in HYMAS.

Within HYMAS the parameter estimation procedures can be divided up into two distinct groups. The first group is associated with the estimation of a set of standard physiographic variables which describe the physical characteristics of the catchment being modelled. The second group deals with the model parameter values themselves.

The standard physiographic variables include topographic, channel, soil, vegetation, geological and climate indices. Some are referred to as primary variables, in that their values are estimated from other processes or entered directly. Others are secondary variables which are estimated from the primary variable data. The % area of a sub-catchment that is occupied by soils falling into five depth classes and five textural classes are examples of primary variables, while the mean soil depth, porosity and field capacity are examples of secondary variables. The equations used to calculate the values of the secondary variables are contained within a text file as Reverse Polish notation equations and can be modified by individual users if necessary. There are several programs within HYMAS that allow digitised topographic data to be used to estimate some of the primary variables. At present these programs only allow the estimation of some of the topographic variables, such as areas, slopes, lengths, drainage density and channel order. The developers hope to expand this part of HYMAS, using better interfaces with GIS and DTM packages, to allow more of the primary variables to be evaluated automatically.

Having established a data file of physiographic data for the sub-areas of the distribution system of a specific application, initial values of some parameters of some models can be determined. The first time that a parameter data file is established, default values are calculated from the physiographic data, where possible. This is not always possible for all parameters of a model as there may be no definable relationships between the parameters and any of the physiographic variables. The form of those relationships that do exist are contained within a text definition file using Reverse Polish notation and can be modified by individual users as necessary. The parameter data files can be edited, using a spreadsheet type utility, to allow the default values to be changed. Whenever changes are made to a parameter value, the default values are displayed so that the user is always aware of the original estimate.

HYMAS contains additional facilities to allow parameter values to change within a period of modelling. This is referred to as 'time slicing' and is used by defining time periods within the total period where one or more parameter values will change. The changes can be established as linear over the 'time slice', or instantaneous at the start of the slice. This facility has been used to account for land use changes and dam construction or raising, for example.

3.3.2 Establishing time series inputs to models.

There are several types of time series data that the models within HYMAS require as input. These include rainfall, observed discharge, upstream inflow, evaporation, as well as reservoir draft and observed storage volumes. These data may also be available in a large number of different formats. Consequently, HYMAS includes several routines to convert different formatted data to a standard format, as well being able to read directly from several standard

formats normally available within South Africa (usually from the Computing Centre for Water Research).

The rainfall data compilation routines are divided up into two groups; the first to compile distributed variable time interval rainfall input for each of the sub-areas of a distribution system and the second to carry out the same operation, but for fixed time interval data (daily or monthly). Both use the same inverse distance squared interpolation procedure to determine average sub-area rainfall depths from several raingauges based on a matrix of distances from the gauge location to the sub-area centres. A facility is available for the fixed interval routines to further weight the sub-area rainfalls by the ratio of the average of the median monthly rainfalls for all the elements of a grid within the sub-area to the median monthly rainfall at each rainfall station. The full details of all the rainfall building processes are explained more fully in the HYMAS user manual and some further discussion of the variable time interval approach is provided in the section in this report on the Variable Time Interval model. The period within the overall available observed time series of rainfall that is to be used for modelling is selected at the time when the rainfall input file is constructed, simply by specifying the starting and finishing dates.

The input data files for the other time series data are only built after the rainfall data files. There are several data abstraction programs included within HYMAS to allow time series of evaporation, observed discharge, etc. to be compiled from the original data files and which are coincident in time with the rainfall input data. In the case of observed discharge data, it is also possible to create a HYMAS data file of a complete observed record (including missing data). This facility allows an observed flow record to be created in the absence of a rainfall data file so that some of the statistics (flow duration curves, for example) or results analysis programs can be used on the complete flow record.

While the available HYMAS procedures cover a wide variety of possible raw data formats, the developers accept that some users may have their data in formats which are not yet compatible. The form of the HYMAS data files is very simple and straightforward such that it is usually a trivial exercise to add new options for data conversion. However, this will also be dependent on the complexity of the raw data format.

3.3.3 Setting up and running models.

Having established the time series input data and the parameter data file, running the model is normally a trivial operation. However, in some cases, the models contain optional approaches to some of their components. The user may then select which options are required, check the compatibility of the choices, and link the choices together with the main part of the model to form the final executable model program.

3.3.4 Assessing the model results.

Several procedures have been included in HYMAS to evaluate the simulation results. Some of these are common to all models, while others have been developed to satisfy the specific features of a single model. The output file generated by a model consist of one containing the time series of downstream runoff and one containing a number of the input, internal state and output variables for each sub-area of the distribution system. The former is included so

that output from one application (a simulation of the monthly runoff volume from a catchment, for example) can be used as input to another application (a simulation of the water balance of a reservoir, for example). The latter is the data file that is normally used in assessing the model results.

The results analysis routines fall into four categories; listing results data, graphical displays, summary statistics and low flow analysis.

Listing results data.

These procedures allow the user to select one or more of the output variables for a single sub-area of the distribution system, as well as the time period within the total simulated period and list these data to the screen, a printer or a text file. The facility is especially useful for exporting the results data to an external package that provides graphical or statistical capabilities not available within HYMAS. A sub-option also allows monthly total or mean values of the output variables to be generated and written to a file.

Graphical analysis routines.

Two options are available within this category. The first is a facility to plot the time series of the output data using screen graphics. The screen image consists of two graphs and the user may select one or more variable and/or sub-area to plot on each graph. There are some restrictions such as only being able to plot data with the same units on the same graph and not being able to plot more than one histogram on the same graph. The way in which the data are plotted (line graph or histogram) are determined by simple numeric codes within a text file that is associated with the output files for a specific model. There are various commercial screen dumping facilities available that allow the contents of the screen to be written as a graphics image to a file (for importing into a word processor, for example), or to a hard copy output device (printer or plotter). There are no internal HYMAS routines for printing or plotting the graphs.

The second graphical option is a scattergram facility, where the user can select two variable/sub-area combinations (observed and simulated discharge, for example) and generate a scattergram plot. There are facilities for transforming the data values to natural logs, to select a range of months to include and for selecting either ordinary data or cumulative data. The latter is quite useful for compiling double mass curves of either rainfall over two sub-areas, or rainfall versus runoff for one sub-area. This program also computes some statistics (mean, standard deviation, maximum, minimum, regression statistics and coefficient of efficiency) for the two variables and the relationship between them.

Both graphics programs allow the user to examine the whole time series simulated, or any part of it.

Summary statistics.

These procedures are highly model specific and depend upon the type of summary information normally required from the models. For example, the summary statistics for the reservoir simulation model calculates the annual means and standard deviations of the major

components of the water balance and provide some information on the percentage time certain drafts were achieved or defined proportions of the full supply volume were maintained. More details of the information contained within the output from the statistics programs are given in the user manual.

Low flow analysis.

This set of procedures are currently being extended as part of another Water Research Commission project on low flow hydrology, but the results do not only pertain to low flows. One of the programs that has been partially completed begins with the normal selection of the output variable to be analysed and the time period of interest and displays a duration curve for the variable. The elements of the curve may be printed to a file or printer and the user is able to define up to 10 'thresholds' on the duration curve. The program continues by computing histograms of the distribution of times that the variable chosen was above and below the chosen 'thresholds'. This is referred to as spell analysis.

Further programs are currently being developed to compute a much wider range of low flow statistics including recession statistics and baseflow indices and to carry out low flow frequency analyses.

This section has provided a very brief overview of HYMAS and any potential users are referred to the user manual or hands on experience of the system itself for more information.

4. MODEL DEVELOPMENT

4.1 INTRODUCTION

This section of the report describes some of the model developments that have been carried out during the project. The main development has been the Variable Time Interval model which has followed on from the results of a number of the process studies referred to in section 2 of this report, as well as literature reviews of the variety of approaches adopted by other catchment hydrology model developers. Other model developments have taken place in response to demands external to this project where attempts to satisfy these demands could be seen as part of the broad terms of reference of the project as a whole. These demands have given rise to the modifications made to an existing reservoir simulation model, the design of a model to simulate nutrient wash-off from developing urban areas (PEXP model) and the formulation of a simple model to evaluate the usefulness of raintanks as a supplementary water supply in developing communities. The other models referred to in this section have been included in the current version of HYMAS because they were perceived by the project team to potentially offer something that the other models do not. One model that is included that is not referred to in detail in this section is the Pitman model. The authors considered that this model is so widely known and used, that it is not necessary to repeat the details in this report. It is however referred to in the HYMAS user manual as one of the possible model options and guidelines to implementing the model via HYMAS are explained.

The latter point illustrates the philosophy behind the approach used in developing HYMAS. Instead of attempting to develop a single model that attempts to simulate many different aspects of catchment hydrology or water resources, the approach has been to include a range of different models in an integrated system with common programs to support the setting up and running of all the models in the system. This approach has allowed the project team to establish models, covering a wide range of potential user requirements, within HYMAS quickly and relatively efficiently. Some of these models are very similar or more or less identical (the Pitman model, for example) to existing approaches, while others are new.

Before discussing in detail any of the developments that have taken place, the next section provides some brief explanations of the way in which models are designed or adapted for inclusion in the HYMAS package.

4.1.1 Designing or adapting models for HYMAS

The details of how the HYMAS package is structured are covered by the user manual, but it is pertinent to refer to some of the techniques used to establish model programs in this part of the report. All of the computer programs used by HYMAS are called from a single master program, which also passes all the necessary information on the types, directory source and names of the data files that are to be used by the programs. Consequently, any model designed to be used with the system must include appropriate computer code to accept this information passed to it. All of the data files used within HYMAS are also in a standard format and therefore any existing models will need to be adapted to be able to read or write

data in such formats. These formats are fully explained in the user manual. These are the only two necessary changes that would have to be made, for existing model computer code to be incorporated as part of HYMAS. There are, however, other changes that could be made to make the operation of a new model more consistent with those already included. These are also highlighted further in the HYMAS user manual.

A facility is incorporated into the HYMAS structure to allow the components of any single model to be simulated using one of several optional approaches. This is achieved by developing several sub-routines for the same component, compiling them as object code and linking the user's choices with the main module of the model. The number of external components and the number of options for each one are specified in one of the HYMAS text definition files, which can be easily edited whenever new options or components are added or removed. The choice of which option to use, as well as the final model linking process are part of the model set-up procedures and the selections are stored as part of the parameter data input file.

The main parameter input to the models is all included in a single binary file which contains a matrix of values for each sub-area and each parameter. However, a facility also exists for allowing the parameter values to change during the time-series period. This is referred to as 'time-slicing' in the user manual. The time slices are established as part of the parameter input and editing procedure by identifying specific periods within the complete time series over which the values of some parameters may change. The changes can be gradual over that period (as with growth of forestry, for example), or instantaneous at the start of the slice (as with clear felling of forest, or the raising of a dam wall, for example). Within the models it is therefore necessary to identify the start and finish times of all the established time slice periods and modify the parameter values as and when necessary.

In some of the models, there are parameters where two values are specified, one for the summer and one for winter. These two values define the extremes of an annual distribution which is then used to determine the values in other months of the year. This avoids having to specify 12 individual values in the parameter file to describe the monthly distribution of the parameter. Where 12 values of a monthly distribution are used (commonly for mean evaporation data and draft data in the reservoir simulation model), these do not form part of the parameter file, but are contained within a separate data file, referred to as the 'mean monthly data' file in HYMAS. The default distribution used is a sine-curve, but this can readily be modified by a user.

Most of the models that have been included in HYMAS to date can be run in two different ways. The first is the most economical approach and simply displays the point in the time series that the modelling process has reached as the model runs. The second approach uses a schematic diagram of the processes that are being modelled and displays the values of some of the input (e.g. rainfall), internal state (e.g. soil moisture, groundwater levels, etc.) or output variables (e.g. runoff) for each time step of the modelling process. The user is also able to interrupt the modelling process to look in more detail at some part of the time series. It is possible to reverse the time to further investigate the conditions during previous time steps or to view the results one step at a time in either direction, or exit the detailed display and continue modelling with the simple display. This approach has been found useful for teaching students about the way in which models operate and improving their overall

appreciation of what is involved in the development and application of hydrological models. Incorporating this approach into existing models is not difficult as all the necessary computer code is contained within a standard set of sub-routines.

None of the models within HYMAS contain code to assess the modelling results. The HYMAS approach has been to keep these two operations separate. There already exist some standard approaches to analyse the results regardless of the model. These include simple listing of some of the output variables (either to the screen, printer or a text file for later analysis using a proprietary statistics or graphics package), screen displaying of some output variables for all or part of the time series, a two variable scattergram plot and regression analysis and a set of time series analyses (duration curves, spell analysis, etc.). The developers have also written some model specific output analysis routines to supplement the more general ones. Therefore, the requirement to add additional analysis routines when another model is added will depend upon the type of analysis that is typically used for interpreting the model results.

While all the models currently within HYMAS have been coded in 'C' language, there is no reason why models coded in FORTRAN, or other languages, cannot be included. The main consideration is the ability of the model executable program to be called from the master HYMAS program and to accept the transfer of some filename information. In taking existing models (e.g. RAFLES - see a later section of this report) and incorpoarting them, the project team have recoded them into 'C', but this is more a matter of personal preference.

4.2 VARIABLE TIME INTERVAL (VTI) MODEL

The history of the development of deterministic catchment hydrology simulation models began with relatively simple and empirical formulations which were usually based on highly simplified conceptualisations of real physical hydrological processes (O'Connell, 1991). Most of the earlier models treated the whole catchment as a single lumped unit, ignoring spatial variation in rainfall-runoff response. Such models have often been demonstrated to satisfactorily reproduce time series of observed runoff, albeit after manipulation of the parameter values through calibration. Some of these models are still in use today, providing estimates which are used in water resource planning and management (Pitman and Kakebeeke, 1991). One of the responses of the hydrological community to the development of this type of model was to design mathematical and statistical techniques to improve either the efficiency or objectivity (or both) of the calibration exercise (Soorooshian, 1991). However, most of these techniques become irrelevant given the fact that there are often few data upon which to base calibrations and rarely enough to allow stable calibrations to be determined (O'Donnell and Canedo, 1980; Görgens, 1983). Attempts to develop techniques to transfer parameters from gauged to ungauged catchments have also met with limited general success (Hughes, 1989).

More recently, the modelling literature has concentrated on the development of models which are more physically-based, spatially distributed and where many, or all, of the parameters can be measured from field, map or other information sources (O'Connell, 1991). However, the application of this type of model is not without problems (Beven, 1989; Grayson, et al., 1992). Many of the physical equations used have been developed and tested at very small spatial scales. To incorporate them, largely unmodified, into catchment models, where the spatial scale of modelling is commonly several orders of magnitude greater, presents at least two problems. Firstly, the detailed parameter values required are not available in most applied situations and whatever methods are used to estimate them introduces a degree of empiricism, the effect of which will depend upon the validity of the estimation technique. Secondly, the effects of spatial variability, or the action of processes not recognised as important at the small scale, may make the application of the algorithm(s) inappropriate at the scale of the model distribution system.

The interaction between the component algorithms and the time interval of modelling may be equally important. For example, a model which purports to simulate infiltration rates, using the physical laws governing this process, can only truly achieve this if the iteration interval is short enough and the input data of a high enough resolution to reflect the real rainfall intensity (Hughes, 1993).

Although great strides have been made in the theoretical development of models, there is still a need for a better understanding of the interactions that exist between the complexity of the modelling approach and the practicalities of applying models. A model may be soundly based on 'real' hydrology, but its data requirements so stringent that they cannot be met with a reasonable degree of accuracy. The reliability of the results will be unpredictable unless extensive calibration and verification of the parameter values is carried out. The authors believe that this is no different to using a much simpler model which has parameters that have to be defined through calibration.

It seems inevitable that a compromise solution is required, where, for practical application purposes, the component algorithms of a model will be based on a mixture of physically measurable and empirically estimated parameters. A number of models of this type have been developed in recent years (for example, Arnold, et al., 1993). Coupled with this should be parallel developments in parameter estimation procedures which are adaptable to the type and amount of information available. The VTI model has been developed with this type of 'compromise' philosophy in mind and throughout the period over which the model has evolved, consideration has been given to three main points :

- The suitability of the algorithms for representing hydrological processes at the scale of sub-catchments in a practical semi-distributed modelling system.

- The availability of information on physical catchment properties and how this can be used to estimate parameters, without introducing too high a degree of empiricism.

- The model and parameter estimation procedures should be applicable to a range of climate types, excluding those where the hydrological response is significantly affected by either frozen ground or snowmelt.

Some of the details of this model have been published in two scientific papers (Hughes, 1993; Hughes and Sami, 1993).

4.2.1 The variable time interval philosophy

At small (detailed) scales and during high rainfall input, hydrological processes operate at much greater rates than if the processes are integrated over large areas or during periods of little or no rainfall input. Reported values for saturated hydraulic conductivities are orders of magnitude greater than unsaturated values and runoff during storm events, whether by infiltration excess or saturation excess surface flow, pipe flow or rapid saturated sub-surface flow is generally much more rapid than baseflow in the same catchment. The necessity to minimise the required computing and data resources, yet achieve an acceptable degree of accuracy or reliability has meant that models have generally been constructed for specific purposes and are rarely interchanged. However, if more than one type of model is applied to the same area for the purpose of generating a range of different output information, it is not always possible to ensure that the models are simulating the hydrology in a compatible way. A compromise solution is to operate on a relatively coarse time scale between events and then switch to an event type model, operating at shorter time intervals (or designed to simulate the basic characteristics of the event, such as the peak, time to peak and volume) for the duration of significant events (Dunsmore, et al., 1986).

Distributed models were developed in response to the need for models to more closely correspond to the levels of spatial variability found in real catchments. It is therefore somewhat surprising that less attention has been given to the temporal resolution in models as has been given to the spatial resolution. Hughes and Herald (1987) illustrated the problem of varying the time step of modelling using an event type model (Hughes, 1989) applied in three different catchments. The catchments consisted of a steep, sub-humid area of 34km^2, a semi-arid area of 83km^2 (both in South Africa) and an arid catchment of 8km^2 situated near Tombstone, Arizona, USA. Comparison of the mean standard errors of estimation of the

peak flows, times to peak and volumes of the simulated events for the Tombstone catchment, showed a marked loss of model accuracy when the time interval exceeded 15min. The benefits of shortening the interval from 1hr for the other two catchments, were less obvious.

Fixed interval hydrological models suffer from the problem of either 'over kill' during relatively dormant process periods in short interval models, or loss of resolution during active process periods in long interval models. The intensity of rainfall is of primary importance in determining runoff, particularly in semi-arid areas, and the real intensity can rarely be adequately represented in a long interval model. Equally, the problem of defining antecedent conditions in event type models (Dunsmore, et al., 1986) can be more satisfactorily solved by using a continuous model with a variable time interval, in that the event then becomes just one part of a continuous water balance estimation procedure. These aspects may assume great importance given the need to develop models which satisfactorily link hydrological processes to the movement of solutes (chemical water quality) and solids (sediment erosion and transport).

Variable time interval models will inevitably take longer to run and require more input information than coarse time interval models, but they should be more efficient with respect to both the required computer resources and the level of detail contained within the model results. The actual success of an individual model will obviously depend upon the validity of the assumptions used in the formulation of the model and particularly the way in which the change over from one length time interval to another is made.

An approach that has been used in variable interval modelling is to adopt one model for the coarse interval (1 day for example) and to overlay a finer time resolution model when the rainfall exceeds a defined amount. This procedure is used in the ACRU model (Dunsmore, et al., 1986; Schulze and George, 1987; Schulze, 1989) where a distributed daily water balance model forms the core and an SCS based flood simulation model is superimposed to provide estimates of flood hydrograph characteristics during high rainfall days. The alternative adopted in the present study is to modify an existing single event model (Hughes, 1989) to operate on a continuous basis.

The time interval structure used for each sub-area in the distribution system is determined using a pre-modelling program that builds the sub-area rainfall input data. The input to this program is assumed to consist of files of gauging station rainfall data stored with a high enough time resolution to adequately define the intensity (often referred to as 'break point' format). The exact resolution required will depend on the nature of the rainfall regime.

Rainfall depth thresholds are specified for a series of time intervals of between 1 day and 5 mins. For example, a user may specify 10mm thresholds for 1 day and 1 hour intervals and set the shortest interval to be used to 15 min. The model input rainfall series would then be built at 1 day intervals while the sub-area rainfall is less than 10mm. For the remaining days the input would be generated in hourly steps, while during any hour with rainfall in excess of 10mm the time step would be reduced to 15 min.

There is obviously little point in trying to generate rainfall input to the model with a time resolution which generally exceeds that of the original data, unless some form of temporal disaggregation procedure is involved. No such procedure is included in the rainfall building

program. If a single period is encountered in the raw station data where the total recorded exceeds the threshold set, the total rainfall would be simply disaggregated into equal rainfall amounts over the next shortest interval. There is, however, nothing to prevent users from developing their own dissagregation routines which could be applied to more commonly available daily data. The only consideration is that the output file from such a routine should be compatible with the HYMAS data formats. The thresholds are applied after mean sub-area rainfalls have been built for the finest time interval using an inverse distance-squared weighting interpolation procedure on the station rainfall data. The user may specify the number of gauges to use for interpolation as well as the maximum separation distance between the gauges and the sub-area centre. Each sub-area therefore has it's own time interval structure and the model accounts for this by skipping over the sub-areas which have coarser intervals at any point in the overall simulation period.

If the time interval organisation procedure and the calculation of rainfall input from the raw station data were used within the model itself, the amount of computer time taken would be prohibitively high, due to the large number of iterations required to establish the sub-area rainfalls from the original gauge data. By making the organisation of the rainfall input a pre-processing function, the amount of computer time taken for repeated runs of the model (for calibration purposes or to evaluate parameter sensitivity, for example) is minimised.

4.2.2 The Model structure

Figure 4.1 illustrates the basic structure of the model and it is made up of the following 9 interlinked components which are discussed in the following sections.

Potential evaporation estimation.
Interception estimation.
Rainfall intensity controlled runoff estimation.
Main moisture accounting and runoff generation component.
Actual evapotranspiration estimation.
Groundwater-surface water interaction component.
Sub-area routing including depression and small dam storage components.
Channel transmission loss estimation.
Channel routing component.

Figure 4.2 illustrates in more detail the moisture accounting and runoff generation routines, including the interactions with groundwater.

The model employs a semi-distributed system, whereby the catchment is divided into sub-areas, each having its own set of parameter values and rainfall input time-series. The current limit to the number of sub-areas is 30. This approach has been adopted as a compromise between lumping the whole catchment into a single unit and methods which use higher resolutions of spatial disaggregation, such as grids or slope elements. This approach also recognises that, while information may be available about broad differences in catchment characteristics, it is rare for model users to have sufficient information to be able to uniquely define differences in parameter values over even a moderately dense grid or at the scale of slope elements. As later sections illustrate, a probability distribution approach (Moore, 1985) is used to account for the spatial variation of some variables within each sub-area.

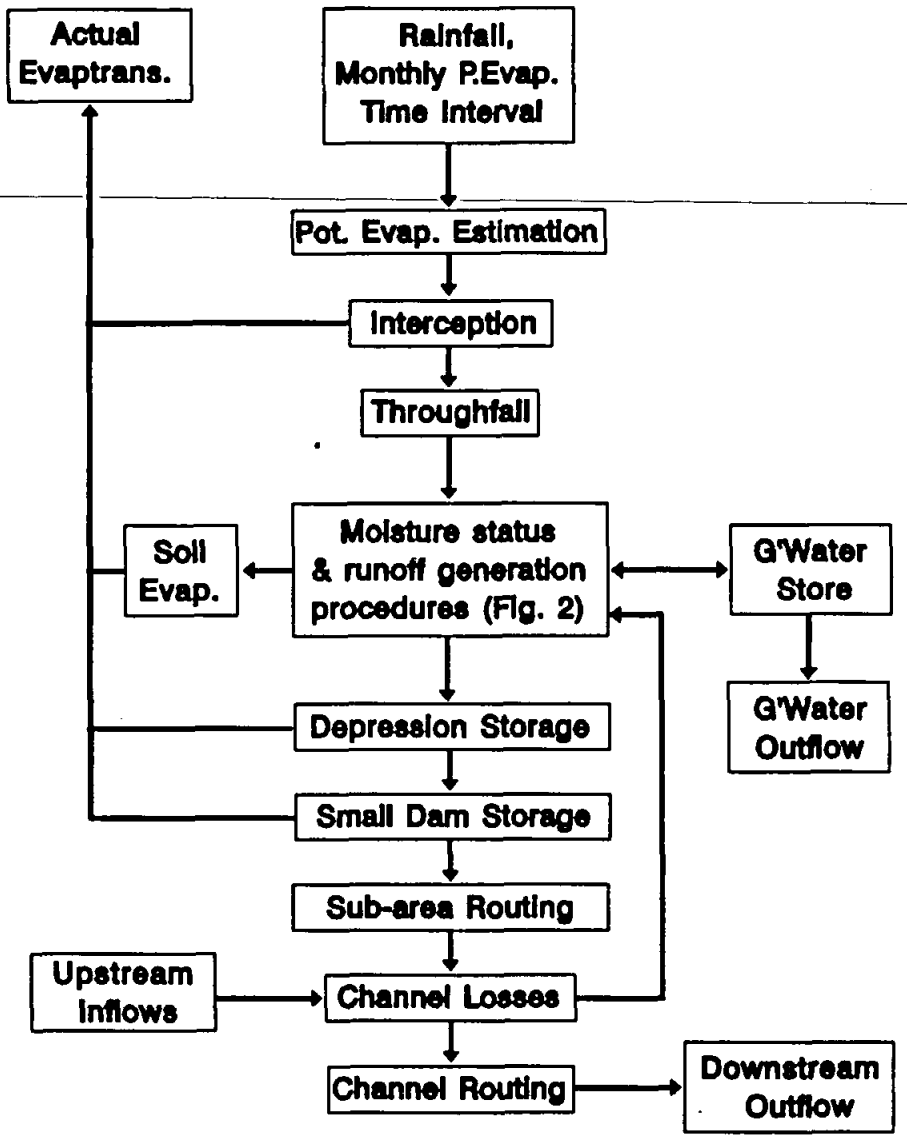

Figure 4.1 Basic structure of the Variable Time Interval model.

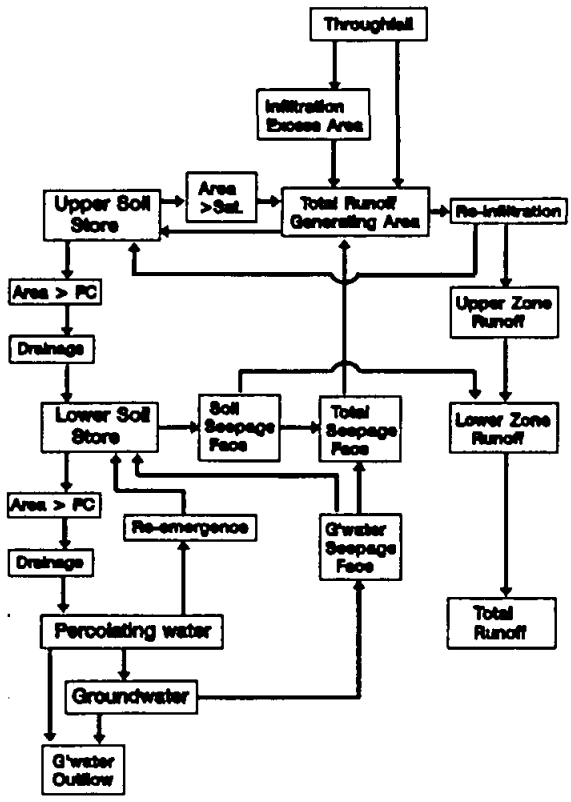

Figure 4.2 Structure of the moisture accounting and runoff generation components.

Potential evaporation.

Estimates of potential evaporation (PEVAP) are made by distributing mean monthly pan evaporation values, corrected to free water surface evaporation, equally over the days of a month and using a sine curve distribution for intervals of less than one day. A correction factor which has the effect of reducing the potential evaporation on wet days and increasing it on dry days is also applied. It is based on a non-linear relationship between mean daily pan evaporation and the actual pan evaporation that occurs on days with differing depths of rainfall (RAIN mm).

$$\text{Correction factor} = EA * RAIN^{-EB} \quad \text{Eq. 4.2.1}$$

Where EA and EB are parameters that can be determined from regional rainfall and pan evaporation figures. Losses from surface water (interception, depression and small dam storages and saturated soil surfaces) are assumed to occur at the potential rate.

Interception.

The interception component uses a simplified Rutter (Rutter, et al., 1975) method involving three parameters; the proportion of vegetation cover (COV), leaf area index (LAI) and the canopy capacity (ICAP). All three parameters are estimated from the proportion of the sub-

area under several broad vegetation cover classes. Seasonal variation is accounted for using a sine curve distribution with an amplitude defined by summer and winter values. Changes in storage are estimated using:

$$\Delta IS = COV * LAI * [RAIN - PEVAP * IS / ICAP] \quad \text{Eq. 4.2.2}$$

where IS is the current level of interception storage (maximum = ICAP),
and ΔIS is the change in storage.

The balance of RAIN and any overflow from storage constitute throughfall.

Rainfall intensity controlled runoff.

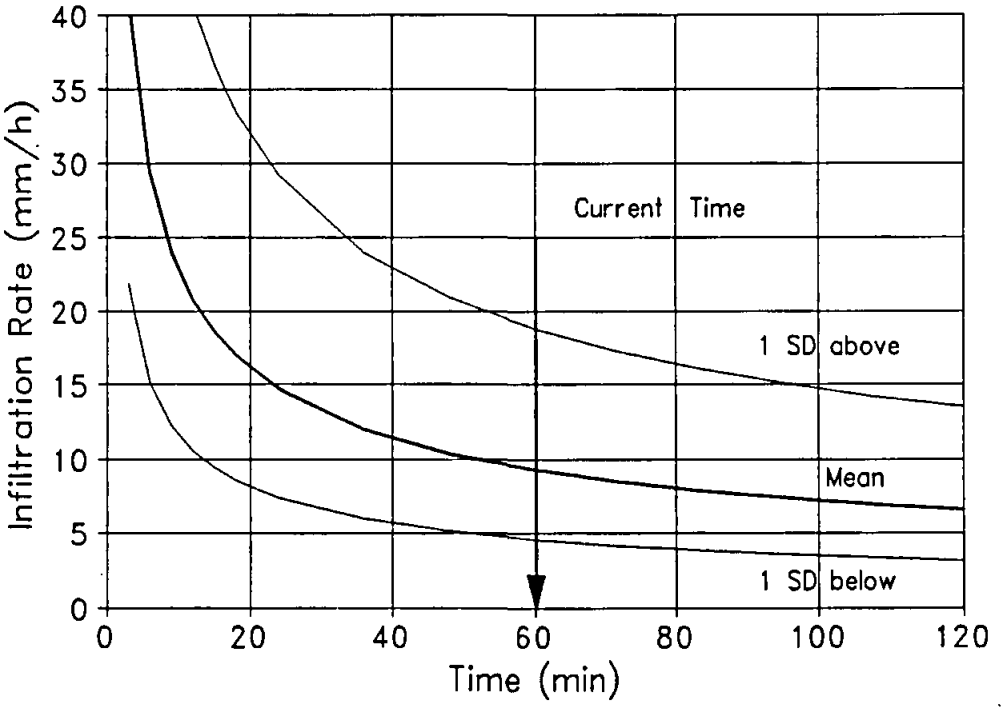

Figure 4.3 Illustration of the infiltration rate approach, showing the mean curve (centre line) as well as the upper and lower curves represented by the standard deviations of a Log Normal distribution.

The model includes two main runoff generation components; one controlled by soil moisture content (see next section) and one controlled by rainfall intensity. The latter makes use of an infiltration function of the form (Kostiakov, 1932) :

$$\text{Infiltration rate} = k * c * T^{(k-1)} \quad \text{Eq. 4.2.3}$$

where T is the cumulative time (mins) incremented from the start of a rainfall event and decremented between events. Spatial variation within each sub-catchment is allowed for by assuming that infiltration rates are defined by distribution functions, rather than single values (fig. 4.3). Mean and variability parameters for each of k and c determine the distribution shapes. The variability parameters represent the upper standard deviation of a log-Normal distribution. Seasonal variation in the means of k and c is allowed for using the same sine curve approach used in the interception function. All of the k and c parameters (seasonal means and variabilities) are estimated from relationships with soil texture and other soil properties as explained in the section on parameter estimation and table 4.1. The proportion of the sub-area contributing to runoff (IROP) is assumed to be equivalent to the proportion of the frequency distribution lying below the rainfall intensity (estimated using Simpson's rule) during a specific time interval (fig. 4.4).

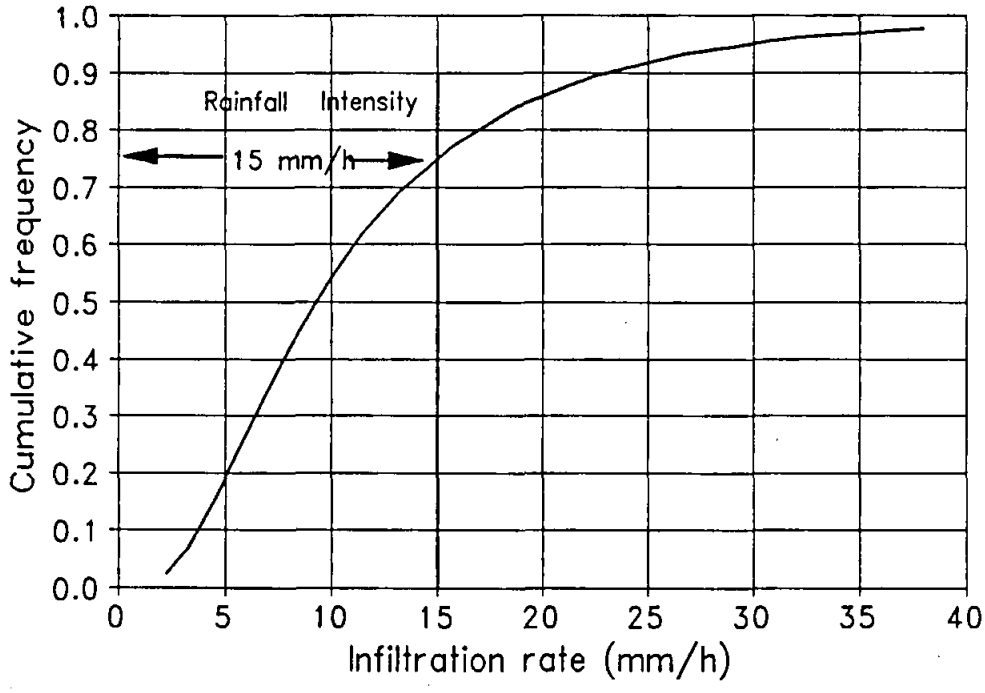

Figure 4.4 Cumulative frequency distribution of infiltration rates at time 1 hour from storm start (fig. 4.3). For a rainfall intensity of 15 mm h^{-1} the figure illustrates that the proportion of the sub-area contributing to infiltration excess runoff will be 0.75.

The calculation of the runoff rate (IRAIN, expressed as a proportion of the sub-area) accounts for the fact that the infiltration rate will be exceeded by the rainfall intensity by differing degrees over the contributing area (IROP). The initial amount of runoff generated by this component is passed to the soil moisture accounting component where it is subjected to re-infiltration along with some of the other runoff elements.

When the time step is set to be greater than the seasonally varying storm duration parameter (table 4.1), an iteration procedure is used to provide a better estimate of rainfall intensity to compare with the current infiltration rate.

Soil moisture accounting and runoff.

The total soil profile is divided into two layers (fig. 4.2); a surface layer 150mm deep and a lower layer the balance of the mean sub-area soil depth. To attempt to account for variations within individual sub-areas, the moisture content of the soils in both layers are represented by Normal distribution functions. The means of these distributions are calculated from the water balance equations using :

$$\Delta\text{mean} = \text{RAIN} + \text{Balance of Drainage} - \text{Evaporation} - \text{Runoff} \quad \ldots . \quad \text{Eq. 4.2.4}$$

where the 'Balance of Drainage' is the input from above (for the lower zone) less the output to a lower layer and the mean moisture storage is expressed relative to the soils porosity and the estimation methods for runoff and evaporation are explained below.

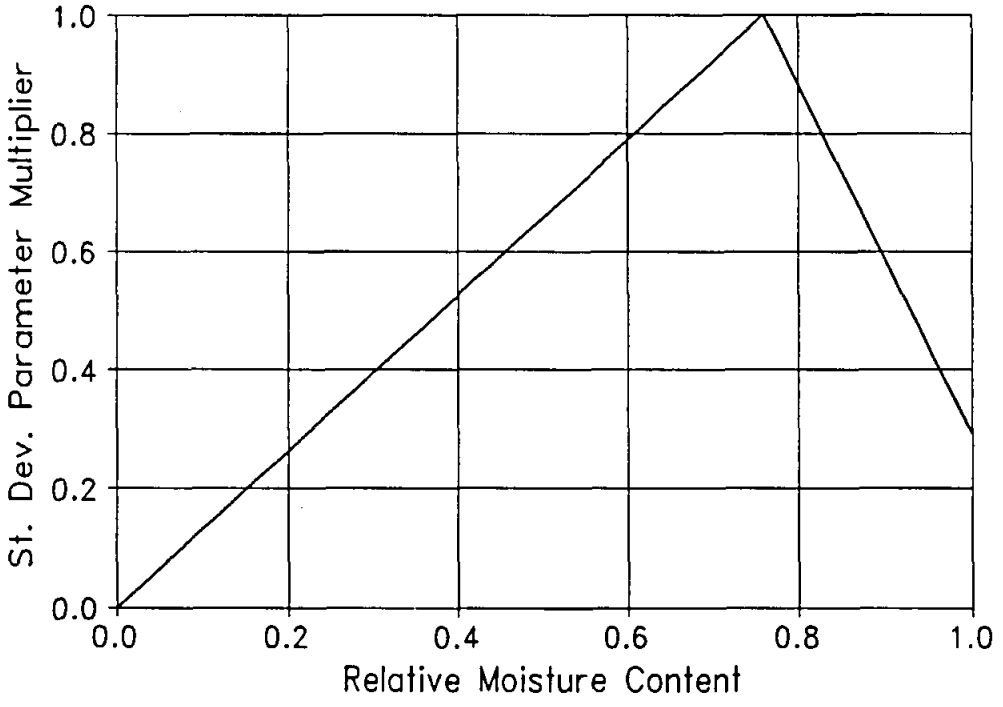

Figure 4.5 Illustration of the relationship between the mean relative moisture content and standard deviation of the soil moisture distribution. The values plotted on the vertical axis are multiplied by the nominal standard deviation parameter.

A single parameter is used to define the nominal standard deviation of the distributions, which is assumed to apply when the relative moisture content is 0.76, and reduces linearly

either side of that value (fig. 4.5) to zero at relative moisture contents of 0.0 and 1.1. The moisture content equivalent to the maximum standard deviation has been set at a fairly arbitrary value (0.76) based upon limited observations of soil moisture contents in a small (20ha) semi-arid catchment. It is possible that information from other areas may reveal that this figure is related to soil texture or other soil characteristics. The proportion of each soil layer that is saturated is assumed to be the area under the distribution which exceeds a relative moisture content of 0.98. Similarly, the proportion in excess of field capacity is the area under the distribution that exceed the ratio of field capacity to porosity. The effect is illustrated in figure 6 for mean relative moisture contents of 70% and 100% (with the standard deviation parameter = 0.2 and field capacity = 0.68 * porosity).

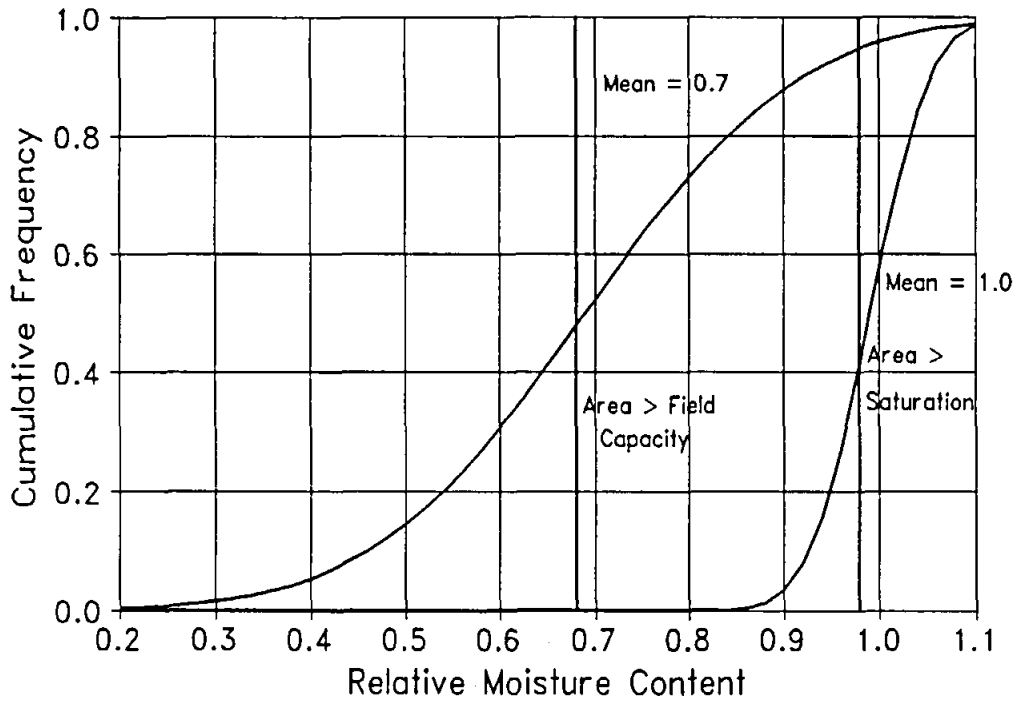

Figure 4.6 Cumulative frequency distributions of relative soil moisture content when the mean is 70% and 100% of porosity. The nominal standard deviation parameter is 0.2 and the proportions greater than field capacity (68%) and saturation (98%) are illustrated.

Figure 4.6 illustrates the proportions of the distributions which are above saturation (0.04 for the drier and 0.6 for the wetter conditions) and field capacity (0.52 for the drier and 1.0 for the wetter conditions). It is clear that the mean relative moisture content must be greater than 100% to achieve a saturated proportion of close to 1.0, implying that the mean cannot be constrained to be less than or equal to porosity. The mean value required to produce total saturation of either layer will depend upon the standard deviation parameter but will only be slightly higher than 100% as the standard deviation is very small in this region (fig. 4.5). As such conditions are rare, this deviation from reality is not considered to be serious.

The distribution functions merely provide estimates of the proportions of the sub-area soils that are above field capacity or saturation. These proportions are then used to estimate the parts of the sub-area which contribute to vertical drainage and runoff from source areas as explained below. However, the distribution functions do not account for the spatial position of such areas nor their vertical distribution in the soil profile. Spatial position could be important if the model is to be applicable to a wide range of situations, such as those where variable source areas occur adjacent to channels, as well as those where saturated areas are more related to the position of shallow soils. Similarly, the vertical position of saturated parts of the soil could be important. At the beginning of an event the wetter parts of a soil are more likely to be lower in the soil profile than in the middle of an event. The implication is that a similar saturated proportion should give rise to different size source areas and runoff quantities depending on the length of time that lateral and vertical drainage has been taking place.

To account for these two considerations a 'lateral distribution factor' (LDF) and a 'vertical distribution factor' (VDF) are calculated for each time step and combined with the estimates of the proportions greater than saturation and field capacity to estimate the final saturated source area, as well as the amounts of re-infiltration and drainage (fig. 4.7).

The LDF is designed to account for the likelihood that saturated parts of the soil are concentrated in valley bottom areas. LDF is constrained to lie between 0 and 1 and is incremented during each time interval by an estimate of the lateral drainage rate within the soil using a function of the lower layer moisture content, catchment slope, hydraulic conductivity, porosity, slope to valley soil depth ratio and time interval. It is then decreased as a function of the amount of water draining from the upper to lower soil layers. The effect is to produce high LDF values for consistently wetted soils with high lateral drainage potentials (typical of many humid areas), but low values where the soil remains dry for a large part of the time, or where drainage rates are low relative to the rate of drying through evaporation (typical of more arid areas).

The vertical distribution factor ($0 < VDF < 1$) is incremented in each time interval by the proportion of the upper layer draining to the lower layer and decremented by the proportion of the lower layer below field capacity. VDF therefore gradually decreases after storm events but increases as the upper soil zone becomes wet and promotes drainage at the start of an event. A low VDF value therefore represents moisture concentration in the lower parts of a soil layer. The LDF and VDF concepts are illustrated in figure 4.7 which shows a conceptualised hillslope cross-section, including the two soil zones, as well as a plan projection of a sub-area.

A soil 'seepage face' (SSF) is estimated as the product of the saturated proportion (LROP) of the lower layer moisture distribution and the LDF value. This is conceptualised as the extent of any residual source area which is related to antecedent conditions rather than the rainfall during the current or immediately past time intervals. If the groundwater level intersects the surface, the groundwater (GSF) and soil 'seepage faces' are considered to overlap and the largest of the two taken to be the total 'seepage face' (TSF) used to estimate saturation excess runoff (see below). The shaded area representing the saturated proportion in the upper plan diagram of figure 4.7 illustrates a 'seepage face'.

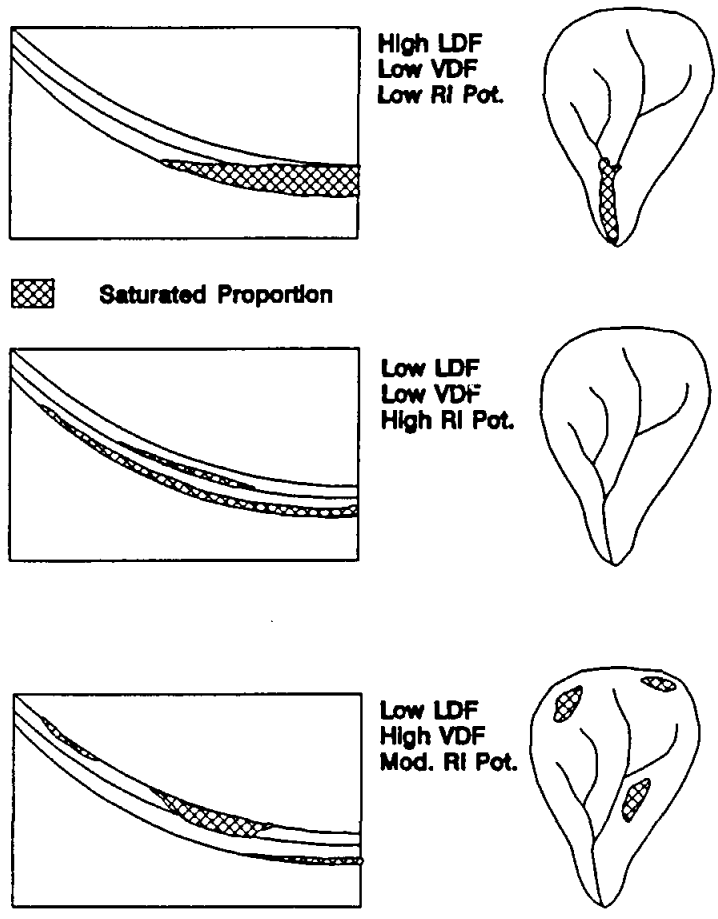

Figure 4.7 Illustration of the meaning of the LDF and VDF factors. RI Pot. refers to the the re-infiltration potential of runoff occuring from the saturated proportions shown. The upper part of the diagram is more typical of a humid catchment, while the lower two are more typical of semi-arid catchment situations.

Apart from the intensity controlled runoff component (previous section), the model simulates three other runoff components :

- Saturation excess runoff caused by rain falling on saturated areas.
- Saturated sub-surface flow re-emerging from saturated parts of the upper layer.
- Saturated lower layer sub-surface flow from the 'seepage face.

The intensity controlled runoff component and the first two of the above are subjected to a re-infiltration function based on the proportion of the upper layer that is not contributing to any form of surface runoff :

$$RIP = 1.0 - (UROP * VDF + IROP + TSF) \quad \text{Eq. 4.2.5}$$

where RIP is the proportion of runoff that re-infiltrates,

UROP is the proportion of the upper layer above saturation,
IROP is the proportion of the sub-area contributing to intensity excess runoff,
and RIS = 1.0 - RIP and is the proportion that does not re-infiltrate.

The components of runoff are then estimated as follows :

Saturation
Excess Runoff = RAIN * ((UROP * VDF) * RIS + TSF) . . . . . Eq. 4.2.6

Infiltration
Excess Runoff = RAIN * IRAIN * RIS . . . . . Eq. 4.2.7

Sat. Upper
Sub-Surface Flow = UROP * VDF * Ksat * SLOPE * dt * RIS . . . . Eq. 4.2.8

where Ksat is the soil saturated hydraulic conductivity (mm h^{-1}),
SLOPE is the sub-area mean slope (km km^{-1}),
and dt is the time interval (h)

Saturated Lower
Sub-Surface Flow = TSF * Ksat * CSLOPE * dt . . . . . Eq. 4.2.9

where CSLOPE is a slope factor which varies non-linearly between the channel slope, at low TSF values, and the catchment slope when TSF equals 1.0.

If there is available storage in the channel transmission loss zone (see later) at least part of the lower sub-surface runoff component will be absorbed.

The drainage components are estimated from the following :

Drainage from
the upper zone = (UFC - SSF - VDF*(LROP-SSF)) * Ksat * 0.5 * dt Eq. 4.2.10

where UFC is the proportion of the upper layer above field capacity,
and SSF + VDF*(LROP-SSF) represents the upper part of the lower soil zone that is saturated and therefore retstricts drainage from above.

Drainage from
the lower zone = LFC * KGsat * 0.5 * dt . . . . . Eq. 4.2.11

where LFC is the proportion of the lower layer above field capacity and includes corrections to account for any lateral concentration in valley bottom areas and the fact that drainage will not occur above the groundwater 'seepage face' (GSF),
and KGsat is the adjusted vertical aquifer hydraulic conductivity (see groundwater section).

The rate of half the saturated hydraulic conductivity parameter is used for vertical drainage

under partially saturated conditions following the recommendation of Bouwer (1969). The estimations account for the restriction that drainage will not occur into a deeper zone over those parts of the deeper zone that are saturated.

The final part of the water balance estimation procedure increments the upper moisture content with that part of the rainfall that does not contribute to either intensity controlled or saturation excess runoff after re-infiltration. The soil moisture accounting routines also include checks to ensure, amongst other things, that conservation of mass principles are adhered to. For example, the combined areas contributing to surface runoff cannot exceed unity and no drainage occurs to the lower layer if its mean moisture content already exceeds saturation.

Actual evapotranspiration.

The total amount of evapotranspiration that takes place from the soil is considered to be made up of three components :

The potential evaporation demand is partially satisfied from the saturated proportion of the upper layer ($AEVAP_I$ mm) at the potential rate :

$$AEVAP_I = PEVAP * UROP \quad \text{Eq. 4.2.12}$$

The remaining potential demand is then apportioned, as residual potential demands, to the non-saturated parts of the upper and lower ($RESP_U$ and $RESP_L$) soil layers based on an empirical power function of a seasonally varying crop factor (CROP).

$$RESP_U = (PEVAP - AEVAP_I) * 1.7^{-CROP} \quad \text{Eq. 4.2.13}$$

$$RESP_L = (PEVAP - AEVAP_I) * (1.0 - 1.7^{-CROP}) \quad \text{Eq. 4.2.14}$$

The division of the total residual demand ($PEVAP - AEVAP_I$) into the rates for the two soil layers is illustrated in figure 4.8.

The relationship between soil water content and actual evaporation for both layers is controlled by a non-linear function that accounts for the concept that for similar relative moisture contents, moisture in a clay soil is retained at higher tensions than in a sandy soil.

For $RAT < FC/POR$

$$EFACT = 0.9 * (1.0 - RAT + FC/POR)^{power} \quad \text{Eq. 4.2.15}$$

For $RAT \geq FC/POR$

$$EFACT = 0.9 - 0.1 * (RAT - FC/POR) / (1.0 - FC/POR) \quad \text{Eq. 4.2.16}$$

where EFACT is the proportion of the residual potential rate for each soil layer,
'power' is a function of FC/POR and the standard deviation of the moisture content distribution parameter,

RAT is the relative soil moisture content in each soil layer,
and FC/POR the ratio of field capacity to porosity.

The relationship between EFACT and the relative moisture content of either soil layer is illustrated in figure 4.9 for three values of FC/POR. Loss from the un-saturated part of the upper layer ($AEVAP_2$ mm) is then estimated from :

$$AEVAP_2 = RESP_U * EFACT_U * (1.0 - UROP). \quad \ldots\ldots\ldots \text{Eq. 4.2.17}$$

A similar function, which incorporates the crop factor, is used to estimate the actual evapotranspiration ($AEVAP_3$ mm) from the lower layer :

$$AEVAP_3 = RESP_L * EFACT_L * CROP. \quad \ldots\ldots\ldots\ldots\ldots \text{Eq. 4.2.18}$$

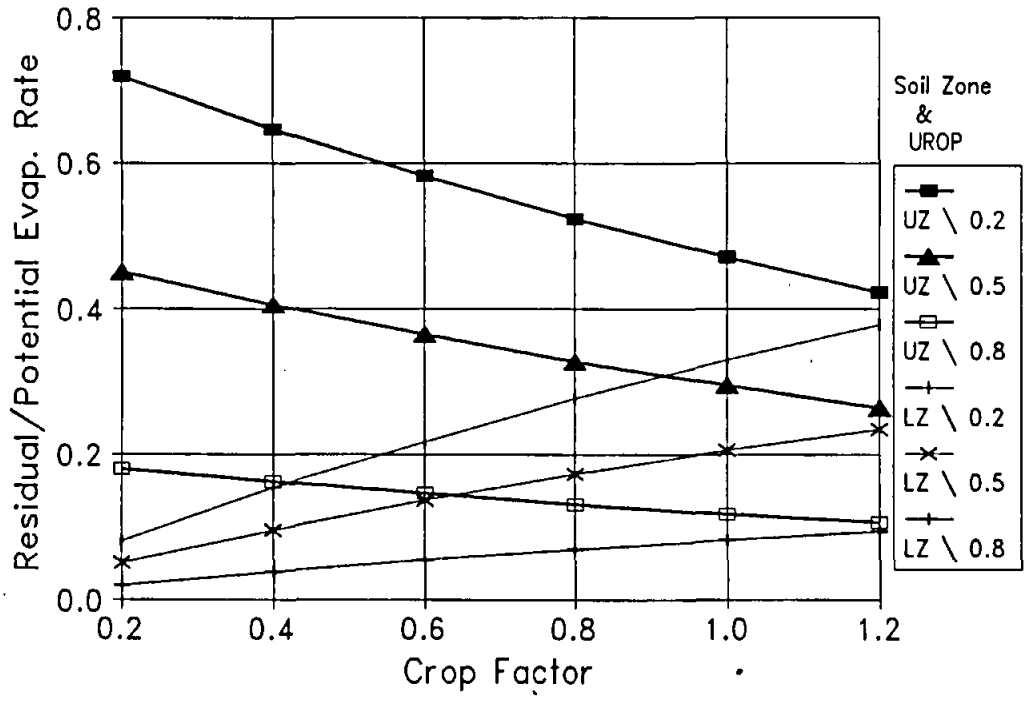

Figure 4.8 Illustration of the residual potential evaporation demand rates applied to the non-saturated proportions of the upper (UZ) and lower (LZ) soil zones for different values of the crop factor parameter.

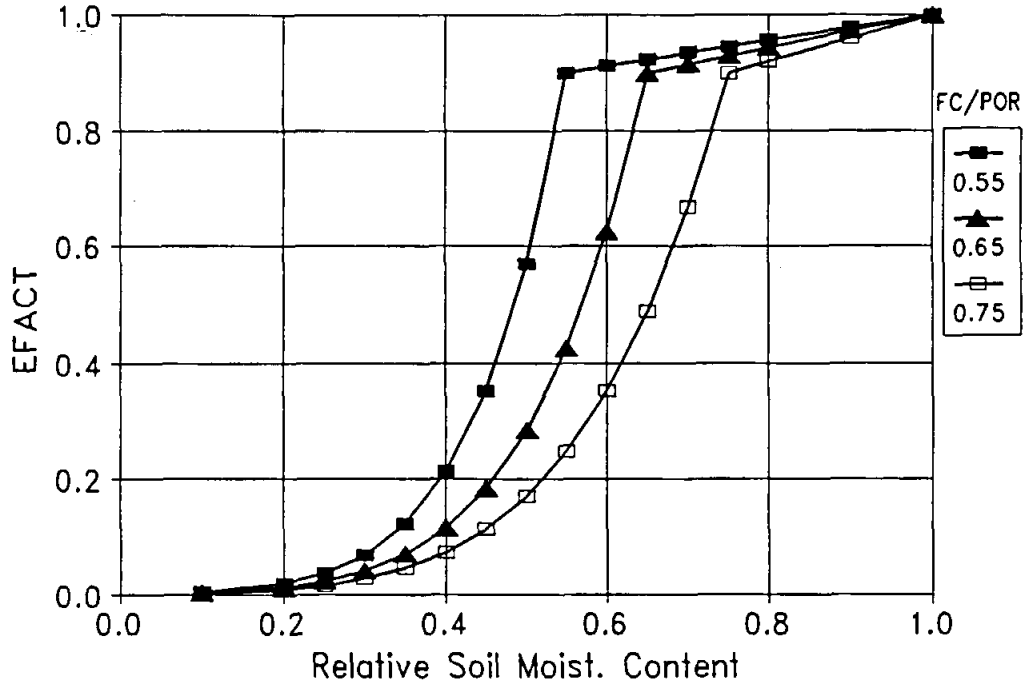

Figure 4.9 Illustration of the relationship between actual evaporation as a proportion (EFACT) of the residual potential rate for different soil types (defined by FC/POR) over the range of moisture contents.

Where sub-catchments have channel transmission loss zones, equations similar to 4.2.14, 1,5 16, and 18 are used to estimate their evaporative losses.

Groundwater-surface water interactions and recharge.

The groundwater-surface water interaction component consists of five functions designed to link the sub-catchment lower soil layer to aquifer storage. The physical processes simulated by these functions are:

- Drainage from the lower layer (equation 4.2.11) into a storage which conceptually represents percolating water which has not yet reached the water table.
- The re-emergence of percolating water as springs above the regional water table.
- The increment to groundwater resulting from recharge and the resultant rise in the water table.
- Groundwater seepage resulting from the intersection of the water table with the surface.

- Transfers into and out of aquifer storage by groundwater flow and abstraction.

Additions to groundwater occur as drainage from that proportion of the lower layer considered to be over field capacity at a rate referred to as the adjusted aquifer vertical hydraulic conductivity (KGsat):

$$KGsat\ (mm\ h^{-1}) = TM / DEPTH * S * 1000/24 \quad \ldots\ldots\ldots\ldots \text{Eq. 4.2.19}$$

where TM is transmissivity ($m^2\ day^{-1}$),
S is storativity or specific yield,
DEPTH is aquifer depth (m).

The use of storativity to adjust the conductivity value accounts for the fact that some of the potential recharge area may be underlain by unfractured rock or rock not hydraulically connected to the main groundwater body. This adjustment has been found to be particularly necessary in fractured rock situations, where the opportunity for drainage from even saturated soil layers is limited by the occurrence of surface fractures.

Water leaving the lower soil layer as recharge (equation 4.2.11) increments the percolating groundwater store (PSTORE in mm of water). Water in PSTORE is considered to be evenly distributed throughout the area above the water table (fig. 4.10). Water is transferred from PSTORE either as increments to the water table, transfers to adjacent sub-area PSTORE's, or baseflow directly into the stream channel. The re-emergence of percolating water as baseflow may reflect two processes lead to the development of subsurface seepage above the regional water table:

- Flow along geological discontinuities which impede vertical percolation and dip less steeply than the surface topography.

- Flow through fractures hydraulically connected with the surface.

The fraction of PSTORE which may re-emerge is determined by that proportion of the zone above the water table (PROP) that also lies above a groundwater drainage vector (DVECT) line which intersects the sub-area surface (fig. 4.10). The drainage vector slope represents the resultant of the lateral and vertical components of percolation. For example, drainage through an unconsolidated layer would be represented by a large vector slope (e.g. > 20), whereas lateral flow over a gently sloping impermeable horizon would have a low vector slope. For re-emergence to occur, the slope of the drainage vector must therefore be less than the mean catchment slope.

The rate of emergence is dependent on the degree of saturation in PSTORE and KGsat:

$$\text{Re-emergence (mm)} = PROP * PSTORE/TOTAL * KGsat * tdt \quad \ldots \text{Eq. 4.2.20}$$

where TOTAL is the maximum potential percolating store at the groundwater level

Losses from PSTORE to adjacent sub-areas (or outside the catchment) are determined using the same approach as for re-emergence. The fraction of water which may be transferred

through the percolating zone (PTRANS) is defined by the area above DVECT when the origin of DVECT is at the current groundwater depth minus PROP. Consequently, if the groundwater depth is above the surface PTRANS is equal to zero. Loss to other sub-areas can be sub-divided into two components determined by two outflow distribution vectors (table 4.1). The two directions of flow can be either into adjacent sub-areas or external to the total catchment.

Increments to the groundwater (GWATER) are calculated from the fraction of PSTORE which lies below DVECT, however, KGsat is corrected by an anisotropy adjustment:

GWATER (mm) =
(1-PTRANS-PROP)*PSTORE/TOTAL*KGsat/ANTPY*tdt . . . Eq. 4.2.21

where ANTPY is an anisotropy adjustment = $90°/Tan^{-1}$(DVECT),
with DVECT the drainage vector slope (km km^{-1}).

Since KGsat is calculated from transmissivity in eq. 4.2.19, it relates to horizontal conductivity. To take into account lower conductivities in the vertical direction in structured formations, the anisotropy adjustment corrects KGsat according to the lateral flow component during percolation.

Drainage from groundwater can occur as flow to other sub-areas, groundwater abstraction and seepage into the lower soil layer if the water table intersects this zone. The seepage rate is calculated using Darcy's equation, with the saturated 'seepage face' set equal to the length of intercept between lines representing the hydraulic gradient and the catchment slope (fig. 4.10). The conductivity is assumed to be the soil hydraulic conductivity and the gradient the mean catchment slope.

Groundwater transfers between sub-areas also use Darcy's equation. To account for increasing flow rates as the saturated depth of the aquifer increases, the transmissivity parameter is incremented as the water table rises above the depth defined by a rest water level parameter:

Transmissivity =
TM + (TM/DEPTH / ANTPY * S/SMAX * (RWL - GWD)) . Eq.4.2.22

where SMAX is an upper limit to storativity, defined as 0.2
RWL is the rest water level parameter
GWD is the current groundwater depth

The weighting of the transmissivity increment by S relative to SMAX and by ANTPY is designed to have different effects under various hydrogeologic regimes. In unconsolidated unconfined aquifers ANTPY will be low and S/SMAX will be high, consequently the adjustment to TM will become increasingly significant as the water table rises and the area conducting flow increases. Under confined conditions, however, recharge to the aquifer does not result in a significant increase in the cross-sectional area of flow, therefore, the transmissivity adjustment would be low. As confined aquifers have low storativities and would be characterised by a lower DVECT value due to lateral flow above the confining

layer, the S/SMAX ratio would be low while ANTPY would be high. Consequently, the adjustment to TM would be low.

The hydraulic gradient used in the groundwater flow equation also increases as the water table rises, being close to zero at the rest water level parameter and rising to a maximum defined by a regional groundwater gradient parameter. The lateral distribution vectors (table 4.1) are also used to distribute groundwater outflow into adjacent sub-areas or external to the whole catchment. These vectors can be set to either represent the strike(s) of the regional joint/fracture pattern in aquifers where flow is structurally controlled or the direction of the hydraulic gradient in porous aquifers.

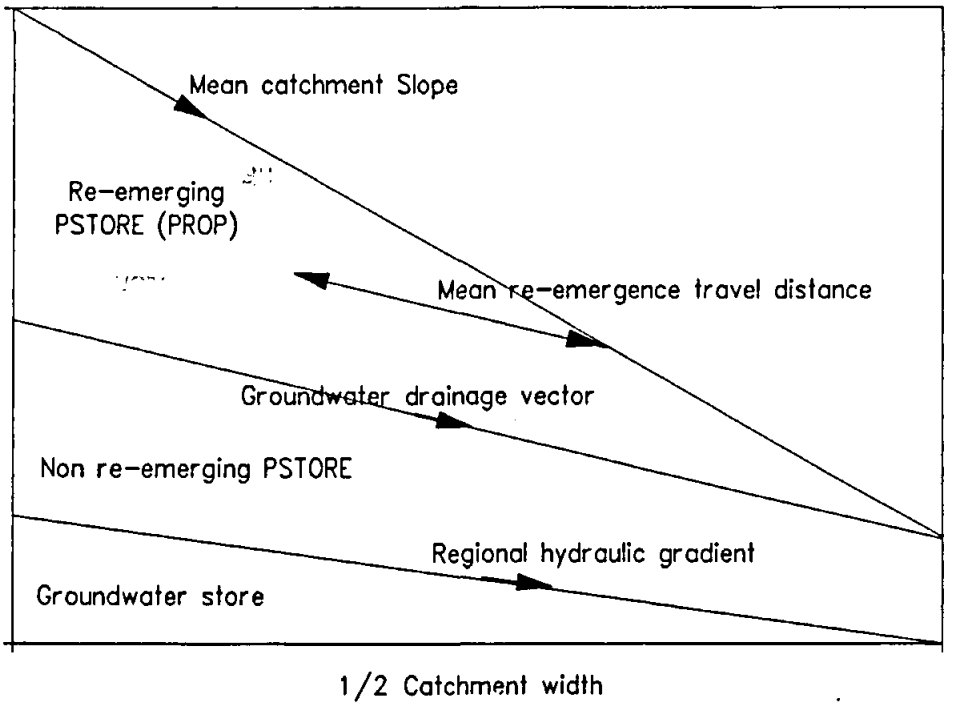

Figure 4.10 Conceptualised distribution of groundwater storage in relation to catchment slope, drainage vector and regional hydraulic gradient parameters.

Sub-area (catchment) routing.

This section includes three separate components; the retention of runoff by depression and dam storage and attenuation of runoff through routing within the sub-catchment. Dam storage is used to account for any impoundments (lakes, reservoirs and farm dams) that individually may have a small effect on runoff, but considered together may impact significantly on the long term volume of sub-catchment runoff.

The total depth of runoff first has to satisfy any available depression storage and then small dam storage. Evaporation (at the potential rate) from small dam storage is calculated after the surface area is estimated as a power function of stored volume. The storage available at any time, expressed as depth of runoff, is estimated from the volume and takes into account the proportion of the sub-area that is upstream of the dams. An additional parameter also allows the collective volume of dam storage to be reduced by a fixed daily draft.

Attenuation of the runoff generated within a sub-area is achieved using a non-linear storage routing function, using the solution recommended by Hughes and Murrell (1986).

$$S = K * Q^n \quad \text{Eq. 4.2.23}$$

where S is storage, Q discharge and K, n parameters.

The parameter K is allowed to vary seasonally in the same way as several of the parameters referred to earlier. Hughes and Murrell (1986) refer to a technique developed for a FORTRAN program operating in a main frame computer environment. In the model referred to here, a similar algorithm (Runge-Kutta formula) in 'C' language code has been drawn from Press et al. (1988). The advantage of this solution technique is that the number of iterations required to achieve an accurate result is established automatically.

Channel transmission losses.

Before being subjected to channel transmission losses, all runoff generated within a sub-catchment is added to that generated from upstream areas. The cumulative time since flow began (up to a maximum of 2h) is used to estimate an initial channel infiltration rate using the same type of equation as for rainfall infiltration.

$$\text{Initial infiltration rate} = CHk * CHc * T^{(1-CHk)} \quad \text{Eq. 4.2.24}$$

where CHk and CHc are the parameters of the Kostiakov (1932) infiltration equation.

Two weighting factors are then applied to the initial estimate of the infiltration rate. The first (WF1) represents an infiltration decay factor to account for a declining hydraulic gradient below the surface as the channel loss storage is incremented. WF1 is estimated as a power function of the ratio of the currently available channel loss storage (CLS mm) to the maximum (LSMAX mm) as follows :

$$\text{Total soil volume} = SA * SWSTORE / \text{Porosity} \quad \text{Eq. 4.2.25}$$

and also

$$\text{Total soil volume} = (SA-CHA) * SSD + CHA * VSD \quad \text{Eq. 4.2.26}$$

where SA is the total sub-catchment area (km^2),
SWSTORE is the sum of the soil zones moisture storage at saturation (mm),
CHA (km^2) is a parameter defining the flow infiltration area,
SSD is the mean soil depth on the slopes,
VSD is the mean soil depth in the valley bottoms,
and SA-CHA = Area of slopes.

The flow infiltration area represents the maximum area over which channel losses are assumed to occur and may be the channel bed area, or a floodplain area if overbank flows are known to occur. Dividing by valley soil depth and re-arranging the equation gives:

$$LSMAX = SA * SWSTORE / (CHA + (SA - CHA) * SLV) \quad \text{Eq. 4.2.27}$$

where SLV is a parameter representing SSD / VSD.

Thus :

$$WF1 = (CLS / LSMAX)^{CLP1} \quad \text{Eq.4.2.28}$$

where CLS is the currently available storage,
and CLP1 is an empirical power parameter.

The second weighting factor (WF2) represents a correction to adjust the flow infiltration area parameter to account for variations in flow width and depth with upstream inflow and is calculated from :

$$WF2 = (Q * Manning's\ n / CSLOPE^{0.5})^{CLP2} \quad \text{Eq. 4.2.29}$$

where Q is the mean upstream inflow ($m^3\ s^{-1}$) during a single time step,
CSLOPE is the channel slope,
and CLP2 is an empirical power parameter.

With

$$\text{Channel losses } (m^3) = \text{Infiltration rate} * WF1 * WF2 * CHA * dt \quad \text{Eq.4.2.30}$$

Although both weighting factors are based on some difficult to quantify empirical parameters, they do represent the processes that are expected to occur during the process of channel transmission losses. Further research into improved channel transmission loss algorithms is currently in progress at Rhodes University.

Checks are carried out to ensure that no more is lost than is available and that the available storage is not exceeded. A function is also included to allow the channel loss storage to drain to groundwater using the same approach as for the lower soil zone. Similarly, evapotranspiration can occur from the channel loss storage zone (see actual evaporation routine).

During periods of zero channel flow, the level of storage in the channel loss zone is gradually adjusted to the same relative moisture content in the soils of the sub-catchment as a whole. This allows the drying of the channel loss zone to lag behind the overall drying of the sub-catchment. During any period when the sub-catchment soils are wetted by rainfall, without significant runoff occurring, increasing storage in the channel loss zone will similarly lag behind.

If a seepage face is present in the lower soil zone and there is spare capacity in the

transmission loss zone, the drainage occurs to the transmission loss zone and not to the channel.

Channel routing.

The attenuation component of channel routing, from one sub-catchment to the next downstream, is achieved using the same form of storage-routing equation as for catchment routing described earlier. An additional parameter specifies the delay component, or time shift between runoff generated in any sub-catchment and its appearance as a contribution to flow at the outlet of the whole catchment. Some problems have been experienced with the use of the non-linear storage-discharge equation solution method at low K values and high values of runoff. This has been identified as at least partly related to the variable time interval. Consequently, an alternative function can be selected which allows the user to 'turn off' channel routing.

4.2.3 Parameter estimation routines.

HYMAS includes a file of brief descriptions for over 90 standard physiographic variables. Some are primary variables (catchment area, slopes, proportions of sub-catchments under different soil or vegetation covers, etc.), which are quantified from maps, air photos, field data or other sources and some are secondary variables (indices of soil or vegetation characteristics, etc.) which are estimated from the primary ones. The file also contains Reverse Polish notation equations defining the secondary variable estimation equations. HYMAS also includes procedures for processing digitised topographic data to calculate the values of some primary physiographic variables. The details of these procedures are explained more fully in the HYMAS user manual.

The model contains 48 parameters, of which 9 have summer and winter values, making a total of 57 which have to be quantified. The parameters can be divided into three main types.

- Those (4) that can be directly measured from normally available information (e.g. the size and shape parameters).

- Those (46) that can be measured in the field, given sufficient resources, or estimated using relationships with some of the physiographic variables. The reliability of these estimates will inevitably depend upon the applicability of the estimation relationships, as well as the availability of information to quantify the physiographic variables (e.g. most of the soil and groundwater parameters).

- Those (7) that are largely empirical and difficult to determine except through calibration (e.g. channel transmission loss power parameters).

The three evapotranspiration parameters are largely empirical, although the crop factor is a physically based index based on vegetation type and designed to reflect rooting depth and density. Typical values have been generated for southern African conditions by the Department of Agricultural Engineering at the University of Natal (Schulze, Pers. Comm.).

The three interception parameters are derived by dividing the sub-catchment up into broad classes of vegetation cover (table 4.1).

The infiltration function is controlled by five parameters. The storm duration parameter is used to dissaggregate rainfall during daily time intervals and may be evaluated from regionalised information on typical storm durations. The infiltration k and c parameters are determined from the areal distribution of five soil texture classes and adjusted by indices of macropore development, soil structure, sand grade, compaction, surface organic matter and roughness (table 4.1). The range of k and c values has been designed to bracket the infiltration curve shapes defined in the literature for different soil textures. An example is the theoretical range of Green-Ampt parameters found in Rawls and Brakensiek (1983).

Soil moisture retention and redistribution, as well as the main runoff generation component, is regulated by six parameters. Soil moisture storage in the upper 150 mm soil layer is determined from porosity, which in turn is estimated from the distribution of soil textures, weighted by indices of organic content, structural development and sand grade. The capacity of the lower soil zone is determined from the same porosity estimate and mean soil depth less 150mm. A default field capacity value is estimated from typical values reported for the five texture classes (Schulze, et al., 1984) and saturated hydraulic conductivity from indices of permeability, macropore and structural development, organic content and sand grade. The soil moisture variability parameter is derived from the weighted coefficient of variation of soil depth, where the weighting factor is partly dependent on permeability.

The groundwater component of the model contains 11 parameters many of which can be determined from estimates of transmissivity, aquifer depth, storativity and water levels. The two outflow vectors allow percolating water and groundwater outflow to be routed in up to two directions, either internal or external to the total catchment.

The remaining parameters listed in table 4.1 are discussed in the previous sections which outline the model components.

4.2.4 Limitations of the model

The more complex a model becomes, the greater are its information requirements and the greater are the expectations of the model's ability to accurately simulate the details of a catchments hydrology. However, there are few situations where enough information is really available and any model is necessarily an approximate conceptualisation of reality. The VTI model uses a sub-catchment distribution system and although attempts have been made to incorporate effects of spatial variations within sub-areas, there are inevitably limitations to this approach. A number of simplyfying assumptions have been made to allow the authors conceptualisations of physical hydrological processes to be translated into mathematical algorithms and it is never possible to state categorically that these assumptions will apply in all catchment situations.

Table 4.1 Variable Time Interval model parameters, descriptions and brief explanations of their derivation (the 'S' indicates that two values are specified, defining the seasonal extremes of the parameter, while the '*' indicates those parameters which are largely empirical and difficult to estimate from available information).

PARAMETER NAME		DESCRIPTION AND/OR DERIVATION
Shape and size parameters :		
Downstream sub-area number		Quantified from topographic maps using GIS (or similar) software and extracted directly from the physiographic data file.
Sub-area area - SA (km^2)		
Sub-area shape (L/W)		
Mean sub-area slope		
Evaporation and interception parameters :		
Evaporation reduction EA	*	Scaling and power factors in $EA/rain^{EB}$ used to reduce potential evaporation during rain periods.
Evaporation reduction EB	*S	
Crop factor - CROP	S	Veg. factor in actual evaporation component.
Proportion vegetation cover - COV	S	All derived from the proportions of the sub-catchment under five different vegetation cover classes (dense tree, bush/sparse tree, dense crop/ground, sparse crop/ground and bare soil).
Leaf area index - LAI	S	
Canopy capacity - ICAP	S	
Infiltration excess runoff parameters :		
Storm duration factor (h)	S	Storm duration to distribute daily rainfall.
Infiltration k	S	Inf. curve parameters based on texture and modified for structure, macropores, sand grade, compaction, surface organics and surface roughness indices.
Infiltration c (mm min^{-1})	S	
Infiltration k variability		Variability of Inf. curve parameters based on texture and compaction (K & C), structure, macropores, sand grade, surface organics and roughness (C).
Infiltration c variability		
Main moisture accounting and runoff generation parameters :		
Upper soil store (mm)		From estimate of porosity in upper 150 mm.
Lower soil store (mm)		From estimate of porosity and mean soil depth.
Field capacity / porosity - FC/POR		Ratio of estimated field capacity to porosity.
Slope/valley soil depth - SLV		Ratio of soil depth on slopes to valley bottoms.
Mean soil hydraulic conductivity ($mm\ h^{-1}$) - Ksat		Estimated from a permeability index based on texture, macropores, organic content, structure and sand grade.
St. deviation soil moisture distribution		Derived from soil depth and permeability characteristics.

Groundwater interaction parameters :		
Groundwater outflow dist. vector 1		User defined vectors to distribute groundwater outflows from sub-catchment (integer part = direction, decimal part = proportion distributed in the direction).
Groundwater outflow dist. vector 2		
Groundwater drain. vector (DVECT)		User defined vector slope of percolating drainage.
Adjusted aquifer hydraulic conductivity (mm h^{-1}) - KGsat		Derived from transmissivity, aquifer depth and storativity estimations.
Max. regional hydraulic gradient		User defined
Storativity - S		Estimates of groundwater parameters applicable during dry season (lower or 'rest' level of groundwater table). Level taken from sub-catchment outlet height.
Transmissivity - TM (m^2 d^{-1})		
Rest water level (m)		
Groundwater demand (Ml day^{-1})		User defined
Groundwater flow velocity - GWVEL (m h^{-1})		Derived from other aquifer parameters (not used in the current model version)
Initial Groundwater depth (m)		User defined initial condition.
Sub-area routing parameters :		
Max. depression storage (mm)	*	User defined
Max. small dam storage (Ml)		Quantified from topographic maps or air photos and extracted directly from the physiographic data file.
Area above small dams (%)		
Area-volume A (Area = A.Vol.$^{B)}$		Scale and power parameters in the relation between dam area (km^2) and volume (Mill. m^3).
Area-volume B		
Demand from dams (Ml day^{-1})		User defined
Sub-area routing constant - K	S	Derived from indices of slope, permeability and infiltration rates.
Sub-area routing power - n		
Channel transmission loss parameters :		
Channel losses power - CLP1	*	User defined power in channel loss equation.
Flow infiltration area - CHA (km^2)		Derived from channel length and width
Manning's n * $slope^{-0.5}$		Flow weighting factor in channel loss equation.
Channel infiltration - CHk		Derived in a similar way to the soil infiltration parameters.
Channel infiltration - CHc (mm min^{-1})		
Channel infiltration-storage power - CLP2	*	User defined power parameter relating channel inf. rate to channel loss storage.
Channel routing parameters :		
Channel routing delay (h)		Derived from channel reach distance, roughness and time of concentration characteristics.
Channel routing constant		

While every attempt has been made to use parameters which have some direct physical meaning in the context of a sub-catchment type distribution system, there are a number of model parameters that are totally empirical. These form part of the model because it has not been possible to find more physically based substitutes that can realistically be evaluated from information which is available even in ideal situations. One reason for this is that the operation of some of the processes being simulated are not sufficiently understood at the spatial scale of the model. An example of this is the transmission loss component which contains several difficult to estimate empirical parameters.

Even those parameters which have direct physical meanings have to be estimated from a wide variety of different types of information source. The parameter estimation routines included as part of HYMAS have been based on information and relationships found in the literature. A great deal of this information is based on case studies carried out in small areas, where the full details of the physical characteristics of the area are not reported. In integrating these seperate sources into parameter estimation routines which are designed to be fairly comprehensive, it is inevitable that simplyfying assumptions are made and a great deal of 'smoothing' is necessary. Users are therefore warned that the parameter estimation routines are mainly guidelines to obtaining initial estimates of the parameter values.

The only initial value quantified in the parameter set is the groundwater level. Other initial values are quantified within the model using some assumptions of the 'average' conditions that are expected to occur. Examples are the soil moisture storages and the level of the percolating water store. The model developers accept that the assumptions made will not be valid for all situations and that a 'warm up' period of modelling may be necessary to allow some of the internal model state variables to find their own acceptable levels. The length of time required will be extremely variable and may be highly dependent on the charateristics of the initial part of the input rainfall time series. For example, a large event at the start of the modelled period may be poorly simulated itself but establish acceptible levels for the state variables for subsequent periods.

Although the model has two soil layers, their characteristics are defined by one set of parameters. This has already been found to be a problem with soils which have very different textural properties between the upper and lower horizons (duplex soils for example). To correct this problem is relatively simple, but would be carried out at the expense of including more parameters and the need to evaluate additional physiographic variables.

The adjusted aquifer hydraulic conductivity parameter is particularly difficult to estimate in fractured rock aquifers as it must take into account the likely spatial correspondence of saturated lower soil layers and upper aquifer fracture zones. In addition, the model does not contain any facility to add external (apart from other sub-areas) groundwater inflows to sub-areas at present. If such inflows constitute an important component of the aquifer water balance, the only way to account for them would be to adjust the maximum regional hydraulic gradient parameter and reduce the resulting groundwater outflow. This could, of course, have implications for adjacent sub-areas.

The model is designed to be operated with variable time intervals that account for the variable rates at which processes operate during different rates of rainfall input. However,

it is also recognised that rainfall data with time resolutions of less than one day are not readily available. There are routines within the model to compensate for the fact that it may be operated with just daily rainfall inputs, but the effectiveness of these, compared to running the model with higher time resolution rainfall data need to be further evaluated. Hughes (1993) carried out some tests using data from two semi-arid areas where there are extreme variations in rainfall intensity over short periods. The conclusions indicated that the model will not work very successfully with just daily rainfall in these situations. Two approaches to solving this problem are possible. The first is to modify the model to try and account for these effects and the second is to use or develop a technique for disaggregating the daily rainfall data before using them as input ot the model.

At present there are few water consumption and abstraction routines included in the model and where they exist they are highly simplified. For example, the small dam routine is part of the sub-area routing procedure and cannot cater for small dams on the main channel, through which upstream runoff would be routed and potentially consumed. Similarly there are no routines to allow 'run of river' abstractions, nor for integrating an abstraction demand to be satisfied from a combination of surface and groundwater, depending upon availability. These issues are expected to be attended to in later versions of the model and will be included as the need for them arises in practical applications.

This section has identified some very general limitations of the VTI model, while some of the later sections of this report, where several applications of the model are discussed, will identify some more specific problems.

4.3 MULTIPLE RESERVOIR SIMULATION MODEL

4.3.1 Background to the model development

In water resource planning and management there is often a need for simulation models that allow long time series of available rainfall and evaporation data to be used to generate similar length series of catchment runoff data, groundwater levels or reservoir storage volumes. Once such models have been calibrated (if necessary) and validated they can be extremely useful to examine the effects of changes in such as, upstream land use, gross water requirements or the operating rules and management approach to water utilization as well as examining such things as the frequency of drought conditions of different severities or storage-yield relationships.

In practice, the choice of which type of simulation model to use is commonly constrained for several reasons. In the field of practical water resource planning, there may be insufficient available data to determine the parameter values of a complex model or insufficient time and funds to collect such data (Hughes, 1991). Similarly, the resolution, accuracy and reliability of the results obtained from the careful application of simpler models may be adequate for the purposes of long-term planning and the development of management strategies. It is extremely difficult to generalise, as the specific requirements and amount of available information will dictate the best choice of model. The extensive use and general acceptance of the 'Pitman' model (Pitman, 1973) for water resource planning in South Africa is a testament to the principle that users will often prefer a relatively simple model with a proven track record to a more complex one whose abilities have not been thoroughly demonstrated.

This section of the report describes a reservoir simulation model based on a monthly time step and using the same basic water balance approach adopted by the developers of the RESSIM model (Middleton et al., 1981). The original model has been expanded to allow several closely linked reservoirs to be simulated together and incorporates a number of functions to describe the format of the linkages. The incentive for modifying the original RESSIM model derived from several requests to the Institute for Water Research at Rhodes to assist in determining the yield that could be expected from a group of several dams that form part of the same system. The developments have attempted to avoid including unnecessarily complex algorithms and to use parameters whose values can be evaluated from generally available information. It therefore remains as relatively simple and easy to operate as the original RESSIM model, but contains additional functionality to allow more complex water resource schemes to be simulated. The details of the model and some examples of its application have been published elsewhere (Hughes, 1992).

4.3.2 The reservoir model structure

The water balance of a single reservoir may be described by the following equation :

$$dS/dt = Qin - Qout + P - E - Sp \quad \text{Eq. 4.3.1}$$

where dS/dt represents the rate of change of storage in the reservoir;
Qin represents the inflow volume to the reservoir and is made up

		of natural inflow from the upstream catchment area (Qcin) and regulated input from other sources (Qrin);
	Qout	represents water released to other reservoirs (Qrout) and drafts to consumers (Qdout);
	P	precipitation onto the reservoir surface;
	E	evaporative loss from the surface;
and	Sp	uncontrolled overflow or spillage from the reservoir.

The time series of natural inflow for each reservoir (Qcin) could be derived from observed data at gauging stations or may be simulated using a suitable modelling approach. Within Southern Africa, the so-called Pitman model (Pitman, 1973) or the more up to date version of the same model contained within the water resources systems model, WRSM90 (Pitman and Kakebeeke, 1991) are appropriate for this purpose. Other deterministic rainfall-runoff or stochastic streamflow models could also be used.

Time series of precipitation data (P) are available at a large number of sites using the Weather Bureau monthly rainfall data base accessible via the Computing Centre for Water Research (CCWR) at the University of Natal, Pietermaritzburg. A composite time series using several gauges, as well as gridded values for median monthly rainfall can be developed using the standard HYMAS routines referred to earlier in this report or the HYMAS user manual. Similar records of pan evaporation (E) are available from the same source but at far fewer sites and usually shorter record lengths. Alternatively, the model allows a mean monthly distribution of pan evaporation values (corrected to represent free water surface area evaporation depths) to be used. Information on regional values for southern Africa are available in the Surface Water Resources of South Africa volumes (e.g. Middleton et al., 1981), while information at a more detailed spatial scale is available from the work being undertaken at the Department of Agricultural Engineering, University of Natal, Pietermaritzburg (Schulze and Maharaj, 1991).

Draft information (Qdout) can also be supplied as a time series of monthly requirements or as a mean monthly distribution. If the latter approach is used, it is also possible to define up to five reserve levels (expressed as a % of reservoir capacity) and associated lower monthly distributions of lower drafts. If the reserve level is specified as greater than 100%, the parameter value will be reduced by 100% and the model will assume that the reserve level is to be based on the total water stored in all dams. Otherwise, the reserve level will be based only on the individual dam. There is therefore reasonable flexibility in the users ability to define the draft operating rules of the individual reservoirs in the system.

The remaining time series (Qrin, Qrout, Sp) are calculated within the model using algorithms defined by the values of some of the model parameters. A complete list of the parameter set is given in the next section, while the details of the algorithms used to control the input, interchange and output of water in the reservoir system are discussed below.

Draft calculations.

The required draft may be specified in two different ways. The first is by simply specifying the draft as a monthly volume (either as an input time series or as a mean monthly distribution). The second is to specify the area of land (Parameter 8, see table 4.3) that the

reservoir is to be used to irrigate as well as information on the monthly required depth (mm) of irrigation water. A further parameter (9) specifies the proportion of monthly rainfall input effective rainfall) that contributes toward satisfying irrigation requirements. The required draft from the reservoir is the remaining amount of irrigation water required.

Thus:

$$Qdout = IA * (ID - Par9 * P) * 10.0 \quad \text{Eq. 4.3.2}$$

where Qdout — actual required draft in one month (m^3);
IA — defined irrigation area (Parameter 8, ha);
ID — required depth of irrigation water (mm);
and Par9 * P — effective rainfall on the irrigation area (mm).

Clearly, if the effective rainfall is equal to or greater than the irrigation requirements a zero draft will result. Similarly, if more water is required than available, Qdout will be reduced to the amount available.

The storage volume at the end of the previous time step is temporarily updated to include natural inflows, regulated inflows from reservoirs higher in the system and the first estimate of the usable draft. This new volume is used to estimate the surface area using :

$$Area\ (km^2) = Par5 * Volume\ (10^6.\ m^3)^{Par6} \quad \text{Eq. 4.3.3}$$

where Par5 & Par6 scale and power parameters, respectively, in the reservoir area - volume relationship.

The volume of evaporation is estimated from the product of the current reservoir surface area and the net evaporation depth (evaporation - rainfall). The new storage volume is then further adjusted to account for evaporative losses. If the calculated volume is less than dead storage (Parameter 3), the achieved (or usable) draft volume is adjusted downwards to compensate.

Spillage calculations.

Spillage is assumed to occur if the above components of the water balance equation result in a stored volume exceeding the dams defined capacity (Parameter 1 adjusted during the time series by Parameter 4). As this spillage could be utilised by other reservoirs lower (further downstream) in the system, it is necessary to specify the components in the correct order. Spillage can only contribute to reservoirs which have a higher number in the ordering system (i.e. Dam 1 can spill to Dams 2 and 3, but Dam 3 cannot spill to Dams 1 and 2). Regulated releases (see below) are treated in a different way. The calculated volume of spillage can be distributed through a maximum of three downstream dams on the basis of several parameters related to the spilling dam as well as the receiving dams.

Natural flows are known to be temporally variable and it is not straightforward to adequately account for variations in the actual monthly time distribution of flows within a monthly time step model. A pragmatic approach has been adopted that uses a single parameter (19)

referred to as the spill time distribution factor. This parameter can assume values between a maximum of 30 and a minimum that is only constrained to be greater than zero. A low value implies a very 'flashy' regime where the total volume of spillage is assumed to occur over a much shorter time period than the model time interval of one month. A value of 30 assumes an even distribution of spillage during the month. The use of this parameter to control re-distribution is explained below.

Parameter 20 is used to specify the volume of compensation flow released from a dam each month. This flow is added to any spillages that occur before the downstream dam calculations are performed.

Each of the specified downstream dams has a priority level associated with it that controls the maximum proportion of the spillage that can be assigned to that dam. If the priority level for a downstream dam is specified as zero, it is assumed to have a direct channel link and spillages can be received in an unrestricted manner. If the sum of these priority levels is set to less than 100%, the remainder of the spillage will pass downstream (unless one or more of the downstream dams has been specified as directly connected). Each of the receiving dams also has two other parameters which potentially control the amount of spilled water and regulated releases that they can accept. The first of these represents the maximum storage capacity (18) to accept controlled spillage or regulated releases. The second parameter (16) represents the monthly capacity of the system (canals or pipelines for example) used to transfer water between the dams.

The distribution of spillage is therefore controlled by four factors:

- the capacity of the distribution system (if not a direct channel connection),
- the assumed monthly distribution of the spillage,
- the allowed maximum capacity of the receiving dam (if not a direct channel connection),
- the priority level of shared distribution (0 for a direct channel connection).

The spill time distribution factor is used to correct the capacity of the distribution system to absorb natural overflows from an upstream reservoir. An example is the best way to explain the approach used.

Suppose there are three dams in a system, an upstream balancing dam (Dam 1) supplying two others via weirs across the outflow channel and two canal systems. Table 4.2 lists some of the parameter values and variables at a specific step in the simulation. Using Parameter 18, Dams 2 and 3 can be increased by spillage from Dam 1 to maximums of 540 and 320 Ml, indicating that they may accept 340 and 20 Ml, respectively. The spillage is corrected to 10*30/15 = 20 Ml (using the spill time distribution factor) for the purposes of comparison with the inflow capacity values.

The priority levels will allocate up to 14 Ml (70%) and 6 Ml (30%) of adjusted spillage to Dams 2 and 3 respectively. The former is greater than the capacity of the relevant canal and

only 10*15/30 = 5 Ml is received by Dam 2. The latter is less than the capacity of the canal feeding Dam 3 and 6*15/30 = 3 Ml can be passed through to Dam 3. Both amounts will not raise the dam levels above their defined receiving limits and therefore no further restrictions are applied.

Of the available 10 Ml of spillage, 5 Ml will be used in Dam 2, 3 Ml for Dam 3 while 2 Ml will continue downstream. The remaining capacities of the two canal systems are :

supplying Dam 2, 5 Ml (10 - 5)
supplying Dam 3, 17 Ml (20 - 3).

These capacities are available to accept regulated releases into the two dams which are now at storage volumes of 205 and 313 Ml respectively.

Table 4.2 Some parameters and variables for a three dam system example.

Parameter or variable.	Dam 1	Dam 2	Dam 3
Par1 - Capacity (Ml)	1000	600	400
Par16 - Inflow capacity (Ml)	N/A	10	20
Par18 - Limit for receiving dam input (% capacity)	N/A	90%	80%
Par19 - Spill time distribution factor	15	15	15
Canal take-off Priority level	N/A	70%	30%
Storage before spill and release (Ml)	1000	200	310
Spillage (Ml)	10	N/A	N/A
Storage after spillage distribution (Ml)	10	205	313
Available for regulated release (Ml)	900	N/A	N/A
Regulated inflow (Ml)	N/A	5	7
Storage after regulated inflow (Ml)	988	210	320

Had the priority levels of Dams 2 and 3 both been set to 100 %, which implies a 'first come first served' basis for allocation, the inflow to Dam 2 would be unaffected as it is limited by the capacity of its canal. The available inflow to Dam 3 would then be 5 Ml, which even after correction for the spill time distribution would still be below the capacity of 20 Ml, and Dam 3 could have absorbed the complete amount, leaving no spillage to continue downstream.

Regulated release calculations.

Much the same procedure used to estimate the distribution of spillages is used for regulated releases. An additional parameter (17) for the releasing dam is involved, which is the maximum amount of water that can be released, expressed as a % of the available volume.

The example used in the previous section can be continued with the additional assumption that the value of Parameter 17 for Dam 1 is 90%, suggesting that 0,9 * 1 000 = 900 Ml is available for release. The canal take-off priorities suggest that maximums of 630 and 270

Ml could be released to Dams 2 and 3 respectively. However, there is only 5 Ml of canal capacity remaining for Dam 2 and therefore its stored volume will increase to 210 Ml. The remaining inflow capacity to Dam 3 is 17 Ml, but Parameter 18 indicates that it can only be raised to 320 Ml, such that only 7 Ml is released to this dam. It should be noted that other components of the water balance (drafts, rainfall and evaporation) are ignored in this example for the sake of simplicity.

The way in which the release calculations are described above demonstrates releases to downstream dams (higher values in the dam numbering system). However, the model also accommodates regulated releases (not spillages) to upstream dams. No additional parameters are required to achieve this, but it should be noted that the releases will only be included in the water balance of the upstream receiving dam in the time interval after the releases occur.

Other considerations.

The full parameter list include those that allow a relatively simple economic analysis of the dam system to be carried out. The initial capital costs of the dam and water supply works (irrigation canals, for example) can be specified, as well the repayment interest rate and the repayment period (or design life). Two further parameters specify the profit value of successful supply and the penalty cost for supply failure. These parameters are not used within the model itself but by a separate program that summarises the performance of the reservoir system over the period of time being simulated.

If it is required to simulate a system of upstream inflows and dams that is too complex for a single set-up of the model a 'batch mode' operation is included as part of HYMAS. This allows several set-ups of either the same, or different, models to be linked together and includes a set of time series management routines as well. An example might be where two dams are far enough apart that natural inflows between the dams need to be simulated.

A separate implementation of the reservoir model carries out a storage-yield analysis for a single dam, or all dams in the system in a similar way to Professor Alexander's (University of Pretoria, undated) OPRULES program. This program uses the same time series data files as the normal model but simulates in reverse time sequence to calculate the required storage to satisfy drafts of 10 to 90% of the mean annual inflow.

4.2.3 Information requirements

Table 4.3 list the parameters of the model, most of which should be readily available from the design of the dam and required water supply system. In addition to these, information on the hydrometeorological inputs are required as well as the monthly distribution of the required drafts or irrigation water requirements (depending on the units specified by parameter 7). If the yield analysis version of the program is to be used, the absolute draft and capacity parameters can be ignored as the model assumes the latter to be a set of fixed percentages of the mean annual inflow. The yield analysis does not consider the operating rules for transfers between dams nor for reserve drafts, but essentially treats all the dams in the system as a whole. In practice the model is normally used for design purposes and many of the parameters are varied to determine the optimum design.

Table 4.3 List of model parameters.

No.	Parameter description	Source of information
1	Reservoir Capacity (Ml).	Available from the reservoir design.
2	Initial storage (Ml).	
3	Dead storage (% capacity).	
4	Annual decrease in capacity ($Ml.a^{-1}$).	Based on sediment input rate.
5	Scale parameter in area-vol. relationship.	Available from the reservoir design.
6	Power parameter in area-vol. relationship.	
7	Draft units (-1=Ml*10^3 : 0=Ml : 1=mm ha^{-1}).	Available from the design of the abstraction requirements.
8	Annual draft (Ml*10^3 or Ml) or Irrigation area (ha).	
9	Effective rain on irrigation area (%).	From a knowledge of rain, soil and cover characteristics.
10	Number of reserve levels (maximum of 5) for lower drafts.	Available from the reservoir, abstraction system and operating rule design.
11-15	Reserve level 1 - 5 (% capacity).	
16	Inflow capacity (Ml).	From the design of the water transfer works.
17	Max. release (% storage).	From the operating rules design.
18	Limit for no release input (% capacity)	
19	Spill time distribution factor.	From available information on the natural flow regime.
20	Compensation releases ($Ml.month^{-1}$).	From any downstream users requirements.
21	First downstream dam number.	All of these parameters are part of the operating rules design.
22	Canal take-off priority (% or 0 for direct connection).	
23	Second downstream dam number.	
24	Canal take-off priority (% or 0 for direct connection).	
25	Third downstream dam number.	
26	Canal take-off priority (% or 0 for direct connection).	
27	Capital cost of reservoir works ($R.m^{-3}$).	All of these parameters are part of the costing analysis for the dam, abstraction works and supply system.
28	Capital cost of supply works ($R.m^{-3}$ or $R.ha^{-1}$).	
29	Repayment interest rate (%).	
30	Repayment period (years).	
31	Profit for successful supply ($R.m^{-3}$ or $R.ha^{-1}$).	
32	Supply failure penalty ($R.m^{-3}$ or $R.ha^{-1}$).	

4.3.4 Model limitations

It should first of all be recognised that this model is commonly used in conjunction with a monthly time-step rainfall runoff model, which will be prone to some inaccuracies, related to the simplicity of the modelling approach and the coarse time step used. The use of a monthly time step in any water resource simulation model is always problematic, particularly in a country such as South Africa that has a highly variable hydrological regime.

In reality, the individual processes that make up the water balance equation operate continuously. However, without any internal iteration, the use of a monthly time step requires that a decision has to be taken to perform parts of the water balance equation before others. As the processes are not always independent of each other, the order in which the calculations are made can effect the results. However, to incorporate an iterative procedure would increase the amount of computer time taken to carry out a simulation.

The spill time distribution parameter has been incorporated to allow the inter-month variability to be accounted for in one part of the model. However, this has been done at the expense of a parameter which may be difficult to quantify in some situations.

It is inevitable that the definition of reservoir operating rules within a relatively simple model will have limitations. Draft volumes can be specified as a monthly distribution. Five lower draft distributions can be defined and are used depending on the current relative storage volume in either a single dam or all the dams in the system. It is possible that such a simple procedure will not cater for all the likely operating rule procedures.

The yield analysis form of the model is simpler in structure than the normal model and does not include all the water transfer components. It is designed to be used for a first approximation of the potential yield of the complete system of dams. Further analysis can be carried out by running the full implementation of the model with several configurations of dam size, water demand and operating rules. The results can then be examined using one or more of the HYMAS results analysis programs.

Despite these limitations, the model is flexible enough to define a wide variety of multiple dam configurations. If a more complex system is to be simulated, the HYMAS 'batch mode' procedures can be used to link several implementations of this model as well as a monthly rainfall-runoff model. However, water transfers, between dams in seperate implementations of the model, cannot be easily established. The reliability of the simulations will be largely determined by the amount and quality of the available data that can be used to define the configuration of the system, the input time series as well the parameter values.

As referred to earlier, the VTI model does not contain any routines to allow for reservoir abstractions on the main channel. Nor can the reservoir model, discussed in this section, operate at anything finer than a monthly time resolution. It may therefore be of benefit to create a daily (or variable interval) version of the reservoir model such that it can be used in conjunction with the VTI model. This would allow reservoir dynamics to be assessed at a finer time resolution than monthly, or the effect of a major reservoir on streamflow patterns to be assessed at a daily time step or less.

4.4 NUTRIENT EXPORT MODEL (PEXP)

4.4.1 Background to the model development

Two of the problems associated with developing urban areas are the determination of the impact of nutrient loads generated in runoff and the development of ameliorative management approaches. Part of the problem is quantifying the time distribution of the non-point source load relative to that of point-source loads derived from sewage treatment works. The CSIR (Grobler, et al., 1987) has developed techniques for translating socio-economic data into information on the source and quantities of phosphorus that are likely to form the input to the phosphorus budget in developing urban areas. Depending upon the methods of waste disposal that operate in a specific case, some of this input phosphorus will be removed to sewage works, some will enter the catchment below the surface or enter the soil profile, while the remainder will lie on the surface. It is the fate of the latter two components and how their fate relates to natural hydrological runoff events that is the topic of this paper.

One of the observations that was made in a previous study (Grobler et al., 1987) on a developing urban area in the Orange Free State was that the non-point load is mainly derived from wash-off of surface phosphorus storage during large storm events. As this coincides with relatively high volumes of runoff, which tend not to be retained in downstream impoundments, their impact is relatively minor compared to the continuous point-source loads from sewerage works. The critical issue is therefore the relative time distribution of the two loads. The logical method for approaching this problem would therefore seem to be to apply a suitable time series simulation model which links the hydrology of the urban catchment with the generation of nutrient loads.

In designing an initial approach to modelling nutrient washoff and stormwater runoff several points have to be considered. Are there likely to be sufficient spatial variations to warrant adopting a distributed rather than a lumped approach? At least a semi-distributed, or sub-catchment approach is probably necessary and sufficient, while a fully distributed type of approach is unlikely to be justified, at least until the processes are better understood.

The time interval over which model iterations are to be carried out is of equal importance. In South Africa, the main national rainfall database is at a resolution of one day and this seems to be a logical time step to use. A monthly time step is unlikely to be adequate as much of the runoff and nutrient wash-off is storm event driven.

The choice of which type of approach to use to simulate the rainfall-runoff processes is difficult. There are many such approaches available, ranging from simple empirical to complex physically based. The final model is expected to be used in a management framework, where long time-series need to be simulated to enable mean, median and extreme representative conditions to be evaluated. It seems sensible to adopt an approach that is not so complex that the amount of time taken to simulate a number of representative years would be restrictive. It also seems to be unnecessary at this stage to use a highly sophisticated hydrological model when the linking processes with nutrient wash-off are poorly understood. The requirement to be management orientated also suggests that a lot of time spent on quantifying parameter values would negate the usefulness of the model.

4.4.2 The model Structure

The nutrient export model included in HYMAS is a semi-distributed, daily time-step model that links an SCS (Soil Conservation Service of the United States) type runoff generation algorithm with a storage-depletion nutrient mass balance function. It's basic structure is illustrated in figure 4.11.

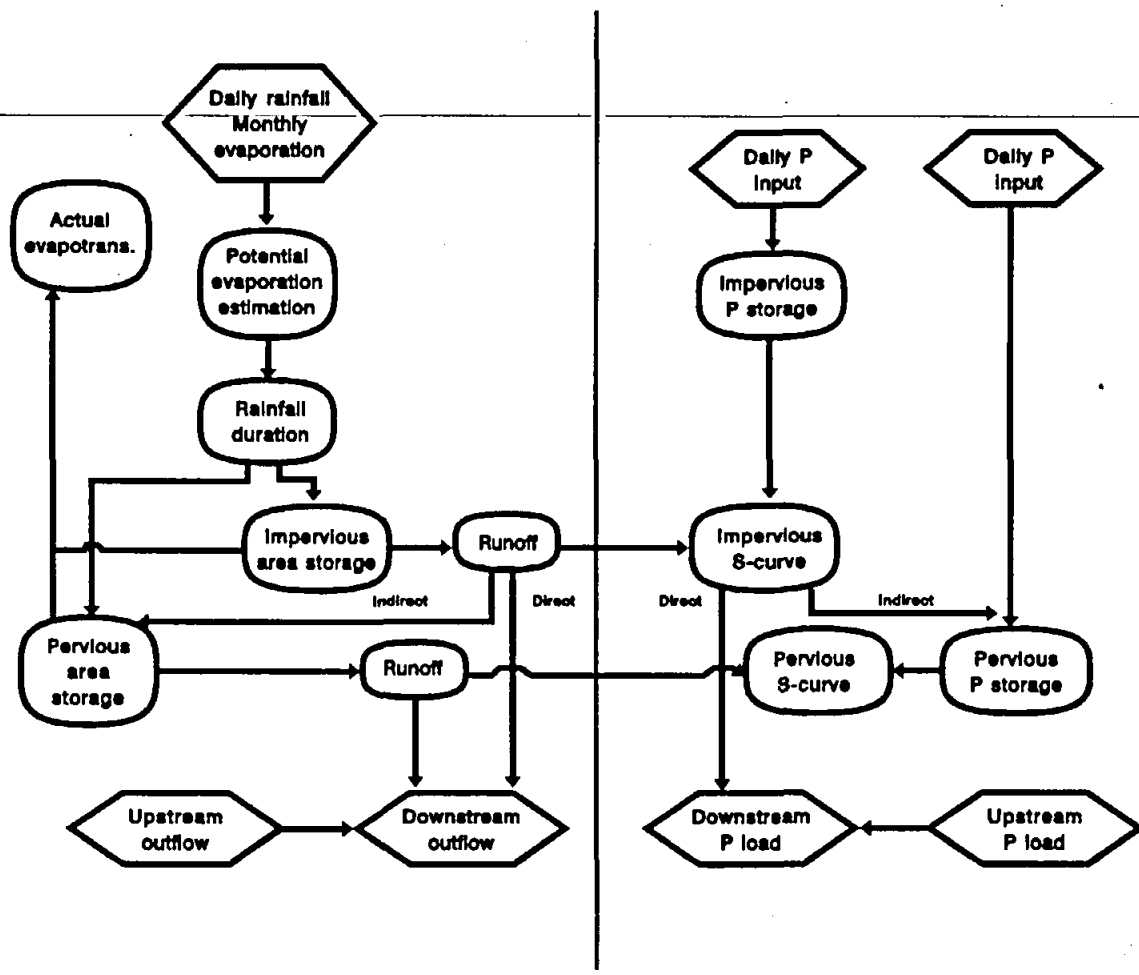

Figure 4.11 Structure of the phosphorus export model.

Each sub-area of the distribution system is sub-divided into three zones; direct and indirect impervious areas and pervious areas. The direct impervious areas are those sealed surfaces conceptualised to be directly connected to the sub-area outlet system via channels. Examples could be roads, compacted, tarred or concreted surfaces or roof areas where down pipes or drainage systems direct runoff into the stormwater system. The indirect impervious areas are those which have no direct connection and runoff would therefore pass over a pervious area before being able to reach a channel system. A typical example would be roof areas whose runoff is channelled onto gardens.

An SCS approach (Schmidt and Schulze, 1987) is used to simulate the runoff from both impervious and pervious areas using the equation :

$$Q = (P - I_a)^2 / (P - I_a + S) \quad \text{Eq. 4.4.1}$$

where	Q	=	Runoff depth (mm)
	P	=	Rainfall depth (mm)
	S	=	Potential maximum storage (mm)
	I_a	=	Initial abstraction
		=	cS
with	c	=	Initial loss coefficient.

In any time interval, water storage is estimated from the basic water balance equation such that :

$$\text{Changes in storage} = P - Q - \text{Evaporation} \quad \text{Eq. 4.4.2}$$

Absolute maximum potential storage can be defined as the total water storage capacity (mm) of a sub-area, i.e. the water that can be absorbed when the sub-area is at it's driest. For the impervious areas the absolute maximum storage (surface ponding, raintank storage, etc.) is a model parameter, while the absolute maximum pervious storage is defined by specifying the depth and water holding characteristics of the soil. The potential maximum storage (S in equation 4.4.1), in any time interval and for both types of surface is therefore the difference between the current level of storage and the absolute maximum.

Schulze and Arnold (1979) found the initial loss coefficient to be dependent on season and antecedent condition factors, while Schulze, et al. (1984) added rainfall amount, duration and intensity to the list of factors. In this model an initial loss coefficient parameter (c) is defined for both types of surface. These are then modified by a seasonally varying rainfall distribution or intensity parameter (RDIST). The RDIST parameter (a value < 24) refers to the likely duration of rainfall in a day and is used as follows :

$$\text{Actual c value} = \text{c parameter} * (\text{RDIST} / 24)^{1/2} \quad \text{Eq. 4.4.3}$$

The effect is to decrease the initial loss coefficient when RDIST is small and is designed to account for decreased infiltration rates if the typical rainfall intensities are high.

Actual evaporation occurs at the potential rate from impervious storage and a function similar to that used in the Pitman model (Pitman, 1973) controls evapotranspiration from the pervious areas. The latter uses a single parameter to define the nature of the relationship between the soil water storage and the ratio of actual to potential evapotranspiration. Potential evapotranspiration is currently estimated from mean monthly pan evaporation data (A or Symons), corrected to represent free water surface evaporation.

When the soil water storage level is above a 'field capacity' parameter a non-linear baseflow function estimates the amount of drainage, which is also controlled by a maximum daily baseflow parameter. The function is essentially an S-curve relationship between the level of soil water storage and the amount of drainage and is defined by a single parameter

(BFLambda) which controls the shape of the S-curve. Figure 4.12 illustrates this approach, but for the baseflow function the horizontal axis represents the difference between the maximum water content (saturation) and field capacity, while the vertical axis represents the drainage rate relative to the maximum. A value of 1.0 for this parameter implies a symmetrical S-curve about the coordinate point {0.5, 0.5}. High values of this parameter imply that little drainage (relative to the maximum value) will occur until the soil water is close to saturation, while low values (or negative) imply that the maximum drainage rate will occur close to field capacity.

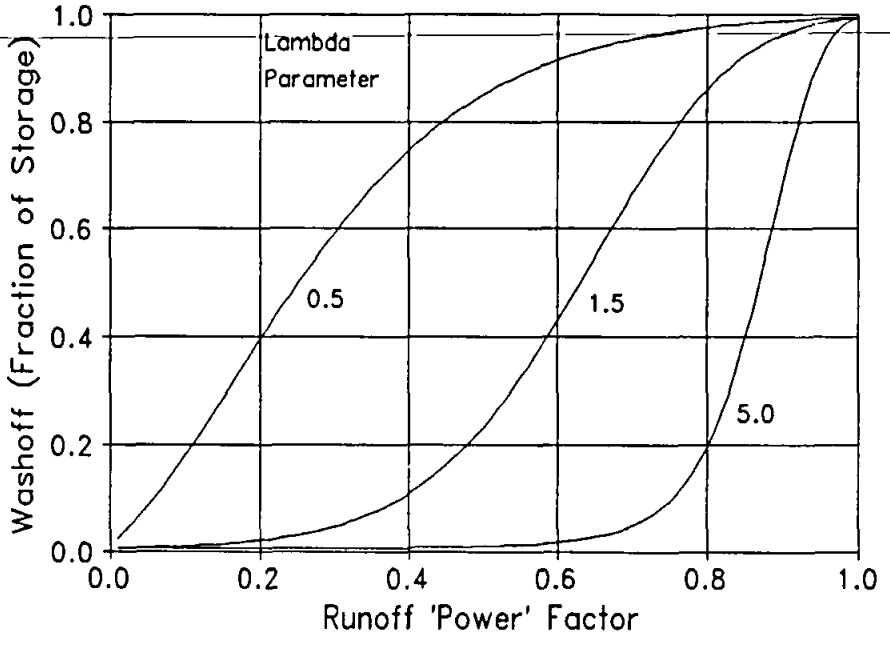

Figure 4.12 Illustration of the relationship between non-dimensional runoff 'power' and the proportion of stored nutrients that are washed off.

The dynamics of the nutrient storages are controlled by parameters defining the daily input to storage and daily export values which are dependent on the runoff and rainfall amounts. Separate nutrient input parameters are evaluated for the two types of surface and can vary seasonally. The seasonal variation is determined by specifying summer and winter values for the Daily Nutrient Input parameters and estimating the actual value in any one month on the basis of a Sine curve with an amplitude defined by the summer and winter extreme values.

The daily load is calculated from S-curve functions similar to that used for baseflow estimation and represent relationships between a non-dimensional index of runoff 'power' and the proportion of stored nutrient that is washed off in one time interval (figure 12). The shapes of these relationships are defined by separate lambda parameters for the pervious and

impervious areas. The calculation of a non-dimensional index of runoff 'power' is based on several considerations.

- The runoff 'power' will increase with the energy of the runoff, which in turn will be dependent on the volume of runoff, as well as the slope and hydraulic roughness of the surface over which flow is occurring.

- The runoff 'power' will increase with the energy of the rainfall, which is partly dependent on the seasonally varying rainfall distribution parameter.

- The runoff 'power' will increase in proportion to the ratio of runoff to rainfall. Given that the runoff is calculated from the SCS approach, this implies that higher runoff 'power' will be associated with lower initial abstractions caused by lower initial loss coefficients or storage states close to the maximum (i.e. full or saturated).

To account for these considerations, the runoff 'power' index is therefore calculated in the model from three components.

$$Fac1 = (Q / 1000)^{2/3} * S^{1/2} / n \quad \text{Eq. 4.4.4}$$

Where Q is the runoff depth (mm)
S is the sub-area slope factor (m m^{-1})
and n is Manning's n Roughness Coefficient

Fac1 (equation 4.4.4) represents the component that is designed to account for the energy of the runoff and is a representation of the Manning Formula for velocity in open channels. In the absence of any information on the depth of runoff, Q / 1000 has been used as a surrogate. The slope parameter would normally be set to the mean sub-area slope, but could also be modified (increased) to account for highly concentrated flow such as may occur if most of the runoff is concentrated in roadside gutters.

$$Fac2 = (24 / RDIST)^{1/2} \quad \text{Eq. 4.4.5}$$

Where RDIST is the Rainfall Distribution Parameter

Fac2 (equation 4.4.5) represents the component that is designed to account for rainfall intensity variations, although the next equation also incorporates this effect.

$$Fac3 = Q / P \quad \text{Eq. 4.4.6}$$

Where P is the rainfall during the time interval.

Fac3 (equation 4.4.6) represents the component that accounts for the ratio of runoff to rainfall and the final index is computed from :

$$\text{Runoff 'Power' Index} = Fac1 * Fac2 * Fac3 \quad \text{Eq. 4.4.7}$$

With the further constraint that the Index ≤ 1.0.

Runoff and exported nutrients for both direct impervious and pervious areas increment the total outputs from the specific sub-area. However, outputs from the indirect impervious area are assumed to flow onto the pervious area and therefore increment the storages (water and nutrients) of the pervious zone.

The S-curve type function for determining the proportion of storage that is exported has been adopted in the absence of adequate information on the real processes that control the relationships between rainfall, runoff and exported nutrient loads. The function allows a high degree of flexibility in the form of the relationship which can be controlled by the single lambda parameter (figure 4.12). The use of equations 4.4.4 to 4.4.7 to non-dimensionalise the estimated runoff is again a pragmatic solution to representing the nature of a physical process about which there is a paucity of information. Only after extensive or intense rainfalls, when the water storages are close to their maximums and the runoff 'power' is high, can the non-dimensional index become close to unity and all the existing stored nutrients be exported.

If more than one sub-area is used in the distribution system, the outputs of runoff and nutrient load are accumulated to determine the totals for the catchment as a whole.

The exported load will clearly depend upon the relative sizes of the areas of the impervious and pervious zones, their maximum storage potentials, loss coefficients, hydraulic properties and the parameters specifying the daily input of nutrients and the shapes of the S-curves (lambda parameters).

4.4.3 Information requirements

The parameters of the PEXP model are listed in table 4.4. Apart from these values, information on the monthly distribution of pan evaporation and a time series of daily rainfall is all that is required. The rainfall input can be constructed from one or more available gauges, as well as gridded information on the median monthly rainfalls using the normal HYMAS routines for this purpose.

Table 4.4 provides some indications of how the sources of information might be used to quantify the parameter values and it is clear that some of them will be difficult to estimate. The highly empirical nature of some of the algorithms and their associated parameters, suggests that some kind of calibration will be necessary.

4.4.4 Model limitations

The model has not been validated in the usual way due to the lack of readily available time series data on either the runoff or the phosphorus loads being washed off urban catchments. Some initial tests of the model (Hughes and van Ginkel, 1993) have been carried out and are reported in section 5 of this report. More data are expected to become available in the future from a study being carried out in Grahamstown and more rigorous tests of the model will be carried out at a later stage.

Table 4.4 Parameter list for the PEXP model

Parameter	Source of Information
Sub-area size (km^2)	From topographic maps or orthophotos and the user defined spatial distribution system. The extent of the different surfaces can be obtained from a study of large scale maps or inferred from a knowledge of the nature of the surface drainage pattern, the extent of tarred or compacted surfaces and the building landscape. The slope factor can be simply the mean sub-area slope, or can be adjusted to account for flow concentration in such as gutters.
Downstream sub-area No.	
Direct impervious area (km^2)	
Indirect impervious area (km^2)	
Pervious area (km^2)	
Sub-area slope factor	
Manning's n - Imp.	From a knowledge of the nature of the surface conditions including vegetation cover.
Manning's n - Perv.	
Imp. area surface storage (mm)	Includes the effects of any storages (ponds, raintanks, etc.)
Soil depth - under imp. area (m)	These parameters can be quantified from a knowledge of the soil types and distribution within the sub-area. The impervious area soil depth parameter is used to allow lateral re-distribution of water that has entered the soil profile via the pervious areas.
Soil depth - pervious area (m)	
Porosity	
Field capacity	
Wilting point	
Initial loss coeff. - Imp.	Values for these parameters should be obtained from other publications on the SCS methods, although may require some calibration adjustment.
Initial loss coeff. - Perv.	
Daily P input - Imp./Summer (T km^{-2})	Obtained from a study of the socio-economic conditions prevailing in the urban area using an approach similar to Grobler, et al. (1987).
Daily P input - Imp./Winter (T km^{-2})	
Daily P input - Perv./Summer (T km^{-2})	
Daily P input - Perv./Winter (T km^{-2})	
P Export Lambda - Imp.	Difficult to obtain parameters as very little information is available about the nature of the relationship between runoff and the proportion of stored phosphorus that is washed off.
P Export Lambda - Perv.	
Baseflow Lambda	These parameters define a very simple baseflow function and are difficult to relate to any physical processes.
Max. depth of baseflow / day (mm)	
Annual Pan evaporation depth (mm)	Obtained from observed data or regionalised figures.
Evap./Soil moisture parameter	Related to the nature of the vegetation cover.
Rain dist. factor (RDIST) - Summer (h)	Related to the typical rainfall intensities expected during the different seasons of the year and obtained from a knowledge of the nature of rainstorms prevailing in the area.
Rain dist. factor (RDIST) - Winter (h)	
Initial P store - Imp. (T km^{-2})	Starting values for the phosphorus storage calculations. Can be set after some initial runs of the model.
Initial P store - Perv. (T km^{-2})	

One of the major uncertainties is the difficulty of adequately quantifying the nutrient Lambda parameters, defining the shape of the S-curve, to represent the real relationship between runoff, phosphorus storage and wash-off for a specific situation. This function is far from being an explicit representation of the processes involved, mainly for the reasons already given that these processes are not clearly understood. It is also not clear that this type of function adequately represents the processes involved. For example, storage is assumed to increase at the rate of the daily input parameters and is only depleted during runoff events. If any processes that cause in-situ depletion of *available* phosphorus are considered to be important then they should be added to the model in some way.

The natural occurrence of phosphorus in soil is known to be quite low (Emsley & Hall, 1976; Malherbe, 1950) and remains fairly stable because the majority occurs as insoluble inorganic phosphates. The minerals that bind to phosphorus and form insoluble bonds, are calcium, iron and aluminium (Emsley & Hall, 1976) and acidic conditions in the soil are required before soluble inorganic phosphates (available phosphate as H_2PO_4) can be utilised for plant growth. The processes involved in determining the fate of phosphorus discharged onto soil surfaces is not discussed in detail in the literature.

Phosphorus is more readily washed out of sandy, acid or water logged soils than from clay soils (Emsley & Hall, 1976; Gower, 1980) and the amount of phosphorus in drainage water is controlled as much by the nature of the soil as by the amount of phosphorus applied to the surface. According to Emsley & Hall (1976) only a small amount of soluble soil phosphate is leached out by rain, and an even smaller amount of the fixed phosphate in the soil is eroded away. The greatest phosphorus loss from the soil seems to be related to uptake by plants. This may then be returned to the surface (as available phosphorus) by the decay of vegetation or by grazing and subsequent deposition of animal wastes.

More information about the following processes would seem to be needed to improve the model conceptualisation :

- The rate of phosphorus uptake into the soil under South African conditions.
- The rate of plant uptake and release of phosphorus to the surface for different vegetation cover and land use characteristics.
- The mineral characteristics of the soil and the extent of phosphorus bonding.
- The conditions required for the removal of soluble phosphates within the soil.

The model only allows for soil uptake through the interpretation of the phosphorus input information derived from the socio-economic survey. A subjective consideration of the vegetation and cover characteristics can be used to estimate that proportion of the total input phosphorus that can be considered available. Whether or not this approach will account for all soil uptake cannot be stated with any certainty.

While it may be possible to estimate (or measure) the proportions of impervious and pervious areas, it is less easy to apportion the total input nutrient load between these two surface conditions. The method based on the socio-economic surveys (Grobler, et al., 1987)

provides some information about how to achieve this, but the model is very sensitive to both the relative proportions of the surface types and their daily nutrient inputs. This factor would assume additional importance if in-situ reduction in *available* phosphorus, associated with one or more of the above processes, were identified as important.

An additional process that is not accounted for in the model is the depletion of phosphorus load during the processes of flow in river or drainage channels. If the phosphorus washed off is attached to sediment, it is likely that channel sedimentation processes may play an important role in some situations.

A monthly modelling approach developed by Watertek (CSIR - Council for Scientific and Industrial Research) links a monthly flow series with a USLE (Universal Soil Loss Equation) type of approach to determine the sediment yield of a catchment (Weddepohl and Meyer, 1991). Phosphorus in its soluble form is assumed to be washed off in proportion to the surface runoff intensity and particulate phosphorus in proportion to the sediment yield. The method has been designed more for large catchments rather than individual urban areas and it is not clear whether the processes related to sediment yield are adequate to represent the phosphorus yield from developing urban areas. All the sediment mobilised on the surface of a catchment during an event rarely reaches the outlet of the catchment over the duration of that event. It is reasonably well understood that sediment moves more gradually through a drainage system and can take quite a long time to leave the system entirely. The model described here assumes that if the runoff 'power' is high enough, all the stored nutrients can be removed within a single event. The question arises as to whether there exists a sufficient understanding of the processes to know whether this is a realistic assumption.

A further process that has yet to be incorporated into the model is runoff and nutrient wash-off that is independent of rainfall. This occurs as a result of reticulated domestic water being discarded onto the surface of the catchment, rather than into sewerage systems. If some of the input nutrients are associated with this water (particularly relevant to phosphorus contained in washing powder), the effect would be to generate continuous background runoff volumes and nutrient loads, as well as cause continuous depletion of the storage levels.

The PEXP model represents an initial attempt to represent the relationships between rainfall, runoff and nutrient wash-off from developing urban areas. Unfortunately, conceptualising the relationship between runoff and nutrient wash-off is extremely difficult owing to the lack of either a reasonably thorough understanding of the processes or observed time series data to illustrate the effects of these processes. It has therefore been impossible to include anything but highly empirical algorithms for defining some of the components of the model.

4.5 OTHER MODELS CURRENTLY WITHIN HYMAS

The remaining models were incorporated into HYMAS because they have a potential to address problems in the broad field of water resources that the previous models are not capable of solving. The first is a version of the PITMAN, monthly time step, rainfall runoff model, the second a modified implementation of a model developed in the Water Systems Research Programme at the University of the Witwatersrand, the third a model to simulate the potential of raintanks for supplementing water supplies and the fourth a very simple design flood model. The PITMAN model is qdequately described elsewhere and will not be referred to further in this section. The second and the last have not been tested in any great detail and should be used with caution at this stage of their development. They are therefore not described in detail in this report.

4.5.1 RAFLES MODEL (University of the Witwatersrand, Water Systems Research Programme)

The original version of this model (Paling, et al., 1989; Stephenson and Paling, 1992) was designed to simulate monthly runoff based on inputs of monthly rainfall and using simplified hydrodynamic equations for overland flow and Green Ampt infiltration. An extension to the model includes simulations of erosion and sediment yield. The Institute for Water Research has modified the original model by converting it to a daily time step model and re-organising some aspects of the structure. The basic modelling conceptualisation, however, remains the same. The main reason for including the model into HYMAS was related to its potential capabilities of modelling erosion and sediment yield.

Hydrological components.

Figure 4.13 provides a diagrammatic representation of the main hydrological components of the model. The primary inputs are a time series of daily rainfall and mean monthly potential evaporation estimates. The daily time step has been chosen on the basis of the type of rainfall data that is commonly available for the majority of regions in South Africa. However, as the modelling approach explicitly estimates infiltration rates, an attempt to account for seasonal variations in the duration of rain within a day is included in the model. Each day is divided up into rain and non-rain parts, where the duration of the rain part is estimated using a random sample from frequency distributions defined by mean and standard deviation parameters for each month of the year. The rainfall is first subjected to interception loss determined by the rainfall intensity and an interception capacity parameter. The remaining rainfall must satisfy any available depression storage before incrementing a surface flow film depth. Losses from interception, depression storage and the surface flow film occur at the potential rate.

The model allows for two subsurface layers; the upper being considered as the unsaturated zone, which may include a perched saturated layer. The lower layer may be thought of as an aquifer proper, or alternatively as a lower soil layer. If the latter is chosen, then the model does not have a groundwater interaction component. However, a parameter allows losses to occur from the lower layer in proportion to it's relative water content, which could be conceptualised as groundwater recharge.

The surface flow film, as well as depression storage, are subject to infiltration into the upper unsaturated zone, with the amount determined using the lesser of the three following estimations :

- An amount calculated from a simplified Green & Ampt formulation (Stephenson and Paling, 1992).
- The amount of water available on the surface.
- The amount of storage available in the upper soil zone.

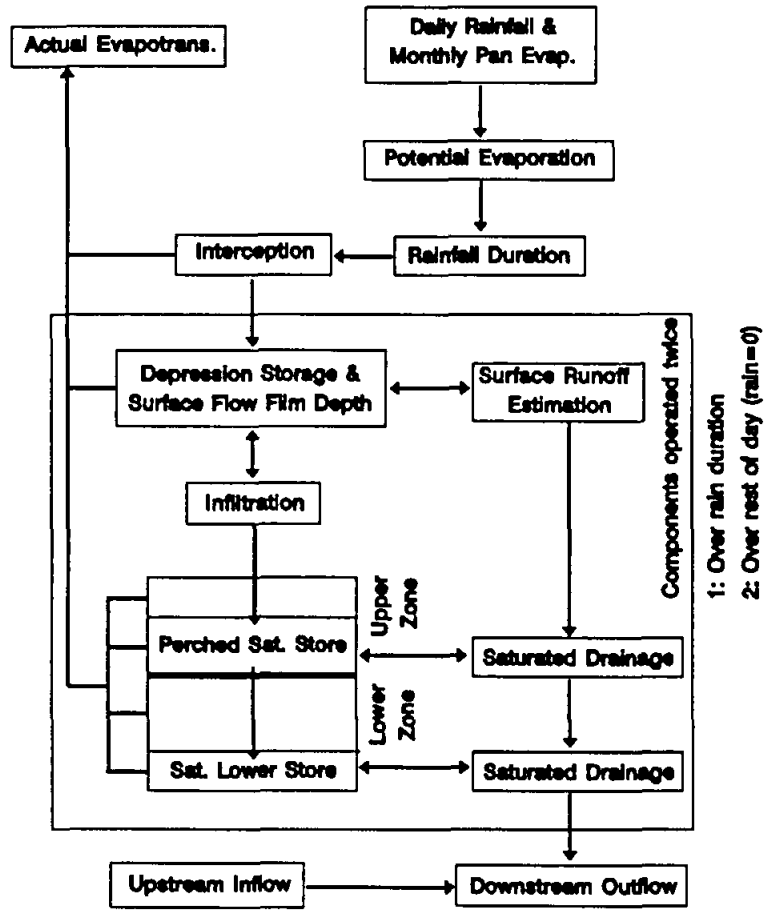

Figure 4.13 Structure of the RAFLES model.

Seepages occur from the unsaturated zone to a perched saturated zone and from there into the saturated part of the lower zone, both being estimated using a Green-Ampt approach with constraints based on the amount available for seepage and the capacity of the receiving layer. Evapotranspiration occurs from the two zones as functions of their total water content, the potential evaporation and a crop factor.

The surface flow film depth is used together with a rill ratio parameter, catchment width,

slope and Manning's n roughness in a kinematic flow equation to estimate the amount of surface runoff. Runoff also occurs from the saturated parts of both layers and is calculated using Darcy's equation.

The depression storage, infiltration, runoff and storage adjustment routines are repeated for the remainder of the day when no rainfall is considered to be occurring. The final total runoff volume is then added to inflow from upstream sub-areas to represent the downstream outflow. An additional function is available to simulate reservoir storage and outflow if required.

The hydrology components of the RAFLES model therefore represent a compromise solution between fully distributed models and simpler approaches. The model inevitably includes some empirical parameters (rill ratio, for example) in an attempt to make some of the physically based algorithms (Green-Ampt, Darcy's and the kinematic flow equations), normally used to describe the operation of processes at very small spatial scales, applicable at the scale of sub-catchments. One of the main uncertainties about the model is whether or not this approach can be applied successfully (Beven, 1989).

Sediment components.

The catchment surface is considered to consist of a layer of loose soil, which is available for transport, underlain by soil which is not loose but is available for detachment and therefore conversion to loose material. The model includes algorithms to compute the amount of erodible soil that is added to the loose soil through fragmentation and through raindrop detachment. The latter is controlled by the detachment coefficient, soil erosivity, effective rainfall intensity and the combined depth of water and loose sediment. The sediment load generated from the surface of the catchment is computed using a bed load transport equation (Paling et al., 1989) based on the flow depth, density of the sediment and the particle size.

The bed of the channel is also considered to consist of a layer of loose sediment overlying a layer of erodible material. Only the loose sediment is considered active in the model and is incremented in each time step with the sediment washed off from the catchment or flowing in from upstream channel modules. Channel sediment transport is assumed to occur as both bed load and suspended load. Bed load is estimated using the same equation as for the catchment surface component, except that the flow depth is replaced by the channel hydraulic radius. The suspended load is estimated from the average flow velocity multiplied by the sediment concentration at mid flow depth. The latter is estimated from a conventional concentration distribution function (Paling et al., 1989).

RAFLES also includes reservoir water and sediment budget routines, further details of which are available from Paling et al. (1989).

Table 4.5 provides some information on the parameters which have to be quantified for the HYMAS version of the RAFLES model. It is clear that there are a number of parameters that can be considered very difficult to estimate in the context of a sub-catchment type distribution scheme.

Table 4.5 Parameters of the HYMAS implementation of the RAFLES model.

Parameter	Source of Information
Downstream Sub-area No.	Taken from the distribution system set-up. The module type refers to catchment/channel or reservoir.
Module Type (1 or 2)	
Catchment / Dam length (km)	Available from topographic maps (for catchment modules or reservoir design data for dam modules).
Catchment width (km)	
Channel length (km)	
Channel / Spillway width (m)	
Spillway dependent on depth (Y:1 , N:0)	Available from reservoir or dam wall design data.
Spillway coefficient	
Dam depth at crest (m)	
Catchment longitudinal slope (%)	From topographic maps.
Overland flow Mannings n	Estimated from catchment surface characteristics.
Channel longitudinal slope (%)	From topographic maps.
Channel flow Mannings n	Estimated from channel characteristics.
Left channel bank slope (%)	
Right channel bank slope (%)	
Mean aquifer depth (m)	Refers to soil characteristics and can be estimated from the standard HYMAS physiographic data files.
Upper aquifer layer depth (m)	
Interception capacity (mm h^{-1})	Estimated from the vegetation cover characteristics (can use the HYMAS physiographic data).
Interception storage capacity (mm)	
Depression storage capacity (mm)	Largely empirical and difficult to estimate.
Soil suction (m)	From soil characteristics.
Rill ratio	Largely empirical and difficult to estimate.
Unsaturated seepage factor (< = 1)	
G'water seepage factor	
Max. non-resurfacing g'water (m day^{-1})	
Aquifer porosity (fraction)	Estimated from the soil and groundwater physical variables in the standard HYMAS physiographic data files.
Min. moisture content (fraction)	
Ksat for upper layer (mm h^{-1})	
Ksat for lower layer (mm h^{-1})	
Area under irrigation (km^2)	From water demand information.
Average monthly water demand (mm)	
Water abstractions (m^3 day^{-1})	

Density of loose sediment (T m^{-3})	From detailed surface soil characterstic data for the catchment and generally difficult to estimate.
Sediment particle size (mm)	
Sediment fall velocity (m s^{-1})	
Detachment coefficient	
Soil fragmentation rate (mm $month^{-1}$)	
Erosivity factor	
Catchment cover density	From catchment vegetation characteristics.

4.5.2 A rainwater tank resource evaluation model

This model is based on an input of a daily rainfall series, together with an estimate of the likely intensity using seasonally varying parameters of the mean and maximum rainfall intensity. The latter are used to define the shape of a log Normal distribution, from which a random sample is taken for the intensity to be used for any single day within the modelling period. Two roof loss parameters are applied; the first is a fixed loss depth to account for the initial wetting of the roof material (or ponding storage in the gutter system), while the second is a continuing loss rate (mm h^{-1}) to account for the fact that a minimum intensity may be required to generate runoff.

Additional losses are accounted for if the capacity of the gutter or downpipe systems are exceeded. The gutter system flow capacity is estimated from the dimensions and slope of the gutter with Manning's formula for discharge. The downpipe system flow capacity is estimated from the maximum head and the total diameter of the downpipes. Neither losses have been found to be limiting except where the gutter system is inadequate for the roof area, or the rainfall intensities are extreme.

The sub-area system of the model currently only applies to the roof runoff and all sub-area runoff volumes are routed to a single tank (sub-area 1 parameters). The remainder of this part of the model simply carries out a water balance of the raintank, accounting for the daily required demand.

The final (optional) part of the model run carries out a yield analysis of the raintank by setting the daily demand at 9 values between 0.5% and 4.5% of mean monthly runoff volume and calculating the capacity required for a 100% assured yield. This is carried out in the same way as the reservoir yield program, by calculating the water balance equations with the time series of inflow data (calculated during the first part of the model) read in reverse order. The inflow volume, required capacity and actual tank level are displayed graphically for each of the 9 daily demands and the maximum required capacity calculated. The final graphics screen displays the capacity yield curve, which can be used to assist with redefining the parameters to obtain the optimum tank size and demand for a specific roof.

The normal HYMAS results display routines can be used to examine the output results (time series of runoff volume, tank volume, achieved supply and shortfalls, for example) in more detail.

The parameters of the model are listed in table 4.6, together with some ideas of how they might be estimated. One possible area for improvement is to define the demand requirements on a seasonal basis, because in regions where the rainfall is highly seasonal it will be impractical to expect the tank to supply the same daily rate throughout the year.

Table 4.6 Parameters of the raintank resource model

Parameter	Source of Information
Plan area of roof (m^2)	All estimated from the geometry of the roof, gutter and downpipe systems. These values are simple to obtain.
Downstream roof no.	
Effective width of gutter system (m)	
Effective depth of gutter (m)	
Mean slope of gutter (%)	
Number of downpipes	
Diameter of downpipes (m)	
Mean summer rain intensity (mm h^{-1})	Estimated from a knowledge of the rainfall characteristics of the region. The maximum values actually represent the intensity at 2.3 times the upper standard deviation of a log Normal distribution.
Mean winter rain intensity (mm h^{-1})	
Max. summer rain intensity (mm h^{-1})	
Mean winter rain intensity (mm h^{-1})	
Initial roof wetting losses (mm)	Estimated from a knowledge of the wetting characteristics of the roof material. There are, however, few guidelines.
Continuing roof losses (mm h^{-1})	
Capacity of raintank (m^3)	Estimated from the size and position of the offtake point of the tank.
Dead storage (m^3)	
Initial storage (m^3)	
Daily water requirements (l $person^{-1}$ day^{-1})	Estimated from the expected water requirements of the household that can be met from the tank.
Size of household (persons)	

4.5.3 A simple design flood model

This model has been added to allow users the capability of estimating design floods of various return periods from design rainfall data using the Muskingham excess rainfall routing methods described in Bauer and Midgley (1974). The design rainfall information is derived from total storm rainfall and duration parameters, as well as a file of standard rainfall distribution proportions (Bauer and Midgley, 1974) for each hour of the duration. The rainfall building procedures are therefore different to any of the other models and a separate HYMAS menu option is included.

As with all the other models, the total catchment area can be distributed into several sub-areas, each having its own set of parameters and rainfall input. Two options are available for estimating the losses and the proportion of the rainfall that will be routed to form the flood hydrograph. The first is a simple constant runoff proportion applied to each hour of

the rainfall hyetograph. The second uses an infiltration curve equation (Kostiakov, 1933) of the form :

$$\text{Infiltration rate} = k.C.\text{Time}^{(k-1)} \quad \ldots\ldots\ldots\ldots\ldots\ldots \quad \text{Eq. 4.5.1}$$

where k and C are the parameters
and Time is the cumulative time since the start of the rainfall.

Before being routed the excess rainfall is reduced by any available dam storage capacity. The total dam storage is estimated from the combined volume of dams in the sub-area as well as the proportion of the catchment area above the dams (table 4.7).

Two delay parameters (table 4.7) are used to define the time differences in the runoff. The first accounts for any time differences between the rainfall inputs to the sub-areas, while the second accounts for routing delays in the generation of the runoff. The other component of the routing function is the attenuation, which is calculated using a Muskingham storage routing formula of the form (Bauer and Midgley, 1974) :

$$O2 = C0 * I2 + C1 * I1 + C2 * O1 \quad \ldots\ldots\ldots\ldots\ldots\ldots \quad \text{Eq. 4.5.2}$$

where O1, O2 are the downstream discharges at the start and end of the time step,
I1, I2 are the upstream inflow at the start and end of the time step,

and
$$C2 = 1 / EXP(dt / K) \quad \ldots\ldots\ldots\ldots\ldots\ldots \quad \text{Eq. 4.5.3}$$
$$C1 = K * (1 - C2) / dt - C2 \quad \ldots\ldots\ldots\ldots\ldots\ldots \quad \text{Eq. 4.5.4}$$
$$C0 = K * (C2 - 1) / dt + 1 \quad \ldots\ldots\ldots\ldots\ldots\ldots \quad \text{Eq. 4.5.5}$$

with K, the routing coefficient estimated from $A * \text{Area}^B$
dt is the time interval (hrs),
Area is the catchment area (km^2),
and A, B the routing coefficients (table 4.7).

The model therefore represents a relatively simple approach to determining design floods which is flexible enough to allow large catchment areas to be divided up into sub-areas. This approach reduces the dependency of the results on the use of areal reduction factors to determine spatially averaged design rainfall input. The typical approach to using the model would be to define design rainfalls over several durations and select the appropriate design runoff hydrograph from the array of results.

Table 4.7 Parameters of the simple design flood model

Parameter	Source of Information
Sub-catchment area (km^2)	From topographic maps.
Downstream sub-area	
Muskingham routing coefficient A	Regionalised variables available from Bauer and Midgley (1974).
Muskingham routing coefficient B	
Routing delay (h)	From information on the size, shape and channel characteristics of the sub-area.
Total storm rainfall (mm)	Available from information about design storm rainfall for a given return period. The delay is estimated from an understanding of the patterns of movement of storms over the total catchment.
Rainfall duration (h)	
Rainfall timing delay (h)	
Runoff proportion (%)	From an understanding of the runoff response of the sub-area.
Infiltration curve k	
Infiltration curve C	
Maximum dam storage (Ml)	From a knowledge of the volume of dam storage in the sub-area and the position of the dams in the drainage network.
% catchment above dams	

5. MODEL APPLICATION EXAMPLES (VTI - Model)

5.1 INTRODUCTION

This section of the report is designed to illustrate the validity of the VTI model by applying it to simulating the hydrology of several different regions. The regions have been chosen on the basis of information availabilty, as well as the extent to which they may be useful to test different aspects of the model and identify shortcomings in the model structure or formulation. Each set of catchments are briefly described in terms of their catchment characteristics, the perceived patterns of hydrological processes and the information that is available to establish the time series and parameter inputs to the model. The simulation results are reported and the implications with respect to any identified model deficiencies are discussed.

The final section attempts to draw some general conclusions about the applicability of the VTI model based on these examples.

5.2 THE BEDFORD CATCHMENTS

5.2.1 Catchment characteristics and hydrological processes

The details of the characteristics of the Bedford catchments are discussed in a separate volume (Hughes and Sami, 1993) of the final report and need not be fully described in this section. However, for the benefit of the reader who does not wish to study the other volume at length, a short summary is included here as well.

Topography :

The topography over the majority of the catchments area consists of relatively gently sloping terrain. There are, however, some more steeply sloping areas on the north western boundary and very steep slopes occur over a short section of the northern boundary.

Geology :

The area is underlain by gently dipping Karroo sandstones and mudstones. East-west trending dolorite dykes occur in some parts of the catchment.

Climate :

The mean annual rainfall is approximately 460 mm, with seasonal peaks in spring and autumn. Rainfall occurs as either short duration convective storms, or much longer duration and generally lower intensity events which can have total depths exceeding 100 mm. Regional values for Symons Pan evaporation indicate that the potential, or reference, evaporation is of the order of 1400 mm. Maximum summer temperatures are generally in excess of 35° C, while winter minimum temperatures are frequently below 0° C.

Soils :

The soils of the catchment are very variable in depth, the deepest (> 1 m) being found in association with valley bottom alluvial and colluvial sediment deposits. Many parts of the slopes and hilltops are covered with thin (< 300 mm) and rocky soils. However, the relationship between topographic position and soil depth is not at all clear, as thin soils are also found in many lower slope and valley bottom areas. Soil textures vary from clay loams to sandy loams, although most seem to fall into the sandy clay loam category. Where vegetation cover is poor, the soils suffer from relatively severe surface crusting.

Vegetation and landuse :

Basal vegetation cover varies from grassland to karoo shrubs and both have varying densities of thornbush (Acacia Karoo) associated with them. The main landuse is grazing of sheep, goats and cattle, with a few small areas of irrigated pasture land. The present day vegetation cover is strongly influenced by the history of grazing management. Overgrazing in some parts has led to extensive and dense thornbush cover. Within the grassland areas, the density of the base cover is relatively dynamic and influenced by the immediately antecedent rainfall conditions, as well as season and grazing practices. There are a large number of small farm dams within the catchment, which are mainly used for stock watering.

The prevailing hydrological processes appear to vary with the type of rainfall event experienced. The majority of the convectional storms do not produce widespread streamflow. Where the intensities are high enough to exceed infiltration rates, localised slope runoff has been observed to occur, but this does not survive for long distances from the source. If it does not re-infiltrate into deeper soils lower down slope where the vegetation cover is better and infiltration rates higher, it rarely survives for long distances in the small headwater channels. The longer duration events that also have high total depths are the only events that produce any widespread streamflow and based on the limited observations available, these occur approximately once or twice a year. During these events the shallow to moderate depth soils become at least partially saturated and give rise to saturation excess slope runoff. As with the intensity excess runoff, generated during convectional storms, some of this runoff has been observed to re-infiltrate into drier soils down slope. There are some parts of the catchment where relatively deep alluvial deposits give rise to the potential for streamflow to be significantly reduced by transmission losses (Hughes and Sami, 1992 and an earlier section of this report).

During the majority of the year, rain storms are too small and widely separated and evaporation rates too high, for the antecedent soil moisture conditions to reach levels that are conducive to runoff generation. Soil moisture observations indicate that deeper soil horizons have relatively constant moisture contents and frequent fluctuations only occur in the upper 300 mm.

5.2.2 Available data

As with the other information on these catchments, the available data has been adequately summarised in other sections of the final project report. There are 7 flow gauging sites, 28 rainfall recording sites, 2 automatic weather stations and observations of soil moisture

available from three areas. While the majority of the data are of good quality, the same can not be said of the streamflow data. The project team has experienced continual problems with data logging water level recorders. These problems have been difficult to solve partly due to the infrequent and largely unpredictable nature of the events coupled with the amount of time taken to travel to the catchments from the IWR's base in Grahamstown. One of the main problems has been that the recordings have frequently failed soon after the start of events (despite working properly when no events occur).

The topographic data have been digitised and stored using GIS, allowing some of the HYMAS routines for automatically estimating the area, slope and distance physiographic variables to be used. Some initial attempts at interfacing DTM data, generated using DEMIURGE (Depraetere, 1992), with HYMAS physiographic data files have been carried out and were quite successful. The main problems experienced are related to the initial generation of the DTM from digitised contour data an the existence of spurious 'pits' which affect the calculations of drainage direction. These have been found to be difficult to remove if the region has relatively low slopes and the grid is fairly dense relative to the map scale (for example a 50 m grid generated from 1:50 000 source data). DEMIURGE generates rectangular grid coverages of altitude, slope direction, etc. and the project team have begun to develop additional software to use these coverages for automatic definition of catchment areas and the generation of some of the physiographic variables used to estimate the parameters of the VTI model. While the draft procedures to estimate the area, slope and distance variables have been completed, further work is still required on the procedures that link the identification of terrain units to soil characteristics defined on land type maps. The ultimate aim is to use these to automatically estimate the distributions of soil and vegetation cover.

Three groups of example applications are reported below, which together are deemed to provide a reasonably representative impression of the applicability of the VTI model to the Bedford catchments and similar regions. The first is a simulation of the soil moisture conditions, within the 0.18 km^2 headwater catchment above gauging station NYQ07, over a an 880 day period. The results are compared with observed soil moisture conditions, estimated from observations taken at approximately two week intervals at 13 neutron probe access tube sites (table 5.2), as well as with simulations using the RAFLES, PEXP and Pitman models.

The second application of the model is a simulation of groundwater recharge and water table levels for the north western part of the catchment where groundwater levels have been monitored at roughly monthly intervals at a number of borehole sites. This area has also been the subject of a geochemically based groundwater recharge study (Sami, 1991 and an earlier section of this report).

The third group are applications of the model to three of the gauged sub-catchments (NYQ03, NYQ05 and NYQ06) to simulate streamflow variations and compare the results with the available observed streamflow. Within one of these sub-catchments (NYQ03), channel transmission losses are known to be a major factor and the simulations of these processes are compared with any available observed information.

5.2.3 Simulation results - Soil moisture variations

This application represents a test of the ability of the VTI model to simulate the soil moisture variations within a small semi-arid catchment and compares the results with three of the other models that form part of HYMAS.

Summary of model differences.

Table 5.1 summarises the approach adopted for the main components of each of the models and illustrates their differences. The table indicates that the VTI and RAFLES models are the most similar, explicitly simulating more physical processes than either of the other two. The Pitman model is the most different, having a time step (1 month) which is much longer than the others. Table 5.1 indicates that the complexity of the models is reflected in the number of parameters and the amount of information required to estimate them.

There are a number of similarities between the VTI and RAFLES models in that both allow two soil layers to be set-up and both attempt to simulate similar runoff processes. Apart from the potentially different time interval structure, one of the main differences is that surface runoff is estimated as volumes ($m^3\ h^{-1}$) in the RAFLES model using a kinematic approach with functions of catchment width, slope and water depth and rate of flow. The VTI model estimates surface runoff as depths (mm) from contributing areas relative to the total sub-catchment area and are only converted to volumes during the sub-area routing component. The subsurface flow components of the two models are more similar. The VTI model also attempts to include a 3-dimensional effect and account for spatial variations in soil water conditions and the effect on runoff generation processes within each sub-area of the distribution system. While this is achieved at the expense of introducing a degree of empiricism, RAFLES also contains a number of empirical components designed to make some of the physically based equations applicable to the scale of the distribution system.

With respect to the different types of runoff processes simulated, the PEXP model is the most different, in that, apart from a relatively minor empirical baseflow function, all the runoff is generated from one SCS algorithm. The division of each sub-area into pervious and impervious is largely irrelevant to this application as the study area is not urbanised.

While the models use the same potential evaporation input data (mean monthly corrected S pan values) the methods for estimating actual evaporation vary from relatively simple linear functions dependent on relative moisture content (PEXP and Pitman) to more complex non-linear functions including a crop factor designed to account for the nature of the vegetation cover and it's rooting characteristics.

Parameter estimation.

The first step in the parameter estimation procedure made use of the physiographic, soils and vegetation information that was available together with the HYMAS routines established to provide initial estimates of most of the critical parameters of the VTI model (table 5.3). After an initial run of the model, minor adjustments were made to some of the more empirical parameters, but no generalised calibration of the parameter values was carried out.

Table 5.1 Summary of model components and their differences.

Component	VTI	RAFLES	PEXP	PITMAN
Parameter info. requirements	High, but empirical estimates from physical data are available.	Moderately high with some estimated from physical data.	Moderate to low.	Low and regional parameter values available for South Africa.
Rainfall Input	Variable time interval (5 mins. to 1 day).	Daily (split into wet & dry part using duration sampled from a seasonal distribution).	Daily (duration determined from a fixed seasonal pattern).	Monthly (four internal iterations).
Interception	Modified Rutter approach.	Similar to VTI model.	None	Tank type storage.
Soil Zones	Two (fixed 150mm surface & defined lower).	Two (defined by parameters).	Single	Single
Intensity Excess Runoff	Kostiakov equation & distribution of infil. rates.	Green Ampt Equation used to determine infiltration from surface water film. Saturation excess when upper soil layer saturated.	Runoff generated using SCS equation. Initial loss coeff. dependent on seasonally varying rainfall intensity factor.	Triangular Distribution of catchment absorption rates.
Saturation Excess Runoff	Based on saturated proportion of upper soil zone distribution.			Runoff occurs when single soil store is full.
Runoff from soil layers	Sub-surface flow from the saturated proportions of both soil layers.	Saturated sub-surface flow from both soil layers.	Non-linear relationship with soil water over defined minimum.	Non-linear relationship with soil water over defined minimum. Divided into soil & g'water flow.
Drainage between soil layers & to groundwater	Drainage from soil layers from proportion of soil water distributions > field capacity at rate of 0.5 sat. hydr. cond.	Drainage from upper soil layer using water content & hydr. cond. Proportional rate of loss from lower layer.	None	None
Actual evapotrans-piration	Non-linear functions of water contents of two soil layers with a crop factor.	Functions of relative water contents of two soil layers with a crop factor.	Linear relationship with soil water storage.	Linear relationship with soil water storage.
Groundwater rise	Estimate of groundwater flow into lower soil zone.	None (if lower layer is taken as a soil zone).	None	None
Sub-area routing	Non-linear storage routing after loss to depressions & small dam storage.	Kinematic flow of the surface flow film.	None	Simple lag function. G'water baseflow lagged separately.
Transmission losses	Estimate of infiltration into a channel loss storage zone.	None	None	None
Channel Routing	Non-linear storage routing.	None	None	None

Table 5.2 Position and depths of readings for soil moisture monitoring sites.

Site	Position	Soil Depth (mm)	Reading Depths (mm)
8/01	Lower catchment, Top-slope	300	150
8/02	Lower catchment, Mid-slope	310	150
8/03	Lower catchment, Valley bottom	1750	150, 300, 500, 750, 1000, 1500
8/04	Lower catchment, Mid-slope	400	150, 300
9/01	Middle catchment, Top-slope	430	150, 300
9/02	Middle catchment, Mid-slope	500	150, 300
9/03	Middle catchment, Valley bottom	1230	150, 300, 500, 750, 100
9/04	Middle catchment, Mid-slope	750	150, 300, 500
10/01	Upper catchment, Top-slope	290	150
10/02	Upper catchment, Mid-slope	2100	150, 300, 500, 750, 1000, 1500, 2000
10/03	Upper catchment, Valley bottom	1800	150, 300, 500, 750, 1000, 1500
10/04	Upper catchment, Mid-slope	1560	150, 300, 500, 750, 1000, 1500
10/05	Upper catchment, Top-slope	500	150, 300

As many of the parameters of the other models share similar meanings with the VTI model, the VTI parameter values were used to assist with estimates of the parameter values of the other models. In a similar way to the VTI model, adjustments were made to some of the less physically related (more empirical) parameters before finalising the simulation results. For the Pitman model, regional parameter values, recommended by Middleton et al. (1981), were used except for the maximum level of the main moisture storage. This value was set to correspond with similar parameters in the other models.

Results

The time series simulated covers a period of some 880 days from November 1989 to March 1992. Within this period a total of 50 separate soil moisture observations were available from each of the access tube sites (table 5.2). The results of the simulations are presented in tables 5.4 to 5.6 as well as figures 5.1 to 5.5. The observed data values have been compiled from weighted means of the various access tube readings. The weights are based on the extent to which each sample depth in each access tube is representative of the whole catchment. Figure 5.1 illustrates the variation in the moisture content of the upper (lower line on the graph) and lower (upper line) soil layers as simulated by the VTI model and includes a representation of the rainfall time series. In this figure all the data points have been plotted after an initial warm up period of 100 days. Figures 5.2 to 5.5 compare the time series of observed soil moisture content with the simulated values for all the models. In these figures only the data points corresponding to times of moisture measurement are plotted, producing a much smoother pattern of variation than can be seen in figure 5.1. In figure 5.5 (Pitman model) the simulated monthly values are repeated where more than one measurement data point occurs in the same month. This explains the stepped appearance of

the graph. Table 5.6 provides some comparisons of the estimated durations and intensities of rainfall for the two daily models (RAFLES and PEXP) with the real values used as input to the VTI model.

Table 5.3 VTI model parameters.

Area (km^2)	0.18
Mean Catchment Slope (%)	7.0
Channel Slope (%)	4.0
Shreve Channel Order	1.0
Crop Factor	0.5
Canopy Capacity (mm)	0.05
Soil Porosity (% Vol.)	37.6
Field Capacity (% Vol.)	28.4
Wilting Point (% Vol.)	16.8
Mean Soil Depth (mm)	48.2
Soil Hydr. Cond. ($mm\ h^{-1}$)	1.8
Infiltration Curve k	0.45
Infiltration Curve C	128.1
St. Dev. of Moist. Content Dist.	0.26
Max. Depression Store (mm)	2.0
Aquifer Storativity	0.005
Aquifer Transmissivity ($m^2\ day^{-1}$)	15.0
Depth of Aquifer (m)	50.0
Adjusted Aquifer Hyd. Cond. ($mm\ h^{-1}$)	0.03
G'water Drainage Vector (Fraction)	1.0
Regional G'water Slope (%)	1.3
Sub-area Routing Coeff. (K)	1.4

The immediate impression provided by figures 5.2 to 5.5 as well as table 5.4 is that the VTI model simulates the observed soil moisture variation most successfully, largely because there are fewer extreme deviations from the observed values. The monthly time step Pitman model generates the worst results, but this is not unexpected as the model was never designed to accurately simulate soil moisture at this resolution.

The better results generated by the VTI model are difficult to ascribe to any single model component. Table 5.6 suggests that the variable time interval approach is likely to be contributing, in that the estimated durations (and consequently the assumed rainfall intensities) used for the main rainfall events in the RAFLES and PEXP models, are frequently very different from the real durations. The increased complexity of some of the other VTI model components may also be helping, but part of this contribution may be

related to the authors experience of this model and determining the parameter values. There are several more empirical type parameters in the RAFLES model, which after additional adjustment could result in improved simulations. However, it was not the intention to carry out detailed calibrations of the parameters against the observed moisture data.

Table 5.4 Sum of squares differences between simulated and observed moisture contents (mm) for the total soil profile as well as surface and deep layers (where applicable). The figures are based on 50 data points.

Model	Surface layer (0 - 150 mm)	Deeper layer (150 - 482 mm)	Total profile (0 - 482 mm)
VTI Model	1205	2604	4543
RAFLES Model	2195	7145	9216
PEXP Model			6120
Pitman Model			18864

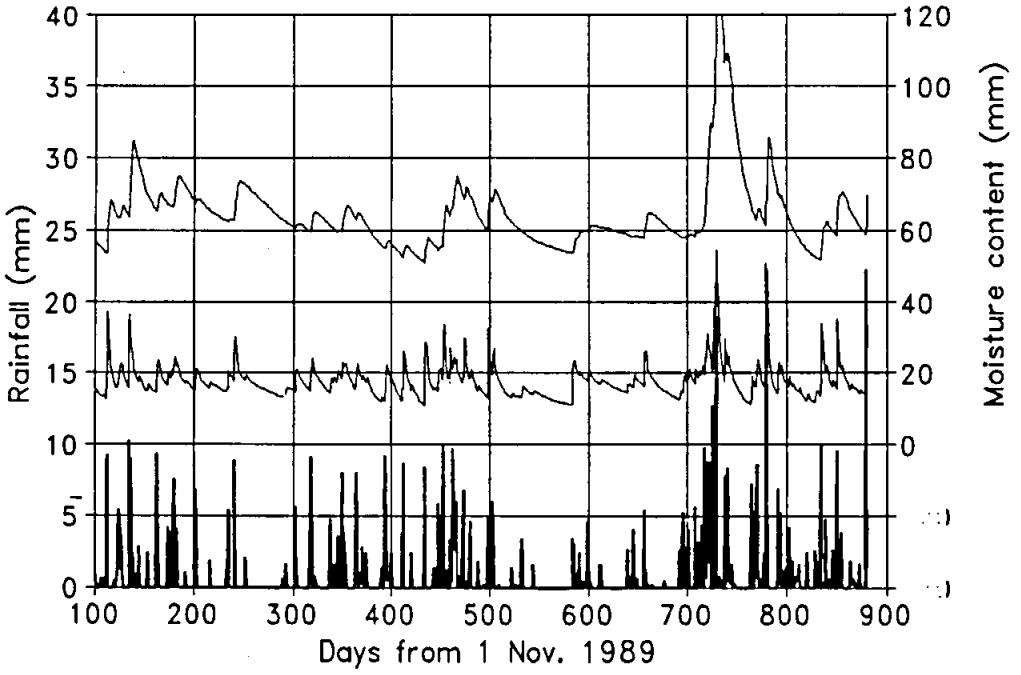

Figure 5.1 Rainfall and simulated soil moisture (upper and lower soil layers) for all time intervals of the VTI model after an initial warm up period of 100 days.

The VTI model does appear to overestimate the amount of variation demonstrated by the observed water contents of the lower zone for this catchment. This may be partly related to the widely spaced sampling interval of the observed data. It may also be attributable to an overestimate of the amount of drainage to the lower zone and evaporation from that zone. All of the other models produce even higher degrees of variation in the total water content than the VTI model. In the case of the PEXP and Pitman model this result can be at least partly ascribed to the single soil storage used. The effects within the RAFLES model are likely to be related to similar problems of drainage and evaporation estimation as in the VTI model.

It is somewhat surprising that the simpler, single soil storage, PEXP model simulates the total soil moisture content better than the two-layer RAFLES model. Both have relatively simplified evapotranspiration routines, but while the RAFLES model uses a non-linear relation with soil moisture, the PEXP model relation is linear. The main differences appear to be that the RAFLES model produces higher water contents in the deeper soils after wetting and excessive drying over prolonged dry periods (days 500 to 700). This is consistent with the differences in the evapotranspiration algorithms used in the two models as well as the fact that RAFLES includes a lower zone drainage routine.

Although the evapotranspiration approach used in the PEXP model is very similar to that used in the Pitman model, the effect on the simulated results is very different. This can be attributed to the different time steps used. The relatively long periods between days of rainfall which are sufficient to cause some recharge of soil moisture in the daily models are not reflected as such extreme dry periods in the monthly model. Similarly, relatively dry months, especially in summer during high potential evaporation, may be made up of a series of days with low, but significant, rainfall events which may somewhat offset evaporation losses and maintain higher moisture levels in the daily models. It is hardly surprising that some of the peaks and troughs of moisture content in the monthly model are out of phase with those in the daily models.

All of the models over-simulate the main wet period at about day 720, but this feature may be more related to small differences (less than one day) in the relative timing of observed and simulated values. The models suggest that the soil moisture levels approach saturation (approximately 180mm for the total profile) at the peak of this period, while the observed data only just exceed field capacity (approximately 120mm). In reality, even if it reached that level, the moisture content is unlikely to remain there for very long and may have been missed at the time of observation.

Table 5.5 compares the simulated runoff volumes for all the days and months of the complete 29 month period when runoff was generated by any one model. It is apparent that, in general terms, there are few differences between the models except that the RAFLES model consistently generates more flow during the main runoff periods and that the monthly Pitman model generates small volumes of flow when the other models do not. Unfortunately, there are insufficient observed flow data to evaluate these simulated flows.

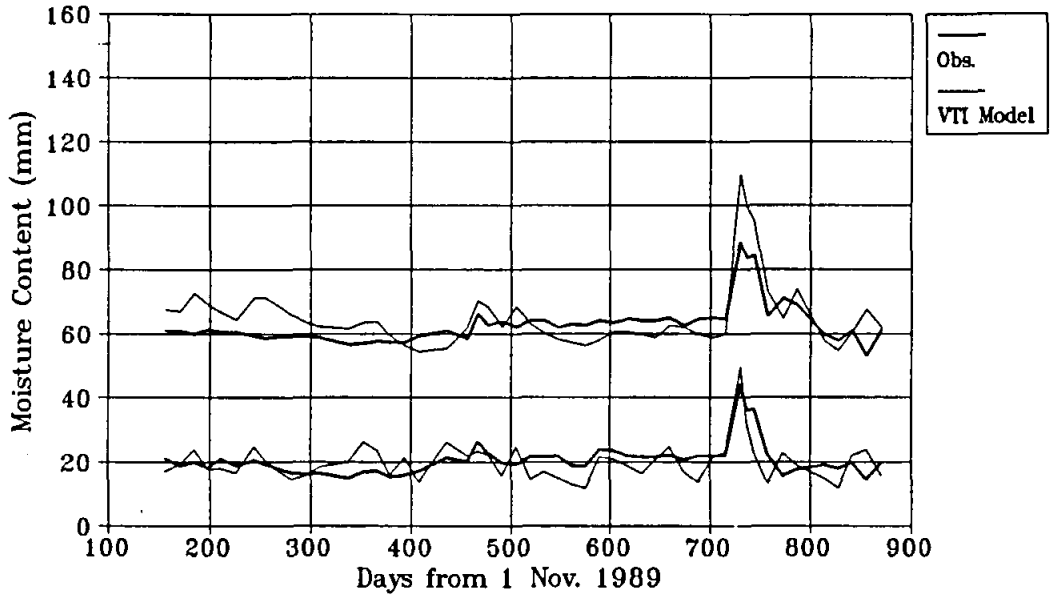

Figure 5.2 Comparison of observed and simulated soil moisture variations for the upper and lower soil layers using the VTI model.

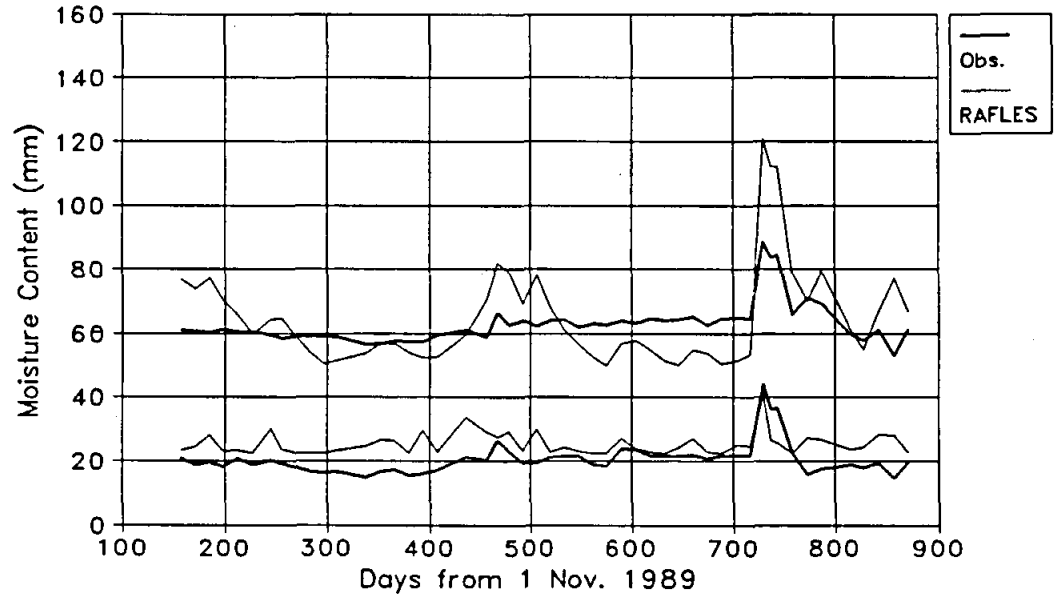

Figure 5.3 Comparison of observed and simulated soil moisture variations for the upper and lower soil layers using the RAFLES model.

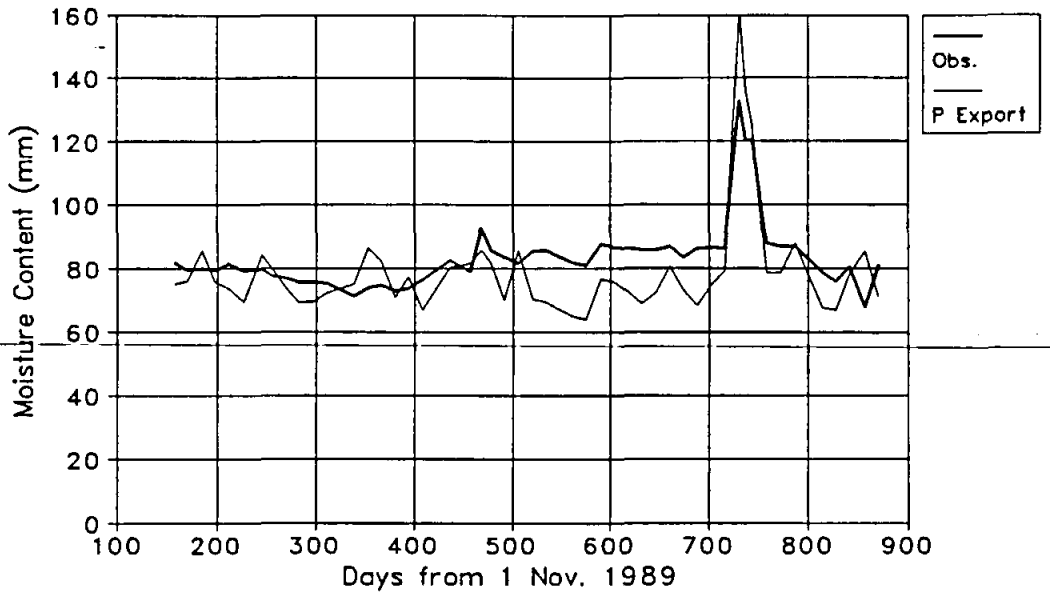

Figure 5.4 Comparison of observed and simulated soil moisture variations for the total soil profile using the PEXP model.

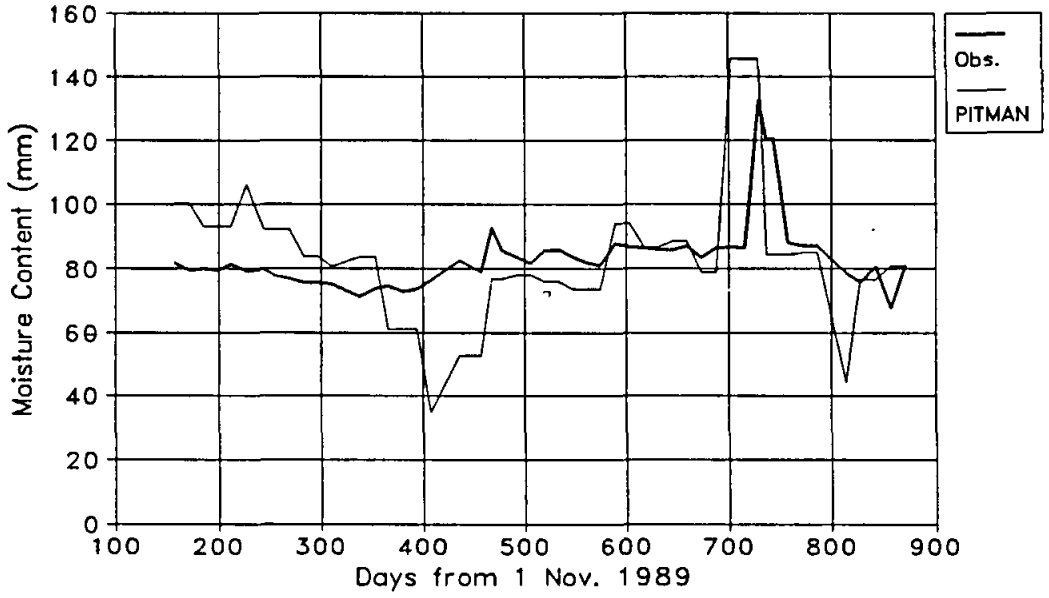

Figure 5.5 Comparison of observed and simulated soil moisture variations for the total soil profile using the monthly Pitman model.

Table 5.5 Monthly rainfall and runoff volumes simulated using the four models (where appropriate individual daily values are also listed).

			Runoff volume (Ml)			
Month (from Nov. 1989)	Day	Rain (mm)	VTI Model	RAFLES Model	PEXP Model	Pitman Model
	14	44.4	0.92	1.31	0.61	
	15	92.9	9.58	14.03	8.68	
	16	13.7	1.76		0.93	
	18	6.2			0.07	
1		199.7	12.26	15.34	10.29	9.37
3		55.2	0.0	0.0	0.06	0.06
	134	28.2			0.01	
4		36.4	0.0	0.0	0.01	<0.01
5, 6 & 12		142.4	0.0	0.0	0.0	0.12
15		63.8	0.0	0.0	0.0	0.12
16		60.0	0.0	0.0	0.0	0.09
17		39.3	0.0	0.0	0.0	0.01
	727	22.0	0.01		0.11	
	728	31.0	0.81	2.42	1.29	
	729	38.5	4.07	4.38	4.24	
24		175.3	4.89	6.79	5.64	6.32
25		30.0	0.0	0.0	0.04	0.0
	779	51.8	1.41	3.08	1.03	
	780-781	0.0	<0.01			
26		97.8	1.41	3.08	1.03	0.78
28		64.6	0.0	0.0	0.0	0.13
29		44.4	0.33	0.0	0.0	0.02
Total runoff (Ml)			18.89	25.21	17.06	17.01

With respect to the origin of the simulated flows, all of the Pitman and RAFLES models flows and greater than 99% of the PEXP model flows are generated as surface runoff. Different types of surface runoff are not distinguished in these three models. For the three major events (days 14-16, 779-780 and 727-729) the VTI model simulates between 65 and 90% of the flow as saturated area runoff, between 7 and 30% as intensity excess over infiltration type runoff and 3 to 5% as saturated sub-surface runoff. The relatively minor contribution of sub-surface flow is consistent with field observations.

Table 5.6 illustrates the likely effect that the daily rainfall 'dissagregation' routines in the RAFLES and PEXP models will have on the runoff simulation results by comparing the estimated rainfall durations or intensities with the real ones as input to the VTI model. This table provides at least a partial explanation for the differences between the runoff generated by the VTI and RAFLES models. The durations estimated by the RAFLES model for the two highest rainfall days (15 - 92.9mm and 779 - 51.8mm) are substantially lower than the real values and this partially accounts for the higher amounts of runoff generated compared to the VTI model. The impact on the PEXP model does not appear to be as noticeable, which may be related to the use of a far more empirical runoff generation function in this model.

Table 5.6 Comparison of rainfall durations on some days used for the two daily models with the real duration used within the Variable Time Interval model.

		RAFLES		PEXP	VTI	
Month	Rain (mm)	Duration (h)	Intensity (mm h^{-1})	Duration (h)	Duration (h)	Mean and St. Dev. of Intensity (mm h^{-1})
Nov. 1989	44.4	13.2	3.4	9.3	8.0	5.5 (6.4)
Nov. 1989	92.9	9.2	10.1	9.3	24.0	3.9 (2.8)
Nov. 1989	13.7	8.5	1.6	9.3	12.0	1.1 (1.3)
Jan. 1990	32.7	7.1	4.6	8.0	18.0	1.8 (0.6)
Feb. 1990	28.2	8.1	3.5	8.3	8.0	3.5 (3.8)
Oct. 1991	22.0	14.3	1.5	10.9	6.0	3.6 (2.4)
Oct. 1991	31.0	14.8	2.1	10.9	11.0	2.8 (3.7)
Oct. 1991	38.5	8.9	4.3	10.9	11.0	3.4 (6.7)
Dec. 1991	51.8	2.5	20.9	8.3	4.0	6.6 (10.5)

Given the fact that most of the parameters were derived directly from measured physical characteristics without further calibration and that evapotranspiration losses are based on mean monthly input data, the VTI model has simulated the soil moisture variations reasonably well. The most difficult parameter to estimate directly was found to be the crop or vegetation factor, which is used in the actual evaporation routines. More information is certainly required about the best approach to use to estimate values of this parameter from available data about the vegetation cover.

It should be recognised that applying the VTI model to a small first order catchment means that some of the parameters become largely irrelevant. It would therefore be incorrect to assume that equally good simulations can necessarily be achieved on larger catchments. However, this applies more to the generation of streamflow, where the routing and transmission loss routines play a greater role, than to the simulation of soil moisture variations. There are also no interactions between the surface and groundwater in this catchment (except for recharge) and most of the parameters related to this model component

do not play a role in this application. The only one that does is the hydraulic conductivity of the aquifer body which affects the amount of drainage from the lower soil zone.

Some of the better simulation results for the VTI model can be attributed to the greater time resolution allowed for. However, in most practical applications of hydrological simulation models, rainfall data of such a high time resolution are rarely available.

5.2.4 Simulation results - Streamflow

Three of the gauged Bedford sub-catchments have been used in this part of the model testing exercise. The first two are the closely adjacent catchments NYQ05 and NYQ06 to the south af the area and the third is NYQ04 to the north and which includes the area of alluvial valley fill referred to in Hughes and Sami, 1992. These have been chosen at this stage largely because of the amount of reasonably reliable observed streamflow that is available for them. There were four main flow events experienced in these cathments in the period 1989 to 1991; October and November 1989 and October and December 1991.

NYQ05 and NYQ06

These two were treated as a single model project with 6 sub-areas set-up. The outlet from sub-area 3 represents NYQ05 and the outlet from sub-area 5, NYQ06. The outlet from the sixth sub-area represents their combined flow but is not gauged. Table 5.7 lists some of the model parameter values that resulted from the standard estimation procedures using the physiographic variable data. It is apparent that many of the soil and vegetation parameters have been set at the same values for all the sub-areas. This is because there is not enough information to differentiate between them. It is also worth noting the large proportion of the area which drains into small farm dams and the fact that the combined volumes are not insignificant.

Figure 5.6 A, B, C and E show the rainfall and observed and simulated streamflow hydrographs for two events (28 October and 18 December, 1991) at NYQ06. These graphs were extracted from an initial run of the VTI model over a period June to December 1991. The time interval structure was established as follows :

Rain $<$ 10 mm d^{-1}	1440 min time step.
10 mm d^{-1} $<$ Rain $<$ 10 mm $6h^{-1}$	360 min time step.
10 mm $6h^{-1}$ $<$ Rain $<$ 5 mm h^{-1}	60 min time step.
Rain $>$ 5 mm h^{-1}	15 min time step.

The lower threshold to determine the step into 15 minute modelling was found to be necessary to adequately define the temporal resolution of the rainfall input to the October event. A smaller threshold tended to smooth out the higher intensities ($>$ 6mm of rain in 15 min) during this storm relative to the December event.

Figure 5.6 B and E demonstrate that the 'standard' parameter set underestimates the October event and overestimates the December event. A detailed comparison of the two storms characteristics and a check of the observed data (rain and flow) was carried out to try and determine any factors (including poor parameter value estimation) which might be responsible for this situation. The conclusion was that no errors could be found in the data and no amount of parameter value adjustment (where the values remain fixed for the whole period) could significantly improve the simulations. Any attempts to increase the simulated discharges for the October event caused even greater over simulation of the December event. This is largely due to the fact that the major discharge component is related to intensity excess runoff generated as a result of high intensities and the intensities are higher for the December event. The soils are very wet at the end of both events (they have similar total

rain depths of about 50 mm) and there is some saturation excess runoff, but most of the rainfall has already passed by the time significant areas of saturation are developed in the model. Five raingauges are located either within, or close to the boundary of this catchment and the observed data do not demonstrate any spatial variability patterns that have not been reflected in the model input. It is therefore difficult to attribute the poor model results to inadequate spatial resolution of the rainfall input.

Table 5.7 VTI model parameters for NYQ05 and NYQ06 simulations.

Sub-area	1	2	3	4	5
Area (km^2)	9.5	12.0	9.6	10.3	7.4
Next downstream sub-area	2	3	6	5	6
Mean Catchment Slope (%)	6.8	6.2	6.7	6.4	5.3
Channel Slope (%)	1.4	1.3	0.9	1.6	1.2
Shreve Channel Order	6	6	18	9	15
Crop Factor	0.5	0.5	0.5	0.5	0.5
Canopy Capacity (mm)	0.22	0.22	0.22	0.22	0.22
Soil Porosity (% Vol.)	37.6	37.6	37.6	37.6	37.6
Field Capacity (% Vol.)	24.4	24.4	24.4	24.4	24.4
Wilting Point (% Vol.)	13.5	13.5	13.5	13.5	13.5
Mean Soil Depth (mm)	32.5	32.5	37.0	32.5	37.0
Soil Hydr. Cond. (mm h^{-1})	5.6	5.6	5.6	5.6	5.6
Infiltration Curve k	0.53	0.53	0.53	0.53	0.53
Infiltration Curve C	159.0	159.0	159.0	159.0	159.0
St. Dev. of Moist. Content Dist.	0.19	0.19	0.19	0.21	0.21
Max. Depression Store (mm)	1.5	1.5	1.5	1.5	1.5
Aquifer Storativity	0.003	0.003	0.003	0.003	0.003
Aquifer Transmissivity (m^2 day^{-1})	15.0	15.0	15.0	15.0	15.0
Depth of Aquifer (m)	50.0	50.0	50.0	50.0	50.0
Adjusted Aquifer Hyd. Cond. (mm h^{-1})	0.04	0.04	0.04	0.04	0.04
G'water Drainage Vector (Fraction)	1.5	1.5	1.5	1.5	1.5
Regional G'water Slope (%)	4.0	4.0	4.0	4.0	4.0
Sub-area Routing Coeff.	3.2	3.5	3.3	3.4	3.9
Area (%) above small dams	94.0	85.2	11.3	49.1	55.6
Combined dam volume (Ml)	18.7	57.8	2.1	59.7	29.4

A relatively rapid response of the ground cover vegetation to large rainfall events has been observed in these catchments, as well as others in the semi-arid parts of the eastern Cape. This is particularly true if the event follows a long dry period when the ground cover has appreciably deteriorated and if the event occurs in spring or summer when germinating and

growing conditions are favourable. The possible implication is that infiltration characteristics are quite different before such events and afterwards, when the vegetation has had a chance to respond. The 'standard' parameters given in table 5.7 could be overestimating the infiltration rates (7.5 mm h^{-1} @ 120 min) for the October storm and underestimating for the December storm. Figure 5.6 C and F illustrate the simulation results obtained by reducing infiltration rates for the October event (k = 0.45, C = 170; 5.7 mm h^{-1} @ 120 min) and increasing them for the December event (k = 0.56, C = 197; 13.2 mm h^{-1} @ 120 min). Whether or not these values represent the range of infiltration rates that do occur in response to changes in vegetation cover can only be confirmed by detailed field experimentation.

A further possibility is that some part of the model formulation is inadequate to account for the differences in the processes occurring during these two events. The re-infiltration model component, that prevents some of the runoff generated on slopes from reaching the channel, is one possible source of inadequacy and may also be related to surface cover conditions. Even the improved simulations shown in figure 5.6 indicate that the small, but significant, responses to the intense rainfall in the early parts of both storms are underestimated. Both occur at a point when the soil moisture content is relatively low and the re-infiltration potential in the model is high.

Figure 5.7 illustrates the results of extending the simulation period back to 1989 and using the same 'standard' parameter values (table 5.7). As with figure 5.6, the bold lines represent the simulated flows. There are two major storm events (2 to 4 October and 14 to 18 November), which are quite different in character from the 1991 events. Total storm rainfall varies from 90 to 60 mm for the October 1989 event and from 140 to 70 mm for the November 1989 event. There is therefore quite a high degree of spatial variability in these two large events. They also have generally lower rainfall intensities than the 1991 events. The result is that the simulations suggest that saturation excess runoff processes are dominant.

The model has over simulated the October event and reasonably well simulated the November event except for the first part. The excessive flows simulated for the October event are difficult to ascribe to any possible differences in catchment characteristics not represented by the parameter values, such as was hypothesised for the two 1991 events. The November event shows some of the same characteristics as the 1991 events, in that the initial part of the hydrograph has not been simulated. It was suggested earlier that this may be related to an inadequacy in the re-infiltration component of the model. A further possibility is that a fairly rapid response is occurring from a part of the catchment close to the outlet and that the spatial resolution allowed for in the model does not account for this. Closer examination of the position of the farm dams in the lower sub-area of NYQ06 tends to support the latter suggestion. Most of them are located in the upper areas of the catchment, such that any initial response is likely to be more rapid than the overall sub-area routing parameter would suggest.

The sub-area routing parameters are represented by fixed values for any one month and it is possible that the real attenuation varies with the characteristics of the runoff response. For example, there could well be routing differences between runoff generated at different stages of surface layer saturation, or for different levels of infiltration excess exceedence.

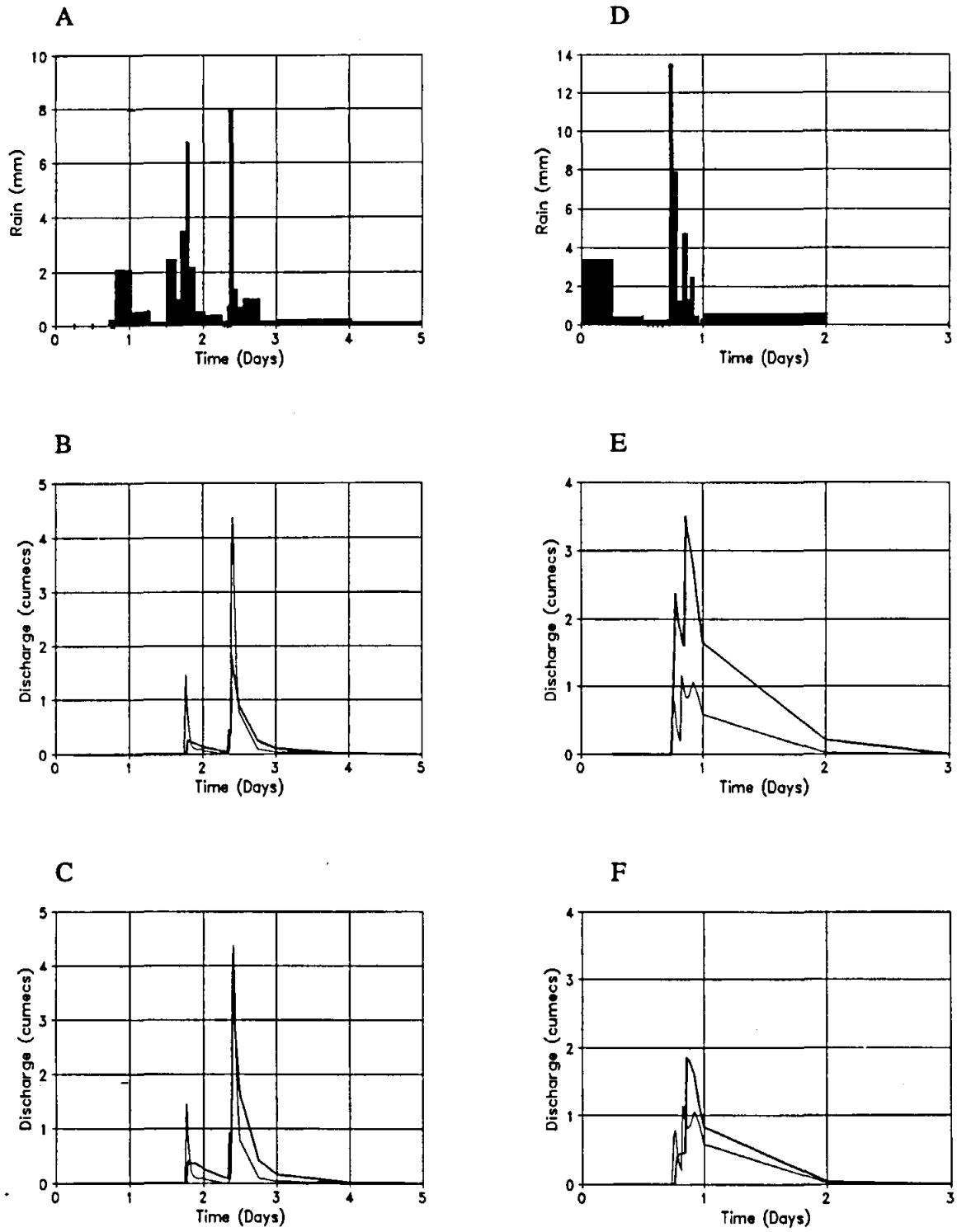

Figure 5.6 Observed rainfall (A & D), simulated (bold lines) and observed flow for the October (B & C) and December (E & F) 1991 events at NYQ06. Graphs B and E represent simulations using the 'standard' parameters and graphs C and D after changes to some parameter values to account for possible changes in the basal vegetation cover and infiltration rates after the October event (the block widths in the rainfall diagrams reflect the variable time intervals used).

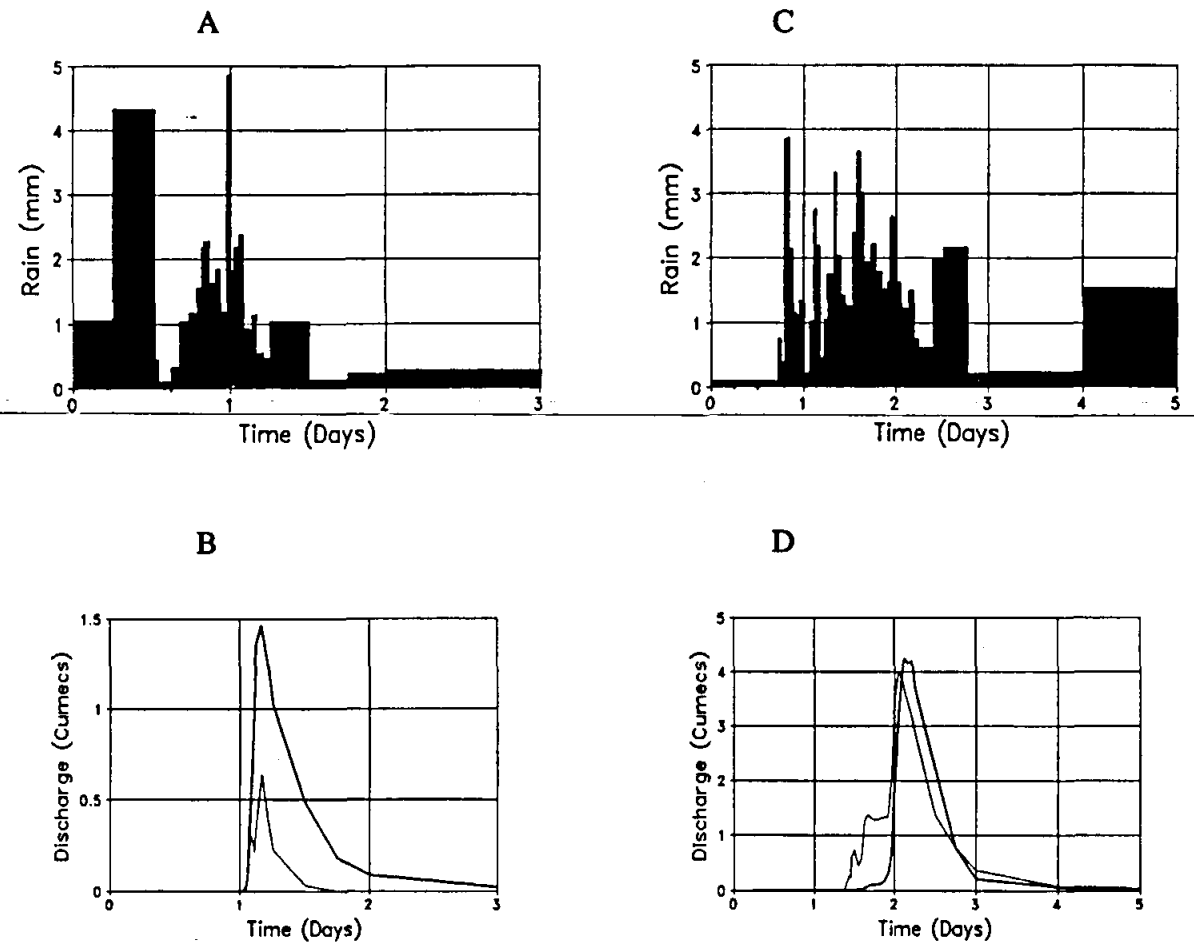

Figure 5.7 Observed rainfall (A & C) and comparisons between simulated (bold lines) and observed flow for the October (B) and November (D) 1989 events at NYQ06 (the block widths in the rainfall diagrams reflect the variable time intervals used).

In general terms, application of the VTI model to NYQ06 has produced mixed results with some storms over- and others under simulated. There do not appear to be any easy determine reasons for this and extensive calibration may improve the results for some storms, but would compromise other events. There is less observed flow data for NYQ05, but that which is available tends to support the conclusions reached about NYQ06. There is some evidence to suggest that a higher spatial resolution (more sub-areas) might be beneficial, however, this presupposes that there is sufficient field information to quantify the parameters over smaller sub-areas.

It should be recognised that the runoff response to all the storms represent less than 7% of the total storm rainfall. Consequently, a small variation in the way in which runoff generation processes are represented in the model may only lead to a small difference in the amount of rainfall that becomes runoff (e.g. 1%), but a large difference in the amount of runoff (e.g. 20%). This is a problem common to the application of most models in arid and semi-arid catchments.

NYQ04

This gauge is situated to the north west of the total Bedford catchment and has been used as an example because of the presence of a significant area of alluvial valley bottom deposits a few km from the gauging weir. It therefore represents an opportunity to assess the application of the channel transmission loss component of the model. The total catchment has been divided up into 9 sub-areas and most of the parameter values (table 5.8) estimated from the information available on the physical characteristics of the area. Some of the parameters (crop factor, depression storage, etc.) have been roughly calibrated as they cannot be directly estimated at present. The two transmission loss power parameters are not reported in table 5.7 but have been set, for all sub-areas, at 0.6 for the flow related power (CLP1, table 4.1) and 3.0 for the storage related power (CLP2, table 4.1). The combination of this set of parameter values suggests an infiltration rate of 99 mm h^{-1} when the storage is about 50% of maximum and the upstream flow rate 5 $m^3 s^{-1}$.

As with the other Bedford catchments there is not a great deal of information about the real spatial variation in soil and vegetation characteristics and some of the differences between sub-areas are inferred from subjective field assessments. There are observed flow data for parts of the 1989 and 1991 events, but this information is incomplete. Reference to Hughes and Sami (1992) and section 2.5 of this report indicates that som estimates of the extent of the channel transmission losses have been made on the basis of soil moisture measurements. The results of the simulations are difficult to evaluate without more complete observed data, however, some observations can be made.

The October 1989 event does not appear to have been simulated very well; the timing is very different to the observed and the flow peak and volume are much greater. The observed peak is about 0.25 $m^3 s^{-1}$ and the simulated 1.4 $m^3 s^{-1}$. Figure 5.8 B indicates that very little flow survives the transmission loss area in sub-area 3, and therefore any over simulation of this event must be due to sub-areas 1 and 2. To reduce the simulated flow to the observed levels it is necessary to change the infiltration and soil moisture storage parameters to values which are very different from the values that otherwise appear to be reasonably acceptable for this catchment. There is no field evidence to suggest that these areas are particularly different to others and the rainfall input to the model would seem to be acceptable, based on the records from nearby gauges. It is therefore difficult to explain why the model generates such poor results for this event. The other possibility is that the observed flow record is inaccurate (this was the first time that this weir had experienced flow since being built and the recording equipment installed). The model estimates that the total transmission losses during this event were some 165 Ml, which also suggests that the flow from the upstream areas is being over simulated, if this figure is compared to the estimates given in section 2.5 of this report 89 Ml. However, it should be noted that the latter figure is a minimum figure based on some unconfirmed assumptions.

The shape, size and timing of the November 1989 event have been simulated much more successfully, although the recession is greatly extended relative to the observed data. The total simulated transmission losses amount to some 179 Ml compared to the soil moisture based estimate of 182 Ml.

Table 5.8 VTI model parameters for NYQ04 simulations.

Sub-area	1	2	3	4	5	6	7	8	9
Area (km^2)	4.6	4.7	6.0	4.5	2.8	2.6	3.9	5.3	5.7
Next downstream sub-area	0	1	1	3	3	5	6	6	6
Mean Catchment Slope (%)	5.4	5.3	8.6	7.5	10.2	9.3	5.7	8.7	9.5
Channel Slope (%)	1.2	1.9	1.1	2.7	1.7	1.8	2.8	2.3	3.3
Shreve Channel Order	27	2	23	2	19	13	4	6	5
Crop Factor	0.6	0.55	0.65	0.5	0.5	0.5	0.5	0.5	0.5
Canopy Capacity (mm)	0.17	0.17	0.22	0.16	0.21	0.16	0.17	0.16	0.16
Soil Porosity (% Vol.)	37.8	37.8	38.6	37.8	38.5	38.5	37.8	37.8	37.8
Field Capacity (% Vol.)	25.2	25.2	22.6	25.2	25.2	25.2	25.3	25.3	25.3
Wilting Point (% Vol.)	14.2	14.2	14.8	14.2	14.2	14.2	14.2	14.2	14.2
Mean Soil Depth (mm)	55.0	49.5	66.0	41.5	42.5	39.0	40.0	39.0	39.0
Soil Hydr. Cond. ($mm\ h^{-1}$)	5.1	5.1	6.3	5.1	6.1	6.1	5.1	5.1	5.1
Infiltration Curve k	0.53	0.53	0.53	0.53	0.53	0.53	0.53	0.53	0.53
Infiltration Curve C	160.0	160.0	160.0	160.0	160.0	160.0	160.0	160.0	160.0
St.Dev.Moist.Content Dist.	0.30	0.30	0.25	0.20	0.20	0.20	0.20	0.20	0.20
Max. Dep. Store (mm)	2.5	2.5	2.5	2.5	2.5	2.5	2.5	2.5	2.5
Aquifer Storativity	0.005	0.005	0.005	0.005	0.005	0.005	0.005	0.005	0.005
Aquifer Trans.($m^2\ day^{-1}$)	15.0	15.0	15.0	15.0	15.0	15.0	15.0	15.0	15.0
Depth of Aquifer (m)	50.0	50.0	50.0	50.0	50.0	50.0	50.0	50.0	50.0
Adj.Aq.Hyd.Cond.($mm\ h^{-1}$)	0.06	0.06	0.06	0.06	0.06	0.06	0.06	0.06	0.06
G'w Drain. Vector (Fract.)	1.5	1.5	1.5	1.5	1.5	1.5	1.5	1.5	1.5
Regional G'water Slope (%)	4.0	4.0	4.0	4.0	4.0	4.0	4.0	4.0	4.0
Sub-area Routing Coeff.	3.4	3.5	2.6	2.6	2.3	2.2	3.3	2.4	2.3
Area (%) above small dams	50.0	78.0	13.1	42.5	19.1	11.7	52.5	55.2	89.2
Combined dam volume (Ml)	12.0	1.9	2.4	2.4	1.1	0.6	1.1	5.4	12.0
Flow Infil. Area (km^2)	0.03	0.03	0.38	0.01	0.01	0.0	0.01	0.0	0.0
Channel Infil. curve k	0.6	0.6	0.6	0.6	0.6	0.6	0.6	0.6	0.6
Channel Infil. curve C	6000	6000	6000	6000	6000	6000	6000	6000	6000

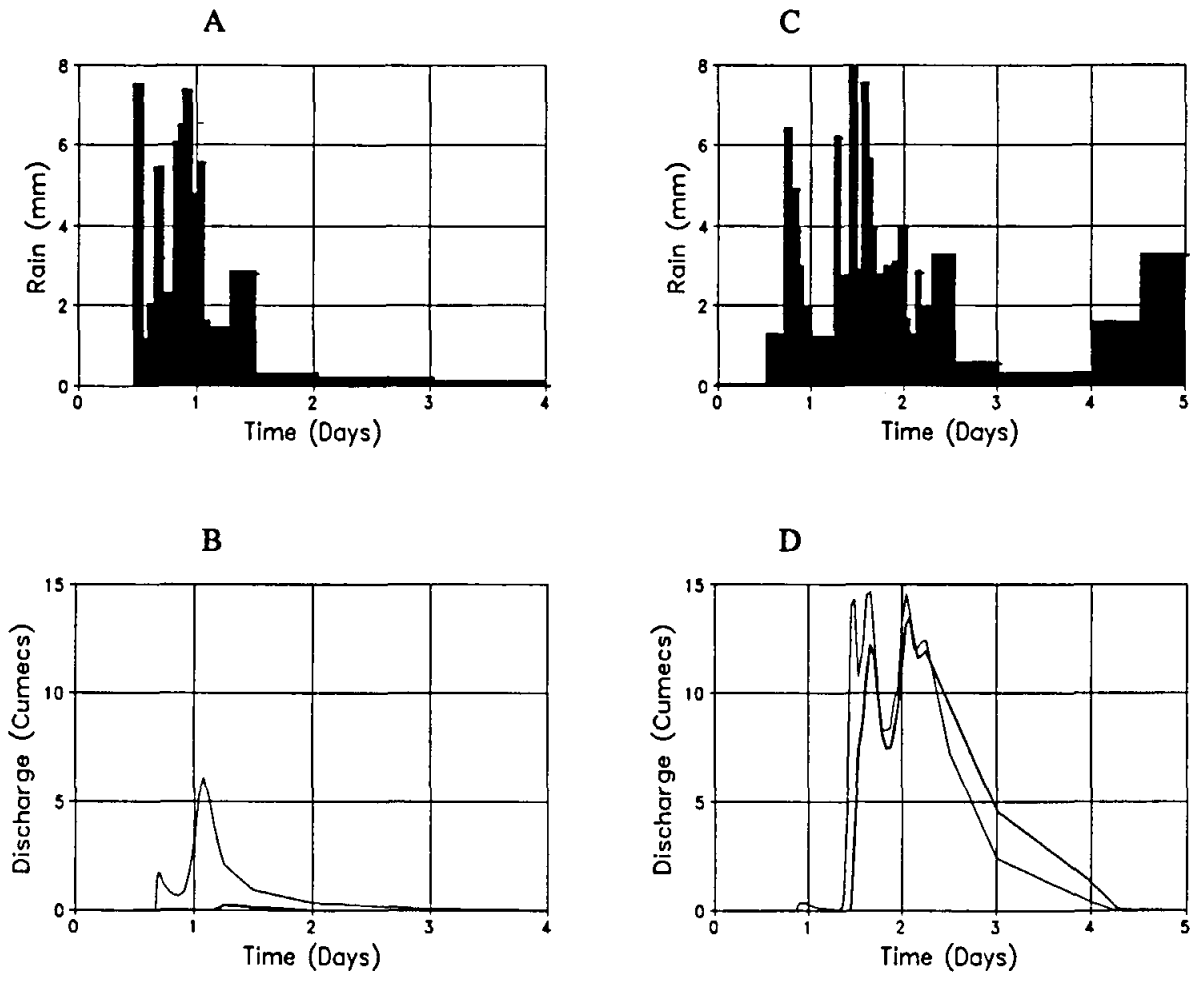

Figure 5.8 Observed rainfall (A & C) and comparisons between simulated (bold lines) and observed flow for sub-area 3 for the October (B) and November (D) 1989 events at NYQ04 (the block widths in the rainfall diagrams reflect the variable time intervals used).

There is little doubt that the empirical nature of the transmission loss parameters mean that it is very difficult to derive *a priori* estimates and that some form of calibration is necessary. However, it has also been found to be very difficult to calibrate these parameters even for a single event. This is largely because they are closely interrelated and it is not a trivial matter to predict the effect of changing one of the parameters on the overall event losses. The current approach has been used in the absence of a more suitable and physically based algorithm, but the developers recognise that this component of the model requires attention before it can be considered useful for anything but research applications. Some further comments will be made about this component in a later section where the simulation results for the Tombstone, Arizona, USA catchments are discussed.

5.2.5 Simulation results - Groundwater recharge

This section focuses on results obtained from the groundwater components of the model and compares the simulated response in several Bedford sub-catchments to observations of fluctuations in groundwater levels and estimates of recharge. Mean annual recharge, and its spatial variability over 12 sub-catchments was estimated from chloride concentrations in groundwater (section 2.5). The simulated time-series of recharge in the same sub-catchments over a 36 year period (1956-1991) is compared to the long term mean calculated from the chloride mass balance. The results show that the model successfully integrates surface and subsurface interactions in fractured rock situations with episodic recharge.

Table 5.9 Key model parameters and physical characteristics.

Sub-area	1	2	3	4	5	6
Area (km^2)	17.74	1.07	4.45	3.52	0.73	17.69
Mean Catchment Slope (%)	3.5	9.5	8.0	5.0	9.4	9.3
Channel Slope (%)	1.17	1.58	1.31	0.94	1.92	1.20
Shreve Channel Order	10	2	9	11	1	20
Crop Factor	0.70	0.50	0.55	0.55	0.50	0.55
Canopy Capacity (mm)	0.74	0.21	0.24	0.24	0.17	0.19
Soil Porosity (% Vol.)	37.61	37.61	37.61	37.61	37.65	37.65
Field Capacity (% Vol.)	23.56	23.56	23.56	23.56	24.4	24.4
Wilting Point (% Vol.)	13.34	13.34	13.34	13.34	13.5	13.5
Mean Soil Depth (mm)	645	390	450	560	390	465
Soil Hydr. Cond. (mm h^{-1})	7.33	7.33	7.33	7.33	6.15	6.15
Infiltration Curve k	0.54	0.54	0.54	0.54	0.53	0.53
Infiltration Curve C	160.5	160.5	160.5	160.5	155.8	155.8
St. Dev. of Moist. Content Dist.	0.16	0.16	0.15	0.16	0.20	0.22
Max. Depression Store (mm)	1.0	1.0	1.0	1.0	1.0	1.0
Max. Dam Store (Ml)	28.98	1.10	1.70	7.30	0.16	25.60
% Area above Dams	53.8	64.6	76.1	29.7	84.1	29.8
Aquifer Storativity	0.001	0.001	0.001	0.001	0.001	0.001
Aquifer Transmissivity (m^2 day^{-1})	15.0	15.0	15.0	15.0	15.0	15.0
Depth of Aquifer (m)	50.0	50.0	50.0	50.0	50.0	50.0
Adjusted Aquifer Hyd. Cond. (mm h^{-1})	0.008	0.008	0.008	0.008	0.008	0.008
G'water Drainage Vector (Fraction)	15.0	15.0	15.0	15.0	15.0	15.0
Max. Rest Water Level (m)	40.0	50.0	50.0	50.0	45.0	50.0
G'water Dist. Vector (Sub-areas)	12,0	3,11	4	11	6	8,7
(%)	60,40	90,10	100	100	100	80,20
Max. Regional G'water Slope (%)	2.5	2.5	2.5	2.5	2.5	2.5
Sub-area Routing Coeff. (K)	10.66	2.13	2.53	3.56	2.07	2.18

Table 5.9 continued.

Sub-area	7	8	9	10	11	12
Area (km^2)	4.90	6.94	11.65	11.57	19.32	12.18
Mean Catchment Slope (%)	7.5	8.6	5.4	5.0	5.0	5.0
Channel Slope (%)	1.44	1.18	0.71	0.44	0.71	0.67
Shreve Channel Order	4	28	33	36	24	72
Crop Factor	0.55	0.60	0.65	0.60	0.60	0.65
Canopy Capacity (mm)	0.19	0.19	0.25	0.23	0.23	0.35
Soil Porosity (% Vol.)	37.65	37.65	37.65	37.61	37.61	37.61
Field Capacity (% Vol.)	24.4	24.4	24.4	23.56	23.56	23.56
Wilting Point (% Vol.)	13.5	13.5	13.5	13.34	13.34	13.34
Mean Soil Depth (mm)	485	465	580	645	535	735
Soil Hydr. Cond. (mm h^{-1})	6.15	6.15	6.15	7.33	7.33	7.33
Infiltration Curve k	0.53	0.53	0.53	0.54	0.54	0.54
Infiltration Curve C	155.8	155.8	155.8	160.5	160.5	160.5
St. Dev. of Moist. Content Dist.	0.21	0.24	0.16	0.16	0.16	0.15
Max. Depression Store (mm)	1.0	1.0	1.0	1.0	1.0	1.0
Max. Dam Store (Ml)	2.36	0.87	27.09	46.34	229.82	40.47
% Area above Dams	39.2	15.6	36.4	86.0	89.1	38.0
Aquifer Storativity	0.001	0.001	0.001	0.001	0.001	0.001
Aquifer Transmissivity (m^2 day^{-1})	15.0	15.0	25.0	25.0	25.0	25.0
Depth of Aquifer (m)	50.0	50.0	50.0	50.0	50.0	50.0
Adjusted Aquifer Hyd. Cond. (mm h^{-1})	0.008	0.008	0.008	0.008	0.008	0.008
G'water Drainage Vector (Fraction)	15.0	15.0	15.0	15.0	15.0	15.0
Max. Rest Water Level (m)	50.0	50.0	50.0	50.0	50.0	50.0
G'water Dist. Vector (Sub-areas)	8,0	9	10,11	12,11	12,1	0
(%)	60,40	100	60,40	80,20	80,20	100
Max. Regional G'water Slope (%)	2.5	2.5	2.5	2.5	2.5	2.5
Sub-area Routing Coeff. (K)	2.52	2.30	3.74	3.52	3.52	4.52

Simulation results

Rainfall inputs to the 112 km^2 catchment were obtained from the Albertvale Weather Bureau station, located near the catchment outlet, which is the only rain gauge in the vicinity with a sufficiently long rainfall record. Consequently, the model was run on a daily time scale and known spatial variations in rainfall (Hughes and Sami, 1991) were ignored. The effect of using a daily time step will be an under-estimation of infiltration excess runoff, since many events are short duration convective summer storms whose intensities cannot be adequately simulated on a daily time step. As a result, it may be expected that runoff peaks will be

under-simulated and are therefore not considered here. It is also expected that an inadequate representation of rainfall intensities will result in soil moisture conditions following short duration events being too high.

Model parameters have been derived as explained in 4.2.3 using known or subjective values to quantify the physiographic variables. The values of the critical model parameters and those affecting recharge are shown in table 5.9.

Differences in slope, soil and vegetation cover exist between the sub-areas. The lower sub-areas have deeper soils and are covered by sparse thornveld (0-25% crown cover) on the hillslopes and thick thornveld (75-100% cover) in the valley bottoms with thick patches of alluvium. The upper sub-areas are covered by sparse grass and have much thinner soils. Furthermore, the western half of the catchment (sub-areas 5-9) are underlain by duplex soils (Swartlands and Sterkspruits) with a larger clay fraction than the primarily Glenrosa soils in the eastern half. Steeper slopes are found in the northern half of the catchment (sub-areas 2, 3, 5, 6).

Groundwater parameters reflect the authors best guess estimates as pump tests were not considered to accurately reflect regionalised field conditions. Pump tests conducted in the area suggested that transmissivites range from 58-137 $m^2 d^{-1}$ and that storativities were 0.008-0.011. However, given the low rates of recharge and a regional hydraulic gradient of 0.012, it is unlikely that these values are regionally representative of the aquifer's hydraulic properties. Hughes and Sami (1991) have also shown that groundwater conditions are fairly stagnant since lag times of about 400 days were required for lateral recharge from upgradient recharge zones to travel a distance of 8-10 km following a major storm event. It is suggested that several reasons may explain why pump tests over-estimate hydraulic properties:

- Boreholes available for test pumping have been established with a subjective bias, almost exclusively in valley bottoms, in order to tap likely fracture zones.

- A nest of boreholes to serve as pumping and observation holes only exists where the aquifer was found to be especially high-yielding. Alternatively, due to the fracture orientation, the aquifer was found to be extremely anisotropic when observation holes were located along different bearings.

- The spatial variability of transmissivity and storativity in fractured rock aquifers renders it difficult to characterise formation constants from point observations.

- Aquifers are highly localised so boundary effects make analysis of data difficult.

- Rest water levels are often different than the depths where water was struck so aquifers can be considered confined. However, boreholes are usually uncased below 10m so they do not act as true piezometers. Water level does not reflect a true piezometric surface since upwelling water has the ability to seep into fractures located above the transmissive zone. Induced drawdown by pumping causes water in these fractures to flow back into the borehole so estimates of transmissivity and storativity from pump tests are largely influenced by the hydraulic properties of these fracture zones rather than those of the water bearing formation.

The groundwater drainage vector was assigned as near vertical based on field observations that joint sets in sandstone beds, hypothesised as being the predominant recharge pathway, dip at 84° and 90°. The strike of these joint sets tends to be oriented along the axis of the valleys.

A higher transmissivity was arbitrarily assigned to the lower sub-areas (9-12) since groundwater in these sub-areas exhibited a continual rise when an initial model run assumed uniform transmissivities across the catchment. As these lower sub-areas are located on the limb of a minor anticline (dip < 3°) and are oriented along its axis they are likely to have a denser fracture density. This adjustment to initial parameter estimates is therefore considered to be valid. No further calibration was attempted.

Table 5.10 gives a summary of the simulated mean annual water balance of the catchment and the 12 sub-areas. Although no observed runoff data is available to validate the results, the simulated MAR of 3.13% is in close agreement with the 3.19% figure given by Tordiffe (1978) for sub-catchments of the Great Fish river.

Table 5.10 Mean annual results for the simulation period 1956-1991.

Sub-area	1	2	3	4	5	6
MAP (mm)	482.9	482.9	482.9	482.9	482.9	482.9
Actual Evap. (mm)	466.7	449.9	457.3	462.1	442.0	449.5
Sat. Excess Runoff (% runoff)	70.6	77.5	70.1	68.7	78.7	76.6
Inf. Excess Runoff (% runoff)	17.6	10.8	11.9	15.3	14.0	15.3
Baseflow Runoff (% runoff)	11.8	11.6	17.9	16.0	7.3	8.1
G'water Recharge (mm)	5.8	6.4	7.0	8.2	4.7	3.0
Sub-area Runoff (Ml)	0.185	0.028	0.083	0.044	0.026	0.539
Total Runoff (Ml)	0.185	0.028	0.111	0.155	0.026	0.564
Sub-area Routed Runoff (mm)	10.4	26.6	18.6	12.6	36.2	30.4
Runoff Coeff. (%)	2.2	5.5	3.9	2.6	7.5	6.3

continued ...

Sub-area	7	8	9	10	11	12	Total
MAP (mm)	482.9	482.9	482.9	482.9	482.9	482.9	
Actual Evap. (mm)	455.2	463.4	465.2	465.1	465.3	467.2	
Sat. Excess Runoff (% runoff)	76.7	63.2	63.5	68.5	68.1	68.0	
Inf. Excess Runoff (% runoff)	17.3	17.0	21.6	17.5	17.4	18.9	
Baseflow Runoff (% runoff)	6.0	19.7	14.9	14.0	14.5	13.1	
G'water Recharge (mm)	4.7	3.2	6.9	7.2	7.4	6.0	
Sub-area Runoff (Ml)	0.113	0.200	0.142	0.126	0.197	0.120	
Total Runoff (Ml)	0.113	0.791	0.917	1.040	0.352	1.694	
Sub-area Routed Runoff (mm)	23.0	16.3	10.8	10.6	10.2	9.7	15.1
Runoff Coeff. (%)	4.8	3.4	2.2	2.2	2.1	2.0	3.1

Figure 5.9 shows the area weighted temporal distribution of recharge for the entire catchment. Table 5.11 presents the recharge statistics for the 12 sub-areas and the total catchment. These data show that the lowest recharge rates occur in the steeper sub-areas covered by relatively shallow duplex soils (sub-areas 5-8). These soils saturate sooner due to their shallower depth and lower permeability, resulting in a higher proportion of saturation excess runoff during storm events. In spite of this very little difference in soil moisture content can be observed between sub-areas with high recharge (e.g. sub-area 4) and those with low recharge (e.g. sub-area 6 : figure 5.10). The storm events of April and November 1989 and that of December 1991 saturate the lower soil zone of both sub-areas, however, the mean moisture content of sub-area 4 remains above field capacity for a longer period of time (greater than 1 month) following these events. Consequently, a larger proportion of the sub-area will be contributing to recharge.

Although no observed soil moisture data can adequately represent conditions over such a large catchment, observations from a nearby first order catchment (see section 5.2.3) show that soil moisture does not rise above field capacity for any significant length of time. It is therefore probable that soil moisture content is being over-simulated by the model, resulting in an over-simulation of recharge and baseflow. This can be attributed to an under-simulation of intensity excess runoff due to the daily time step of the model run. Alternatively, the model may be maintaining wet conditions in the lower soil zone due to insufficient evapotranspiration resulting from too low a crop factor or too low an estimate of potential evapotranspiration during the summer months.

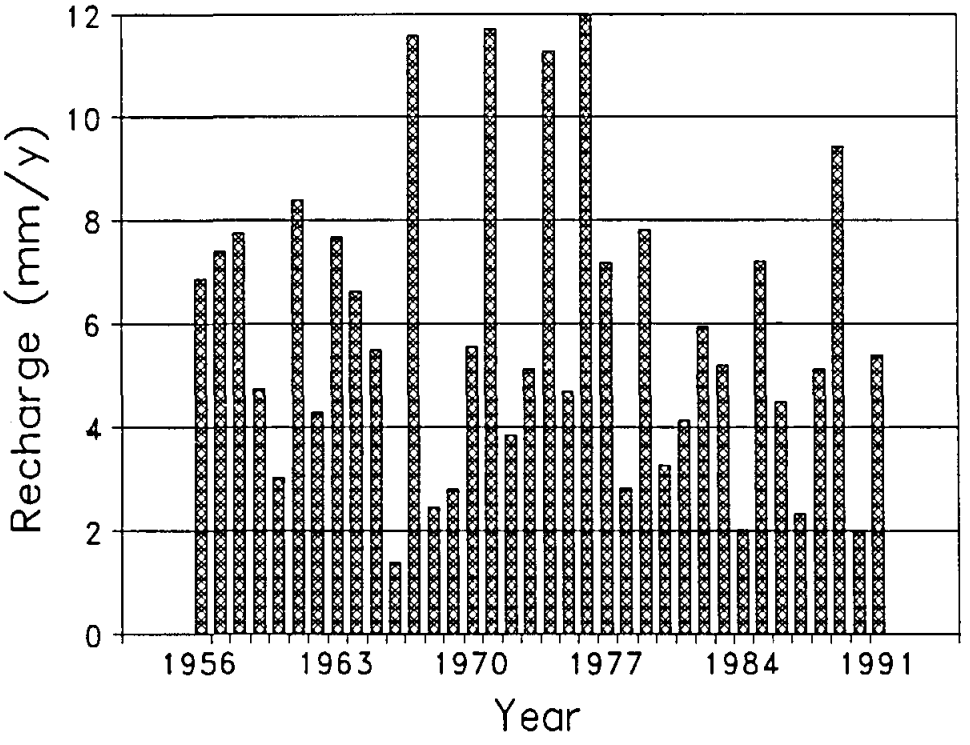

Figure 5.9 Area weighted recharge for the entire catchment, 1956-1991.

Table 5.11 Mean annual recharge statistics for the various sub-areas and the entire catchment.

Sub-area	1	2	3	4	5	6	7	8	9	10	11	12	Total
Mean (mm)	5.80	6.44	7.00	8.17	4.67	2.98	4.70	3.18	6.87	7.15	7.37	6.00	5.80
Med. (mm)	5.22	6.03	6.84	7.88	4.23	2.42	4.24	2.75	6.19	6.78	6.82	5.52	5.29
S Dev. (mm)	3.25	2.82	3.05	3.61	2.19	1.90	2.70	1.79	3.38	3.48	3.49	3.36	2.90
Min. (mm)	1.19	1.17	2.14	2.26	1.14	0.47	1.12	0.61	1.62	1.88	1.86	1.41	1.36
Max. (mm)	13.69	11.33	12.87	17.81	9.01	7.82	10.13	7.24	14.72	15.41	15.59	13.58	11.99
C. Var. (%)	56.1	43.8	43.5	44.2	46.8	107.4	57.5	56.3	49.2	48.8	47.3	55.9	50.1

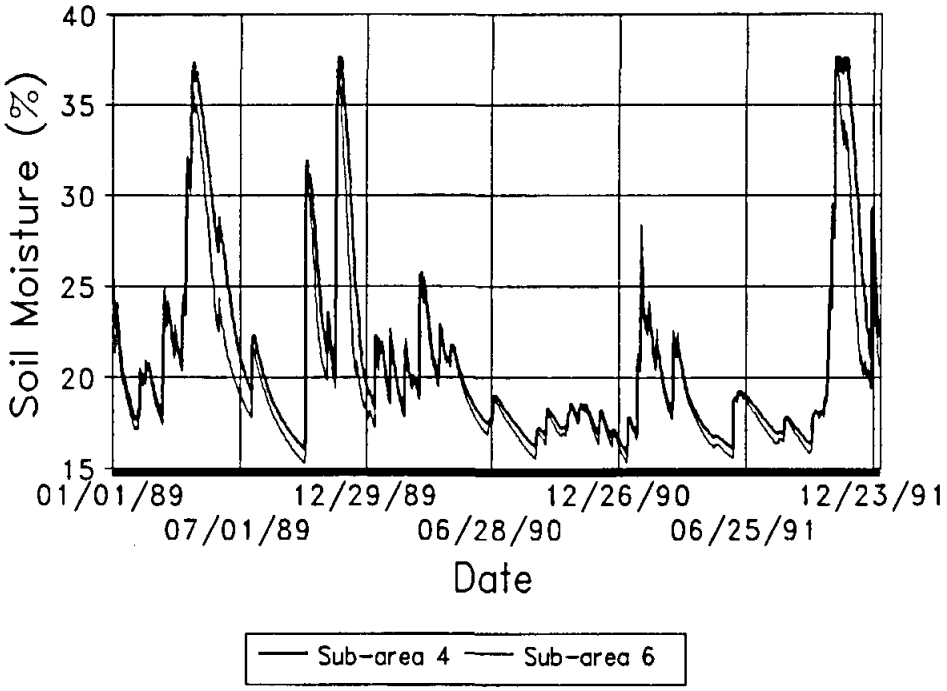

Figure 5.10 Mean soil moisture content of the lower soil layer for 2 sub-areas representing those with deep and shallow soils.

Comparison of recharge estimates

For the overall catchment the simulation yields a mean of 5.8 mm y^{-1} while the chloride method yields 4.5 mm^{-1}, therefore, if no data were available to calibrate simulated recharge the simulation can be considered successful. Figure 5.11 shows a comparison of mean annual recharge as estimated from the VTI model and the chloride balance model for each of the sub-areas. Relatively good results have been obtained for sub-areas 1, 3, 5, and 9, while simulations for sub-areas 4, 6, 8, 10, 11 and 12 can be considered poor. These poor results can be partially explained by horizontal redistribution of chloride. The chloride method assumes that all chloride deposition on a catchment is in equilibrium with chloride

export in groundwater and does therefore not consider its redistribution to other sub-areas by overland flow prior to percolation. For example, since sub-area 6 is relatively steep and has a high runoff coefficient, much of the chloride deposited may be transported to sub-area 8 where it percolates to groundwater via transmission losses through the deep alluvium in this sub-area. Consequently, the chloride model would over-estimate chloride inputs to groundwater in sub-area 6 and under-estimates those in sub-area 8, resulting in an over-estimate of recharge in sub-area 6 and an under-estimate for sub-area 8. The poor results for the other sub-areas can probably be explained by excessively wet conditions being simulated in sub-areas with deep soils, as previously mentioned. This problem could be overcome by calibration of the soil and evapotranspiration parameters. However, it is unlikely that any modelling at a daily time scale could completely overcome the problem.

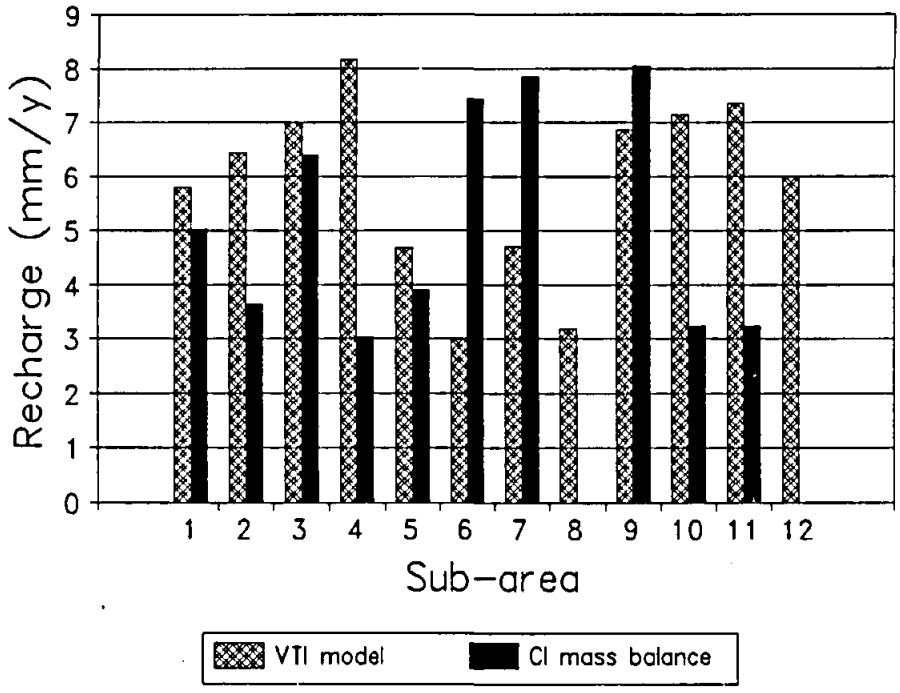

Figure 5.11 Mean annual recharge as estimated by the VTI model and the chloride mass balance model.

Rainfall-recharge characteristics

The relationship between annual recharge and rainfall is shown in figure 5.12. A regression of rainfall and recharge predicts that:

$$\text{Recharge (mm)} = \log(\text{Rainfall}) * 22.4 - 54.1 \quad \text{Eq. 5.2.1}$$

with an r^2 of 0.79. The most probable reason that the relationship exhibits a poorer fit during high rainfall years than low rainfall years is that high rainfall events often occur during the last month of the year, consequently the resulting recharge may be attributed to

the following year due to the lag time in recharge.

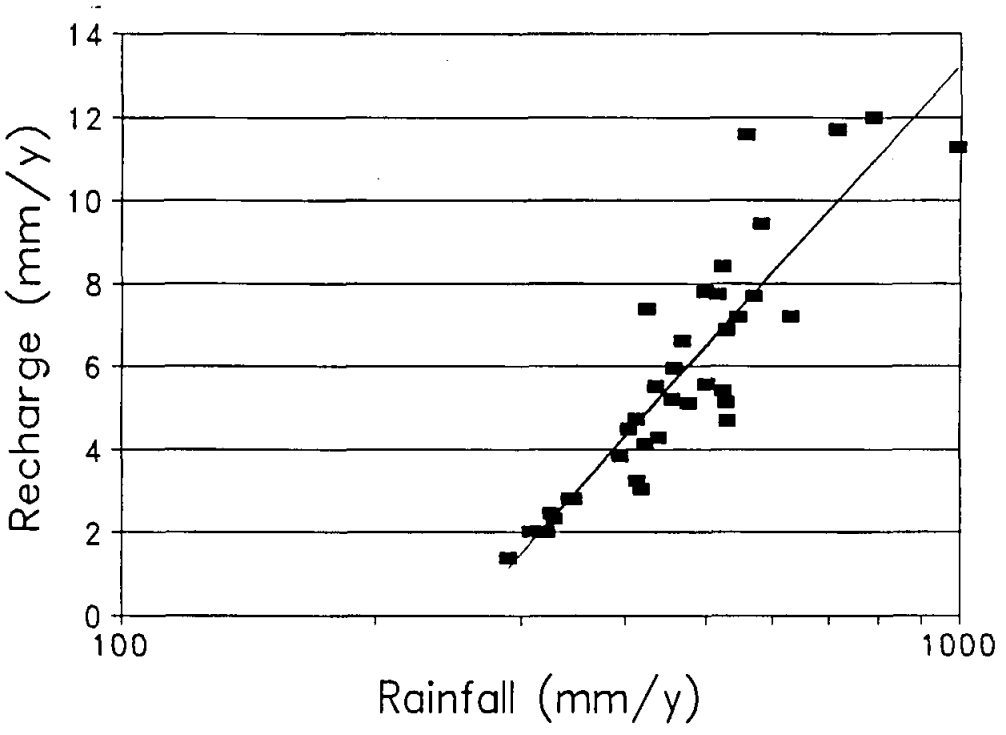

Figure 5.12 The relationship between groundwater recharge and annual precipitation.

Annual and spatial variations in recharge for the sub-areas where good simulations were obtained are shown in figure 5.13. The figure shows that there is not much spatial variation during dry years (less scatter around the regression line), however, during wet years the spatial variation increases (more scatter). Recharge is shown to vary between 0.7% of rainfall during dry years to 1.2% during wet years. This is substantially lower than the 2-4% suggested by Kirchner and Van Tonder (1991) for Karoo aquifers with soils greater than 200 mm thick. Kirchner and Van Tonder suggested that recharge could be estimated by:

$$\text{Annual Recharge (mm)} = 0.023 * (\text{Annual Rainfall} - 51) \quad \text{Eq. 2.5.2}$$

This relationship over-estimates recharge in the Bedford catchments (figure 5.14) and results in a mean annual recharge of 9.9 mm^{-1}. Such generalised relationships must therefore be treated with caution when applied to regions other than where they were derived. The VTI model has been shown to generate recharge estimates which more closely agree with measured values on a catchment scale from regionalised parameters values prior to any calibration.

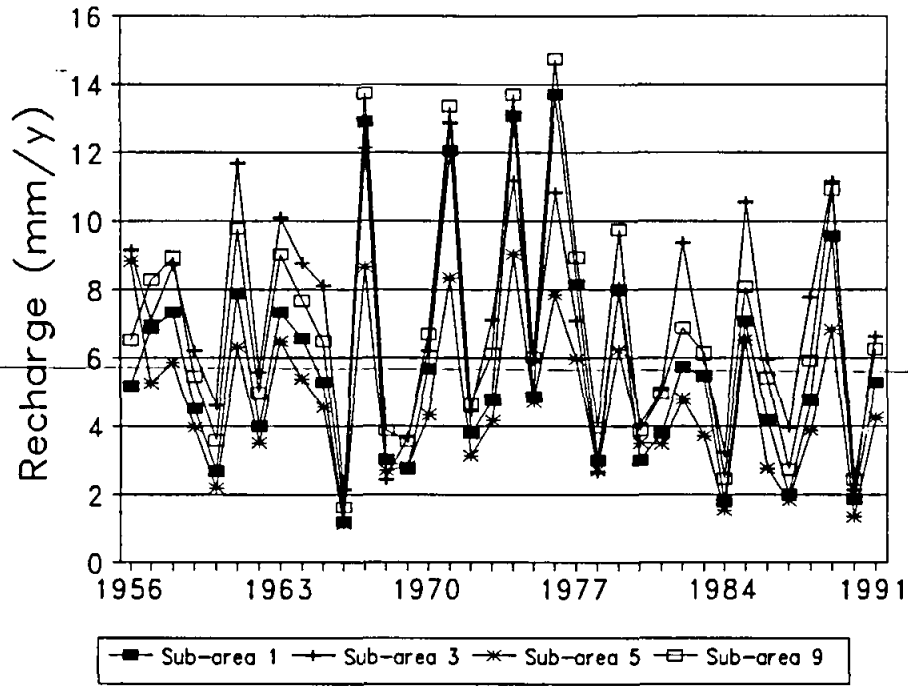

Figure 5.13 Simulated recharge to four sub-areas, 1956-1991.

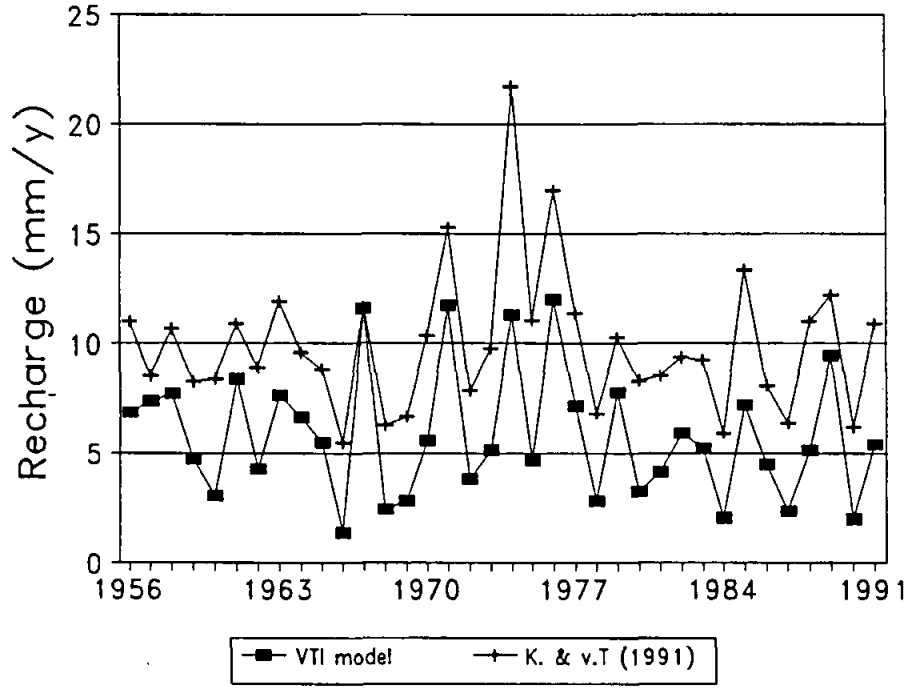

Figure 5.14 Recharge as estimated by the VTI model and by the Kirchner and Van Tonder (1991) relationship for Karoo aquifers.

Groundwater level simulations

The VTI model also includes a component which simulates groundwater levels as a depth below the catchment outlet (see section 4.2.2). The water level function has been used to verify whether estimated parameters values result in stable groundwater conditions. Assuming that estimates of storativity are realistic, this function can also be used to verify estimates of recharge and the lateral redistribution of groundwater if results are compared to observed water level fluctuations. This function was tested in the Bedford catchments against observed water levels in 4 boreholes located near the outlets of sub-areas 1, 2, 8 and 12. The length of time of observation for various boreholes varies due to changes in borehole network introduced in 1990 following an initial study of the groundwater dynamics of the catchment (Hughes and Sami, 1991). Since the model records water level depths as a depth below the stream channel and boreholes are located several metres above this datum, observed water levels have been offset to account for the height of boreholes above the channel bottom. This offset ranged from 0 m in sub-area 2 where the borehole is located next to a shallow first order stream, to 5 m in sub-area 12 where the borehole is located on an alluvial bank approximately 5 m above the channel bottom. Simulated and observed water levels are shown in figures 5.15 to 5.18.

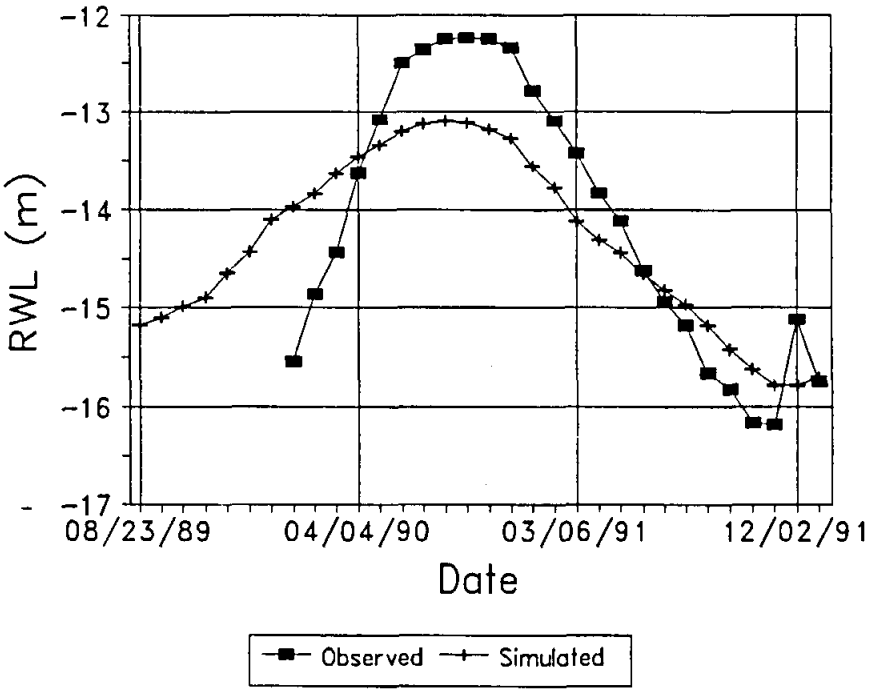

Figure 5.15 Observed and simulated groundwater levels for sub-area 1.

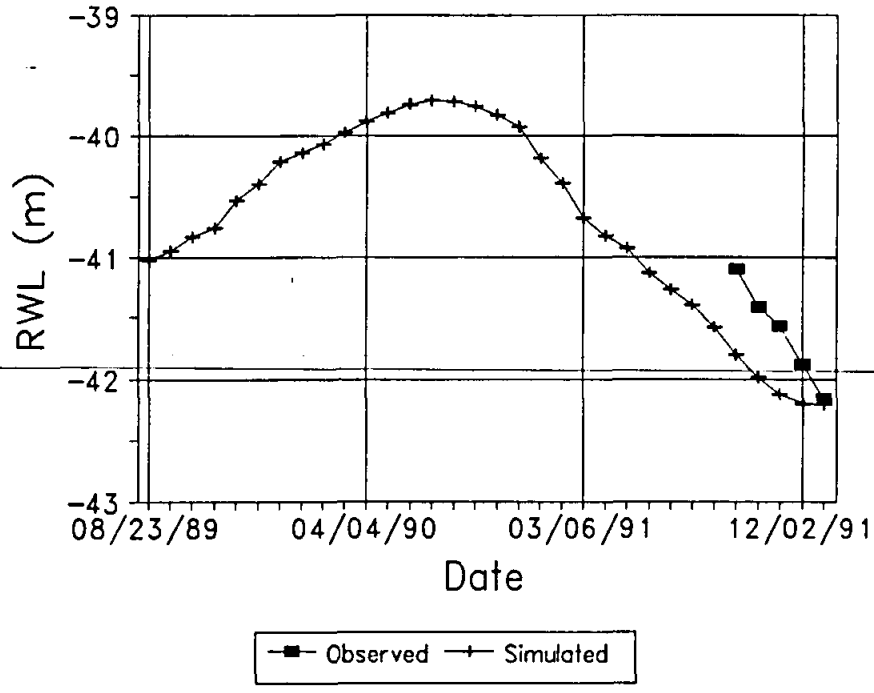

Figure 5.16 Observed and simulated groundwater levels for sub-area 2.

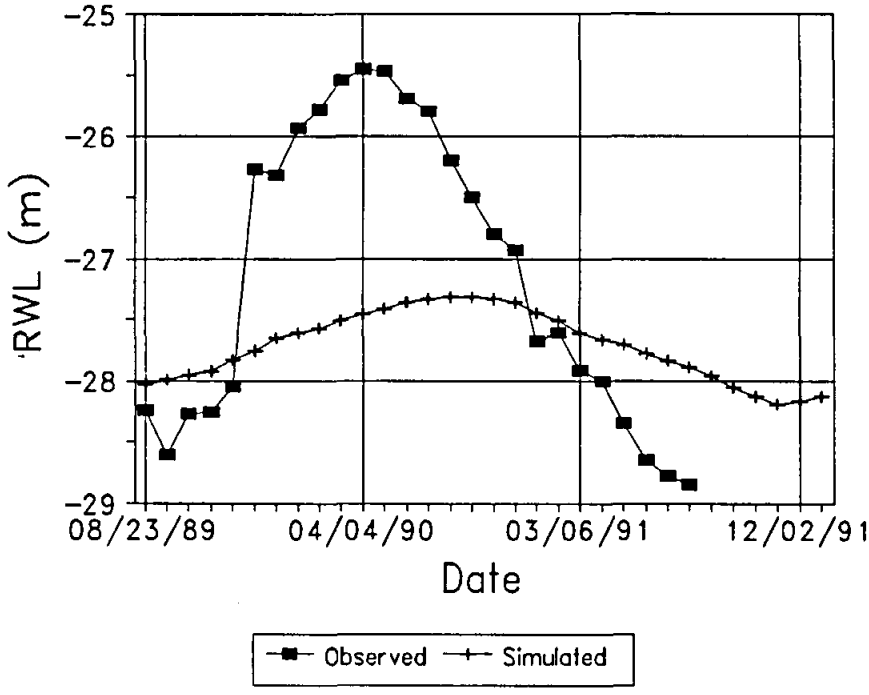

Figure 5.17 Observed and simulated groundwater levels for sub-area 8.

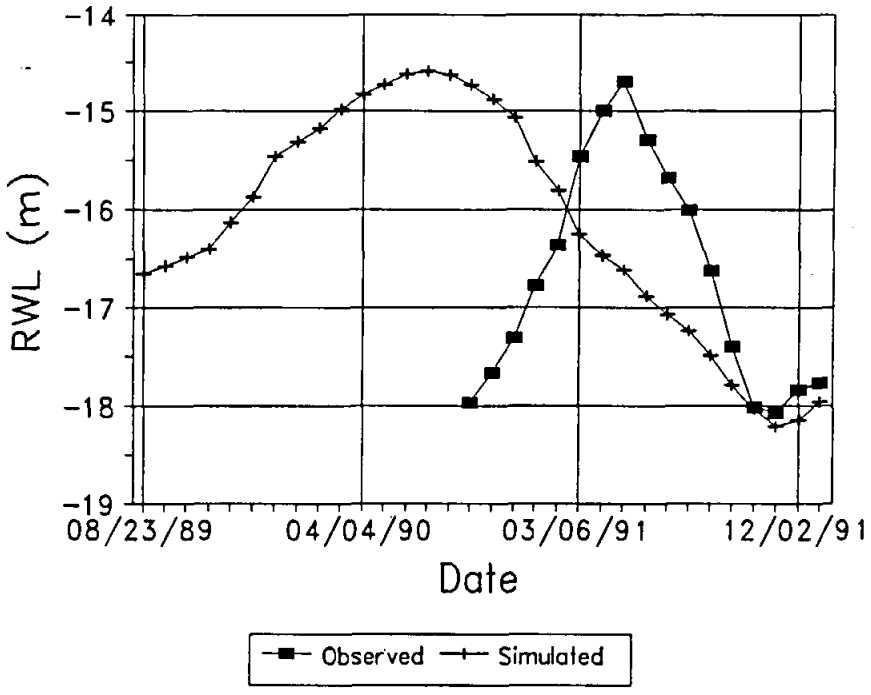

Figure 5.18 Observed and simulated groundwater levels for sub-area 12.

Unfortunately, a sufficiently long record is not available for sub-area 2 and it is not possible to determine whether water levels accurately reflect the recharge dynamics in a first-order catchment. The simulated water level and its rate of decline, however, indicate that groundwater parameters (see section 4.2.3) adequately model the redistribution of groundwater.

Water levels in sub-areas 1, 8 and 12 all reflect more complex processes since they vary with recharge as well as with the balance between groundwater inflow and outflow resulting from groundwater redistribution. Simulated water levels in sub-area 1 indicate that the water level rise is less than was observed in the field (figure 5.15) and that the rise occurred too early following the 1989 events. This suggests that the author's 'best-guess' estimate of inflow to the sub-area may be too low and may have to be upgraded during calibration. The early simulated response probably reflects the lack of routing in the groundwater component of the model. The model assumes that inflows from other sub-areas immediately results in a water level rise at the sub-area outlet. The slow rates of groundwater flow imply that this is unlikely to occur on a sub-catchment scale, therefore, this problem cannot be corrected without introducing routing parameters into the groundwater redistribution function. Although the model has simulated the water level in sub-area 8 reasonably well, water level fluctuations have been under-estimated. This is probably the result of an under-estimate of groundwater outflow from sub-area 7 into sub-area 8 (see distribution vector parameters in table 5.9). The model accurately simulates water levels in sub-area 12, the catchment outlet, as the correct magnitude of fluctuation resulting from recharge and lateral redistribution (figure 5.18). However, the simulated water level rise is also out of phase with observed levels as a consequence of the lack of routing.

It can be concluded that the groundwater functions in the model have performed surprisingly well given the lack of calibration and the regionalisation of the parameter values. Water levels, and in most cases, their fluctuations have been adequately simulated during the initial model run. The lack of groundwater routing is perceived to be the major inadequacy at present.

5.2.6 Discussion

The application of the VTI model to several aspects of the hydrology of the Bedford catchments has revealed the following points about the either the model design itself, or the parameter estimation procedures.

The transmission loss parameters are difficult to estimate as well as being difficult to calibrate. The implication is that this component of the model requires further investigation.

The standard deviation of soil moisture content parameter is estimated from indices of soil depth variability, mean soil depth and soil permeability using a highly empirical equation. There is very little information in the literature about this value and how it varies for different soil water contents. The simulation results can also be very sensitive to this parameter value as it directly affects saturated area runoff and internal soil drainage. The implication is that a better understanding of the real spatial dynamics of soil moisture and how to estimate the relevant model parameter values is required.

Although some of the groundwater parameters are difficult to estimate, the Bedford results indicate that this component of the model works reasonably well in practice.

The groundwater component produces an immediate response to recharge within a sub-area, which is also translated into immediate responses in downstream sub-areas. The model is therefore simulating the response as 'piston' flow, when the observed groundwater data suggests a delayed or 'wave' type of response.

There would appear to be some questions about the conceptualisation of soil water movement within the model. The 150 mm depth for the surface layer was defined on the basis of simulating runoff and may be too shallow for some of the other model components, specifically the actual evapotranspiration routines. The division of the total soil moisture between two layers and the fate of the water in each layer (as drainage or evaporation), is clearly affected by several model components. If too much water is considered to lie in the lower zone and the crop factor parameter is relatively low, the effect will be to generate too much recharge and possible baseflow. The model does not currently allow water to move from the lower to upper zone, via capillary rise, and such a function has now been identified by the developers as being potentially important. A revision of the model, to incorporate this effect, is currently being designed.

If the model is operated with fixed daily time steps, a five level iteration routine is used to estimate the likely rainfall intensities within the day for the purposes of estimating infiltration excess runoff. There is little doubt that this part of the model is not functioning adequately for areas such as Bedford where rainfall intensities can be very high on days with relatively

low total rainfalls. The impact on the groundwater recharge simulation results is that more rainfall enters the soil profile and generates higher recharge, baseflow and saturated area runoff, but lower infiltration excess runoff than is realistic. A more recent version of the model has addressed some of these issues and improved the intensity estimation methods when the time step is longer than the expected seasonal storm duration.

The size of sub-catchments can have a very important effect on the runoff generated in small events. This is largely a result of the spatial variation in runoff generation processes that a relatively coarse spatial scale of modelling cannot account for. In practice, some runoff generated close to the catchment outlet will survive and be measured as observed flow. In the model, all of this runoff may be taken up in depression storage or other parts of the routing procedures. The impact is small in large events, but very noticeable in small events.

5.3 SOUTHERN CAPE CATCHMENTS

The southern Cape catchments (fig. 5.19) have been included as examples for several reasons. First of all the former Hydrological Research Unit has extensive experience of simulating the hydrology of this area, through two former projects. One of these concentrated on simulating the monthly patterns of streamflow volume using the Pitman model and carried out a parameter transfer exercise to try and estimate sequences of monthly flow volume for all the catchments flowing into Swartvlei and the Wilderness lakes (Hughes and Görgens, 1981; Hughes, 1982; Hughes, 1983; Hughes, 1984). The second project concentrated more on the flood hydrology of the catchments and data from some of them were used to test several isolated event models (Hughes and Beater, 1989).

A more recent project, being undertaken for the Department of Environment Affairs, is designed to determine the impacts of land use change and water abstractions on the hydrology of the inflows to the coastal lakes. This project also overlaps with a Department of Water Affairs and Forestry initiative to develop a water quality and quantity management plan for the area. As both projects have identified the need for more detailed streamflow information than monthly volumes, it was considered worthwhile to carry out an initial investigation of the applicability of the VTI model to the gauged catchments of this area. It may then be possible to simulate the flows of the ungauged parts of the catchments and carry out further investigations of the impacts of various water abstraction scenarios on the streamflow regimes, particularly low flows.

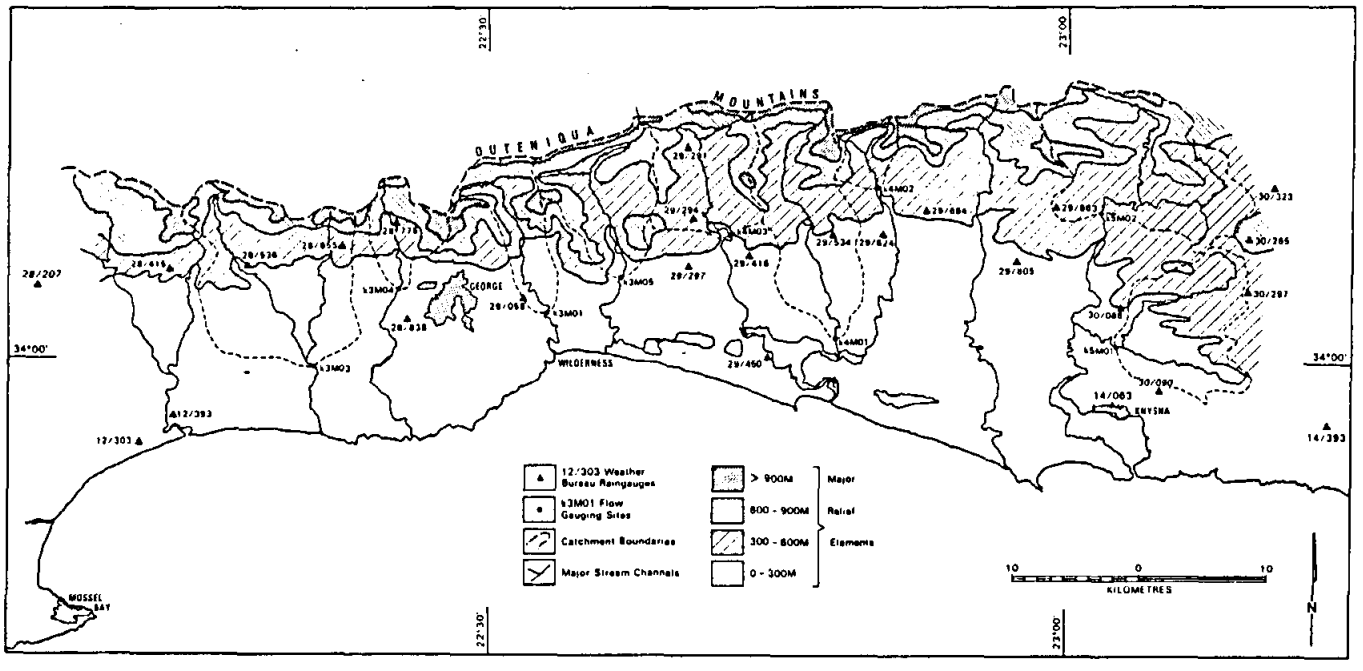

Figure 5.19 Southern Cape coastal region showing gauged catchments and raingauges.

5.3.1 Catchment characteristics and hydrological processes

Some of the characteristics of this area have already been fully described in earlier reports (Hughes and Görgens, 1981; Schafer, 1991, for example).

Topography :

The region is made up of several main landforms including the steeply sloping Outeniqua Mountains, the foothill zone, the heavily dissected plateau region and a coastal embayment consisting of the lakes and dune systems. The three gauged catchments used in this study include the mountain areas, the foothills zone and a small part of the plateau.

Geology :

The mountain areas and foothills are predominantly underlain by sandstones of the Table Mountain Group which are steeply folded and vary between resistant beds, in the ridge and mountain top areas, to softer shales and sandstones in the valleys. The coastal plateau is underlain by pre-Cape granites, phyllites, schists and shales.

Climate :

The area experiences a temperate climate with an all year round rainfall regime dominated by orographic influences. There is a general increase in annual rainfall from about 700 mm close to the coast, to over 1200 mm over the mountain areas. However, this pattern is confused by the influence of localised rainshadow effects caused by some of the ridges extending out from the main east-west trending mountain range. Further details of the climate can be obtained from Tyson (1971), Hughes and Görgens (1981) and Schafer (1991).

Soils :

The most comprehensive description of the soils in the region is provided by Schafer (1991). They vary from shallow residual soils and peaty lithosols in the mountains, through duplex soils with a poorly drained clay subsoil to deep sandy profiles in the coastal aeolianites. In more general terms, the distribution patterns of soil type are complex and related to local topography and underlying geology.

Landuse :

Most of the steep mountain areas are covered with fynbos which is partly managed through selected burning programmes. In the lower mountain areas and the foothills, landuse varies between fynbos, managed pine and gum plantations and dense indigenous forest. These landuses are also represented within the plateau areas, which are also used for cultivation and grazing.

It is clear that the array of hydrological processes active in the region will reflect the complex interplay of the climate, geology, soils and landuse. The large areas of forest cover, both pine plantations and indigenous woodland imply that interception losses and relatively high actual evaporation rates will play important roles. Similarly, the nature of the surface

vegetation cover, the texture of the surface soils and the generally low rainfall intensities suggest that sub-surface flow processes will be more important than infiltration excess surface runoff. All of the gauged catchments in the area are known to experience perennial streamflow, but whether the sustained baseflow is derived from soil water storage, or as groundwater flow from the sub-strata is uncertain. The upper catchment areas, where the soils are relatively coarse textured and which are underlain by the sandstones, are likely to be the major groundwater recharge area. The steep slopes and highly dissected nature of the topography, implies that groundwater outflow in the valley bottoms of the mountain and foothills zones may contribute significantly to baseflows. The lower areas, where duplex soils with a clay subsoil occur and where the substrata consists of granite, phyllites and schists, are less likely to contribute recharge and groundwater outflow may be similarly restricted.

An important component of the areas hydrological response is likely to be the influence of the spatial distribution of localised differences in the soil and vegetation cover. These in turn are strongly influenced by the slope aspect and the presence of any local anomolies in the general trend of increasing rainfall with altitude. North facing slopes are known to be drier, often have stonier soils and certainly have less vegetation cover. Steep south facing slopes appear to remain more permanently wetted and frequently have high surface organic contents. Together with the deeper valley bottom areas, these are likely to be the major source of sustained baseflow.

5.3.2 Available data

Ten long term daily rainfall stations have been operated by the Weather Bureau within the area, however, several have been closed down in recent years. Most are also located at relatively low elevations and the mountainous areas are under-represented. Several autographic gauges were maintained by Rhodes University during the 1980's, but these have unfortunately added little to our understanding of the spatial patterns of rainfall (Hughes and Wright, 1988), except for the purposes of simulating isolated flood events. In most areas of South Africa it is useful to supplement the available gauged rainfall data with the median monthly gridded (1' x 1' grid size) data, estimated by the Department of Agricultural Engineering, University of Natal, Pietermaritzburg (Dent, et al., 1987) and available from the Computing Centre for Water Research. One of the stations used in this spatial interpolation procedure is at a high altitude, but has the lowest rainfall for the immediate region. Unfortunately, this station appears to have a very large influence on the results for the whole region and significantly depresses the estimated values for the upper mountain areas. It was therefore found necessary to increas the median monthly values for many of the grid squares of the area. While the adjustments were based on an understanding of local rainfall patterns and some additional short term rainfall data, they are still largely subjective.

The rainfall interpolation approach for the models contained within HYMAS has already been explained earlier in this report. For each of the southern Cape catchments, the interpolation was based on three raingauges, but in the case of the Touw and Karatara, none of these are within the gauged parts of the total catchment. A heavy reliance is therefore placed on the gridded median monthly values to determine the rainfall input to the model. It is unlikely, therefore that a very good one-to-one correspondence between the simulated flows and the

observed can be expected.

The closest evaporation pan station is at George Airport, which is located within the coastal plateau zone to the west of the region of interest. Regionalised mean monthly S-pan evaporation figures (Hughes and Görgens, 1981), checked against the George data, are therefore probably the best available at present. The future availability of better estimates of A-pan equivalent evaporation estimates from a study undertaken at the Department of Agricultural Engineering, University of Natal, Pietermaritzburg (Schulze and Maharaj, 1991) should improve the situation.

Three streamflow gauging stations are used in this report (Touw River, K3H005; Karatara River, K4H002; Diep River, K4H003 - fig. 5.19). They vary in total size from 22 km^2 to 78 km^2 and have record lengths dating back to the 1960's. The quality of the records is apparently quite good, although, in common with many Water Affairs gauging stations, generally tend to under-estimate high flows.

Quite detailed soils information is available from Schafer (1991), which also provides some information on the nature of the sub-stratum. Some landuse information is available from earlier Rhodes University reports (Hughes and Görgens, 1981), while some more detailed and updated information is available from a current Rhodes University project (Filmalter, et al., 1992).

In general terms, the amount and detail of available information is more than adequate to carry out a test of a hydrological model, assuming that the time step of modelling is limited to no shorter than 1 day. The major deficiency is in the spatial representativeness of the available rainfall data as well as the relatively poor understanding of the importance and dynamics of the surface/groundwater interactions. The spatial scale of the available information does not warrant dividing the gauged catchments up into very small sub-areas and consequently the spatial scale of modelling chosen is relatively coarse (sub-areas of 10 to 40 km^2)

5.3.3 Simulation results

Simulations have been carried out on the total areas (down to their outflows into the coastal lakes) of the three catchments and each has been divided up into four sub-areas. The gauged parts of the catchment are represented by the outflow from sub-area 1 for the Karatara, sub-area 2 for the Diep and sub-area 3 for the Touw. Tables 5.12 to 5.14 list some of the characteristics of the sub-areas, as well as the values for the critical VTI model parameters. The parameter values have been derived in the normal way for this model by using as much information on the topography, soils, vegetation and landuse, as well as the standard HYMAS parameter estimation routines. Some of the main differences are between the soils and landuse, where the relevant parameter values strongly reflect the spatial position of the sub-areas with respect to the main land types identified by Schafer. The aquifer parameters are difficult to estimate from the available information and have been quantified on the basis of the presumed characteristics of the Table Mountain Sandstones (TMS) and the adjacent pre-Cape rocks, as well as the influence of the contact between these two sequences. The TMS is thought to have the highest transmissivities, except for the near surface shallow weathered zone of the granites.

Apart from the groundwater parameters, the crop factors are the most difficult values to determine for this model. The actual evaporation and soil water conditions are very sensitive to these values, yet the model developers have few clear indications about the best way to estimate them. In relative terms they have been set at values which should reflect the water usage of the different landcover types and the extent to which they are represented within the sub-areas of the three catchments. In absolute terms, their values are uncertain.

The groundwater parameter values were largely determined by a combination of *a priori* estimation, based on assumed aquifer properties and some calibration. As there is no actual observed data to calibrate the groundwater parameters against, the main aim was to achieve a degree of long term stability in the groundwater levels; that is no systematic rise or fall over the duration of the simulation period.

The simulation results are illustrated in tables 5.15 to 5.17 and figures 5.20 to 5.22. It should be noted that the output depths (evaporation, runoff and recharge) will not necessarily equal the input rainfall depth. This is because there may be imbalances between soil water storage at the start and end of the simulation period and because some of the baseflow may be derived from groundwater which is fed by recharge. The observed mean annual runoff is given for the appropriate sub-area in each case and the last row of the tables include some statistics of the relationship between the observed and simulated flows. Figures 5.20 to 5.22 illustrate the differences between the observed (bold lines) and the simulated flow duration curves.

Table 5.12 Touw River (K3H005) characteristics and model parameters.

Sub-area	1	2	3	4
Area (km^2)	36.0	22.0	22.0	17.0
Mean Catchment Slope (%)	32.0	36.0	34.0	24.0
Channel Slope (%)	2.0	2.9	2.4	0.8
Shreve Channel Order	100	38	182	217
Crop Factor	0.8	1.0	1.0	0.85
Canopy Capacity (mm)	0.86	1.48	1.12	1.46
Soil Porosity (% Vol.)	37.3	37.8	41.8	42.5
Field Capacity (% Vol.)	21.1	24.5	31.2	31.2
Wilting Point (% Vol.)	11.7	14.3	19.4	19.4
Mean Soil Depth (mm)	515	570	685	700
Soil Hydr. Cond. (mm h^{-1})	9.28	6.32	5.74	6.23
Infiltration Curve k	0.69	0.62	0.57	0.57
Infiltration Curve C (mm h^{-1})	193.0	168.1	124.5	124.5
St. Dev. of Moist. Content Dist.	0.17	0.19	0.17	0.16
Max. Depression Store (mm)	0.0	0.0	0.0	0.0
Max. Dam Store (Ml)	0.0	0.0	0.0	0.0
% Area above Dams	0.0	0.0	0.0	0.0
Aquifer Storativity	0.006	0.006	0.004	0.003
Aquifer Transmissivity (m^2 day^{-1})	40.0	40.0	30.0	25.0
Depth of Aquifer (m)	90	90	80	70
Adjusted Aquifer Hyd. Cond. (mm h^{-1})	0.11	0.09	0.06	0.05
G'water Drainage Vector (Fraction)	5.0	5.0	5.0	5.0
Regional G'water Slope (%)	0.7	0.7	0.5	0.8
Sub-area Routing Coeff. (K)	3.1	4.1	3.2	5.0

Table 5.13 Karatara River (K4H002) characteristics and model parameters.

Sub-area	1	2	3	4
Area (km^2)	23.5	30.0	26.5	21.5
Mean Catchment Slope (%)	43.0	25.0	20.0	20.0
Channel Slope (%)	2.3	2.1	1.5	0.4
Shreve Channel Order	49	114	158	211
Crop Factor	0.75	1.10	0.9	1.0
Canopy Capacity (mm)	0.90	1.77	1.02	1.23
Soil Porosity (% Vol.)	37.6	39.0	41.8	41.5
Field Capacity (% Vol.)	19.4	23.0	31.1	27.2
Wilting Point (% Vol.)	10.4	12.5	19.3	16.3
Mean Soil Depth (mm)	385	505	670	700
Soil Hydr. Cond. (mm h^{-1})	12.91	8.67	6.06	10.80
Infiltration Curve k	0.71	0.63	0.57	0.62
Infiltration Curve C	207.5	177.3	124.9	153.2
St. Dev. of Moist. Content Dist.	0.21	0.20	0.20	0.20
Max. Depression Store (mm)	0.0	0.0	0.0	0.0
Max. Dam Store (Ml)	0.0	0.0	0.0	0.0
% Area above Dams	0.0	0.0	0.0	0.0
Aquifer Storativity	0.005	0.004	0.003	0.006
Aquifer Transmissivity (m^2 day^{-1})	50.0	35.0	35.0	25.0
Depth of Aquifer (m)	80	70	70	70
Adjusted Aquifer Hyd. Cond. (mm h^{-1})	0.13	0.08	0.02	0.05
G'water Drainage Vector (Fraction)	5.0	5.0	5.0	5.0
Regional G'water Slope (%)	0.5	0.2	0.6	0.5
Sub-area Routing Coeff. (K)	2.5	6.0	4.5	4.5

Table 5.14 Diep River (K4H003) characteristics and model parameters.

Sub-area	1	2	3	4
Area (km^2)	35.0	36.0	13.3	14.0
Mean Catchment Slope (%)	30.0	25.0	18.0	15.0
Channel Slope (%)	1.2	1.7	1.3	2.7
Shreve Channel Order	103	159	182	204
Crop Factor	0.95	1.15	1.2	0.75
Canopy Capacity (mm)	1.39	2.27	2.21	0.55
Soil Porosity (% Vol.)	37.5	38.0	41.8	42.0
Field Capacity (% Vol.)	24.0	24.5	31.2	31.2
Wilting Point (% Vol.)	13.8	14.3	19.3	19.3
Mean Soil Depth (mm)	605	700	700	725
Soil Hydr. Cond. (mm h^{-1})	7.35	6.67	6.06	6.23
Infiltration Curve k	0.62	0.63	0.58	0.57
Infiltration Curve C	171.2	168.4	126.1	124.9
St. Dev. of Moist. Content Dist.	0.17	0.17	0.18	0.17
Max. Depression Store (mm)	0.0	0.0	0.0	0.0
Max. Dam Store (Ml)	0.0	0.0	0.0	0.0
% Area above Dams	0.0	0.0	0.0	0.0
Aquifer Storativity	0.005	0.005	0.006	0.006
Aquifer Transmissivity (m^2 day^{-1})	40.0	40.0	80.0	80.0
Depth of Aquifer (m)	80	80	10	15
Adjusted Aquifer Hyd. Cond. (mm h^{-1})	0.10	0.10	2.50	1.67
G'water Drainage Vector (Fraction)	5.0	5.0	100.0	100.0
Regional G'water Slope (%)	0.6	0.3	10.0	10.0
Sub-area Routing Coeff. (K)	4.23	7.66	9.38	3.70

Table 5.15 Simulation results (mean annual values) for the Touw River (period 1970-1978).

Sub-Area	1	2	3	4
MAP (mm)	791	770	700	706
Actual Evap. (mm)	618	593	513	539
Sat. Excess Runoff (mm)	55	50	49	56
Int. Excess Runoff (mm)	0	0	4	5
Baseflow Runoff (mm)	104	106	138	75
Groundwater Recharge (mm)	136	73	26	30
Sub-area runoff (Ml)	5676	3402	4175	2322
Total Runoff (Ml)	5676	3402	13253	15575
Observed Total Runoff (Ml)	N/A	N/A	11747	N/A
	Slope of Regression Line	Intercept of Regression Line	Regression Coeff.	Coeff. of Efficiency
Fit Statistics (sub-area 3)	0.90	-0.01	0.52	0.51
Log Statistics (sub-area 3)	0.82	-0.66	0.42	0.28

Table 5.16 Simulation results (mean annual values) for the Karatara River (period 1962-1970).

Sub-Area	1	2	3	4
MAP (mm)	1019	887	733	695
Actual Evap. (mm)	644	692	487	568
Sat. Excess Runoff (mm)	115	72	77	52
Int. Excess Runoff (mm)	0	1	4	0
Baseflow Runoff (mm)	234	126	143	64
Groundwater Recharge (mm)	241	94	13	45
Sub-area runoff (Ml)	8201	5970	5925	2508
Total Runoff (Ml)	8201	14171	20094	22602
Observed Total Runoff (Ml)	11195	N/A	N/A	N/A
	Slope of Regression Line	Intercept of Regression Line	Regression Coeff.	Coeff. of Efficiency
Fit Statistics (sub-area 1)	0.80	0.15	0.49	0.44
Log Statistics (sub-area 1)	0.78	-0.18	0.55	0.38

Table 5.17 Simulation results (mean annual values) for the Diep River (period 1962-1976).

Sub-Area	1	2	3	4
MAP (mm)	771	775	802	740
Actual Evap. (mm)	569	634	378	381
Sat. Excess Runoff (mm)	77	58	25	54
Int. Excess Runoff (mm)	2	1	4	6
Baseflow Runoff (mm)	82	70	30	160
Groundwater Recharge (mm)	103	84	509	306
Sub-area runoff (Ml)	5625	4625	781	3065
Total Runoff (Ml)	5625	10250	11031	14096
Observed Total Runoff (Ml)	N/A	8954	N/A	N/A
	Slope of Regression Line	Intercept of Regression Line	Regression Coeff.	Coeff. of Efficiency
Fit Statistics (sub-area 2)	0.59	0.09	0.65	0.33
Log Statistics (sub-area 2)	0.70	-0.51	0.55	0.42

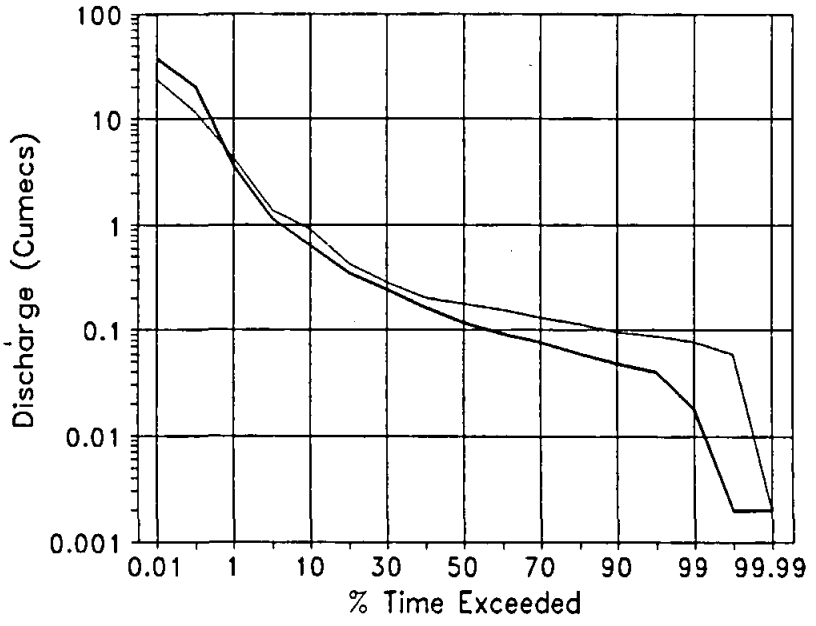

Figure 5.20 Flow duration curves for the Touw River (the bold line represents the observed flows).

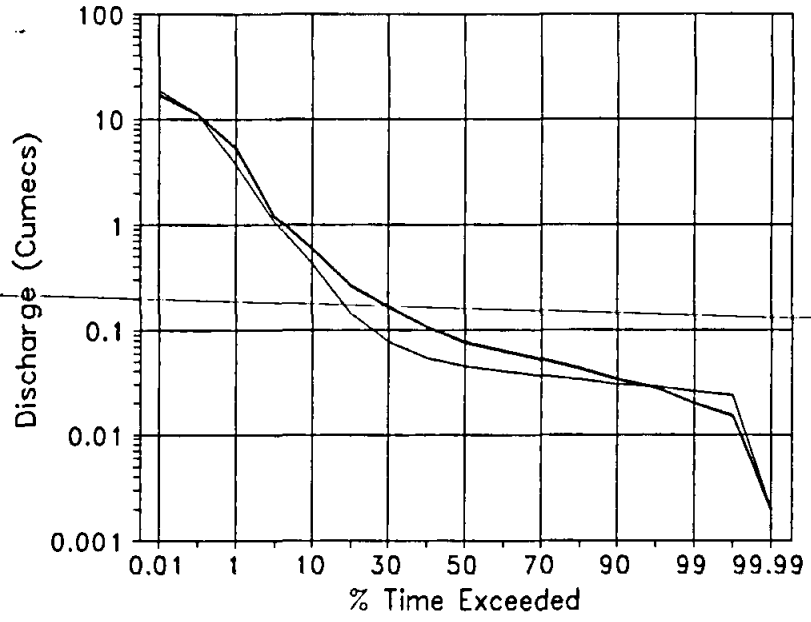

Figure 5.21 Flow duration curves for the Karatara River (the bold line represents the observed flows).

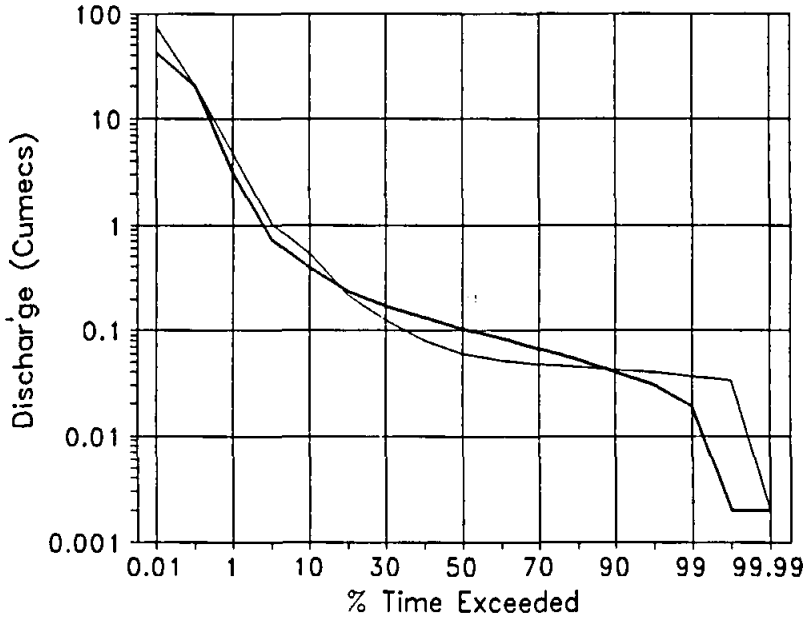

Figure 5.22 Flow duration curves for the Diep River (the bold line represents the observed flows).

5.3.4 Discussion

Although presented in the results tables, the simulations for the sub-areas below the gauging stations cannot be properly evaluated. This discussion will therefore concentrate on the gauged parts of the catchments and only refer to the other sub-areas where any of the results point to potential deficiencies in the model formulation or the way in which parameter values have been estimated in this application.

As expected, given some of the deficiencies in the available data, the one-to-one correspondence between the observed and simulated daily flows is relatively poor. In general terms most of the problems appear to occur with moderate to low flows.

Touw River Results.

The majority of the Touw River is covered by fynbos and plantations only occur in the upper parts of sub-area 2, while a small part of sub-area 3, close to the gauging station, is covered by indigenous forest. The relatively low evaporation depth (table 5.15) in the latter sub-area appears to be related to the lower rainfall and finer textured soils, while the higher baseflow is a consequence of the presence of the contact between the TMS and pre-Cape schists and phyllites. This contact has been effectively represented in the model as a restriction to the downslope flow of groundwater, causing it to rise within this sub-area. Should this be an erroneous assumption, the overall simulation of baseflows and the low flow part of the duration curve (fig. 5.20) for the gauged catchment would improve.

Although the observed duration curve indicates that close to zero flows occur (fig. 5.20), this is an artifact of the original data. Zero daily flows appear in the record for at leats one day either side of missing data and only a few missing data periods are required to depress the duration curve in the extreme low flow part. The rapid fall in the observed duration curve after about 95-99% exceedence is caused by one period in the 9 year record of some 2 to 3 months where the streamflows are consistently lower than at other times. There is no concomitant decrease in the rainfall over this period, so it is difficult to explain this feature of the observed record.

The use of a daily time step in this model is expected to under-predict extreme events due to the inadequate representation of the real rainfall intensities (Hughes, 1993), although the impact is not expected to be too great in an area experiencing relatively long duration and low intensity rainfall events. However, at the same time, the extreme flood flows are also expected to be underestimated by the observed record due to the fact that the gauging weirs are not designed for high flows and given that the observed data represent mean daily flows and not instantaneous discharges. It is difficult to determine what the combined effects of these factors will be when comparing the observed and simulated high flows. If they can be considered to cancel each other out then the simulation of the Touw River has certainly underestimated the high flows and the general overprediction of MAR (table 5.15) is due to oversimulation of the moderate to low flows.

From a parameter point of view, greater attention may be required in defining the soil and vegetation properties of sub-area 3, as well as the groundwater parameters of all sub-areas. From a model formulation perspective, the authors consider that attention should be focused

on the applicability of the surface/groundwater interaction components and their applicability in this steeply sloping catchment.

Karatara River Results.

In this case the general trend is an under-simulation of the MAR (table 5.16), and specifically the moderate flows occurring a large proportion of the time (fig. 5.21). It is possible that the soils are really somewhat shallower, or coarser in texture, than has been specified by the parameters (table 5.13). It is also possible that the rainfall could be higher or the vegetation cover and crop factor lower for this area. However, apart from steeper slopes, the gauged Karatara catchment is thought to be similar to the upper reaches of the Touw River, where an increase in the simulated runoff does not appear to be warranted. A further possibility may be related to the fact that the periods used for the simulation of the Touw and Karatara are different and there may have been some differences in the veld burning management practice.

The differences in the simulation results of the Touw and Karatara, illustrate the difficulties of ascribing any discrepancies between observed and modelled flows to specific problems in either the model formulation, the parameter values or the observed data.

Diep River Results.

The Diep catchment has far greater coverage of pine plantations than either of the previous two. A large proportion of sub-area 1 and virtually all of sub-area 2 are covered with plantations. The relatively lower depths of simulated actual evaporation and baseflows (table 5.17) are partly a result of the lower rainfall in this catchment where local rainshadows are known to occur. The main cause for the overall (MAR) overestimation appears to be related to excessive moderate to high flows, which is not offset by under-simulation of the flows occurring most of the time (fig. 5.22). The extreme low flow part of the observed duration curve suffers from the same problem as with the Touw data in that there are a number of periods of missing data with which are associated zero flows. As with the other catchments in the southern Cape it is difficult to speculate on the reasons for the errors in the simulated flows compared to the observed record.

The lower sub-areas (3 and 4) are underlain by pre-Cape Granites, which have been assumed to have high transmissivities and storativities in a shallow weathered zone. Translating these characteristics into model parameters produces high rates of groundwater recharge and, in the case of sub-area 4, relatively high baseflows which may be unrealistic. It is possible that if these really are the characteristics of the sub-areas, it is also likely that some evapotranspiration demands would be met from this type of shallow aquifer. The model does not take this into account.

Overall.

In general terms and given the representativeness of the available rainfall information, as well as the lack of data on the groundwater characteristics of the area, the results are reasonably acceptable and to a large extent the model can be considered to be applicable to this region. One aspect of the models formulation that may need some attention in the future is the

surface/groundwater interactions and, particularly, the methods used to estimate the parameter values of these routines from typically available information. The relationships between groundwater recharge and re-emergence as baseflow within the same sub-area in steeply sloping catchments is not clear and a better understanding of these processes would perhaps lead to some modifications that would be beneficial. The need to allow evapotranspiration from shallow groundwater bodies may also require some attention in the model.

5.4 NORTH DANVILLE CATCHMENTS

These catchments are located in Caledonia County, Vermont State in the north eastern United States and are part of the Connecticut River basin. They have been included as they represent a steep and forested area, similar to the southern Cape catchments of South Africa, but under a different climate regime. They were also previously used by Hughes and Beater 1989) to test single event models developed at Rhodes.

The available data have been acquired from the United States Department of Agriculture and consist of breakpoint rainfall and streamflow records, which have been converted into the standard Rhodes IWR format. Data from two streamflow gauges have been used in this application. One is at the outlet of a 41.8 km^2 catchment and the other at the outlet of an internal sub-area of size 8.2 km^2. Rainfall data are available from a total of 14 gauges which are reasonably evenly distributed in and around the larger catchment.

Information about the physical characteristics of the area has been obtained from the USDA (1955-1973) publications, which were kindly loaned to Rhodes by Prof. Schulze of the University of Natal, Pietermaritzburg.

5.4.1 Catchment characteristics and hydrological processes

Topography :

These catchments represent the sloping to steep New England area. Table 5.18 indicates that the mean catchment slopes are relatively uniform over the whole catchment at about 12%. The main slope variation appears to occur in the headwater sub-areas (1, 3 and 4) where a steeper ridge forms the catchment boundary.

Geology :

The underlying strata are made up of interbedded calcareous schists and quartzites which are very dense and have no solution chambers. Overlying these is a dense and largely impervious glacial till or boulder clay which varies in depth from very shallow to about 15 m. This is the most important geological characteristic from a hydrological point of view.

Climate :

Mean annual precipitation is about 950 mm and while evenly distributed throughout the year, much of the winter precipitation occurs as snowfall. Mean daily temperatures are in excess of 15°C during the summer months, while five months of the year experience sub-zero mean daily temperatures and there is a spring snowmelt runoff period during the months April to May. The summer rainfall events vary from high intensity and short duration convective storms to much longer events with generally lower intensities. There are also quite large differences in the degree of spatial variability between events.

Mean monthly A-pan evaporation values have also been obtained from the US Department of Agriculture and vary (excluding winter months) between 50 mm for October and 120 mm for July.

Soils :

The available soils data suggests that depths vary between 300 mm and 700 mm, although few fall within the lower depth category. The soil texture does not seem to vary a great deal and most are loams or silty loams and have moderate to rapid permeabilities and only weak structure. There is insufficient soils information to adequately define the spatial variability. The only information available is the differences between the soil descriptions for the two gauged catchments (one which is within the other).

Landuse and Vegetation :

Hardwood forest, with scattered spruce, pine and fir softwoods cover about 67% of the area. The remainder is occupied by pastureland with a small cultivated percentage.

The rivers are perennial and the first point to note about the hydrological response of this region is that the VTI model will be unable to simulate the winter conditions during snowfall and probably frozen ground conditions. Nor will the model be able to simulate the spring snowmelt event. Consequently, although a continuous time series simulation, for the period April 1970 to October 1973, has been carried out, only the response for the months June to October have been examined.

The nature of the surface cover suggests that infiltration excess runoff is most unlikely in this area and that the predominant runoff mechanisms will be saturation excess (source area) runoff and saturated sub-surface flow. The impermeable nature of the sub-stratum, together with the relative frequency of rainfall events (70 for June to October), suggests that the lower soil layers are likely to be maintained at relatively high water contents, sustaining baseflows. The implication is also that a fairly permanent saturated area will exist in favourable parts of the catchment giving rise to at least some response from even relatively minor rainfall events. This may take the form of a small increase in baseflow levels or small peaks superimposed on the background baseflow. The fact that many of the rainfall events have relatively high spatial variabilities suggests that the response of the small to medium sized events will be equally spatially variable, giving rise to some quite complex relationships between average catchment rainfall and streamflow at the catchment outlet.

5.4.2 Simulation results and discussion

The total catchment area of some 42 km^2 has been divided up into 6 sub-areas, of which number 1 represents the other gauged catchment. The distributed rainfall inputs were compiled using a maximum of three of the available raingauges and a time interval system based on 1 day, 12, 6, 1 hour and 15 minute intervals. A depth threshold of 10 mm was used in all cases to determine the step down from one interval to another. The distance of the furthest gauge (i.e. the third of three) from the sub-area centres varies from 3.1 to 4.0 km, suggesting that any spatial variations at a scale of less than about 10 km^2 (area of a circle with radius of 0.5 * max. distance) will be smoothed out.

Some of the physical characteristics of the sub-areas and the more important model parameter values are listed in table 5.18. It can be seen that few sub-area variations in the soil and vegetation parameters have been allowed for due to the lack of any information to

satisfactorily define these. The majority of the parameter values were estimated using the standard HYMAS approach of specifying physiographic variable values from available information and accepting the default estimations of the parameter values. The only parameters that were calibrated were those controlling the groundwater levels (initial values of percolating store and groundwater depth, as well as regional gradient). These were calibrated to achieve a degree of long term stability, but were not found to be all that important in this area where the sub-stratum is relatively impervious and the aquifer shallow.

Table 5.18 North Danville characteristics and model parameters

Sub-area	1	2	3	4	5	6
Downstream sub-area	2	6	6	5	6	Out
Area (km^2)	8.2	7.2	7.7	8.4	5.8	5.4
Mean Catchment Slope (%)	13.9	12.0	12.0	12.5	11.0	12.5
Channel Slope (%)	3.3	1.8	3.7	3.5	3.1	3.4
Shreve Channel Order	3	6	3	4	7	14
Crop Factor (Summer)	1.0	1.0	1.0	1.0	1.0	1.0
Canopy Capacity (mm - Summer)	1.7	1.7	1.7	1.7	1.7	1.7
Soil Porosity (%)	41.6	42.2	42.2	41.6	42.2	42.2
Field Capacity (%)	24.8	25.1	25.1	24.8	25.3	25.3
Wilting Point (%)	13.3	13.7	13.7	13.3	14.0	14.0
Mean Soil Depth (mm)	610	610	610	610	610	610
Soil Hydr. Cond. (mm h^{-1})	10.5	11.6	11.6	10.5	11.5	11.5
Infiltration Curve k	0.68	0.68	0.68	0.68	0.68	0.68
Infiltration Curve C (mm h^{-1})	177.3	177.3	177.3	177.3	177.3	177.3
St. Dev. of Moist. Content Dist.	0.22	0.16	0.16	0.16	0.16	0.16
Max. Depression Store (mm)	0.0	0.0	0.0	0.0	0.0	0.0
Aquifer Storativity	0.1	0.1	0.1	0.1	0.1	0.1
Aquifer Transmissivity (m^2 day^{-1})	0.2	0.2	0.2	0.2	0.2	0.2
Depth of Aquifer (m)	15.0	15.0	15.0	15.0	15.0	15.0
Adj. Aquifer Hydr. Cond. (mm h^{-1})	0.06	0.06	0.06	0.06	0.06	0.06
G'water Drainage Vector (Fraction)	10.0	10.0	10.0	10.0	10.0	10.0
Regional G'water slope (%)	2.0	2.0	2.0	2.0	2.0	2.0
Sub-area Routing Coeff. (K)	6.0	5.5	7.5	6.0	5.0	5.5

Taking into account only the June to October results, the success of the simulation exercise is very mixed. There are extended periods where the baseflows as well as the minor events (up to about 1 m^2 s^{-1}) are well simulated. However, there are also periods where the baseflows are consistently over simulated for sub-area 6 and under simulated for sub-area 1. Similarly, there are many of the intermediate sized peaks that are relatively poorly simulated

for both sub-areas. Figures 5.23 and 5.24 demonstrate that the largest event in the simulation period has been successfully modelled at both gauging sites and this is generally the case for the larger events. The very good representation of the shapes of the hydrographs (rising limbs, secondary peaks and recessions) implies that the routing delay and attenuation parameters are set at acceptable values. The illustration of the rainfall time distributions are very generalised and there are more intensity variations during the storms than the horizontal resolution on the graph will allow to be shown. The differences in the simulation results between the low to moderate events and the moderate to high events are strongly reflected in the fit statistics (table 5.19), where using ordinary data, the larger events dominate the results. However, the log statistics, which reflect the influence of the moderate to low flows, are not as good.

Table 5.19 Simulation results. The mean annual values should be treated with caution as they are based on less than 4 years of data and the winter and spring month runoff regimes are not simulated using snowfall and melt. The fit statistics are based on months June to October only.

Sub-area	1	2	3	4	5	6
MAP (mm)	1138	1033	1169	1057	1042	1224
Actual Evap. (mm)	500	510	530	490	520	520
Sat. Excess Runoff (mm)	88	83	71	67	60	89
Int. Excess Runoff (mm)	4	5	9	5	4	10
Baseflow Runoff (mm)	467	313	437	394	346	483
G'water recharge (mm)	93	131	129	115	125	135
Sub-area Runoff (Ml)	4595	2903	3981	3914	2378	3160
Total Runoff (Ml)	4595	7498	3981	3914	6292	20931
Obs. Runoff (Ml)	5685	N/A	N/A	N/A	N/A	23106
Statistics based on June to Oct.	% Error Maximum Flow	% Error Mean Flow	Slope of Regression Line	Intercept of Regression Line	Regression Coeff.	Coeff. of Efficiency
Fit Statistics (sub 1)	7.2	-22.2	0.95	0.11	0.81	0.80
Log Statistics (sub 1)	2.9	5.4	0.67	-0.54	0.34	0.25
Fit Statistics (sub 6)	18.9	5.4	0.82	0.2	0.88	0.84
Log Statistics (sub 6)	4.9	-43.6	0.75	-0.42	0.33	0.24

Part of the reason for the sometimes poor simulation of the minor peaks may be related to the spatial rainfall variations and the inadequacy of the available rainfall data to represent this. A similar reason may be the fact that the use of three raingauges to interpolate for sub-area rainfall input has excessively smoothed the spatial variations during some events.

The observed baseflow output from the total catchment (42 km^2) is some 2.5 to 3 times that from sub-area 1, which is about one fifth of the area (8.2 km^2). The mean baseflow response of all the sub-areas is 406 mm, which is some 90% of the baseflow response for sub-area

1. The implication is that there is more variation in the responses between the sub-areas (with at least some of the others having a lower response than 1) than has been accounted for by the model parameters. The alternative is that there exists some channel or riparian process that consumes flow in the channel.

A further possible influencing factor is the effect of the spring snowmelt on the soil moisture regime in the early part of summer. The model is currently assuming that the soil is draining continually during the winter months and is likely to be lower than field capacity at the start of June. In reality, the influence of the snowmelt during the April to May months may be such that it starts the summer season at a higher water content than the model suggests. This will not be important if a large event occurs early in the summer season as in 1973. It is worth noting that the 1973 baseflows are simulated more successfully than the other 3 years.

The mean percentage contribution to total flow of baseflow is 83%, while that for saturation excess runoff is 16%. The minor contribution of infiltration excess runoff is as expected and consistent with a comparison between the final mean infiltration rate (@ 120 min) of 26.4 mm h^{-1} given by the mean infiltration k and C parameter values. There are only a few situations where 15 min rainfalls are high enough to allow a significant proportion of a sub-area to generate infiltration excess runoff.

In general terms, and given the amount of information available to the authors, the simulations have been reasonably successful and the model may be considered to be applicable to the summer months of this region. It is very definitely not applicable to the winter and spring months, but it was never intended to simulate the effects of snowfall and the resulting spring snowmelt flow regime. The fact that the winter and spring seasons can not be modelled correctly has obviated any possibility of testing the seasonal variations in the vegetation parameters (interception and crop factor, etc.), which would be expected to vary considerably in a deciduous forest situation.

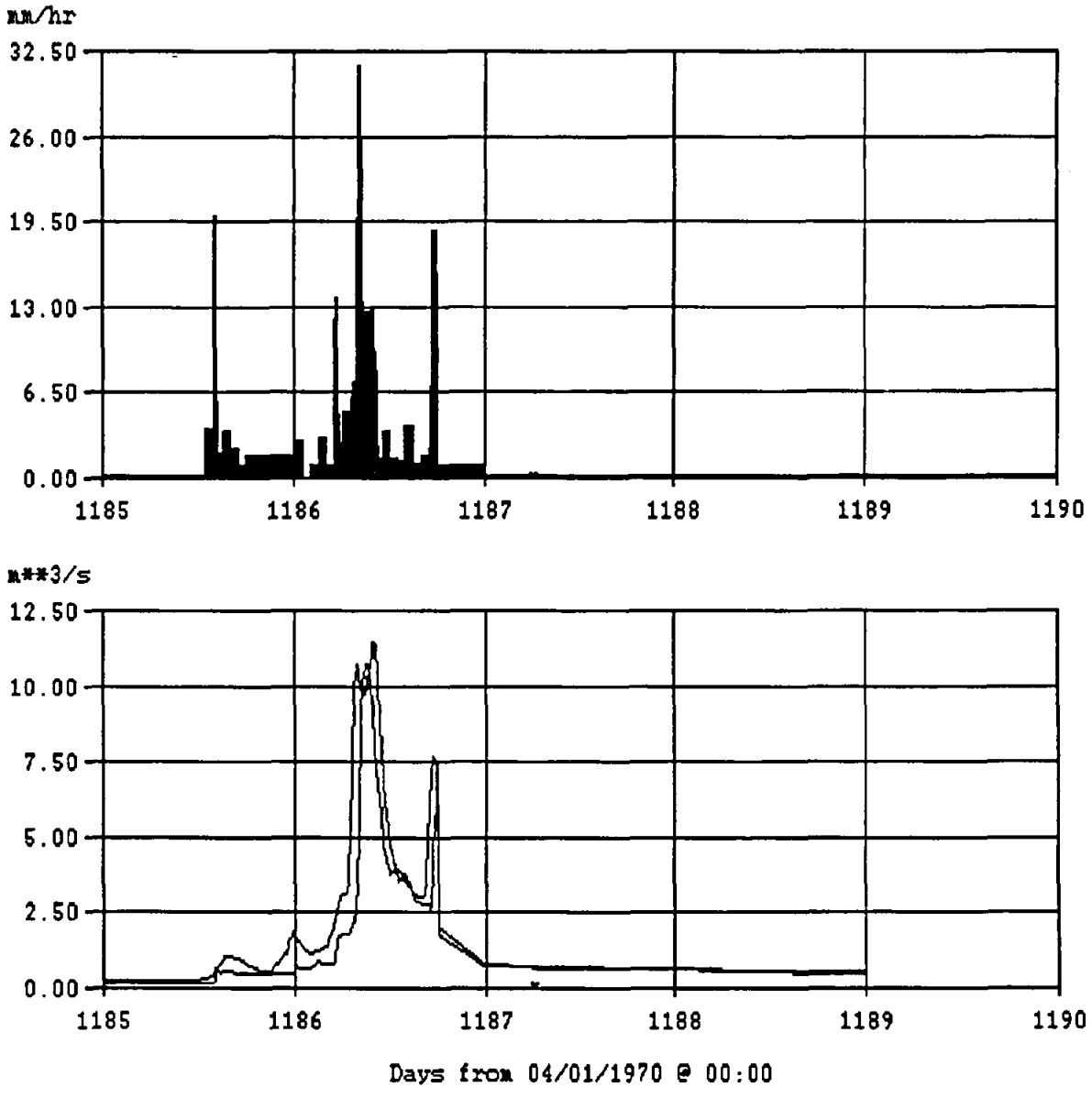

Figure 5.23 Rainfall intensity and runoff distribution for a June 1973 event, sub-area 1 (the simulated runoff is represented by the slighlty lower line at the start of the hydrograph).

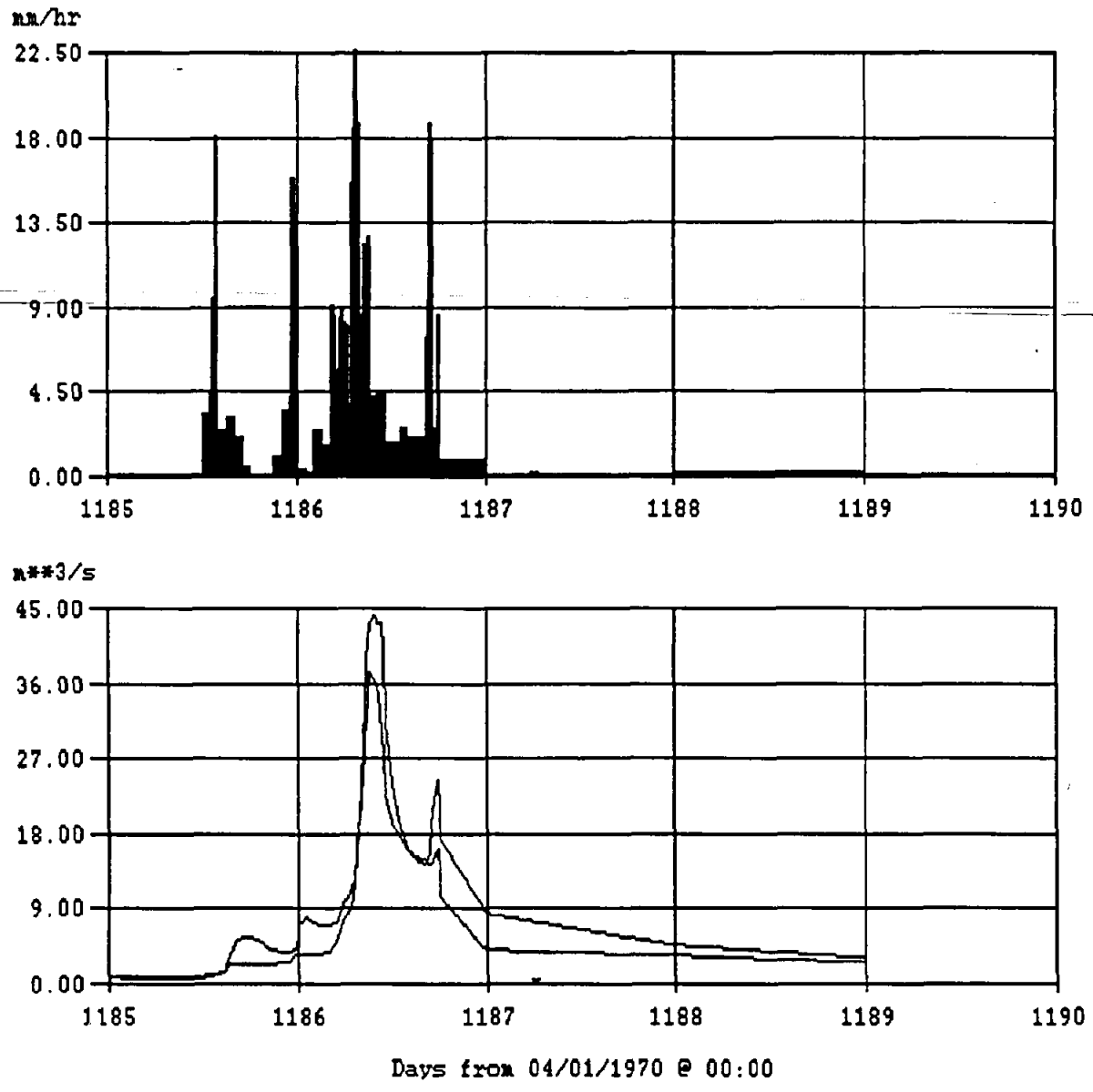

Figure 5.24 Rainfall intensity and runoff distribution for a June 1973 event, sub-area 6 (the simulated runoff over-estimates the two peaks).

5.5 TOMBSTONE, ARIZONA CATCHMENTS

The Tombstone catchments lie within the United States Department of Agriculture's Walnut Gulch Experimental Watershed, which is located in Cochise County, Arizona. The catchments modelled incorporate two gauged nested catchments within this watershed, W-8 and W-11. Their inclusion in the study allows several important aspects of the model to be tested. First, the region is semi-arid with ephemeral streams subject to heavy transmission losses. These losses have been relatively well documented (Lane et al., 1971) and therefore provide an ideal opportunity to test the transmission loss and indirect recharge functions incorporated into the VTI model. Second, rainfall events are of small areal extent and extremely variable spatially. Furthermore, they are often of high intensity and short duration. However, the existence of a dense network of recording rain gauges exists (approximately 1 gauge per 0.65 km^2) allows the problem of estimating weighted sub-area rainfall inputs to be overcome. This situation allows the model's intensity runoff and re-infiltration routines to be evaluated.

5.5.1 Catchment characteristics and hydrological processes

Topography:

The catchments occupy part of broad alluvial filled basin surrounded by intrusive Mesozoic and Tertiary igneous and metamorphic mountain blocks between cover a total of 15.49 km^2 and are made up of low undulating hills with moderate slopes which are dissected by well defined ephemeral stream channels. Slopes range from 0-35% but generally lie between 3-10% with a mean catchment slope of 7.9%.

Geology:

The entire catchment area is underlain by Quaternary and Tertiary alluvium of the Tombstone pediment. The alluvium is made up of permeable lensed and inter-bedded sand, gravel, discontinuous conglomerate and caliche conglomerate and some clay. The mean thickness of the alluvium is about 2 metres. The porosity of the material ranges form 30-45% with a mean of about 36%. The corresponding values for specific yield are between 9-33% with a mean of 27% (Lane et al., 1971). Two series of conglomerate lie unconformably beneath the recent alluvium. These conglomerates persist to depths exceeding 400 m. The regional groundwater is approximately 140 m deep (USDA, 1955-1973).

Channel characteristics:

The principal channel is approximately 13 km long with two major tributaries. The principal channel is shallow but well defined, varying in width from 5-15 m with a mean of 12 m. Caliche conglomerates which are resistant to erosion form steep but low cliffs in the channel. The channel has a slope of 1.2% with a sand and gravel bed ranging in thickness from 0-4 m. Flow events are typically flash floods lasting from 2-5 hours with a runoff peak within 15-30 minutes. Lane et al. (1971) monitored a 6.5 km reach of this channel, recording up to 100% peak reductions and estimating that the water absorbing capacity of the transmission loss zone below the channel was between 30 000 - 43 000 m^3.

Climate:

The area represents a hot desert grassland range with a mean annual rainfall of about 300 mm and clear peaks in July and August. These summer storms are high intensity convective events and typically exhibit a high degree of spatial variability. For example, total rainfall may vary from 0-60 mm within 0.8 km. Frontal storms lasting up to several days may also occur from November to June. There is no available data on evaporation for the catchment, however, the average annual class A pan evaporation for Tucson, Arizona is about 2200 mm.

Soils:

No information is available for these catchments, however, some soil data is available for adjacent catchments in the experimental watershed. These soils are moderately permeable calcareous gravelly loams. The lenticular nature of the geology and the presence of conglomerates suggests that the soils may also vary from sands to sandy silts.

Landuse:

The catchment is covered by desert grasses and shrubs. Two-thirds of the area is dominated black grama, sideoats grama and curly mesquite grasses with a basal area of about 2.5%, interspersed by desert shrubs with a crown spread of about 5%. The remaining third is dominated whitethorn, creosotebush and tarbush shrubs with a crown spread of 30% and an understorey of grasses with a less than 1% basal area.

Hydrological processes:

The predominant factor controlling runoff generation is rainfall intensity. The permeable nature of the soils suggest that only periods of intense rainfall are capable of generating infiltration excess runoff. The short duration of rain events, together with the low relief and thickness of the alluvial material, imply that it is unlikely that any saturated areas develop in the soil, so subsurface probably play an insignificant role in runoff generation. The thickness of the alluvium relative to rainfall volumes also suggest that direct groundwater recharge is unlikely. Recharge occurs primarily from channel transmission losses, and from lateral inflow of seepage from the adjacent mountain blocks which will not be accounted for in the model simulation.

5.5.2 Available data

Break-point rainfall data from 24 rain gauges and runoff from the two nested catchments covering the period June 1968 - December 1970 was obtained from the USDA. The network of rain gauges cover the catchments being modelled and the surrounding catchment boundaries.

The high degree of spatial and temporal variability of rainfall, even within one storm event, suggests that simulation results will be sensitive to the rainfall interpolation approach. For example, if sub-area rainfall for any time interval is calculated from too many rain gauges rainfall estimates will be an average incorporating data from gauges outside the sub-area

which may have received significantly higher or lower rainfall. Similarly, if a too coarse time interval structure is selected sharp peaks and fluctuations in rainfall intensity will be smoothed out resulting in an underestimation of infiltration excess runoff. The distribution of rain gauges demonstrated that sub-area rainfall for every sub-catchment can be adequately covered by four gauges. For this reason, sub-area rainfall calculations are based on the four rain gauges nearest to each sub-area centre. The modelling time interval selected varies from 1 day to 5 minutes, decreasing from intervals of 1 day, 6 hour, 1 hour, 15 minutes to 5 minutes if time interval rainfall exceeded 10 mm.

It is unlikely that such a dense network of rain gauges exists anywhere else in the world and thus this catchment provides a unique opportunity to test the infiltration excess runoff generating functions. Since practical applications are unlikely to have such a rainfall data network, simulations were carried out to test the model's inherent assumptions concerning hydrological processes rather than to test how well the model would perform in similar environments given the usual data constraints.

Given the lack of soils and evaporation data, their representation in the model remains highly subjective. However, since potential evapotranspiration exceeds rainfall by such a large degree it is unlikely that inaccuracies in its estimate and temporal distribution affect simulation results to any degree. Unfortunately, the lack of soils data dictated that their textural distribution and structural parameters be evaluated based on the authors' subjective interpretation of geologic conditions. As intensity excess runoff will be greatly affected by the infiltration rates derived from such estimates, the lack of soil data is the greatest deficiency in characterising the hydrologic response of the catchment.

5.5.3 Simulation results and discussion

Initially, the two gauged catchments were partitioned into six sub-areas of between 2-4 km each and data from only two rain gauges was used. These simulations produced very poor results as a consequence of the inability to accurately represent the spatial variations in rainfall given the size of the sub-areas. As it is not possible to test the model's runoff generating functions unless sub-area rainfall inputs can be reasonably well simulated, it was necessary to further subdivide each sub-area into two and to use data from a much denser network of rain gauges. The large number of sub-areas therefore reflects an attempt to adequately estimate the spatial variability of storm inputs to the catchment rather than any spatial physiographic differences. The gauged parts of the catchment represent discharge from sub-areas 1-6, (USDA nested catchment W-11), and sub-areas 1-12 (USDA catchment W-8).

Parameter values were derived from the available physiographic information wherever possible. Where insufficient data was available, parameters values either reflect the authors' initial 'best guess' estimates without further modifications or have derived after some calibration. Given the lack of data concerning soil texture, soil parameter values have been regionalised and considered uniform across the catchment. They represent subjective values reflecting the authors' speculations about alluvial soils in arid climates. Transmission losses parameters were calibrated in sub-areas 7, 8, 11 and 12, which represent the sections of the channel where losses were estimated by Lane et al. (1971). Initial sub-area routing

parameters estimated by HYMAS generated poor simulations, generally producing excessive lag times and flow duration. This is attributed to the 'flash flood' nature of runoff in this catchment which is difficult to reproduce on a sub-area scale. These values were subsequently altered by calibration against the observed hydrographs. Table 5.20 lists some of the physical characteristics and the critical parameter values used in the final simulation. The major difference between sub-areas exists in the transmission losses parameters. Transmission losses are likely to increase downstream as the channel widens and the channel bed material becomes coarser. Consequently, the relevant parameter values increase in the downstream direction.

Table 5.21 shows some of the components of the simulated water balance of the catchment and the statistics of fit between the observed and simulated flows from sub-areas 6 and 12. Given the rarity and short duration of events, the relationship between simulated and observed discharge is based on relatively few data points. Consequently poor fit statistics were obtained. Most of the observed data points correspond to low flows during the hydrograph recession so that small errors in simulated discharge lead to large discrepancies in the one to one relationship. As a result, these statistics do not adequately describe the performance of the model. A more representative evaluation of the model can be obtained by comparing the differences between the observed and simulated flow-duration curves (figs. 5.25 and 5.26). In general, most of the discrepancies between observed and simulated runoff occur during high flows.

Sub-area 6

Runoff from this sub-area was generally under-simulated (table 5.21). This may be attributed to the insufficient generation of infiltration excess runoff or to the over-estimation of transmission losses. As no information pertaining to channel characteristics or transmission losses was available for these sub-areas, the accuracy of their estimation is unknown. The under-simulation of high flows (fig. 5.25), however, suggests that insufficient runoff was generated. Given the lack of soil and infiltration data, this deficiency is not considered serious since no calibration of the runoff generation parameters was undertaken.

Since 100% of stormflow is generated by infiltration excess runoff (table 5.21), the derivation of reasonable simulations requires an accurate estimation of rainfall intensity and its distribution in space. The study found that it was necessary to model rainfall inputs at a spatial scale of less than 1 km^2 in order to properly characterise rainfall intensities. The use of larger sub-areas led to an under-estimation of rainfall intensities due to the highly localised nature of the convective storms. The variability in subarea rainfall during representative storms is shown in figure 5.27 and 5.28. During these storms, sub-area rainfall varied from 12-35 mm and 22-52 mm across sub-areas 1-6 while no rain fell on sub-areas 7-12. Since large spatial and temporal variations in rainfall intensity were recorded by the various rain gauges, and since up to 80% of rainfall during these events fell in a 10-15 min period, it was necessary to model rainfall at 5 minute time intervals in order to obtain realistic intensity estimates.

Table 5.20 Tombstone characteristics and model parameters.

Sub-area	1	2	3	4	5	6
Area (km^2)	1.5	1.5	1.6	1.6	1.0	1.0
Mean Catchment Slope (%)	7.9	7.9	7.9	7.9	7.9	7.9
Channel Slope (%)	2.3	2.3	2.4	2.4	1.7	1.7
Shreve Channel Order	1	1	3	3	5	5
Crop Factor	0.8	0.8	0.8	0.8	0.8	0.8
Canopy Capacity (mm)	0.03	0.03	0.03	0.03	0.03	0.03
Soil Porosity (% Vol.)	35.7	35.7	35.7	35.7	35.7	35.7
Field Capacity (% Vol.)	17.9	17.9	17.9	17.9	17.9	17.9
Wilting Point (% Vol.)	9.5	9.5	9.5	9.5	9.5	9.5
Mean Soil Depth (mm)	2000	2000	2000	2000	2000	2000
Soil Hydr. Cond. (mm h^{-1})	17.0	17.0	17.0	17.0	17.0	17.0
Infiltration Curve K	0.57	0.57	0.57	0.57	0.57	0.57
Infiltration Curve C	190.6	190.6	190.6	190.6	190.6	190.6
St. Dev. of Moist. Content Dist.	0.06	0.06	0.06	0.06	0.06	0.06
Max. Depression Store (mm)	1.0	1.0	1.0	1.0	1.0	1.0
Max. Dam Store (Ml)	0.0	0.0	0.0	0.0	0.0	0.0
% Area above Dams	0.0	0.0	0.0	0.0	0.0	0.0
Channel Infiltration K	0.65	0.65	0.65	0.65	0.65	0.65
Channel Infiltration C	500	500	500	500	500	500
Channel Infiltration area (km^2)	0.010	0.009	0.010	0.007	0.007	0.004
Channel Losses Power	0.32	0.32	0.32	0.32	0.32	0.32
Infiltration Storage Power	2.0	2.0	2.0	2.0	2.0	2.0
Aquifer Storativity	0.27	0.27	0.27	0.27	0.27	0.27
Aquifer Transmissivity (m^2 day^{-1})	50.0	50.0	50.0	50.0	50.0	50.0
Depth of Aquifer (m)	200	200	200	200	200	200
Adjusted Aquifer Hyd. Cond. (mm h^{-1})	2.81	2.81	2.81	2.81	2.81	2.81
G'water Drainage Vector (Fraction)	0.1	0.1	0.1	0.1	0.1	0.1
Regional G'water Slope (%)	0.01	0.01	0.01	0.01	0.01	0.01
Sub-area Routing Coeff. (K)	0.37	0.37	0.37	0.37	0.37	0.37

Table 5.20 Continued

Sub-area	7	8	9	10	11	12
Area (km^2)	1.05	1.05	0.9	0.9	1.7	1.7
Mean Catchment Slope (%)	7.9	7.9	7.9	7.9	7.9	7.9
Channel Slope (%)	1.4	1.4	2.0	2.0	1.2	1.2
Shreve Channel Order	2	2	5	5	7	7
Crop Factor	0.8	0.8	0.8	0.8	0.8	0.8
Canopy Capacity (mm)	0.03	0.03	0.03	0.03	0.03	0.03
Soil Porosity (% Vol.)	35.7	35.7	35.7	35.7	35.7	35.7
Field Capacity (% Vol.)	17.9	17.9	17.9	17.9	17.9	17.9
Wilting Point (% Vol.)	9.5	9.5	9.5	9.5	9.5	9.5
Mean Soil Depth (mm)	2000	2000	2000	2000	2000	2000
Soil Hydr. Cond. (mm h^{-1})	17.0	17.0	17.0	17.0	17.0	17.0
Infiltration Curve K	0.57	0.57	0.57	0.57	0.57	0.57
Infiltration Curve C	190.6	190.6	190.6	190.6	190.6	190.6
St. Dev. of Moist. Content Dist.	0.06	0.06	0.06	0.06	0.06	0.06
Max. Depression Store (mm)	1.0	1.0	1.0	1.0	1.0	1.0
Max. Dam Store (Ml)	0.0	0.0	0.0	0.0	0.0	0.0
% Area above Dams	0.0	0.0	0.0	0.0	0.0	0.0
Channel Infiltration K	0.65	0.65	0.65	0.65	0.65	0.65
Channel Infiltration C	2300	2300	500	500	2300	2300
Channel Infiltration area (km^2)	0.012	0.008	0.006	0.011	0.018	0.015
Channel Losses Power	0.1	0.1	0.1	0.1	0.1	0.1
Infiltration Storage Power	1.0	1.0	2.0	2.0	1.0	1.0
Aquifer Storativity	0.27	0.27	0.27	0.27	0.27	0.27
Aquifer Transmissivity (m^2 day^{-1})	50.0	50.0	50.0	50.0	50.0	50.0
Depth of Aquifer (m)	200	200	200	200	200	200
Adjusted Aquifer Hyd. Cond. (mm h^{-1})	2.81	2.81	2.81	2.81	2.81	2.81
G'water Drainage Vector (Fraction)	0.1	0.1	0.1	0.1	0.1	0.1
Regional G'water Slope (%)	0.01	0.01	0.01	0.01	0.01	0.01
Sub-area Routing Coeff. (K)	0.37	0.37	0.37	0.37	0.37	0.37

Table 5.21 Simulation results for the Tombstone catchments, May 1968 - October 1971.

Sub-area	1	2	3	4	5	6
Rainfall (mm)	1100	1081	1019	1122	1026	1017
Actual Evap. (mm)	888	877	827	916	825	818
Sat. Excess Runoff (mm)	0	0	0	0	0	0
Inf. Excess Runoff (mm)	42	39	32	31	42	37
Baseflow Runoff (mm)	0	0	0	0	0	0
G'water Recharge (mm)	32	25	20	32	22	23
Sub-area Runoff (Ml)	0.03	0.033	0.025	0.02	0.025	0.02
Transmission Losses (Ml)	0.003	0.003	0.003	0.002	0.002	0.004
Total Runoff (Ml)	0.027	0.057	0.022	0.040	0.023	0.154
Obs. Total Runoff (Ml)	N/A	N/A	N/A	N/A	N/A	0.174
	Slope of Reg. Line	Intercept of Reg. Line	Reg. Coeff.	Coeff. of Eff.		
Fit Stats. (sub-area 6)	0.57	0.02	0.32	0.14		
Log Stats. (sub-area 6)	0.88	-1.06	0.49	0.36		

Sub-area	7	8	9	10	11	12
Rainfall (mm)	1001	966	969	905	1062	1109
Actual Evap. (mm)	835	793	782	728	877	927
Sat. Excess Runoff (mm)	0	0	0	0	0	0
Inf. Excess Runoff (mm)	27	36	33	28	44	38
Baseflow Runoff (mm)	0	0	0	0	0	0
G'water Recharge (mm)	26	22	16	11	36	33
Sub-area Runoff (Ml)	0.013	0.019	0.013	0.011	0.042	0.039
Transmission Losses (Ml)	0.049	0.045	0.003	0.005	0.103	0.091
Total Runoff (Ml)	0.18	0.19	0.010	0.017	0.202	0.262
Obs. Total Runoff (Ml)	N/A	N/A	N/A	N/A	N/A	0.306
	Slope of Reg. Line	Intercept of Reg. Line	Reg. Coeff.	Coeff. of Eff.		
Fit Stats. (sub-area 12)	0.64	0.01	0.38	0.27		
Log Stats. (sub-area 12)	0.58	-0.17	0.25	0.11		

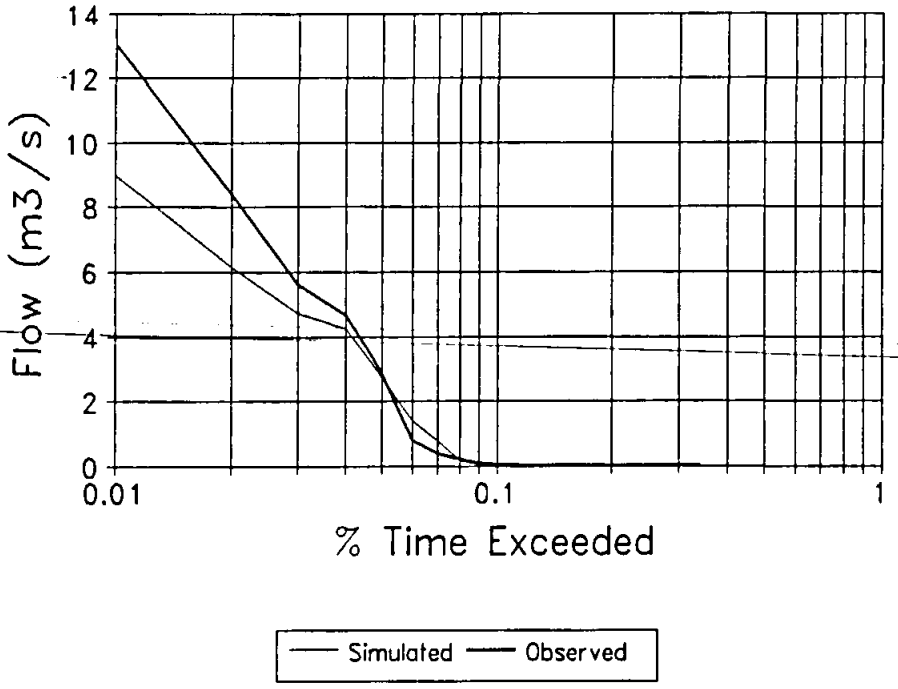

Figure 5.25 Observed and simulated flow duration curves from sub-area 6.

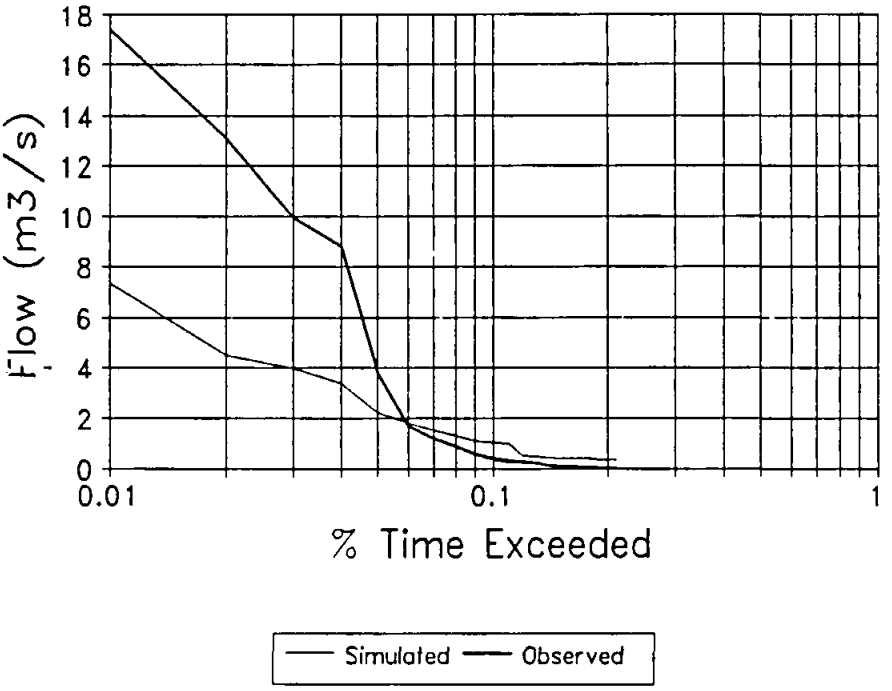

Figure 5.26 Observed and simulated flow duration curves from sub-area 12.

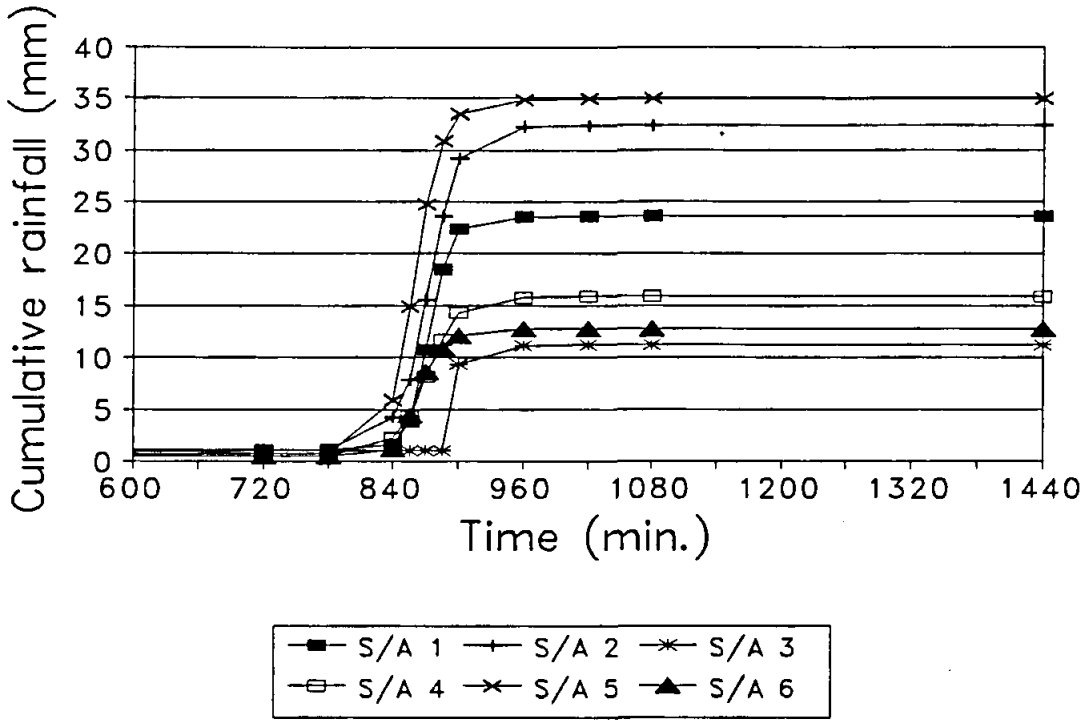

Figure 5.27 Sub-area cumulative rainfall curves for the storm of 2 August, 1968.

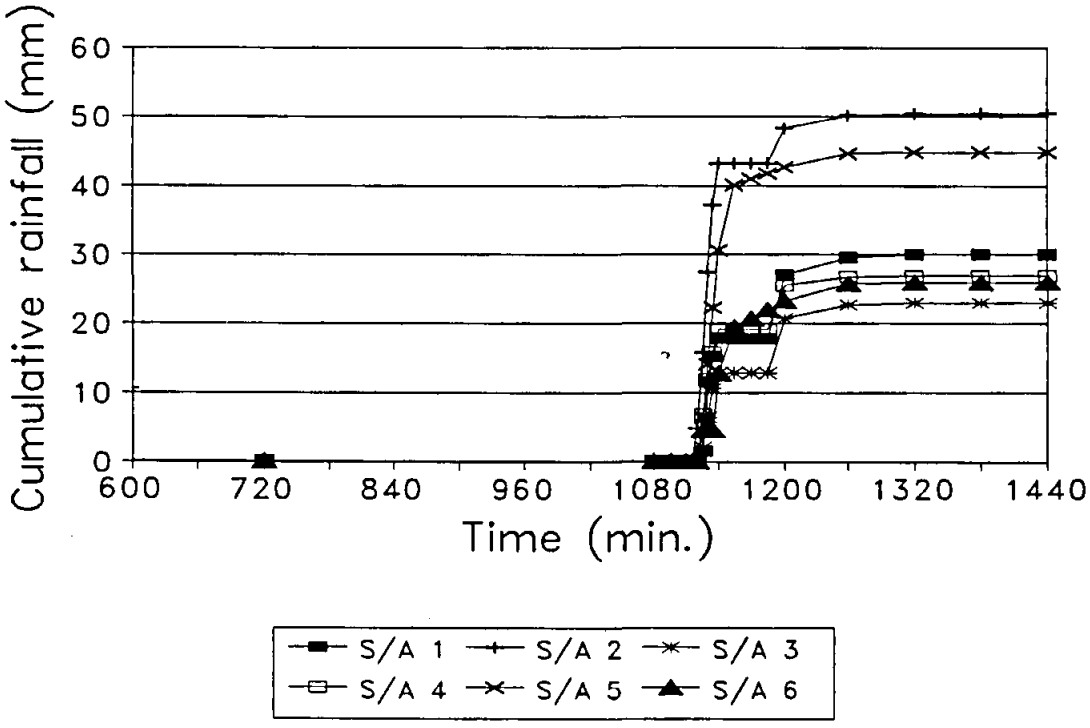

Figure 5.28 Sub-area cumulative rainfall curves for the storm of 5 August, 1968.

The hydrographs generated by these two events are shown in figure 5.29 and 5.30. These show that runoff peaks and volumes were under-simulated and calibration of the infiltration parameters is required. The 2 August event shows a recession tail resembling excessive baseflow, however, this discrepancy does not represent an inadequacy in the simulated flow regime but is rather an attribute of the change in modelling time interval. As rainfall intensities decrease immediately following the hydrograph peak, the model returns to a 1 hour modelling interval. This increased temporal spacing of simulated flow data points results in a line being drawn from a high flow data point to a low flow data point on the plotted hydrograph. Rainfall during the 5 August tapers off more gradually, hence this effect is not present in the simulated hydrograph.

Sub-area 12

Total runoff volumes were under-simulated during the simulation (table 5.21). This under-simulation is attributed to the insufficient generation of high flows (fig. 5.31), probably due to the under-simulation of inputs from sub-areas 1-6. Sub-areas 7, 8, 11 and 12 contain the main channel where transmission losses have been documented. Some calibration of the transmission loss parameters was undertaken. These parameters were difficult to calibrate and mixed results were obtained. In general it was difficult to simulate small events without over-simulating large events. Results for the 2 and 5 August 1968 events are shown in figures 5.31 and 5.32. These show that a poor simulation was obtained for the 2 August event, probably due to insufficient upstream inflows from sub-area 6 and excessive transmission losses. The 5 August hydrograph was reasonably well reproduced, both in terms of runoff volume and timing. The peak was under-simulated due to insufficient inflow from sub-area 6. Small runoff producing storms falling on sub-area 6 could not be simulated due to the high channel loss parameters, hence the low regression slope of the fit statistics (table 5.21). Discharge produced by these events likely represents runoff from rain falling in the vicinity of the catchment outlet and not subject to high reinfiltration and channel losses. This process cannot be reproduced on a sub-area scale where generated runoff is subject to re-infiltration. It is unlikely that runoff from such events can be simulated under conditions where high channel loss parameters have been set.

Conclusions

Mixed results have been obtained, but given the lack of soils information, the infiltration excess runoff generating function performed reasonably well. In general, runoff was under-simulated and further calibration is required. The transmission loss function proved difficult to calibrate and resulted in an inability of the model to reproduce runoff from small localised events. The ability of the model to reproduce the hydrograph shape of the major events suggests that its inherent assumptions concerning hydrological processes and their spatial distribution during intensity driven runoff, are essentially correct. However, most of these processes operate at fine time intervals and are difficult to reproduce at coarser time scales.

The high spatial and temporal rainfall variability required a minimum 5 minute time interval and small sub-areas to achieve any degree of success. Since the density of rain gauges and the fine time interval rainfall data used in this study is rarely available outside research catchments, it is unlikely that intensity driven runoff from such catchments can be reproduced unless more suitable rainfall distribution techniques can be developed.

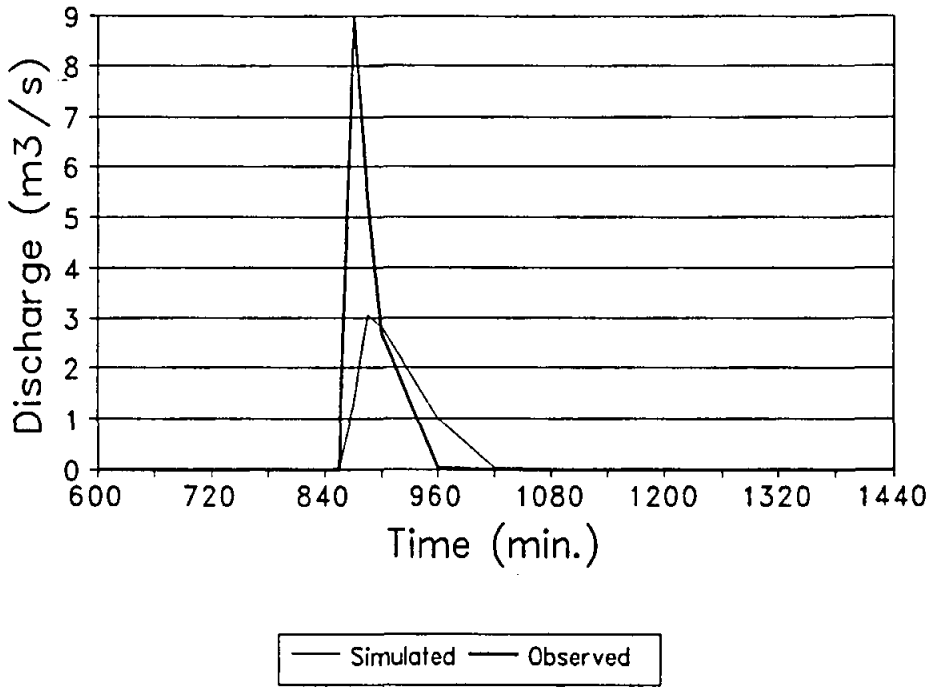

Figure 5.29 Hydrograph of discharge from sub-area 6, 2 August, 1968.

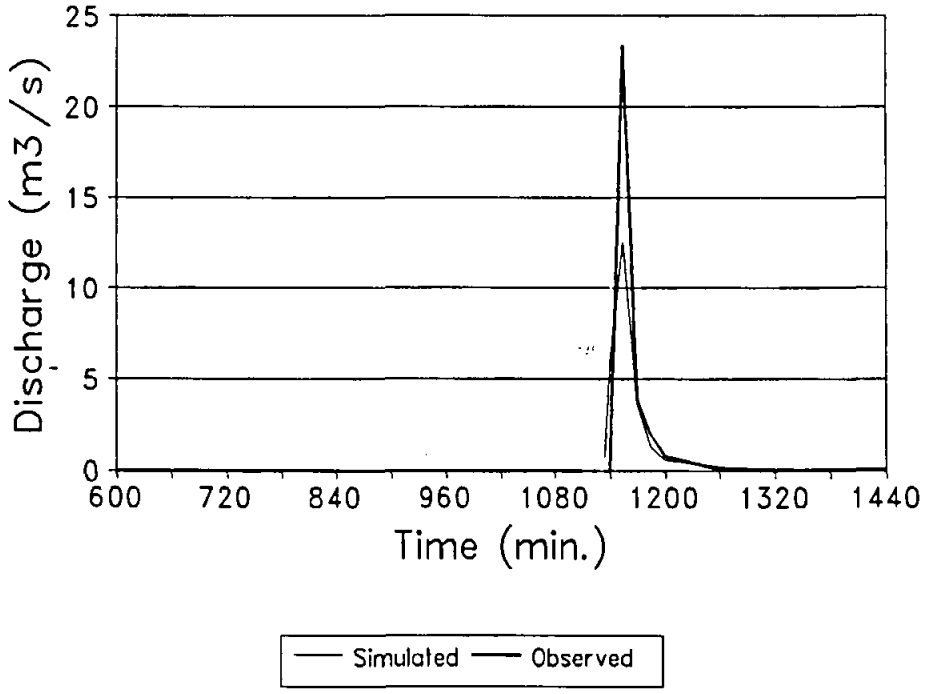

Figure 5.30 Hydrograph of discharge from sub-area 6, 5 August, 1968.

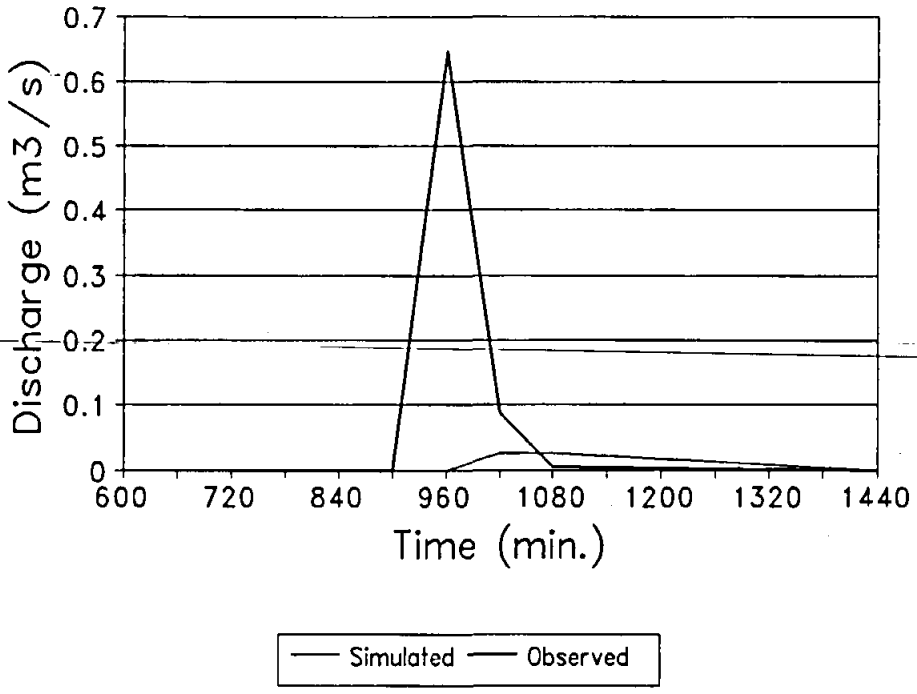

Figure 5.31 Hydrograph of discharge from sub-area 12, 2 August, 1968

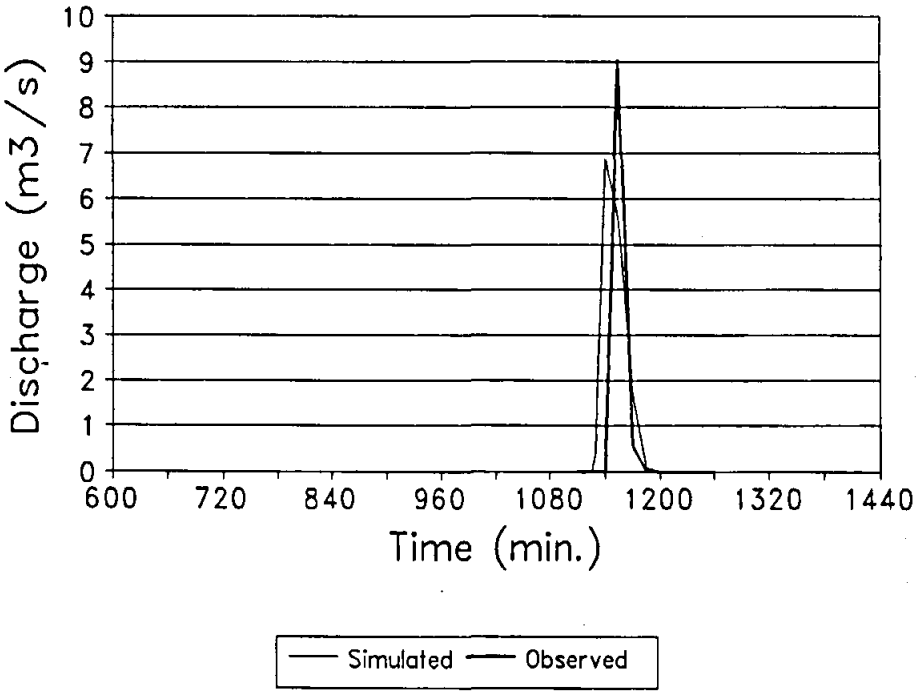

Figure 5.32 Hydrograph of discharge from sub-area 12, 5 August, 1968.

5.6 OXFORD, MISSISSIPPI CATCHMENTS

These catchments are located in Marshall County, Mississippi State in southern central USA (Hughes and Beater, 1989). They represent the moderately eroded uplands in the transitional zone between the southern coastal plain and the southern Mississppi valley uplands. They have been included in this study as they represent catchments with very distinct seasonal variations in runoff response due to landuse changes.

The available data have been obtained from the US Department of Agriculture and consist of breakpoint rainfall and streamflow records for approximately two years (1970 and 1971). Data from three gauged nested catchments have been used (two upstream areas of 30.4 km^2 and 22.4 km^2 and a downstream gauge with catchment area of 80.9 km^2). The total area has been divided up into 9 sub-areas and there are data available from 10 raingauges, fairly evenly distributed within the total area.

Information about the physical characteristics of the area have been obtained from the USDA (1955-1973) publications, which were kindly loaned to Rhodes by Prof. Schulze of the Department of Agricultural Engineering, University of Natal, Pietermaritzburg.

5.6.1 Catchment characteristics and hydrological processes

Topography :

Mean catchment slopes appear to vary from between 6% in the lower sub-areas to about 10% in the upper reaches. Otherwise there are no great variations in topography and main channel slopes within the sub-areas also appear to be similar at about 0.4% (table 5.22).

Geology :

The underlying geology is made up of massive sandstones with a high silt and clay content. Overlaying this, in some places, are mixed alluvial sediments and Loess of recent and pleistocene origin. Some of the lower alluvial valleys are wide and flat. The regional groundwater gradient follows the topography in some parts of the area, but for sub-areas 1 to 3, the gradient is transverse to the topography suggesting groundwater outflow to adjacent areas which are not being modelled. Groundwater levels are generally below the surface, but periodically rise in the lower sub-areas to produce perrenial spring flow at the outlet of the main catchment. Otherwise the rivers are ephemeral.

Climate :

Mean annual precipitation is about 1300 mm and reasonably evenly distributed over the year. There also do not appear to be any great spatial variations in overall rainfall amount. The rainfall quite often falls as high intensity, short duration events, even in winter. Information on potential evapotranspiration is lacking, but mean annual rates seem to be of the order of 1250 to 1300 mm.

Soils :

Soils vary from fine sandy loams to silty clay loams having weak structure and moderate permeabilities. Depths vary from very shallow to over 1.3 m, with most of the area having soils in excess of 0.9 m. There is insufficient information to fully characterise the spatial variations in either soil texture or depth and both have been assumed to be uniform over the sub-areas.

Landuse and Vegetation :

About 20% of the area is cultivated, with corn and cotton being the dominant crops. The remaining area is either idle (broom sedge and grasses - 42%), woodland (21%) and pasture (13%). The seasonal variations in surface cover over the cultivated lands appears to have the predominant effect on the runoff regime. However, there is no information available about the position of the main cultivated areas with respect to the river channels (i.e. in the valley bottoms or on the hill slopes) and this may have a major impact on the generation of runoff.

Hughes and Beater (1989) noted that an average runoff ratio for winter and spring months can be as high as 50%, while the same value for summer, despite higher intensity rainfall, is more likely to be less than 15%. Part of the test of the VTI model was therefore to evaluate the seasonal differences in the parameter values which are normally established by setting a minimum and maximum value and determining the individual monthly values using a sine curve distribution with a peak in July for the northern hemisphere. This procedure applies to the vegetation (interception and evapotranspiration), infiltration and routing parameters.

Table 5.22 Oxford catchment characteristics.

Sub-area	1	2	3	4	5
Area (km^2)	9.2	12.5	8.7	4.3	11.1
Downstream sub-area	2	3	4	5	6
Mean Catchment Slope (%)	7.0	7.0	7.0	6.0	6.0
Channel Slope (%)	0.4	0.4	0.4	0.4	0.4
Shreve Channel Order	42	93	137	14	182

Sub-area	6	7	8	9
Area (km^2)	6.1	10.9	11.5	6.6
Downstream sub-area	9	8	9	-
Mean Catchment Slope (%)	6.0	10.0	10.0	6.0
Channel Slope (%)	0.4	0.5	0.4	0.4
Shreve Channel Order	212	49	99	326

5.6.2 Simulation results and discussion

The total catchment area (referred to as OX32) has been divided into 9 sub-areas varying in size from 4.3 to 12.5 km^2. Gauged catchment OX35 consists of sub-areas 1 to 3 and OX10 of sub-areas 7 and 8 (table 5.22). The distributed rainfall inputs were compiled using a time interval scheme of 1 day, 1 hour and 15 minutes with thresholds of greater than 10mm during a longer interval to determine the change to a lower interval.

Some of the more important model parameter values are listed in table 5.23. The values listed in the first column are those that have been derived using the procedure of entering physiographic information and the HYMAS standard parameter estimation equations where possible. Some of the others were initially estimated from best (informed !) guesses about such as geological characteristics. Only one parameter value is given as there is little evidence for major spatial variations. The major changes that were made to obtain reasonable results were alterations to the infiltration and routing parameter values. Further changes were made to the seasonal distribution weights (table 5.24) as the original sine curve values did not appear to adequately reflect the differences related to landuse during the year. It was extremely difficult to 'calibrate' the seasonal distribution and it is unfortunate that more information is not available about the seasonal variations in cover conditions to check that the modified distribution makes sense.

Table 5.23 Parameter values for Oxford catchments.

Parameter	Initial prameter estimate	'Improved' parameter estimate
Summer Crop factor	0.8	1.1
Winter Crop factor	0.5	0.5
Summer Infiltration curve K	0.711	0.650
Winter Infiltration curve K	0.478	0.370
Summer Infiltration curve C	180.4	380.0
Winter Infiltration curve C	148.0	250.0
Total soil depth (mm)	1055	1055
FC/Porosity ratio	0.66	0.66
Soil Hyd. Cond. (mm h^{-1})	6.6	6.6
St. Dev. Moist content dist.	0.156	0.156
Max. Depression storage (mm)	0.0	0.0
G'water drainage vector	8.0	8.0
Max. regional g'water slope (%)	5.0	5.0
Aquifer Storativity	0.006	0.006
Transmissivity (m^2 day^{-1})	100	100
Summer sub-area routing K	7.6	1.1
Winter sub-area routing K	3.3	1.1

Table 5.24 Sine-curve and modified seasonal distribution weights.

	Jan	Feb	Mar	Apr	May	Jun	Jul	Aug	Sep	Oct	Nov	Dec
Sine-Curve	0.00	0.26	0.50	0.71	0.87	0.97	1.00	0.97	0.87	0.71	0.50	0.26
Modified	0.00	0.00	0.20	0.30	0.70	0.70	0.97	1.00	0.97	0.87	0.70	0.50

Figures 5.33 to 5.36 illustrate the seasonal changes in response and the extent to which the VTI model has successfuly simulated these. The results illustrated in these hydrographs are typical of the whole two year simulaton period and for the three gauged catchments. Many of the events are reasonably well simulated using the modified seasonal infiltration rates and table 5.25 indicates that for the upstream sub-areas most of the runoff is generated as infiltration excess runoff. For the peak summer months (July to September) the balance of runoff generation appears to shift to saturated area type runoff. The events that are simulated the worst are those in July, when the model indicates far more runoff than actually occurs. It is difficult to understand why this should be the case when June and August events are simulated quite well. The higher levels of baseflow for some of the sub-areas indicates that the groundwater level is rising to a point where it intersects the surface. Although the observed data suggests that this does happen in the lower sub-areas (5, 6 and 9), it is unlikely to be the case for sub-areas 1 and 2, suggesting that some of the groundwater parameter values or model functions are inadequate for these catchments.

The imbalance between the total simulated volumes and the poor statistics suggest that more calibration of the parameter values is required, despite some of the reasonable individual event results demonstrated in figures 5.33 to 5.35. The overall results suggest that for some of the time the runoff is derived from a combination of infiltration excess as well as saturated area runoff. However, the model does not always demonstrate a satisfactory capability of achieving the correct balance between these two. It is possible that the size of the sub-areas is too large to adequately simulate the hydrology of this area, however, the scale of the sub-areas is consistent with the spacing of the available raingauges. It is also possible that more information about the spatial position of the major cultivated areas may be beneficial in explaining some of the simulation results. In general terms, it is difficult to know whether smaller sub-areas may improve the simulations given the available knowledge.

Conclusions.

The most obvious conclusion is that the standard parameter estimation routines for infiltration rates and for the routing parameters did not work adequately for these catchments and more calibration than was carried out in this initial test is required. Similarly, the standard seasonal distribution values were equally inadequate. The implication is that the user must beware of making the assumption that the standard values, provided by the initial estimation procedures, are likely to be even close to satisfactory for all catchments. The difficulty is knowing when to accept them and when to modify them. This decision can only be based on further information about either the response of the catchment or its physical characterisics. Typically, this requires either calibration, if runoff data are available, or field investigations, if not.

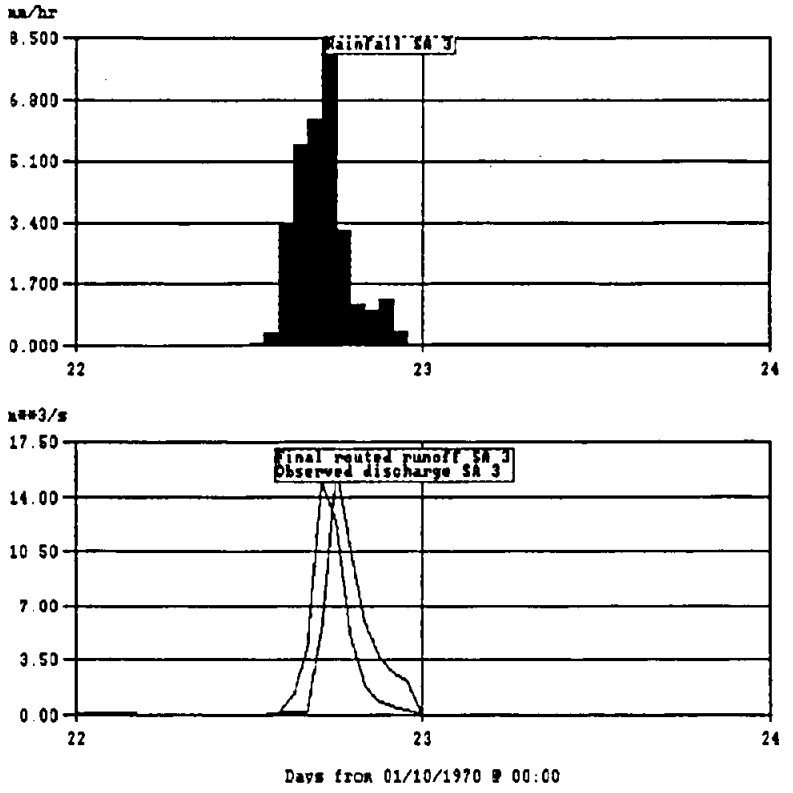

Figure 5.33 February 1970 event for sub-area 3 (the simulated occurs earlier).

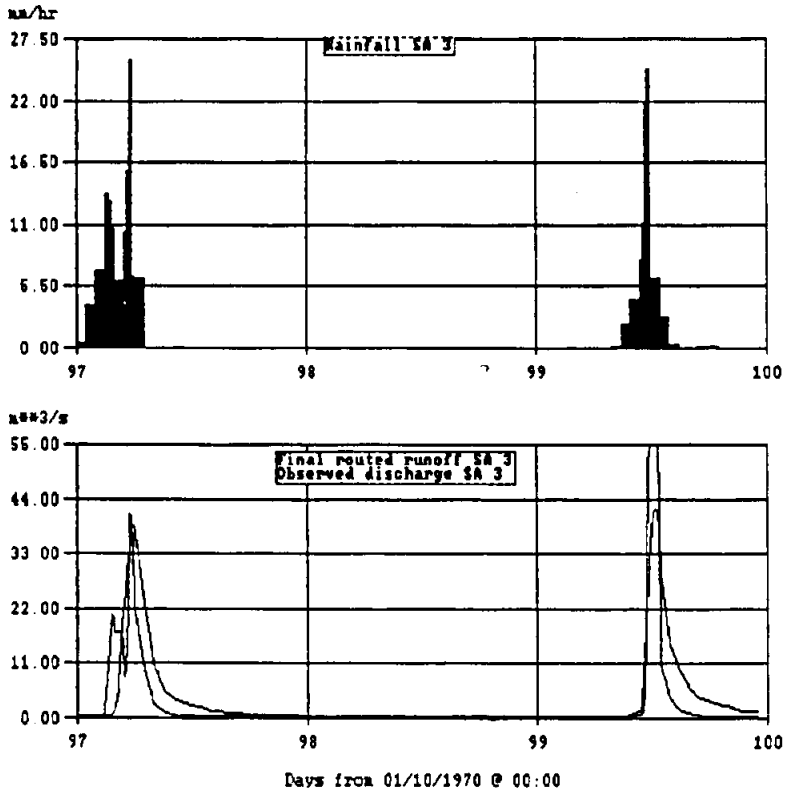

Figure 5.34 April 1970 events for sub-area 3 (the simulated have steeper recessions).

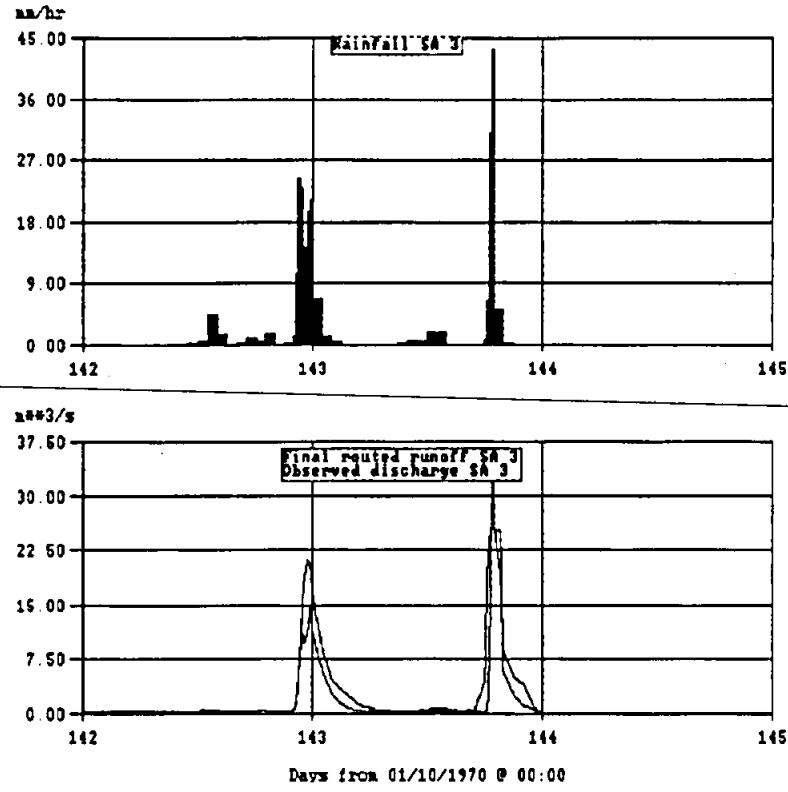

Figure 5.35 June 1970 events for sub-area 3 (1st under-simulated, 2nd over-simulated).

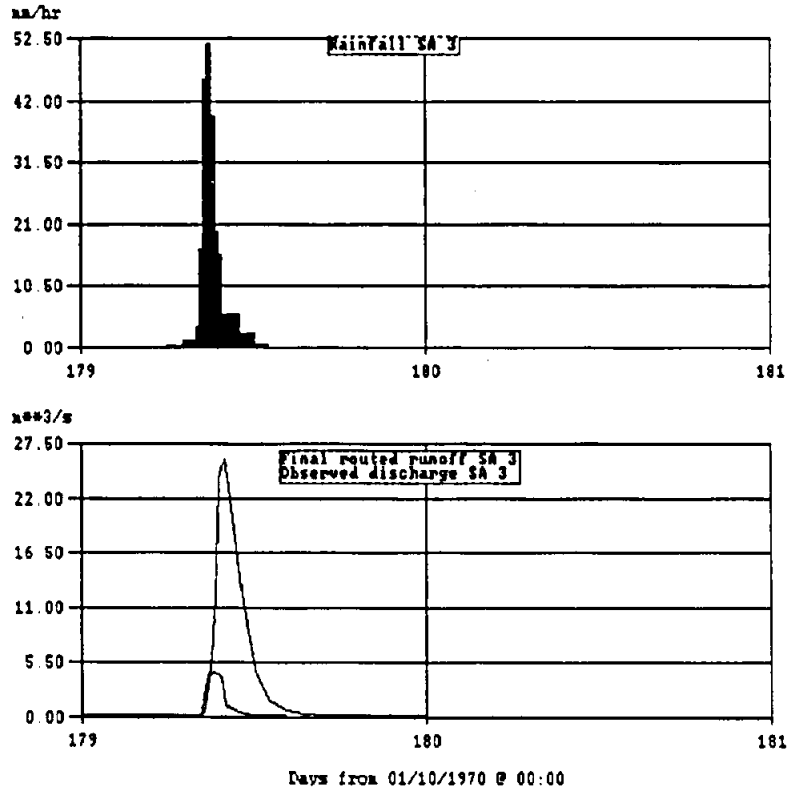

Figure 5.36 July 1970 event for sub-area 3 (the event is highly over-simulated).

Table 5.25 Results for the Oxford catchments, January 1970 - October 1971 (608 days).

Sub-area	1	2	3	4	5
Rainfall (mm)	2139	2262	2180	2112	2043
Actual Evap. (mm)	1286	1356	1315	1245	1223
Sat. Excess Runoff (mm)	92	106	82	62	166
Inf. Excess Runoff (mm)	146	193	160	145	111
Baseflow Runoff (mm)	42	39	15	5	125
G'water Recharge (mm)	427	441	426	426	667
Sub-area Runoff (Ml)	2744	4488	2359	994	4706
Transmission Losses (Ml)	36	119	244	105	137
Total Runoff (Ml)	2705	7074	9189	889	14647
Obs. Total Runoff (Ml)	N/A	N/A	11776	N/A	N/A
	Slope of Reg. Line	Intercept of Reg. Line	Reg. Coeff.	Coeff. of Eff.	
Fit Stats. (sub-area 3)	0.62	0.90	0.50	0.31	
Log Stats. (sub-area 3)	0.48	0.67	0.26	-0.60	

Sub-area	6	7	8	9
Rainfall (mm)	2094	2225	2211	2190
Actual Evap. (mm)	1194	1258	1256	1243
Sat. Excess Runoff (mm)	72	162	185	164
Inf. Excess Runoff (mm)	134	169	140	148
Baseflow Runoff (mm)	22	9	12	93
G'water Recharge (mm)	689	386	374	729
Sub-area Runoff (Ml)	1477	3858	4100	2822
Transmission Losses (Ml)	168	76	229	229
Total Runoff (Ml)	15956	3782	7653	26202
Obs. Total Runoff (Ml)	N/A	N/A	8384	36915
	Slope of Reg. Line	Intercept of Reg. Line	Reg. Coeff.	Coeff. of Eff.
Fit Stats. (sub-area 9)	0.77	2.03	0.40	0.36
Log Stats. (sub-area 9)	0.62	-0.20	0.40	0.24

5.7 APPLICABILITY OF THE VTI MODEL

This section is designed to draw together any general points about the general applicability of the VTI model that have been revealed by the several test applications that have been carried out and reported in detail above.

5.7.1 The parameter estimation procedures

Wherever possible the model has been applied without calibrating the parameter values that can be estimated from the physiographic data. The initial values, taken from the information about the physical characteristics of the areas entered into the physiographic variable data files, have generally been accepted and used to generate the results presented. However, as already stated, not all of the model parameter values can be estimated in this way. This is either due to the empirical nature of the parameters themselves (e.g. the transmission loss parameters), or because there is not sufficient information available to quantify the physiographic variables (e.g. the groundwater parameters in the southern Cape examples).

There is little doubt that more work is required to reduce the number of parameters that are totally empirical and to attempt to improve the representativeness of the other parameter estimation equations. While some appear to be satisfactory for some of the test catchments, there are others that would appear to produce inappropriate model parameter values under certain circumstances. It should be pointed out that these estimation equations should always be viewed as first estimates and if additional information is available to suggest alternative values they should be modified.

The final conclusion is that, while the results suggest that reasonable simulations can be achieved without calibration under some situations, it is still not possible to state that reliable simulations can always be expected without some form of calibration.

5.7.2 Model limitations and deficiencies

One of the major limitations that has been identified is the inadequacy of the model to satisfactorily reproduce the correct amounts of infiltration excess runoff for semi-arid areas with short duration, high intensity rain events when the model time period selected is too long. This has serious implications for South African situations, where many areas experience this type of rainfall and the national rainfall database is at a resolution of one day. It is therefore necessary to investigate the posibility of developing an improved approach to dissagregating daily rainfall values.

The Tombstone simulations illustrate the difficulty of defining a satisfactory channel transmission loss routine that is based on physically meaningful parameters. Although, the algorithms used in the model are thought to reflect the nature of the physical processes involved, the highly empirical nature of some of the relevant parameter values makes this part of the model very difficult to apply in practice.

The model appears to maintain moisture levels in the lower soil zone at artificially high levels, particularly when the crop factor parameter value is relatively small. This is thought to be related to the fact that the model does not allow for water to move from the lower to

the upper zone through capillary rise when the upper zone is dry. As soon as a suitable approach has been identified, the soil moisture component of the model will be modified.

The groundwater recharge application of the model in the Bedford area revealed that there is a potential need to include a delay in the routing of groundwater between sub-areas. The model is simulating this movement as 'piston' type flow, when the observed data indicate that it is really 'wave' type movement.

Care should be taken in quantifying the groundwater drainage vector, as recharge is very sensitive to this parameter when the vector is specified as a shallow angle. This parameter is also difficult to quantify without detailed information about the route that percolating water follows in rock fracture zones.

As already referred to, the model has very little in the way of water abstraction routines and those that have been included are highly simplified. Until improved routines have been added, it will therefore be difficult to apply the model to investigate the impacts of changes in most types of water abstraction.

6. MODEL APPLICATION EXAMPLES (The PEXP model)

6.1 INTRODUCTION

The input of phosphorus to the surface of catchments within developing urban areas and the subsequent washoff of these nutrients is viewed as a potentially major source of pollution in the rivers and storage reservoirs of South Africa. The source of these nutrients includes detergents, food waste and fuel ash, as well as excreted animal and human wastes. Their prevalence in developing urban areas is related to the inadequacy of the waste disposal facilities. Reference has already been made to the techniques developed at the CSIR (Grobler, et al., 1987) which are used to translate socio-economic survey data into information on the input phosphorus budget to the catchment surface. The purpose of this model is to utilize that information, together with a simplified approach to estimating the daily volume of stormwater runoff, to estimate the quantities of phosporus washed off the surface.

The model has been applied to two different areas for which the necessary socio-economic survey data is available to estimate the likely phosphorus input onto the catchment surface. The first is the Botshabelo Township located in the Modder River catchment close to Bloemfontein in the Orange Free State (Grobler, et al., 1987). The phosphorus budget for Botshabelo was determined as part of a study for the Department of Water Affairs and Forestry to assess the impact of low-cost, high-density urban development on water quality in the Modder River. The Grobler, et al. (1987) report suggests a mean annual phosphorus input of 102 tonnes yr^{-1}.

The second area is the Buffalo River catchment in the eastern Cape Province, where several developing townships are situated. One of these is Mdantsane located close to East London on the northern bank of Bridel Drift Dam. The phosphorus budget data (mean annual input of some 55 tonnes yr^{-1}) for this area was determined as part of a broader water quality situation analysis, to assist the Department of Water Affairs and Forestry in assessing the assimilative capacity of the Buffalo River (Van Ginkel, et al., 1993). The perception that nutrients, washed off from these areas during storm runoff, may play a major role in water quality problems within Bridle Drift Dam, prompted the application of the model to this area.

The rainfall input for both areas has been derived from Weather Bureau daily rainfall stations (accessed via the Computing Centre for Water Research, University of Natal, Pietermaritzburg) for a period of 46 years (1930-1975). The two example areas have different characteristics in terms of climate and socio-economic conditions and therefore might be expected to have different nutrient export characteristics.

6.2 SENSITIVITY OF SOME MODEL PARAMETERS

The model was initially applied by quantifying the parameters as far as possible from available information. However, as there is no available information about how to quantify some of the parameters (notably the S-Curve Lambda values for the nutrient export relationships), this section of the report mainly concentrates on a limited sensitivity analysis of the model. Several of the parameters values have been varied and their impact on the simulation results assessed with respect to duration curves of runoff, total phosphorus load and stored phosphorus.

Table 6.1 lists some of the parameter values for the two areas as well as indicating the range (lower and higher values) over which the sensitivity analyses were carried out. The parameters reflect somewhat deeper soils, better developed vegetation and steeper slopes in the Mdantsane Township (relative to Botshabelo), as well as less intense rainfall, particularly in summer. From the available information it has also been assumed that Mdantsane has a higher proportion of pervious areas.

Table 6.1 Main model parameters, their values and those used in the sensitivity analysis.

		Standard Parameter Values		Sensitivity Analysis	
Model Parameters		Botshabelo	Mdantsane	Lower Value	Higher Value
Areas (km^2)	Direct Imp.	8.0	8.6		
	Indirect Imp.	1.5	3.0		
	Pervious	1.5	5.5		
	Total	11.0	17.1		
Slope Factor		0.04	0.08		
Manning's n	Impervious	0.04	0.04	0.02	0.06
	Pervious	0.05	0.05	0.03	0.07
Imp. Area Storage (mm)		10.0	15.0		
Soil Depth (m)		0.3	0.5		
Initial Loss Coeff.'s	Impervious	0.25	0.25	0.10	0.40
	Pervious	0.30	0.30	0.15	0.45
Daily P Inputs ($T\ km^{-2}$)	Impervious	0.019	0.005		
	Pervious	0.067	0.017		
S-Curve Lambda	Impervious	1.5	1.5	0.5	5.0
	Pervious	1.5	1.5	0.5	5.0
Rain Dist. Factor (h)	Summer	3	6	2	10
	Winter	16	18	10	20

Note : The value used for the upper value of the Summer Rain Distribution Factor for Botshabelo sensitivity analysis was 6h.

The results of the sensitivity analysis are presented in tables 6.2 to 6.4, as well as figures 6.1 to 6.4, which illustrate the duration curves for total monthly phosphorus load (tonnes) and mean monthly stored phosphorus (tonnes km^2) for the four groups of parameters and the two townships.

Table 6.2 Sensitivity analysis results - Monthly rainfall and discharge volume (Ml) statistics.

		Mean	St. Dev.	Median	Coeff. Var.	Mn/Med. Ratio	Max.
Botshabelo							
Rainfall (mm)		49.8	50.6	34.3	1.02	1.45	252.0
Standard Values		231.9	298.3	119.9	1.29	1.93	2110.8
Initial Loss Coeff.'s	Lower	247.3	308.1	135.1	1.25	1.83	2144.5
	Higher	218.2	289.8	106.4	1.33	2.05	2083.1
Rain Dist. Factors	Lower	236.5	301.5	124.5	1.27	1.90	2121.4
	Higher	224.5	293.2	113.0	1.31	1.99	2096.1
Mdantsane							
Rainfall (mm)		59.5	57.4	44.1	0.96	1.35	561.5
Standard Values		316.0	569.5	134.1	1.80	2.36	8030.7
Initial Loss Coeff.'s	Lower	346.4	581.2	166.3	1.68	2.08	8068.1
	Higher	293.2	561.3	114.0	1.91	2.57	8019.2
Rain Dist. Factors	Lower	332.5	576.6	148.3	1.73	2.24	8044.4
	Higher	305.2	565.6	125.8	1.85	2.43	8025.9

Note : No results are tabulated for the effects of changing the Nutient Lambda or Manning's n parameters as these have no effect on the simulated runoff.

The discharge statistics for the standard parameters reflect the greater impervious area and higher intensity rainfalls in Botshabelo, resulting in a generally higher runoff response than Mdantsane. For example, the mean monthly runoff depth for Botshabelo is 21.1mm from 49.8mm of rainfall (ratio = 0.42), while the equivalent depths for Mdantsane are 18.5mm and 59.5mm (ratio = 0.31). However, the occasional large and long duration events experienced in the eastern Cape coastal area account for the very large maximum runoff volumes and the high coefficients of variation for runoff. The sensitivity analysis indicates that the initial loss coefficient is the more sensitive parameter and unfortunately it is also the most difficult to determine from normally available information. Schulze (1982) refers to some of the values of this parameter that have been used in different applications of the SCS model and they seem to vary between 0.05 and 0.2. However, most of these applications relate to small rural catchments and there seems to be little available information on the value to use for urban catchment situations. Schmidt and Schulze (1987) used a value of 0.1 throughout their design manual.

Table 6.3 Sensitivity analysis results - Monthly phosphorus load (Tonnes) statistics.

		Mean	St. Dev.	Median	Coeff. Var.	Mn/Med. Ratio	Max.
Botshabelo							
Standard Values		8.6	23.7	1.3	2.76	6.6	247.0
Nutrient Lambda parameters	Lower	8.6	14.8	3.6	1.72	2.4	119.6
	Higher	8.5	26.5	1.2	3.12	7.1	290.5
Manning's n	Lower	8.6	20.1	1.9	2.34	4.5	196.7
	Higher	8.5	25.8	1.5	3.02	5.7	336.2
Initial Loss Coeff.'s	Lower	8.6	20.0	1.9	2.34	4.5	203.3
	Higher	8.6	26.1	0.9	3.05	9.5	276.4
Rain Dist. Factors	Lower	8.6	21.3	1.5	2.48	5.7	211.8
	Higher	8.5	26.9	1.2	3.16	7.1	245.3
Mdantsane							
Standard Values		4.5	16.6	0.46	3.69	9.78	186.2
Nutrient Lambda parameters	Lower	4.6	11.6	1.21	2.39	3.80	87.2
	Higher	4.4	20.4	0.41	4.63	10.7	224.0
Manning's n	Lower	4.6	15.4	0.74	3.35	6.22	176.1
	Higher	4.4	18.2	0.46	4.14	9.56	223.7
Initial Loss Coeff.'s	Lower	4.5	14.3	0.89	3.18	5.06	154.2
	Higher	4.4	18.4	0.19	4.18	23.2	211.5
Rain Dist. Factors	Lower	4.6	14.2	0.91	3.09	5.05	151.9
	Higher	4.4	18.6	0.28	4.23	15.7	214.9

The statistics for the simulated monthly phosphorus loads partly reflect the differences in the simulated flow regimes, but are also affected by other factors. The higher levels of input onto the direct impervious areas of Botshabelo (55 tonnes y^{-1}), relative to Mdantsane (16 tonnes y^{-1}), combined with the higher runoff 'power' from such areas, contribute to relatively higher median and mean monthly loads from Botshabelo. This influence is also affected by the greater seasonality in the runoff and consequent nutrient wash-off in Botshabelo. This factor will contribute to higher levels of storage at the start of the rain season (and higher potential loads), as well as more frequent depletion of storage during the rain season.

Over the range of parameters used in the sensitivity analysis, the shape parameters (lambda values for pervious and impervious areas) of the relationships between runoff and the proportion of storage washed off seem to be the most sensitive and Manning's n least sensitive. The general pattern for all the parameters is that the higher values cause a decrease in the wash-off load at relatively low flows which leads to better sustained storage levels. This serves to increase the potential for high loads to be generated when the runoff is 'powerfull' enough to cause a very high depletion of storage.

Table 6.4 Sensitivity analysis results - Monthly phosphorus storage levels (tonnes km^{-2}). Botshabelo annual input is 9.3 tonnes km^{-2}, while Mdantsane is 3.2 tonnes km^{2}.

		Mean	St. Dev.	Median	Coeff. Var.	Mn/Med. Ratio	Max.
Botshabelo							
Standard Values		9.9	5.2	9.3	0.52	1.06	25.3
Nutrient Lambda parameters	Lower	4.7	2.3	4.6	0.49	1.02	13.9
	Higher	15.4	8.0	14.7	0.52	1.05	39.0
Manning's n	Lower	7.4	3.8	7.3	0.51	1.01	20.3
	Higher	13.3	7.1	12.8	0.53	1.04	33.7
Initial Loss Coeff.	Lower	9.0	4.3	8.8	0.48	1.02	21.1
	Higher	10.9	6.1	9.9	0.56	1.10	28.3
Rain Dist. Factor	Lower	8.4	4.3	8.2	0.51	1.02	21.9
	Higher	13.2	7.5	12.1	0.57	1.09	35.0
Mdantsane							
Standard Values		4.0	2.3	3.8	0.58	1.05	10.7
Nutrient Lambda parameters	Lower	2.2	1.4	1.9	0.64	1.16	5.4
	Higher	5.8	3.1	5.7	0.53	1.02	12.9
Manning's n	Lower	3.4	2.2	3.0	0.65	1.13	10.1
	Higher	5.3	3.0	5.0	0.57	1.06	13.1
Initial Loss Coeff.	Lower	3.4	1.9	3.3	0.56	1.03	9.1
	Higher	4.5	2.8	4.2	0.62	1.07	12.3
Rain Dist. Factor	Lower	3.2	1.9	2.9	0.59	1.10	8.7
	Higher	4.8	2.8	4.5	0.58	1.07	12.4

Some of the differences in the phosphorus storage regimes between the two areas, as well as the effects of changing the parameter values, have already been referred to. It would appear that, despite the build up of storage over the winter dry season, the levels of storage reached in Botshabelo are lower, relative to the annual input, than in Mdantsane. For Botshabelo the median monthly storage level is equal to the annual input, while the maximum build up is about 2.7 times this value. The equivalent figures for Mdantsane are 1.2 (median) and 3.3 (maximum).

These figures raise the question about the fate of nutrients stored on the surface for a relatively long period of time, particularly when this storage is occurring on vegetated pervious areas. The model has no functions which allow the build up of available phosphorus to be reduced in situ. While this may be an important process in the pervious areas, there seems to be little specific information in the literature about the processes involved and the extent of in-situ reduction of available phosphorus.

A.

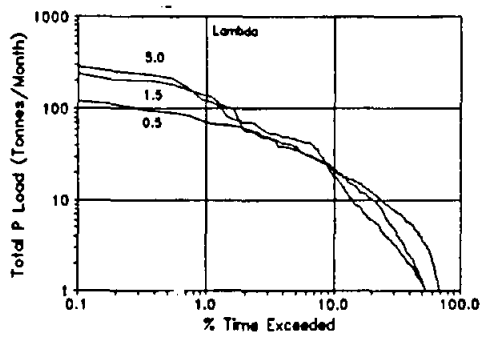

B.

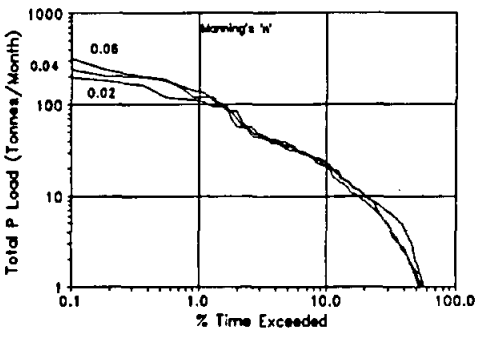

C.

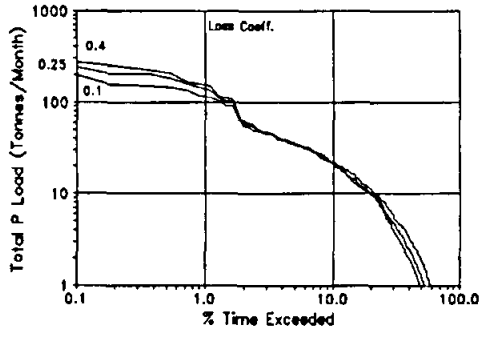

D.

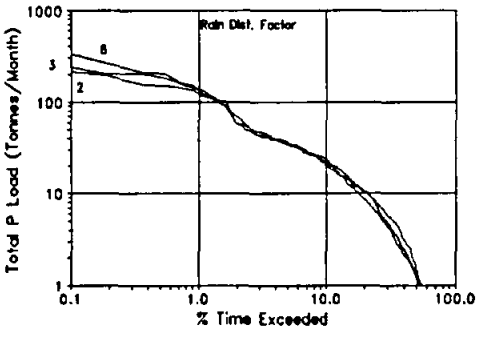

Figure 6.1 Botshabelo - Phosphorus load. Monthly duration curves for the different parameter sets.

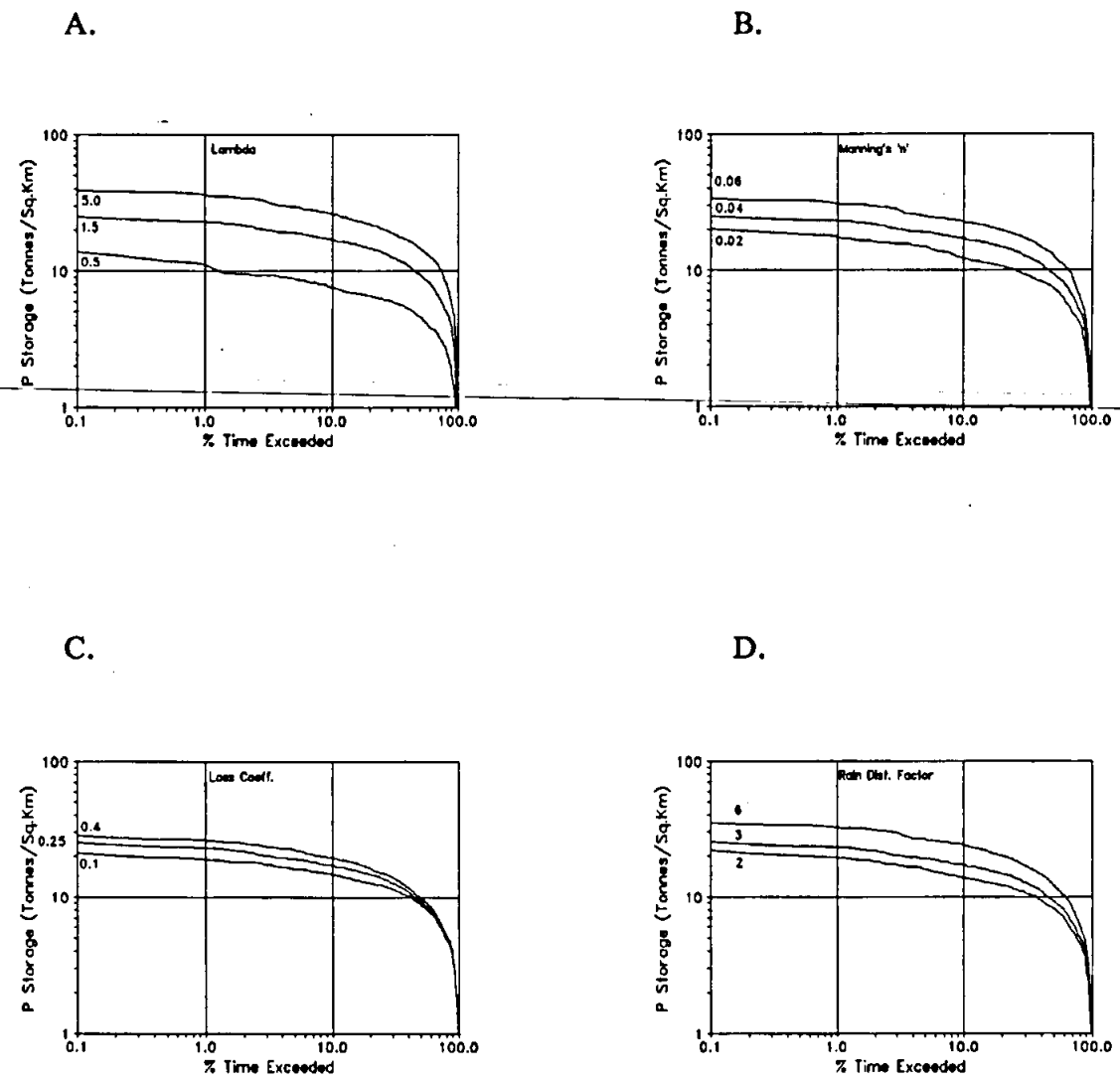

Figure 6.2 Botshabelo - Phosphorus storage levels. Monthly duration curves for the different parameter sets.

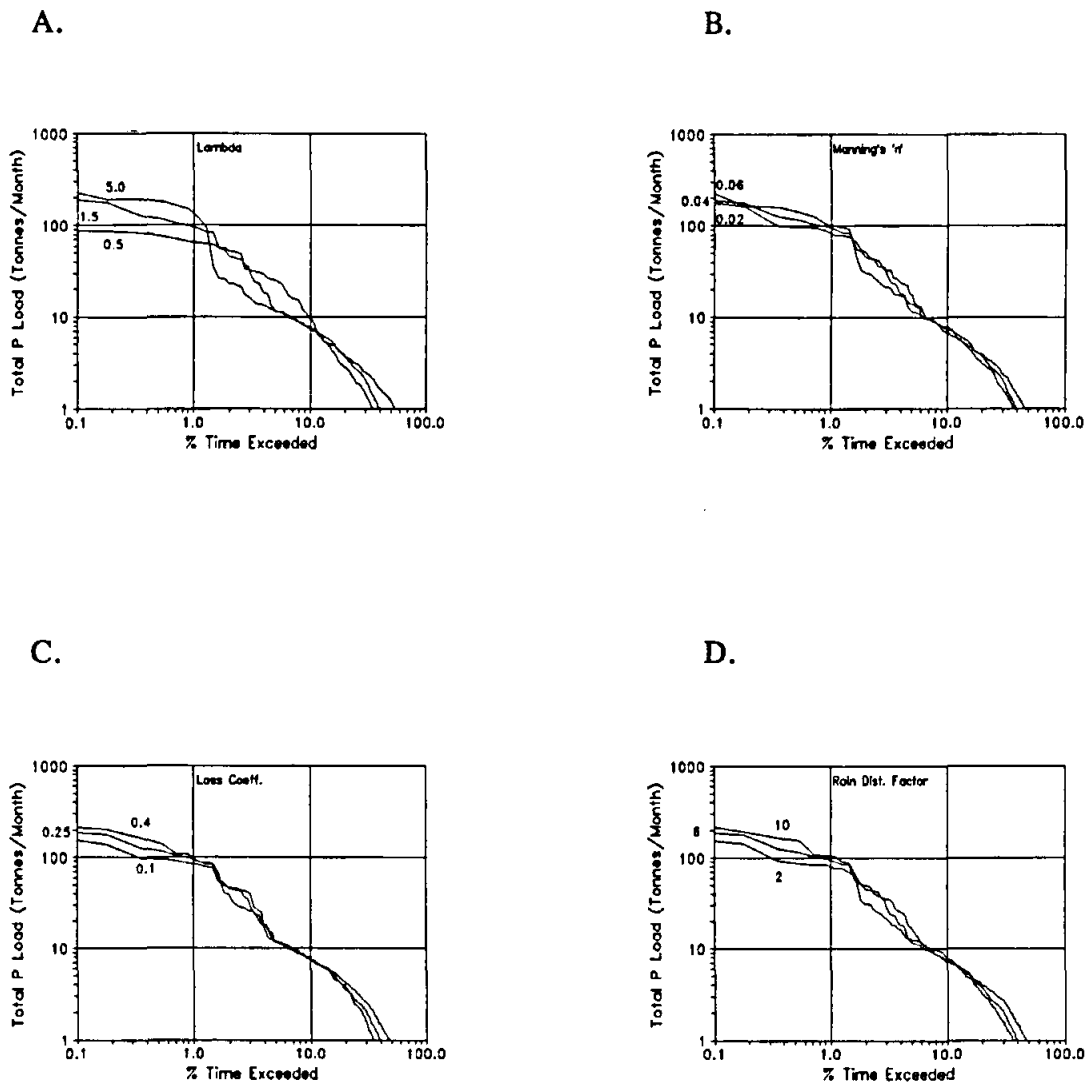

Figure 6.3 Mdantsane - Phosphorus load. Monthly duration curves for the different parameter sets.

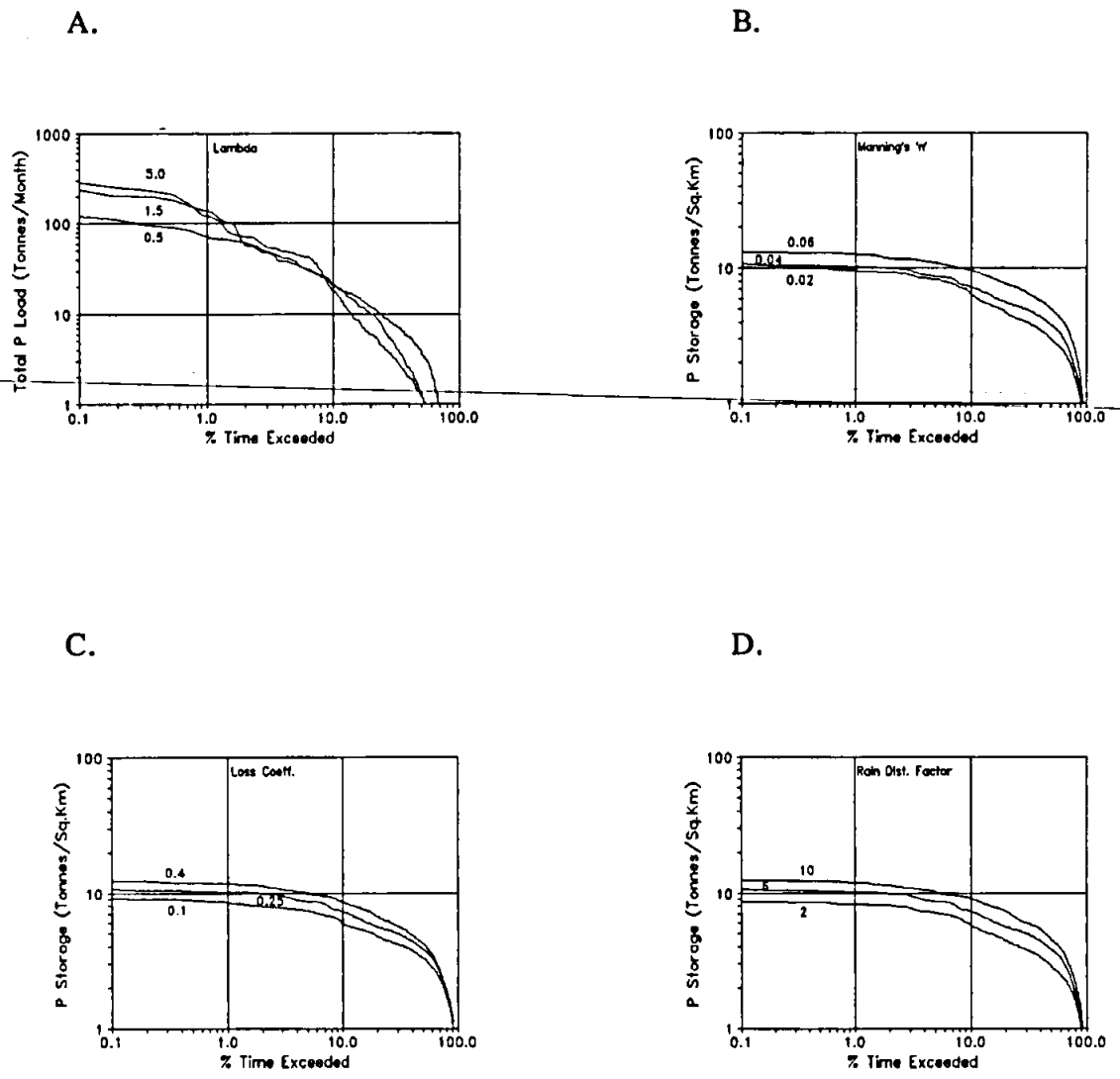

Figure 6.4 Mdantsane - Phosphorus storage levels. Monthly duration curves for the different parameter sets.

6.3 APPLICABILITY OF THE PEXP MODEL

The application of the model to the two areas has done more to highlight the lack of understanding of the processes involved than to provide an adequate test of the simulation approach. However, the authors believe that, in combination with the application of the socio-economic survey approach of Grobler, et al. (1987), it should be capable of providing a fairly quick and approximate impression of the range and time distribution of loads that might be expected from developing urban areas. These may then be compared with the pattern of other sources of nutrients and used for the purposes of planning and management.

A number of limitations of the model were identified in an earlier section of this report and the examples of the model's application have not revealed any further problems. Satisfactory testing of the model and its applicability will necessarily have to await observations of at least some time series of loads and runoff and preferably an improved understanding of the processes. A project is currently being undertaken by the IWR at Rhodes University to monitor stormwater discharge and associated nutrient loads from both the developed and developing urban areas of Grahamstown. The monitoring system has only recently been established and the records are currently too short to be of use to assess the validity of the PEXP model. In addition, no attempt has yet been made to carry out the socio-economic survey necessary to determine the input phosphorus budget. Sufficient information may be available by early 1994 to begin to use the Grahamstown situation as a test of the model.

While the model was developed specifically for estimating phosphorus washoff, it is possible that the same, or similar, approach could be applicable to other nutrients or microbiological pollutants. Attempting to apply the model to other pollutants being washed off urban areas will suffer from the same limitations related to the understanding (or lack of) of the processes involved. However, the model may represent an acceptable starting point for future developments, once a better understanding is available.

7. MODEL APPLICATION EXAMPLES (The Multiple Reservoir Model)

7.1 INTRODUCTION

The few examples of the application of the reservoir simulation model provided in this section are designed to illustrate the way in which the parameters can be set-up to define real situations in a simplified way, as well as illustrating the general availability of the information required. The first example includes a comparison with observed data, but it should be emphasised that the results of the reservoir simulation model cannot be considered independent of the method used to quantify the inputs to the reservoir. There may be observed information on these inflows which can be used to assess the validity of the model used to simulate them. More commonly, there will be no detailed information available and comparisons with such as regional estimates of mean annual runoff and seasonal distribution will have to suffice.

The second example is used to illustrate the way in which the model may be used in a study of a relatively large system with a number of linked components. The final example further illustrates some of the ways in which linkages between two or more reservoirs may be specified and also includes an example of the simple economic analysis associated with analysing the simulation results.

7.2 GRAHAMSTOWN WATER SUPPLY SYSTEM

The first example application is a simulation of seven years (1985 to 1991) of the dynamics of the two main reservoirs constituting Grahamstown's water supply (Hughes, 1992). Settlers Dam is located at the outlet of a 176 km^2 catchment which includes the Howison's Poort Dam catchment as part of it. Howison's Poort Dam is built at the outlet of a 42 km^2 steeply sloping sub-catchment of the total area. Within the other part of the catchment are two major private dams with a total capacity of some 1 000 Ml. Time series of inflow volumes to Howison's Poort and Settlers have been simulated using two separate runs of Pitman's model resulting in mean annual flow volumes of 1 930 and 5 150 Ml, respectively. Observed dam volumes (Figs. 7.1 and 7.2) are available for most of the months during the period selected which contains a number of sequences of dry periods, during which water restrictions were implemented in Grahamstown, interspersed with occasional months of high flow.

The main parameters of the reservoir model for the two dams in the system are listed in Table 7.1, while reference can be made to table 4.3 for more details of the complete parameter set for this model. The capacities and area-volume relationships have been obtained from the City Engineer's Department of Grahamstown Municipality, as has the information required to establish the other parameter values. The water required for Grahamstown is pumped from Howison's Poort Dam, which in turn receives water pumped from Settlers Dam. The available records indicate that the normal monthly water consumption is approximately 177 Ml with little systematic difference between individual

months of the year. Restrictions are commonly enforced when the total volume stored in the two dams is below 40% of capacity. Parameter 11 has therefore been set at 140% (i.e. 40% of the combined storage in Settlers and Howison's Poort Dams). Reserve drafts of 85% of normal draft are used when the total storage falls below 40% of the combined capacity.

The annual direct draft (excluding water pumped to Howison's Poort Dam as regulated releases) of Settlers Dam (parameter 8) is made up of 220 Ml a^{-1} pumped out of the dam by local farmers and an obligation to release water four times a year to downstream riparian users (approximately 680 Ml a^{-1}). This obligation falls away when it is necessary to place restrictions on Grahamstown users. The reserve draft is therefore set at 220 Ml a^{-1} and is applicable when Settlers Dam is below 40% of capacity (parameter 11). This reserve level has no effect on the amount of water transferred to Howison's Poort Dam.

The inflow capacity to Howison's Poort Dam (143 Ml) has been calculated from information about the capacity of the pump used and the length of time over which the pump normally operates. A spill time distribution factor is not relevant for either dam as Howison's Poort Dam only receives controlled releases from Settlers Dam which in turn has a direct channel connection to Howison's Poort Dam and can accept all spillages.

Table 7.1 Parameters for the simulation of Grahamstown's water supply reservoirs.

Parameter		Dam 1 Howisons	Dam 2 Settlers
No.	Description		
1	Capacity (Ml).	848	5 300
5	Scale parameter in area-vol. relationship.	0,17	0,17
6	Power parameter in area-vol. relationship.	0,7	0,7
8	Annual draft (Ml).	2 121	900
11	Reserve level 1 (% capacity).	140	40
16	Inflow capacity (Ml).	143	N/A
17	Max. release (% storage).	N/A	80
18	Limit for no release input (% capacity)	95	N/A
19	Spill time distribution factor.	N/A	N/A
20	Compensation releases ($Ml.month^{-1}$	0	0
21	Downstream dam.	2	1
22	Canal take-off priority (%).	0	100

Given the fact that the simulated inflow time series cannot be checked for accuracy due to the lack of observed data, Figs. 7.1 and 7.2 indicate that the reservoir system performance has been reasonably successfully simulated. The model has generally under-estimated the total amount of water available in the dams and while this may be largely related to under-estimation of the inflow, it is also possible that the Municipal records of water consumption are over estimations. Without further detailed investigation of the available data, it would

be difficult to draw any firmer conclusions.

An extension of the application utilised the same parameter values for both the reservoir model and the Pitman model, but applied with a rainfall time series of some 100 years. The intention was to examine to what extent the demand indicated in table 7.1 could be sustained in the long term and what the pattern of shortfalls would be. This study also investigated changing the number and level of reserve drafts to investigate whether different operating rules could be used to increase the reliability of the supply. The conclusions were in close agreement with the original consulting engineers design that suggested that the storage capacity would be adequate to survive a 1:50 year drought (unspecified duration). The simulation indicated that two failures (inadequate supply even to meet the reserve demand) of supply would occur during a 100 year period.

Introducing water restrictions at a level of 50% and introducing a lower reserve at 20% of capacity, did not affect the number of failures, but did decrease the duration and severity of the failures. It also increased, quite considerably, the number of occasions when water restrictions were necessary.

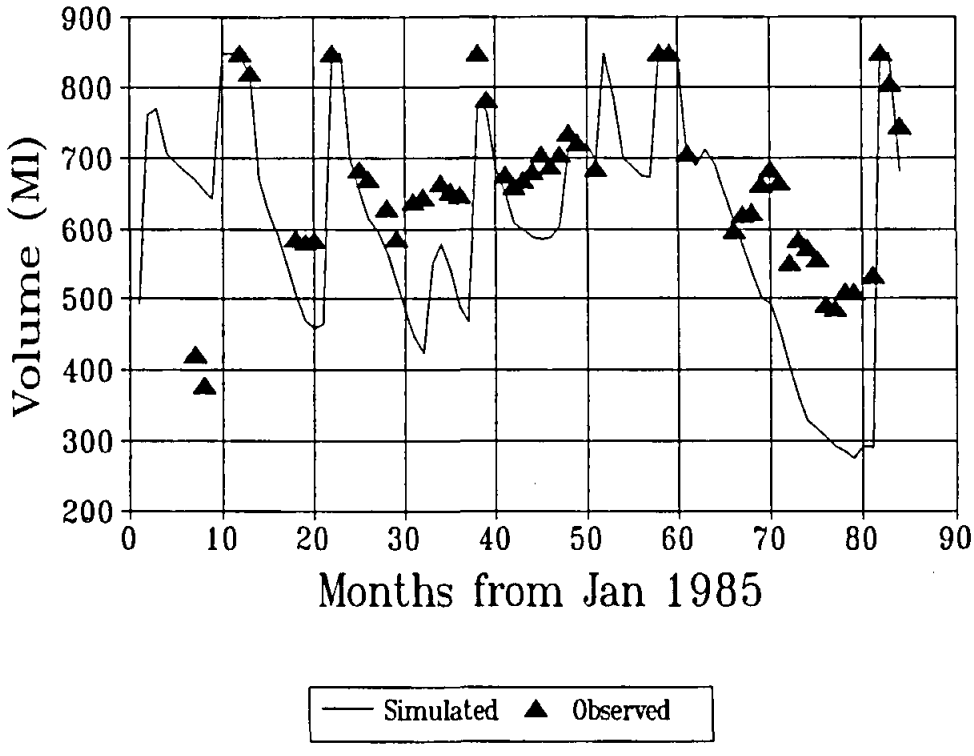

Figure 7.1 Simulated and observed volumes for Howison's Poort Dam.

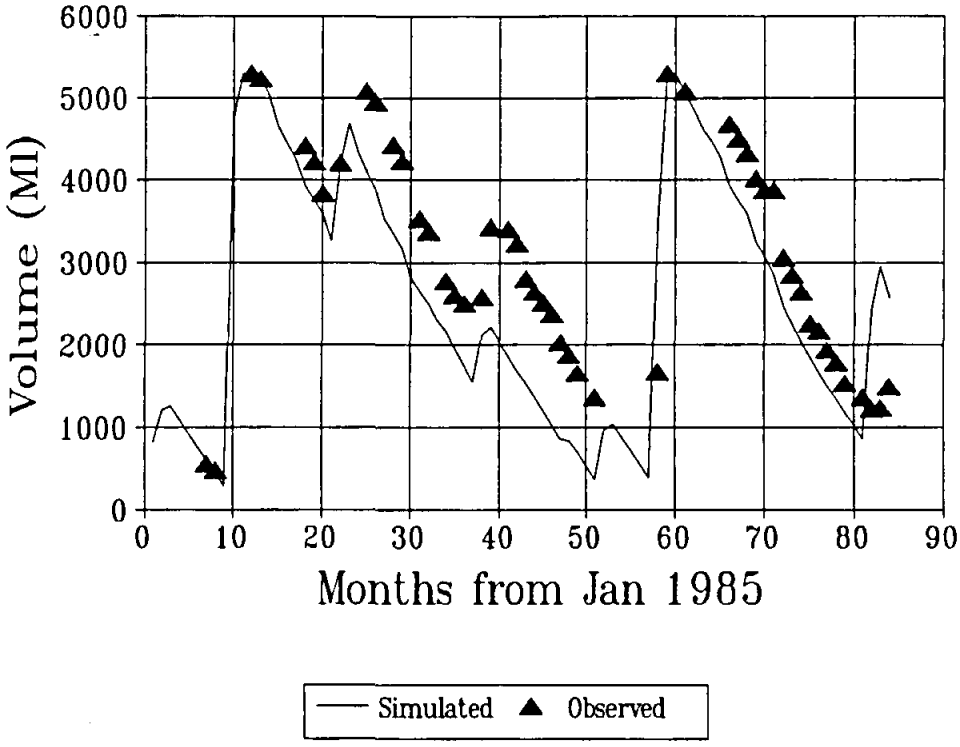

Figure 7.2 Simulated and observed volumes for Settlers Dam.

7.3 THE BUFFALO RIVER CATCHMENT

The main objective of this study was to calibrate one or more monthly time step hydrological models on the available data for the Buffalo River catchment, inland of East London in the eastern Cape Province, so that relatively long time series of streamflow could be simulated for all parts of the total catchment area. This information was then to provide support for an investigation of the water quality situation of the catchment (van Ginkel, et al., 1993).

The total catchment area (down to gauging station R2H002) is 1204 km^2 and there are 8 gauged sub-catchments upstream, varying in size from 15 km^2 to 668 km^2. The record lengths of the streamflow data and of the nearly 30 raingauges in the region are highly variable. There are also four water supply reservoirs within the system; two in the upper reaches (Maden Dam - 31 km^2 and Rooikrantz Dam - 51 km^2) and two lower down on the main Buffalo River (Laing Dam - 913 km^2 and Bridle Drift Dam - 1180 km^2). There are some records of storage, inflow, abstraction and release volumes for Rooikrantz, Laing and Bridle Drift Dams that could be used to assist in the assessment of the hydrological simulations of the total catchment. However, some of the components of the 'observed' water balance of the reservoirs are estimated from real observations of others and can not be considered totally reliable. A further problem existed, in that the best period available

for calibrating the catchment model (10 years from 1964 to 1973) corresponded with a period when abstractions from Laing and Bridle Drift Dam were undergoing a great deal of change. Two of the dam walls were also raised during this period and the records indicate that the capacity was also changing due to sedimentation. Other components of the system that had to be allowed for included the return flows of effluent discharged into the system below the main points of water usage (King William's Town, Zwelitsha and Mdantsane).

The final simulations, designed to provide information on the statistics of the existing situation, involved generating a 46 year record of streamflow data for all points within the system.

The approach used was to divide the total catchment area into 38 relatively homogeneous sub-catchments based on the available information about soils, land use and climate characteristics, as well as the location of streamflow gauging points and of the major abstraction or wastewater return flow points. The simulation exercise involved the progressive calibration of Pitman's monthly rainfall-runoff model, starting in the upstream areas and gradually working downstream to the outlet at R2H002. The reservoir model was used to simulate the historical conditions in the four major reservoirs. This exercise involved 12 separate implementations of the Pitman model (each with between 2 and 6 internal sub-areas defined) and four of the reservoir simulation model, where the output from some implementations formed the input to others. The HYMAS batch processing procedures were used extensively to carry this out. These procedures involved initially setting up the 16 model implementations as separate projects and then linking them all so that they could be run together in a single operation. If the parameter values for one of the upstream catchments were refined it was only necessary to run the batch file (not all the separate projects downstream) to update the simulation results for the whole catchment.

With respect to the reservoir simulation model, the dynamic nature of the abstractions and the reservoir capacities, meant that the HYMAS parameter 'time slicing' facilities had to be used. However, it was not found to be easy to define the changes in abstraction volumes as the observed data indicated that they followed a fairly random pattern over some parts of the simulation period. Although the model has a parameter to define the annual decrease in reservoir volume due to sedimentation, it was found that this process was better reproduced by 'time slicing' the dead storage parameter. An alternative would be to 'time slice' the storage capacity itself.

Despite the limitations of the simulation exercise, the overall results were satisfactory, in that the general pattern of stored volume fluctuations were reasonably well simulated and in particular, the number and length of periods of overflow were accurately reproduced. The latter feature of the simulations were particularly important because of the effects on the flow regimes below the reservoirs and the implications with respect to water quality variations.

7.4 OTHER APPLICATIONS

The reservoir model has been used in conjunction with the Pitman model on many occasions to assist with the design of single small to medium sized dams. Most of these applications have been simple and straightforward and have not really required the multiple dam

capabilities of the model. One example where these capabilities were required was in the assessment of the impact of constructing a balancing dam directly on the stream channel of a catchment supplying 700 ha of irrigated orchards in the Langkloof area of the Southern Cape. The existing situation consisted of several small dams, each supplied from canals fed from weirs built across the river channel. For the purposes of simplicity, all the existing dams and supply systems were combined as a single representative dam of 1 500 Ml (Dam 2 in table 7.2).

The area above the scheme is a 9 km^2 mountain catchment with a mean annual rainfall of about 1000 mm and a relatively high runoff potential. A 55-year time series of monthly streamflows was simulated using the version of the Pitman (1973) model contained within HYMAS and the resulting mean annual runoff volume estimated to be 3 310 Ml. A neighbouring gauged catchment indicates that this figure is acceptable and suggests that the monthly runoff regime is likely to be characterised by relatively frequent short duration storm events superimposed on a generally continuous baseflow. The spill time distribution factor for the streamflow reaching the canal off-take points was set at 12.5 (table 7.2) to account for the assumed flow regime. After the construction of the upstream balancing dam the flow regime of the spillage was assumed to be somewhat attenuated and the spill time distribution factor increased to 17.5. The inflow capacity of the canals serving the irrigation dams were calculated assuming a combined flow capacity of 1 $m^3 \cdot s^{-1}$ operated for an average of 10h a day.

The parameters of the reservoir model are given in table 7.2 for the undeveloped Dam 1 (no dam) and developed situation, as well as for Dam 2 (combination of all the irrigation dams). Some of the unused parameters have been omitted. The economic parameters (27 to 32) have been set at reasonably sensible, but somewhat arbitrary values and are used mainly to illustrate their use.

The initial simulation, given no balancing dam, indicates that of the 3 300 Ml mean annual river flow, 2 000 Ml is drawn off into the irrigation dams. This produces a usable draft of 1 870 Ml out of the total required draft of 3 070 Ml. The economic parameters suggest a mean annual profit of R1.86m. The effect of the balancing dam is to increase the inflow to the irrigation dams to 2 600 Ml and the usable draft to 2 400 Ml. The mean annual profit (after allowance for capital repayments) increases to R2.11m.

Closer examination of the time series of drafts indicates that the critical period appears to be the first four months of the year. In the undeveloped situation, a draft of equal to or better than 90% of that required is only met during 35% of these months over the 55-year period. After the balancing dam is included, the simulation suggests that this figure will increase to 58%.

This example could be extended to assess the effects of different size balancing dams, as well as the additional area of irrigation that could be economically supported if more realistic economic parameter values are used. It would also be possible to break the system down further and to model some of the irrigation dams separately. Although many of the parameters have only been roughly quantified in the example, it does serve to illustrate one of the type of problems that can be analysed by the model. In a situation such as this, where no observed data are available to calibrate the model, an experienced irrigation engineer

should be capable of assessing and interpreting the results to assist in the final decision-making process.

Table 7.2 Parameters for the effect of a balancing dam on an irrigation scheme.

Parameter		Dam 1 (no dam)	Dam 1 (Built)	Dam 2
No.	Description			
1	Capacity (Ml).	N/A	1 000	1 500
5	Scale parameter in area-vol. relationship.	N/A	0.3	0.5
6	Power parameter in area-vol. relationship.	N/A	0.8	0.62
8	Irrigation area (ha).	N/A	N/A	700
9	Effective rain (%).	N/A	N/A	50
16	Inflow capacity (Ml).	N/A	N/A	1080
17	Max. release (% storage).	N/A	100	N/A
18	Limit for no release input (% capacity)	N/A	N/A	100
19	Spill time distribution factor.	12.5	17.5	12.5/17.5
20	Compensation releases ($Ml.month^{-1}$)	0	0	0
21	Downstream dam.	2	2	N/A
22	Canal take-off priority (%).	100	100	N/A
27	Capital cost of dam ($R.m^{-3}$)	N/A	2.5	N/A
28	Capital cost of supply works ($R.ha^{-1}$)	N/A	N/A	N/A
29	Repayment interest rate (%)	N/A	18	N/A
30	Repayment period (years)	N/A	20	N/A
31	Profit for successful supply ($R.ha^{-1}$)	N/A	N/A	5
32	Supply failure penalty ($R.ha^{-1}$)	N/A	N/A	2

7.5 APPLICABILITY OF THE MODEL AND ITS LIMITATIONS

The example applications illustrate the possible uses of the multiple reservoir simulation model. When the model is applied to a single reservoir system, the reliability of the time series of inflow volume is probably of more significance to the results than the way in which the internal water balance of the reservoir is simulated. In all the examples given above, the inflows have been simulated using a monthly time-step rainfall runoff model, which will be prone to some inaccuracies.

When the multiple reservoir capabilities of the model are used, there are some additional water balance processes that have to be quantified. These are represented in the model in a relatively simplified way. Any further detail would be generally incompatible with the relatively coarse time step of the model, as well as with the amount of information available for most applications.

The model does appear to be able to take account of a variety of different reservoir configurations. However, one type of configuration that it is not easily able to account for is where the operating rules of two or more dams, related to satisfying a single demand, are independently related to the storage levels in the individual dams. For example, a percentage of the demand may be satisfied from one dam, while it is above a certain level, but be drawn from one of the other dams at other times. The model is currently not able to simulate this type of relatively complex operating rule.

The dams are also not permitted to exceed their storage capacities; if they do the amount they exceed it by will become spillage volume. While it is well known that many dams do exceed this level during large floods (due to the head of flow over the spillway), in a monthly model the issue may not be critical as the dam will not remain at that level for very long. If any consideration was to be given to converting the model to operate with daily time steps, this issue would have to be addressed.

Several limitations were identified in the earlier section covering the model description. The examples used above to illustrate the application of the model have not revealed any further limitations.

8. CONCLUSIONS AND RECOMMENDATIONS

The separate chapters of this report contain concluding or summary sections and it is therefore unnecessary to repeat such comments in this final chapter. However, reference to the original aims and objectives of the project and the perception of the research team as to the extent to which these have been achieved are included. This chapter also includes some recommendations for further work and suggests some technology transfer actions that could be carried out.

8.1 Achievement of the project aims and objectives.

It is inevitable that, for a project designed some 6 years previous to the appearance of the final report, the objectives will have undergone a certain degree of revision. If this were not the case, it might be concluded that the project had been carried out ignoring other developments that were taking place over the duration. In the case of this project, there have been some modifications, but the basic aim of contributing to an improvement in the applicability of hydrological models has been maintained throughout. The modifications that have occured have been in response to the project teams perceptions of the changing needs of the hydrological and water resources management community within southern Africa.

The first primary objective of the project was :

- To quantify the physical characteristics (relief, soil, landuse, etc.) of the Bedford catchments so that they can be established as long term research areas in a semi-arid environment.

The volume of the final report (Hughes and Sami, 1993) that deals with the characteristics of the Bedford catchments, as well as parts of this volume, which discuss some aspects of the hydrological processes operative in the area, indicate that this primary objective has been achieved. There is now available a reasonable database on the physical and climatological characteristics of the Bedford catchments that provides a basis for any future work in the region. Inevitably, some of the characteristics have been covered in more detail than others, but there is at least some information available on all those relating to the hydrology of this area. It is unfortunate that the water level recording instrumentation did not operate satisfactorily during most of the project and that the streamflow database is less than complete.

The second primary objective was :

- To improve the general applicability of hydrological models through the development of a flexible approach to their basic structure.

This objective is addressed in both this volume of the final report, as well as the User Manual for the HYMAS package. The objective was originally stated in very general terms and the project team has interpreted it to mean that some model developments would be carried out and that several models would be incorporated into a generalised model

application system. Both of these objectives have been achieved, in that several new models have been developed and that a model application package has been created. The HYMAS package has evolved, during the project, into an integrated modelling environment that allows many of the essential pre- and post-modelling procedures to be carried out in a common way for a range of different models. The models that have been currently incorporated into the system include several new ones developed by the project team, as well as others which are either well established (Pitman model), or offer some unique capabilities not covered by the others (RAFLES). HYMAS is designed to make the application of models easier, as well as facilitating the establishment of new models.

The third primary objective was :

- To improve the soil moisture budgeting component of hydrological models by concentrating on monitoring and modelling vertical and lateral moisture fluxes at or near the base of the root zone.

This objective has also undergone some modification and the research work has concentrated on developing an alternative approach to simulating soil moisture dynamics in a practical, semi-distributed model, as well as incorporating surface-groundwater interactions. This work is mainly discussed within the sections of this report that deal with semi-arid hydrological processes and the development of the VTI model. The model incorporates the use of frequency distributions to account for some hydrological processes occurring at scales of less than the elements of the distribution system. A number of application examples of this model are discussed within this report and several issues relating to the usefulness of the model and further modifications that are required are discussed. Together with the development of the model itself, some work has been carried out on the approaches used to estimate the parameter values of the model. This aspect of the application of models has been viewed as being of great importance by the project team and really forms part of the second objective. While some progress has been made during the project, there still remains a high degree of uncertainty about the best approaches to adopt.

While most of the project teams resources have been directed towards development work, the applied nature of the developed project has not been ignored. The HYMAS system and several of the models have been used successfuly during the course of the project to address real water resource problems. While of benefit to the individuals and groups who were responsible for solving the problems, these applications of the research results were also of great benefit to the research team in terms of creating a practical context within which to work, as well as bringing some new problems to their attention.

8.2 Recommendations for further work.

With respect to the Bedford catchments, it is recommended that the baseline monitoring of rainfall, runoff, soil moisture and some climate variables continues indefinitely. To collect a satisfactorily representative hydrological record for a semi-arid area is a long term proposition that involves a substantial effort. There are few detailed observations of semi-arid hydrology within South Africa and yet this is the predominant climate of the country. However, it is also recognised that collecting such information is an expensive business.

It is the intention of the Institute for Water Research to continue with further enhancements to the HYMAS system. A current WRC project being carried out by the IWR is designed to investigate various aspects of the low flow hydrology of South African rivers. As part of this project, a number of methods of characterising low flows are being investigated. As appropriate indices are identified, procedures to estimate them are being incorporated into HYMAS so that they may be calculated for observed and simulated flow sequences.

Some initial work has already been carried out on the use of GIS and DTM's for the semi-automated delineation of catchment boundaries and the estimation of physical catchment characteristics. While the results are promising, there are still some doubts about the general availability of the required input information or the cost effectiveness of this approach. It is recommended that parallel developments should be carried out in the use of this type of approach and in the methods used to estimate model parameter values from physical catchment data. The ultimate aim of such work would be to make parameter estimation procedures more efficient and reliable.

This report has identified some deficiencies in more than one of the models contained within HYMAS which can be corrected without a great deal of additional research. Specifically, the VTI model appears to require an addition to the soil moisture accounting procedures to allow for capillary rise to take place between the lower and upper soil zones. It would also be useful to re-evaluate the channel transmission loss routines and attempt to develop an approach which is less reliant on the quantification of several highly empirical parameters. The WRC project dealing with low flow hydrology is designed to investigate the importance of such processes within South African river systems and any results from this work will be incorporated into refinements of the VTI model. The report also highlights the problem of the distribution of daily rainfalls for intensity excess runoff generation estimation. The current method in the VTI model does not appear to generate sufficiently high intensities for some semi-arid storms, leaving too much water to enter the soil and contribute to baseflow and groundwater recharge. There is very little rainfall information available in South Africa at a resolution of better than 1 day and if the VTI model is to be of widespread use, this component should therefore receive some attention. Additional applications of the VTI model may reveal other areas where some of the components require revision and improvement.

The phosphate export model was developed in the absence of a suitable alternative to investigate the ever increasing problem of nutrient loads derived from developing urban areas within South Africa. The development of the model was not one of the objectives of the project, but was motivated by the requirements of another project being carried out at Rhodes (van Ginkel, et al., 1993). This model is still very much in the development phase and will remain so until it can be tested against some observed information about the processes involved or time series of runoff and nutrient load data. A project initiated in Grahamstown during 1992 is likely to generate some useful information that can be used to carry out further assessments of the value of this model. Data from other projects of a similar type, but being carried out in different climate regions of the country, would also be extremely valuable.

In summary, it is recommended that any future work concentrate on enhancing the usefulness of the HYMAS package, by strengthening some of the pre- and post-modelling routines and

by improving the applicability of the models contained within it.

8.3 Technology transfer actions.

With respect to the Bedford catchment database, it is suggested that the availability of the information and the report be made known to those groups or individuals that may have a potential use for it. The Institute for Water Research will be able to service any requests for information that may arise.

Earlier versions of the HYMAS system have been demonstrated to some groups already. However, if the system is to be made generally available it will be necessary for the project team to organise training and familiarisation workshops for future potential users. These would also allow the project team to obtain additional feedback on the system and the user manual and allow future changes and developments to reflect the needs of the users. Any other groups or individuals within South Africa who would like to suggest additional models for inclusion in HYMAS could be invited to contact the project team. The IWR can then advise or assist them in making the necessary modifications. It is important that, if it is to become a useful tool for hydrological and water resource estimation, HYMAS undergoes continual development and review. While the IWR staff will continue with some of these developments for their own purpoese, the system will be further strengthened and enhanced through inputs from others.

Towards the end of the project, several groups have expressed an interest in using HYMAS, or some of the models contained within it. The system will be available for distribution towards the end of 1993, as soon as some of the already identified 'bugs' have been corrected. It is anticipated that a series of training sessions and workshops on the system will be organised during the early part of 1994 according to the demand from potential users.

A new project, involving the analysis and modelling of catchments from throughout southern Africa, is expected to start at the beginning of 1994. HYMAS will be used in this project and will probably be interfaced with the HYDATA software, available from the Institute of Hydrology, UK. The latter is a hydrological data storage and analysis system which allows a number of standard time series analyses to be performed and incorporates a hydrological database system. While there may be some duplication in the analyses that the two software packages can perform, HYDATA is meant for observed data and is not a modelling package like HYMAS.

9. REFERENCES

Adar, E.M., Neumann, S.P. & Woolhiser, D.A. (1988) Estimamation of spatial recharge distribution using environmental isotopes and hydrogeochemical data, 1. mathematical model and application to synthetic data. **J. Hydrol.**, 97, 251-277.

Allison, G.B. (1987) A review of some of the pysical, chemical and isotopic techniques available for estimating recharge. In: Simmers (ed.), **Estimation of Natural Groundwater Recharge**, NATO ASI ser. C, Vol. 122. Reidel, Dordrecht, 49-71.

Allison, G.B., Barnes, C.J., Hughes, M.W. & Leaney, F.W.J. (1984). Effect of climate on oxygen-18 and deuterium profiles in soils. **Isotope Hydrology 1983**. IAEA, Vienna, 105-123.

Allison, G.B., Stone, W.J. & Hughes, M.W. (1985). Recharge in karst and dune elements of a semi-arid landscape as indicated by natural isotopes and chloride. **J. Hydrol.**, 76, 1-25.

Arnold, J.G., Allen, P.M. & Bernhardt, G. (1993) A comprehensive surface-groundwater flow model. **J. Hydrol.**, 142, 47-69

Bauer, S.W. & Midgley, DC (1974) **A simple procedure for synthesizing direct runoff hydrographs.** Report No. 1/74. Hydrological Research Unit, Univ. of the Witwatersrand, Johannesburg.

Barnes, C.J. & Allison, G.B. (1988) Tracing water movement in the unsaturated zone using stable isotopes of hyrogen and oxygen. **J. Hydrol.**, 100, 143-176.

Beven, K.J. (1989) Changing ideas in hydrology - The case of physically-based models. **J. Hydrol.**, 105, 157-172.

Bouwer, H. (1969) Infiltration of water into nonuniform soil. **Proc. ASCE, J. Irrig. and Drainage Div.**, 95(IR4), 451-462.

Brinkmann, R., Eichler, R. Ehalt, D. & Munnich, K.O. (1963) Uber den Deuterium gehalt von Niederschlags und Grundwasser. **Naturwissenschaften**, 50, 611-612.

Chandrasekharan, H., Navada, S.V. & Jain, S.K. (1988). Studies on natural recharge to the groundwater by isotope techniques in arid western Rajasthan, India. In: Simmers (ed.), **Estimation of Natural Groundwater Recharge**, NATO ASI ser. C, Vol. 122. Reidel, Dordrecht, 205-220.

Cornish, J.H. (1961) Flow losses in dry sandy channels. **J. Geophys. Res.**, 66(6), 1845-1853.

Craig, H. (1961) Standard for reporting concentrations of deuterium and oxygen-18 in natural waters. **Science**, 133, 11702-1703.

Crerar, S., Fry, R.G., Slater, P.M., van Langenhove, G. & Wheeler, D. (1988) An unexpected factor affecting recharge from ephemeral river flows in SW/Namibia. In: I.Simmers (ed), **Estimation of Natural Groundwater Recharge**, Reidol, 11-28.

Dansgaard, W. (1964) Stable isotopes in precipitation. **Tellus**, 16, 436-468.

Depraetere, C. (1992) **DEMIURGE 2.0, Preparation and Processing of Digital Elevation Models (DEM) chain of production and of treatment of ground digital models.** ORSTOM editions, French Institute of Research for Development in Cooperation.

Dettinger, M.D. (1989) Reconnaissance estimates of natural recharge to desert basins in Nevada, U.S.A., by using chloride-balance calculations. **J. Hydrol.**, 106, 55-78.

Dincer, T., Al-Mugrin, A. & Zimmermann, U. (1974) Study of the infiltration and recharge through sand dunes in arid zones with special reference to stable isotopes and thermonuclear tritium. **J. Hydrol.**, 23, 79-109.

Drever, J.I. & Smith, C.L. (1978) Cyclic wetting and drying of the soil zone as an influence on the chemistry of ground water in arid terrains. **Am. J. Sci.**, 278: 1448-1454.

Dunsmore, S.J., Schulze, R.E. & Schmidt, E.J. (1986) **Antecedent soil moisture in design stormflow estimation.** ACRU Report No. 23, Dept. Agric. Eng., Univ. of Natal, Pietermaritzburg, South Africa, pp114.

Edmunds, W.M., Darling, W.G., Kinniburgh, D.G., Kotoub, S. & Mahgoub, S. (1992) Sources of recharge at Abu Delaig, Sudan. **J. Hydrol.**, 131, 1-24.

Emsley, J & Hall, D. (1976) **The chemistry of phosphorus. Environmental, organic, inorganic, biochemical and spectroscopic aspects.** Harper & Row, Publishers, London. 563pp.

Eriksson, E. & Khunakasem, V. (1969) Chloride concentration in groundwater, recharge rate and rate of deposition of chloride in the israel coastal plain. **J. Hydrol.**, 7, 178-197. -

Fontes, J.C. & Edmunds, W.M. (1989) **The use of environmental isotope techniques in arid zone hydrology: a critical review.** Technical documents in hydrology, UNESCO, Paris, 75 pp.

Foster, S.S.D. & Smith-Carrington, A. (1980) The interpretation of tritium in the Chalk unsaturated zone. **J. Hydrol.**, 46, 343-364.

Gat, J.R. & Issar, A. (1974) Desert isotope hydrology: water sources of the Sinai Desert. **Goech. et Cosmch. Acta**, 38, 1117-1131.

Gee, G.W. & Hillel, D. (1988) Groundwater recharge in arid regions: review and critique of estimation methods. **Hydrol. Processes**, 2, 255-266.

Gower, A.M. (ed) (1980) **Water quality in catchment ecosystems.** John Wiley & Sons, Chichester. 335pp.

Görgens, A.H.M. (1983) Reliability of calibration of a monthly rainfall-runoff model: the semiarid case. **Hydro. Sci. Journ.**, 28(4), 485-498.

Grayson, R.B., Moore, I.D. & McMahon, T.A. (1992) Physically Based Hydrologic Modeling 2. Is the Concept Realistic ? **Water Res. Res.**, 26(10), 2659-2666.

Grobler, D.C., Ashton, P.J., Mogane. B & Rooseboom, A. (1987) **Assessment of the Impact of Low-cost, High-density Urban Development at Botshabelo on Water Quality in the Modder River Catchment.** Report to the Department of Water Affairs, Pretoria. 47pp.

Hughes, D.A. (1982a) **Conceptual catchment model parameter transfer studies using data from the southern Cape Coastal lakes region.** Hydrological Research Unit, Report No. 1/82, Rhodes Univ., Grahamstown.

Hughes, D.A. (1982b) The relationship between mean annual rainfall and physiographic variables applied to a coastal region of southern Africa. **South African Geog. Journ.**, 64(1), 41-50.

Hughes, D.A. (1983) **Conceptual catchment model parameter transfer: Application of models to ungauged catchments in the southern Cape Coastal lakes region.** Hydrological Research Unit, Report No. 4/83, Rhodes Univ., Grahamstown.

Hughes, D.A. (1989) Estimation of the parameters of an isolated event conceptual model from physical catchment characteristics. **Hydrol. Sci. Journ.**, 34(5), 539-557.

Hughes, D.A. (1991) Catchment Hydrolcgical Modelling: Where are we and were do we go from here? **Proc. Fifth South African National Hydrological Symposium**, Stellenbosch, South Africa, November, 1991.

Hughes, D.A. (1992) A monthly time step, multiple reservoir water balance model simulation model. **Water SA**, 18(4), 279-286.

Hughes, D.A. (1993) Variable time intervals in deterministic hydrological models. **J. Hydrol.**, 143, 217-232.

Hughes, D.A. (In prep.) Soil moisture and runoff simulated using four deterministic catchment rainfall-runoff models. **Submitted for publication to J. Hydrol. May, 1993.**

Hughes, D.A. & Beater, A.B. (1989) **The application of isolated event conceptual models to simulating floods in areas with different climate and physiographic characteristics.** Report to the Water Research Commission (WRC Rep. No. 138/2/89) by the Hydrological Research Unit, Rhodes Univ., Grahamstown.

Hughes, D.A. & Görgens, A.H.M. (1981) **Hydrological investigations in the southern Cape Coastal lakes region.** Hydrological Research Unit, Report No. 1/81, Rhodes Univ., Grahamstown.

Hughes, D.A. & Herald, J. (1987) The application of deterministic catchment hydrological models: contemporary problems and suggestions for a more unified approach. **Proc. 1987 Hydrological Sciences Symposium, Vol. II.** Rhodes University, Grahamstown, South Africa, September, 1987.

Hughes, D.A. & Murrell, H.C. (1986) Non-linear runoff routing - a comparison of solution methods. **J.Hydrol.**, 85, 339-347.

Hughes, D.A. & Sami, K. (1992) Transmission losses to alluvium and associated moisture dynamics in a semi-arid ephemeral channel system in southern Africa. **Hydrol. Processes**, 6, 45-53.

Hughes, D.A. & Sami, K. (1993) **The Bedford catchments: An introduction to their Physical and Hydrological characteristics.** Final report to the Water Research Commission by the Inst. for Water Research, Rhodes University, Grahamstown.

Hughes, D.A. & Sami, K. (1993) A semi-distributed, variable-time interval model of catchment hydrology - structure and parameter estimation procedures. **J. Hydrol.**, (in press).

Hughes, D.A. & van Ginkel, C. (1993) Nutrient loads from developing urban areas, a simulation approach and identification of information reuirements. **Water SA**, Submiited for publication, April 1993.

Hughes, D.A. & Wright, A. (1988) Spatial variability of short term rainfall amounts in a coastal mountain region of southern Africa. **Water SA**, 14(3), 131-138.

Hutton, J.T. (1976) Chloride in rainwater in relation to distance from the ocean. **Search** 7, 207-208.

Issar, A. & Gat, J. (1981) Environmental isotopes as a tool in hydrogeological research in an arid basin. **Groundwater**, 19 (5), 490-494.

Issar, A., Quijano, J.L., Gat, J.R. & Castro, M. (1984). The isotope hydrology of the groundwaters of central Mexico. **J. Hydrol.**, 71, 201-224.

Johansson, P. (1987) Estimation of groundwater recharge in sandy till with two different methods using groundwater level fluctuations. **J. Hydrol.**, 90, 183-198.

Johnston, C.D. (1987) Distribution of environmental chloride in relation to subsurface hydrology. **J. Hydrol.**, 94, 67-88.

Jordan, P.R. (1987) Streamflow transmission losses in western Kansas. **J. Hydr. Div., ASCE**, 8, 905-918.

Kirchner, J. & Van Tonder, G.J. (1991) **Exploitation Potential of Karoo Aquifers.** WRC Report 170/1/91. Water Research Commission, Pretoria, South Africa.

Knutsson, G. (1988) Humid and arid zone groundwater recharge - a comparative analysis. In: Simmers (ed.), **Estimation of Natural Groundwater Recharge**, NATO ASI ser. C, Vol. 122. Reidel, Dordrecht, 493-503.

Kostiakov, A.N. (1932) On the dynamics of the coefficient of water percolation in soils and on the necessity for studying it from a dynamic point of view for purposes of amelioration. **Trans. 6th Int. Soc. Soil Science, Russian Part A.** 17-21.

Lane, L.J., Diskin, M.H. & Renard, K.G. (1971) Input-output relationships for an ephemeral stream channel system. **J. Hydrol.**, 13, 22-40.

Lane, L.J. (1983) **Transmission losses.** United States Dept. of Agriculture, Washington, D.C.

Lerner, D.N., Issar, A.S. & Simmers, I. (1990) **Groundwater Recharge. A Guide to Understanding and Estimating Natural Recharge**, Vol 8. Verlag Heinz Heise, Hanover, 247-256.

Levin, M., Gat, J.R. & Issar, A. (1980) Precipitation, flood and groundwaters of the Negev Highlands: an isotopic study of desert hydrology. In: **Arid Zone Hydrology:** Investigations with Isotopic Techniques. IAEA, Vienna, 3-23.

Lloyd, J.W. (1986) A review of aridity and groundwater. **Hydrol. Processes**, 1, 63-78.

Malherbe, I de V. (1950) **Soil Fertility.** Second edition. Oxford University Press, London. 296pp.

McKenzie, R.S., Roth, C. & Stoffberg, F. (1993) Orange River Losses. **Proc. Sixth South African National Hydrological Symposium**, Pietermaritzburg, Sept. 1993, 351-358.

Merlivat, L. & Jouzel, J. (1979) Global climatic interpretation of the deuterium - oxygen-18 relationship for precipitation. **J. Geophys. Res.**, 84, pp. 5029.

Middleton, B.J., Lorentz, S.A., Pitman, W.V. & Midgley, D.C. (1981) **Surface Water Resources of South Africa. Volume V, The Eastern Cape.** Report No. 12/81. Hydrological Research Unit, Univ. of the Witwatersrand, Johannesburg.

Mishra, S., Parker, J.C., & Singhal, N. (1989) Estimation of soil hydraulic properties and their uncertainty from particle size distribution data. **J. Hydrol.**, 108, 1-18.

Moore, R.J. (1985) The probability distributed principle and runoff production at point and basin scales. **Hydro. Sci. Journ.**, 30(2), 273-297.

Munnich, K.O. & Roether, W. (1967) Transfer of bomb ^{14}C and Tritium from the atmosphere to the ocean: Internal mixing of the ocean on the basis of Tritium and ^{14}C profiles. In: **Radioactive Dating and Methods of Low-Level Counting**, Proc. Symp. Monaco, 1967, IAEA, Vienna.

O'Connell, P.E. (1991) A historical perspective. In: Bowles, D.S. and O'Connell, P.E. (eds.), **Recent Advances in the Modelling of Hydrologic Systems**, NATO ASI Series, Kluwer Academic, Netherlands. 3-30

O'Donnell, T. & Canedo, P. (1980) The reliability of conceptual basin model calibration. In: **Hydrological Forecasting** (Proc. Oxford Symp., April 1980), IAHS Publ. no. 129, 263-269.

Paling, W.A.J., Stephenson, D. & James, C.S., 1989. **Modular rainfall-runoff and erosion modelling.** Report No. 1/1989, Water Systems Research Group, Univ. of the Witwatersrand, Johannesburg, South Africa.

Payne, B.R. (1988) The status of isotope hydrology today. **J. Hydrol.**, 100, 207-237.

Peables, R.W., Smith, R.E. & Yakowitz, S.J. (1981) A leaky reservoir model for ephemeral flow recession. **Water Resour. Res.**, 17(3), 628-636.

Pitman, W.V. (1973) **A mathematical model for generating monthly river flows from meteorological data in South Africa.** Report No. 2/73, Hydrological Research Unit, Univ. of the Witwatersrand, Johannesburg.

Pitman, W.V. & Kakebeeke, J.P. (1973) The Pitman model - Into the 1990's. **Proc. of the 5th S. Afr. Natl. Hydrol. Symp.**, Stellenbosch, Nov. 1991.

Press, W.H., Flannery, B.P., Teukolsky, S.A. & Vetterling, W.T. (1988) **Numerical Recipes in C. The Art of Scientific Computing.** Cambridge Univ. Press. 735pp.

Rawls, W.J. & Brakensiek, D.L. (1983) A procedure to predict Green and Ampt infiltration parameters. **Proc. National Conference on Advances in Infiltration**, Am. Soc. Agric. Engrs., Dec. 1993, Chicago, Illinois.

Reinders, F.B. & Louw, A.A., 1984. **Infiltration : Measurement and Use.** Div. of Agric. Eng., Dept. of Agric. Tech. Services, Silverton, South Africa.

Renard, K.G. & Keppel, R.V. (1966) Hydrographs of ephemeral streams in the Southwest. **J. Hydraulics Div.**, ASCE, 92(HY2), Proc. Paper 4710, 33-52.

Reynders, A.G., Moolman, J.H. & Stone, A.W. (1985) Water level response in fractured rock aquifers underlying irrigated lands - a study in the lower Great Fish river valley. **Water SA**, 11(2), 93-98.

Rosenthal, E. (1987) Chemical composition of rainfall and groundwater in recharge areas of the Bet Shean-Harod multiple aquifer system, Israel. **J. Hydrol.**, 89, 329-352.

Rushton, K.R. (1987) Numerical and conceptual models for recharge estimation in arid and semi-arid zones. In: Simmers (ed.), **Estimation of Natural Groundwater Recharge**, NATO ASI ser. C, Vol. 122. Reidel, Dordrecht, 449-460.

Rutter, A.J., Morton, A.J., & Robins, P.C. (1975) A predictive model of rainfall interception in forests. II. Generalization of the model and comparison with observations in some coniferous and hardwood stands. **J. Appl. Ecology**, 12, 367-380.

Sami, K. (1991) Modelling groundwater recharge in semi-arid environments. **Proc. Fifth South African National Hydrological Symposium**, Stellenbosch, South Africa, November, 1991.

Sami, K. (1992) Recharge mechanisms and geochemical processes in a semi-arid sedimentary basin, Eastern Cape, South Africa. **J. Hydrol.**, 139, 27-48.

Scanlon, B.R. (1991) Evaluation of moisture flux from chloride data in desert soils. **J. Hydrol.**, 128, 137-156.

Schafer, G.N. (1991) **Forest Land Types of the Southern Cape.** Forestek, CSIR, Pretoria.

Schmidt, E.J. & Schulze, R.E. (1987) **SCS-Based Design Runoff - User Manual.** ACRU Report No. 25, Department of Agricultural Engineering, Univ. of Natal, Pietermaritzburg, South Africa. 81pp.

Schulze, R.E. (1982) **Adapting the SCS stormflow equation for application to specific events by soil moisture budgetting.** ACRU Report No. 25, Department of Agricultural Engineering, Univ. of Natal, Pietermaritzburg, South Africa. 63pp.

Schulze, R.E. (1989) **ACRU: Background, concepts and theory.** Report (WRC 154/1/89) to the Water Research Commission by the Dept. Agric. Eng., Univ. of Natal, Pietermaritzburg, South Africa.

Schulze, R.E. (1993) Personal Communication from the Dept. of Agricultural Eng., University of Natal, Pietermaritzburg, South Africa.

Schulze, R.E. & Arnold, H. (1979) **Estimation of volume and rate of runoff in small catchments in South Africa, based on the SCS technique.** ACRU Report No. 8, Department of Agricultural Engineering, Univ. of Natal, Pietermaritzburg, South Africa. 79pp.

Schulze, R.E. & George, W.J. (1987) A dynamic process-based user-orientated model of forest effects on water yield. **Hydrol. Processes**, 1, 293-307.

Schulze, R.E., George, W.J., Arnold, H. & Mitchell, J.K. (1984) **The coefficient of initial abstraction in the SCS model as a variable.** In Schulze, R.E. 1984, Hydrological models for application in small rural catchments in southern Africa : Refinements and developments. ACRU Report No. 19, Department of Agricultural Engineering, Univ. of Natal, Pietermaritzburg, South Africa. 248pp.

Schulze, R.E., Hutson, J.L. & Cass, A. (1985) Hydrological characteristics and properties of soils in Southern Africa 2: Soil water retention models. **Water SA**, 11(3), 129-136.

Schulze, R.E. & Maharaj, M. (1991) Mapping A-Pan equivalent potential evaporation over Southern Africa. **Proc. of the 5th S. Afr. Natl. Hydrol. Symp.**, Stellenbosch, Nov. 1991.

Sharma, M.L. & Hughes, M.W. (1985) Groundwater recharge estimation using chloride, deuterium and oxygen-18 profiles in the deep coastal sands of western Australia. **J. Hydrol.**, 81: 93-109.

Solomon, D.K. & Sudicky, E.A. (1991) Tritium and Helium 3 isotope ratios for direct estimation of spatial variations in groundwater recharge. **Water Res. Res.**, 27 (9), 2309-2319.

Sophocleous, M. (1991) Combining the soil water balance and water-level fluctuation methods to estimate natural ground-water recharge: practical aspects. **J. Hydrol.**, 124, 229-241.

Sophocleous, M. (1992) Groundwater recharge estimation and regionalization: the Great Bend Prairie of central Kansas and its recharge statistics. **J. Hydrol.**, 137, 113-140.

Sorooshian, S. (1991) Parameter estimation, model identification, and model validation: Conceptual-type models. In: Bowles, D.S. and O'Connell, P.E. (eds.), **Recent Advances in the Modelling of Hydrologic Systems**, NATO ASI Series, Kluwer Academic, Netherlands. 443-467.

Spears, D.A. (1986) Mineralogical control of the chemical evolution of groundwater. In: Trudgill, S.T. (ed.). **Solute Processes**. John Wiley & Sons, Chichester.

Stephenson, D. & Paling, W.A.J. (1992) An hydraulic model for simulating monthly runoff and erosion. **Water SA**, 18(1), 43-52.

Sukhija, B.S., Reddy, D.V., Nagabhushanam, P. & Chand, R. (1988) Validity of the environmental chloride method for recharge evaluation of coastal aquifers, India. **J. Hydrol.**, 99, 349-366.

Thorburn, P.J., Cowie, B.A. & Lawrence, P.A. (1991) Effect of land development on groundwater recharge determined from non-steady chloride profiles. **J. Hydrol.**, 124, 43-58.

Tordiffe, E.A.W. (1978) **Aspects of the Hydrochemistry of the Karoo sequence in the Great Fish River Basin, Eastern Cape Province, with Special Reference to the Groundwater Quality**. Unpubl. Ph.D. thesis. Department of Geology, University of the Orange Free State.

Tordiffe, E.A.W. (1981) The relationship between macro-topography and the groundwater quality in the Great Fish river basin, eastern Cape. **Water SA**, 7(3), 113-138.

Turner, J.V., Arad, A. & Johnston, C.D. (1987) Environmental isotope hydrology of salinized experimental catchments. **J. Hydrol.**, 94, 89-107.

Tyson, P.D. (Editor) (1971) **Outeniqualand: The George-Knysna Area**. South African Landscape Monographs, No. 2, South African Geographical Society, Johannesburg.

USDA (1955-1973) **United States Department of Agriculture, Agricultural Research Service, Hydologic data for experimental watersheds in the United States.** Misc. Publ. Series compiled by H.W.Hobbs, J.B.Burford and J.M.Clark.

Van Ginkel, C.E., O'Keeffe, J.O., Hughes, D.A., Hill, T. & Ashton, P.A. (1993) **A situation analysis of water quality in the catchment of the Buffalo River, eastern Cape, with special emphasis on the impacts of low-cost, high-density urban development on water quality. Vol. 1.** Inst. for Water Research, Rhodes Univ. and Watertek, CSIR. Final report to the Water Research Commission, Pretoria. 70pp.

Van Tonder, G.J. & Kirchner, J. (1990) Estimation of natural groundwater recharge in the Karoo aquifers of South Africa. **J. Hydrol.**, 121, 395-419.

Vogel, J.C. (1963) A survey of the natural isotopes of water in South Africa. In: **Radioisotopes in Hydrology**. IAEA, Vienna, 383-395.

Vogel, J.C., Lerman, J.C., Mook, W.G. & Roberts, F.B. (1972) Natural isotopes in the groundwater of the Tulum Valley, San Juan, Argentina. **Bull. Int. Ass. Hydrol. Sci.**, 17, 85-96.

Vogel, J.C. & Van Urk, H. (1975) Isotopic composition of groundwater in semi-arid regions of southern Africa. **J. Hydrol.**, 25, 23-36.

Walker, G.R., Jolly, I.D. & Cook, P.G. (1991) A new chloride leaching approach to the estimation of diffuse recharge following a change in land use. **J. Hydrol.**, 128, 49-67.

Walters, M.O. (1990) Transmission losses in arid region, **J. Hydr. Engineering**, 116(1), 129-138.

Weddepohl, J.P. & Meyer, D.H. (1992) **Utilisation of models to simulate Phosphorus loads in southern African catchments.** Report to the WRC by the Div. of Water Technology, CSIR (No. 197/1/92). 160pp.

APPENDIX A Publications, reports, conference papers and theses emanating from the project work.

Engelbrecht, G. (1991) **Characteristics of the alluvial sediments in the Bedford catchments.** Unpubl. Undergrad. Thesis, Dept. of Geography, Rhodes University Grahamstown.

Engelbrecht, G. (1993) **The viability of water storage tanks for augmenting drinking water supply.** Unpubl. Hons. Thesis, Dept. of Geography, Rhodes University Grahamstown.

Hensley, M. & Sami, K. (1992) **A description of the soils at selected sites in the Bedford catchments.** Unpubl. report.

Hughes, D.A. (1991) Catchment Hydrological Modelling: Where are we and were do we go from here? **Proc. Fifth South African National Hydrological Symposium,** Stellenbosch, South Africa, November, 1991.

Hughes, D.A. (1992) A monthly time step, multiple reservoir water balance model simulation model. **Water SA,** 18(4), 279-286.

Hughes, D.A. (1992) **Proposed Dam : Uniondale, Hydrological Design.** Confidential report to Liebenburg and Stander by the Inst. Water Research Rhodes University.

Hughes, D.A. (1993) Variable time intervals in deterministic hydrological models. **J. Hydrol.,** 143, 217-232.

Hughes, D.A. (1993) A pragmatic approach to incorporating 'real' hydrology into a catchment simulation model. **Proc. Sixth South African National Hydrology Symposium, Pietermaritzburg,** Sept. 1993.

Hughes, D.A. (In prep.) Soil moisture and runoff simulated using four deterministic catchment rainfall-runoff models. **Submitted for publication to J. Hydrol. May, 1993.**

Hughes, D.A. & Murdoch, K.A. (1991) **The development of a flexible, PC based hydrological modelling system.** Paper and software demonstration presented at the XVI General Assembly of the European Geophysical Society, Wiesbaden, Germany, April 1991.

Hughes, D.A. & Sami, K. (1992) Transmission losses to alluvium and associated moisture dynamics in a semi-arid ephemeral channel system in southern Africa. **Hydrol. Processes,** 6, 45-53.

Hughes, D.A. & Sami, K. (1993) **The Bedford catchments: An introduction to their Physical and Hydrological characteristics.** Final report to the Water Research Commission by the Inst. for Water Research, Rhodes University, Grahamstown.

Hughes, D.A. and Sami, K. (1993) A semi-distributed, variable-time interval model of catchment hydrology - structure and parameter estimation procedures. **J. Hydrol.**, (in press).

Hughes, D.A. & van Ginkel, C. (1993) Nutrient loads in runoff from developing urban areas, a modelling approach. **Proc. Sixth South African National Hydrology Symposium**, Pietermaritzburg, Sept. 1993.

Hughes, D.A. & van Ginkel, C. (1993) Nutrient loads from developing urban areas, a simulation approach and identification of information reuirements. **Water SA**, Submiited for publication, April 1993.

Kent, C.D. (1990) **A preliminary investigation into the space-time variations of rainfall events in the Bedford river catchments.** Unpubl. Hons. Thesis, Dept. of Geography, Rhodes University Grahamstown.

Langton, C.W. (1987) **A hydrogeological investigation into the Nyara River catchment based on a survey of borehole water characteristics.** Unpubl. Hons. Thesis, Dept. of Geography, Rhodes University Grahamstown.

Maclear, L.G.A. (1987) **A hydrogeological investigation of the Nyara River catchment near Bedford.** Unpubl. Hons. Thesis, Dept. of Geography, Rhodes University Grahamstown.

Morgan, M. (1989) **An examination of the relationship between channel morphology and the catchment characteristics of a semi-arid region of the Goba River, Bedford.** Unpubl. Undergrad. Thesis, Dept. of Geography, Rhodes University Grahamstown.

Sami, K. (1991) Modelling groundwater recharge in semi-arid environments. **Proc. Fifth South African National Hydrological Symposium**, Stellenbosch, South Africa, November, 1991.

Sami, K. (1992) Recharge mechanisms and geochemical processes in a semi-arid sedimentary basin, Eastern Cape, South Africa. **J. Hydrol.**, 139, 27-48.

Sami, K. (1993). Estimates of recharge and its variability in a semi-arid region of South Africa. (In prep.)

Sami, K. & Hughes, D.A. (1993) A comparison of recharge estimates from a chloride mass balance and an integrated surface-subsurface semi-distributed model. **Proc. Sixth South African National Hydrology Symposium**, Pietermaritzburg, Sept. 1993.

Scott, D. (1988) **An assessment of streamflow and drought sequences for Settlers Dam catchment using a hydrological modelling approach.** Unpubl. Hons. Thesis, Dept.